UNIVERSITY OF LATVIA

CHARACTERISTICS OF GROWTH PROPERTIES, MARKER EXPRESSION, AND DIFFERENTIATION ABILITY OF HUMAN ADIPOSE-DERIVED STEM CELLS

Doctoral thesis

Department of Molecular Biology
Faculty of Biology

Author: Ance Bogdanova-Jātniece
Supervisor: Dr. habil. biol. Tatjana Kozlovska

Riga 2016

Summary

Human adipose tissue is known to be an attractive and readily available source of mesenchymal stem cells (MSCs). In the last fifteen years the isolated adipose-derived stem cells (ASCs) have experienced a great scientific interest and have become increasingly popular for application in regenerative medicine. The aim of this study was to analyse growth properties, various marker expression, and differentiation ability of human ASCs that have been cultured in the medium supplemented with autologous serum (AS).

The obtained results showed that ASCs can be easily and effectively propagated in the medium containing AS and such culture conditions does not alter their characteristic spindle-shaped morphology throughout the eight tested passages (P). The aggregation of ASCs into four different types of bodies was observed under various stress conditions. The ASC assembly into adherent bodies was triggered by slight changes in the growth environment or the use of different growth surface, such as uncoated glass. Altered composition of a culture medium induced generation of individual floating ASC bodies. Another type of floating cell bodies were detected in early passages that subsequently formed compact and large aggregates of interconnected ASC bodies. The exact reason provoking this type of cell clustering is unknown. Furthermore, single floating ASC bodies of both types were capable of adhering to the surface and converting back to functional monolayer culture, when transferred onto new plastic tissue culture flask. Few ASCs in the monolayer culture showed alkaline phosphatase (AP) activity, thus representing more mature cells. Floating ASC bodies, after their transfer to a new flasks, were AP negative, but a large fraction of cells migrating out of the ASC bodies after their attachment to the surface exhibited AP activity. These observations suggest that spontaneously formed floating ASC bodies may represent more primitive cell subpopulation within the individual ASC culture.

The 8-color flow cytometry analysis at cell passages 2, 3, 4, 5, and 8 showed that ASCs represent highly homogeneous cell population by expressing typical MSC surface markers CD29, CD44, CD73, CD90, CD105 simultaneously, but lacking the expression of such markers as HLA-DR, CD34, CD14, CD19, and CD45. Furthermore, median fluorescence intensity of positive cell surface markers increased with each subsequent passage indicating the overall accumulation of protein expression. The complementary real-time RT-PCR data on positive MSC surface marker genes revealed the increase of gene expression until P4 or P5, except for *CD105* where the peak expression was observed at P2. The investigation of the expression of pluripotency markers in ASCs showed that these cells express such pluripotency markers as *OCT4* isoform A and *SOX2*, but the presence of *NANOG* was inconclusive. At the same time, the expression of *NANOG* pseudogene 8 (*NANOGP8*) was discovered in ASCs. The immunocytochemistry data lead to possibility that in the ASCs of the investigated donor the *NANOGP8* is not only transcribed, but also translated into protein.

The ASC differentiation into cells of mesodermal lineage showed that these cells can be differentiated into adipocytes, osteocytes, and chondrocytes not only at P3, but also at P6. However, their differentiation into cells of endodermal origin or insulin-positive cells was not successful. In total, nine various differentiation protocols were employed on ASCs of four donors to test their ability to give rise to the cells of endodermal lineage. Data from immunocytochemistry or real-time RT-PCR methods showed no solid evidence to suggest the expression of insulin or other markers characteristic to pancreatic cells or cells from any transition state, along the pancreatic differentiation, after ASCs have been subjected to any of investigated protocols.

Kopsavilkums

Ir zināms, ka cilvēka taukaudi ir vērtīgs un viegli pieejams mezenhimālo cilmes šūnu avots (MCŠ). Pēdējo piecpadsmit gadu laikā no taukaudiem iegūtās cilmes šūnas (TCŠ) ir piedzīvojušas ievērojamu zinātnisko interesi, un to popularitāte pielietojumam reģeneratīvajā medicīnā ir kļuvusi arvien lielāka. Šī darba mērķis bija analizēt augšanas īpatnības, dažādu marķieru ekspresiju un diferencēšanās spējas cilvēka TCŠ, kas audzētas barotnē ar autologo serumu (AS).

Iegūtie rezultāti parādīja, ka TCŠ var viegli un efektīvi pavairot barotnē, kas satur AS, un šādi audzēšanas apstākļi nemaina tām raksturīgo vārpstveida morfoloģiju astoņu pārbaudīto šūnu pasāžu (P) laikā. Dažādos stresa apstākļos tika novērota TCŠ agregācija četru dažādu veidu sakopojumos. TCŠ apvienošanos adherentos sakopojumos izraisīja nelielas izmaiņas augšanas vidē vai arī citas augšanas virsmas, piemēram, neapstrādāta stikla, izmantošana. Izmainīts šūnu kultivēšanas barotnes sastāvs veicināja individuālu, peldošu TCŠ sakopojumu veidošanos. Agrās šūnu pasāžās tika detektēti cita veida peldoši šūnu sakopojumi, kas vēlāk izveidoja blīvus un lielus savstarpēji saistītu TCŠ sakopojumu agregātus. Precīzs iemesls, kas izraisīja šāda veida šūnu apvienošanos, nav zināms. Papildus tam, abu veidu atsevišķi peldošie TCŠ sakopojumi spēja piestiprināties pie virsmas un pārveidoties atpakaļ par funkcionālu monoslāņa kultūru pēc tam, kad tika pārnesti uz jaunu plastmasas šūnu kultivēšanas flakonu. Atsevišķas TCŠ monoslāņa kultūrā uzrādīja sārmainās fosfatāzes (SF) aktivitāti, tādējādi reprezentējot nobriedušākas šūnas. Peldošie TCŠ sakopojumi pēc to pārnešanas uz jaunu flakonu nebija SF pozitīvi, bet liela daļa no šūnām, kas migrēja ārā no TCŠ sakopojumiem pēc to piestiprināšanās pie virsmas, demonstrēja SF aktivitāti. Šie novērojumi liek domāt, ka spontāni veidojušies peldošie TCŠ sakopojumi varētu reprezentēt primitīvāku šūnu subpopulāciju individuālā TCŠ kultūrā.

Astoņu krāsu plūsmas citometrijas analīze šūnām no 2., 3., 4., 5. un 8. pasāžas parādīja, ka TCŠ reprezentē ļoti homogēnu šūnu populāciju, vienlaicīgi ekspresējot MCŠ raksturīgos virsmas marķierus CD29, CD44, CD73, CD90, CD105, bet neuzrādot tādu marķieru kā HLA-DR, CD34, CD14, CD19 un CD45 ekspresiju. Turklāt, šūnu pozitīvo virsmas marķieru vidējās fluorescences intensitāte pieauga ar katru nākamo pasāžu, norādot uz vispārējo proteīna ekspresijas uzkrāšanos. Dati par pozitīvajiem MCŠ virsmas marķieru gēniem, no papildus veiktās reālā laika RT-PĶR, atklāja šo gēnu ekspresijas pieaugumu līdz P4 vai P5, izņemot *CD105* gadījumā, kur augstākais ekspresijas līmenis tika detektēts P2. Pluripotences marķieru ekspresijas pētījumi TCŠ parādīja, ka šīs šūnas ekspresē tādus pluripotences marķierus kā *OCT4* izoforma A un *SOX2*, bet *NANOG* klātbūtne nebija viennozīmīga. Tajā pašā laikā, TCŠ tika atklāta *NANOG* pseidogēna 8 (*NANOGP8*) ekspresija. Imunocitoķīmijas dati norādīja uz iespēju, ka pētītā donora TCŠ notiek ne tikai *NANOGP8* transkripcija, bet arī tā translācija proteīnā.

TCŠ diferenciācija par mezodermālās līnijas šūnām parādīja, ka šīs šūnas var tikt diferencētas par adipocītiem, osteocītiem un hondrocītiem ne tikai P3, bet arī P6. Taču to diferenciācija par endodermālas izcelsmes šūnām vai insulīna pozitīvām šūnām nebija veiksmīga. Kopumā tika izmēģināti deviņi dažādi diferenciācijas protokoli, izmantojot četru donoru TCŠ, lai pārbaudītu to spēju pārveidoties par endodermālās līnijas šūnām. Imunocitoķīmijas un reālā laika RT-PĶR rezultāti nedeva pārliecinošus pierādījumus, kas liktu domāt par insulīna vai citu raksturīgu marķieru, kas atrodami aizkuņģa dziedzera šūnās vai šūnās no jebkura aizkuņģa dziedzera diferenciācijas laikā novērojamā pārejas stāvokļa, ekspresiju TCŠ pēc tam, kad tās tikušas pakļautas jebkuram no šajā darbā izmēģinātajiem protokoliem.

Table of contents

Abbreviations

3D	three-dimensional
aa	amino acid
AP	alkaline phosphatase
AS	autologous serum
ASCs	adipose-derived stem cells
BAT	brown adipose tissue
bFGF	basic fibroblast growth factor
BM	bone marrow
BSA	bovine serum albumin
CD	cluster of differentiation
cDNA	complementary deoxyribonucleic acid
C-PEPT	C-peptide
DAPI	4',6-diamidino-2-phenylindole
DAPT	N-[N-(3,5-difluorophenacetyl)-1-alanyl]-S-phenylglycine t-butyl ester
DE	definitive endoderm
DEPC	diethylpyrocarbonate
DMEM	Dulbecco's Modified Eagle Medium
DNA	deoxyribonucleic acid
DNase I	deoxyribonuclease I
EBs	embryoid bodies
ESCs	embryonic stem cells
FBS	fetal bovine serum
FSCs	fetal stem cells
GCG	glucagon
GLP-1	glucagon-like peptide-1
GSK3β	glycogen synthase kinase 3 β
GVHD	graft-versus-host disease
HCl	hydrochloric acid
HIF-1α	hypoxia-inducible factor 1α
HLA	human leukocyte antigen
HSCs	haematopoietic stem cells
INS	insulin
iPSCs	induced pluripotent stem cells
ISCT	International Society for Cellular Therapy
MHC	major histocompatibility complex
mRNA	messenger ribonucleic acid
MSCs	mesenchymal stem cells
NANOGP1, NANOGP2...	NANOG pseudogene 1, NANOG pseudogene 2
NGN3	neurogenin 3
OCT4P1, OCT4P2...	OCT4 pseudogene 1, OCT4 pseudogene 2
ORF	open reading frame
P1, P2...	cell passage 1, cell passage 2
PBS	phosphate-buffered saline
PCR	polymerase chain reaction
PI3K	phosphatidylinositol 3-kinase
RNA	ribonucleic acid
rpm	revolutions per minute
RT	room temperature
RT-PCR	reverse transcription polymerase chain reaction
SCs	stem cells
SST	somatostatin
SVF	stromal vascular fraction
T1D	type 1 diabetes
T2D	type 2 diabetes
TA cells	transit-amplifying cells
TBS	Tris-buffered saline
TGFβ	transforming growth factor β
TNAP	tissue-nonspecific alkaline phosphatase
UC	umbilical cord
WAT	white adipose tissue

Introduction

Stem cells (SCs) are undifferentiated cells that can self-renew and give rise to diverse types of cells. Most adult tissues or organs can serve as a source of somatic, i.e., adult SCs, as they exist in specialized niches within those organs and play an important role in tissue repair and regeneration through our life (Mimeault, Batra 2006). P. Zuk and her colleagues showed that mesenchymal stem cells (MSCs) can be obtained not only from adult bone marrow (BM), but also from adipose tissue (Zuk et al. 2001). Since then the potential use of adipose-derived stem cells (ASCs) has experienced a great increase of scientific interest.

The attraction of MSCs has been furthered by the observations that adult SCs express OCT4 and other pluripotency markers, usually detected in embryonic SCs (ESCs) (Tai et al. 2005, Izadpanah et al. 2006, Ambady et al. 2010). This has led to discussions regarding actual potency of somatic SCs. It is tempting to speculate that adult SCs share greater degree of similarities with ESCs than anticipated. However, the actual characteristics of routinely tested pluripotency markers OCT4 and NANOG are highly confusing. Overlooking these particularities can result into misleading conclusions regarding the expression of those markers in somatic SCs.

Even though it is generally believed that adult SCs possess lower differentiation ability than pluripotent SCs, their potential use in the development of cell-based therapies is growing rapidly (Mimeault, Batra 2006). The potential of MSC in treating bone disorders, neurological diseases, liver diseases, heart damages, diabetes, graft-versus-host disease, as well as healing chronic wounds has been intensely explored (Lindroos et al. 2011, Catacchio et al. 2013). One of those diseases - type 1 diabetes - has gained particular interest, since it can be cured by replacing destroyed pancreatic β cells, thus restoring insulin secretion. A lot of effort has been made to differentiate both ESCs and somatic SCs into insulin-producing cells. This is still hampered by problems, such as the lack of efficient standard method for functional insulin-secreting cell generation, inability to consistently produce clinically significant amounts of insulin, and differentiation on a large scale. These are yet to be overcome before SCs can be used for the treatment of diabetes (Wong 2011).

Furthermore, to ensure the safety of the SCs intended for the clinical use, all possible threats must be eliminated. Although the danger of prion diseases and zoonoses from the fetal bovine serum (FBS), that is used to supplement most of the cell culture media, is considered to be minimal (Doerr et al. 2003), it has been shown that 10^8 MSCs grown in the medium supplemented with 20% FBS would carry 7-30 mg of FBS proteins. It could lead to the possible autoimmune reaction against patient's own SCs (Spees et al. 2004). To avoid this risk, the FBS can be substituted with an autologous serum (AS).

The aim of this doctoral study was to determine characteristics of human adipose-derived stem cells, cultured in the medium containing autologous serum, with respect to their growth properties, various marker expression, and differentiation potential into cells of mesodermal, as well as endodermal origin. In order to achieve this goal the following tasks were set:

- to obtain human ASCs, propagate them in a medium supplemented with autologous serum, and evaluate their growth characteristics;
- to detect the expression of such surface markers as CD14, CD19, CD29, CD34, CD44, CD45, CD73, CD90, CD105, and HLA-DR on human ASCs at different passages using flow cytometry, real-time RT-PCR, and immunocytochemistry methods;
- to determine the expression of pluripotency markers OCT4, NANOG, and SOX2 in human ASCs by means of RT-PCR, sequencing, and immunocytochemistry methods;
- to analyse alkaline phosphatase activity in ASC culture;
- to differentiate human ASCs into adipocytes, osteocytes, and chondrocytes *in vitro* and

assess this differentiation capacity at passages 3 and 6;
- to test the ability of human ASCs to differentiate into insulin-producing cells using various differentiation protocols.

Unless noted otherwise, the author of all the figures presented under "Results and discussion" and "Appendix" is A. Bogdanova-Jātniece.

Part of the main results described in the doctoral thesis is published in three original papers. The list of publications and the author's contributions to each of them are as follows:

Original paper I

Bogdanova A., Berzins U., Bruvere R., Eivazova G., Kozlovska T. Adipose-derived stem cells cultured in autologous serum maintain the characteristics of mesenchymal stem cells. *Proceedings of the Latvian Academy of Sciences, Section B* 2010, 64(3/4): 106-113.

Contributions: performed and optimised the immunocytochemistry method and *in vitro* differentiation of ASCs; wrote the manuscript.

Original paper II

Bogdanova A., Berzins U., Nikulshin S., Skrastina D., Ezerta A., Legzdina D., Kozlovska T. Characterization of human adipose-derived stem cells cultured in autologous serum after subsequent passaging and long term cryopreservation. *Journal of Stem Cells* 2014, 9(3): 135-148.

Contributions: participated in the *in vitro* differentiation of ASCs and gene expression analysis by real-time RT-PCR; collected and analysed the data; prepared the graphical and visual information; wrote the manuscript.

Original paper III

Bogdanova-Jatniece A., Berzins U., Kozlovska T. Growth properties and pluripotency marker expression of spontaneously formed three-dimensional aggregates of human adipose-derived stem cells. *International Journal of Stem Cells* 2014, 7(2): 143-152.

Contributions: carried out the methods of alkaline phosphatase detection and immunocytochemistry; collected and analysed the data; wrote the manuscript.

1. Literature overview
1.1. Stem cells

Stem cells play a major role in the development of multicellular organisms as they can create a new life from only one fertilized oocyte and SCs are indispensable during an adult lifespan since they can regenerate certain tissues undergoing a natural physiological turnover or an injury (Fuchs et al. 2004). SCs are defined as undifferentiated cells that can self-renew (generate precise copies of themselves upon division) and differentiate into diverse cell types (produce specialized cell types) (Mimeault, Batra 2006). They can be classified according to their origin (see Chapter 1.2.), as well as potency. Potency of SCs is regarded as their potential to differentiate into various cell types (Bindu, Srilatha 2011). Three major types are commonly discriminated: totipotent, pluripotent, and multipotent SCs. Totipotent SCs are referred to as cells that can differentiate into embryonic and extra-embryonic cell types giving rise to a new and complete organism on their own. The only totipotent cells are a fertilized egg and early blastomeres up to the 8 cell stage (Pera, Dottori 2005). Pluripotent SCs can differentiate into every cell type of the body, including germ cells. The embryonic stem cells, isolated from the inner cell mass (ICM) of a blastocyst, are the best known example of pluripotent SCs (Mimeault, Batra 2006). Multipotent SCs can give rise to several types of mature cells. One such example is haematopoietic SCs (HSCs) that can differentiate into all types of blood cells. Sometimes bipotent (giving rise to two types of differentiated cells) and unipotent (producing only one cell type) SCs are also discriminated (Pera, Dottori 2005).

In order to sustain a population of undifferentiated SCs and produce differentiated cells as well, SCs employ two cell division strategies: asymmetric and symmetric (Figure 1.1.1.).

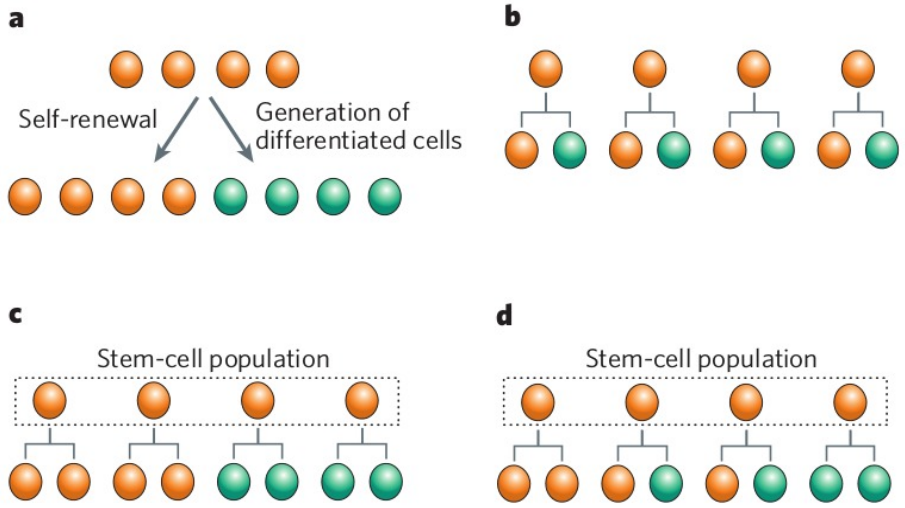

Figure 1.1.1. Figure and caption from Morrison and Kimble 2006: "Stem cell division strategies. (A) Stem cells (orange) must accomplish the dual task of self-renewal and generation of differentiated cells (green). (B) Asymmetric cell division: each stem cell generates one daughter stem cell and one daughter destined to differentiate. (C) Symmetric cell division: each stem cell can divide symmetrically to generate either two daughter stem cells or two differentiated cells. (D) Combination of cell divisions: each stem cell can divide either symmetrically or asymmetrically. C and D represent population strategies that provide dynamic control over the balance between stem cells and differentiated cells."

Asymmetric cell division is defined as a process where each stem cell divides to produce one daughter cell that differentiates and another daughter stem cell to sustain self-renewal (Morrison, Kimble 2006). This strategy helps to maintain the population of SCs at a

steady level, but it does not allow a dynamic control of SCs in case of injury. Therefore SCs also use symmetric cell division creating two stem cells or two more differentiated cells (Shahriyari, Komarova 2013). The more differentiated cells produced during both cell division strategies are termed transit-amplifying (TA) or intermediate cells. The TA cells possess high proliferative index and migratory properties. These cells can further produce other intermediate cell progenitors and more mature cells within tissues or organs of their origin or other, more distant tissues (Mimeault, Batra 2006). It has been recently shown that TA cells also play a regulatory role by activating quiescent stem cells, thus orchestrating tissue regeneration (Hsu et al. 2014). It is believed that most SCs can divide by either division strategies, switching between the modes of asymmetric and symmetric division, and the balance between those two is under control of numerous developmental and environmental signals (Morrison, Kimble 2006) coming from the surrounding tissues and the SCs themselves (Shahriyari, Komarova 2013). A stem cell niche is also thought to participate in the regulation of this balance by precisely orienting the divisions to sustain a correct flow and directionality of the cells (Fuchs et al. 2004).

The stem cell niche is described as a local tissue microenvironment that hosts and influences the actions or characteristics of SCs (Hsu, Fuchs 2012). The niches are composed of the SCs themselves and surrounding differentiated cell types that secrete and organize fertile environment of extracellular matrix and other factors (Fuchs et al. 2004). The functions of SCs depend on cooperation between their intrinsic genetic programmes and extrinsic regulatory signals from the niche (Dzierzak, Enver 2008), as well as feedback mechanisms from differentiated progeny (Hsu et al. 2014). It is thought that inside the niche SCs are usually dormant. There are two possible ways how to activate SCs in the niche. First, SCs are slowly, but constantly, dividing and filling up the niche until excess SCs lose a direct contact with it. When these cells encounter a new environment outside the niche, they progress to differentiate. It seems, that this mechanism is more used during development. Second, SCs stay quiescent within the niche until environmental changes, e.g., from the tissue injury, signal to the niche and SCs become activated in return. This model is believed to function more often in adult tissues (Fuchs et al. 2004). However, a great difference in proliferative abilities of SCs from different tissues and organs have been observed, and not all somatic tissues even contain the SC reserves, and not all cell types can be efficiently regenerated from SCs *in vivo* (Naveiras, Daley 2006). Few of the best-characterised SC niches are hair follicles of mammalian skin, endothelial gut crypts, bone marrow (BM), and mammalian and invertebrate testes (González-Reyes 2003).

The potential therapeutic applications of different types of SCs include their use as adjuvant immunotherapy for diverse cancer types, Parkinson's and Alzheimer's diseases, muscular degenerative disorders, chronic liver and heart failures, diabetes, as well as skin, eye, kidney, and haematopoietic disorders (Mimeault, Batra 2006). Similarly, SCs could be used to prevent graft-versus-host disease (GVHD), correct inborn metabolic errors, and deliver a variety of therapeutic genes into the cells (Tocci, Forte 2003).

1.2. Types of stem cells

According to their origin, three main types of SCs are distinguished: embryonic, fetal, and adult, i.e., somatic SCs. All of them possess ability to self-renew and differentiate under appropriate conditions *in vitro* and after transplantation in the host *in vivo* (Mimeault, Batra 2006) (Figure 1.2.1.).

Embryonic SCs are derived from the inner cell mass of a blastocyst. Firstly they were isolated from mice (Martin 1981) and only later from humans (Thomson et al. 1998). The main characteristics of ESCs are as follows: they are obtained from a pluripotent cell population; they are firmly diploid and maintain normal karyotype *in vitro*; they can be

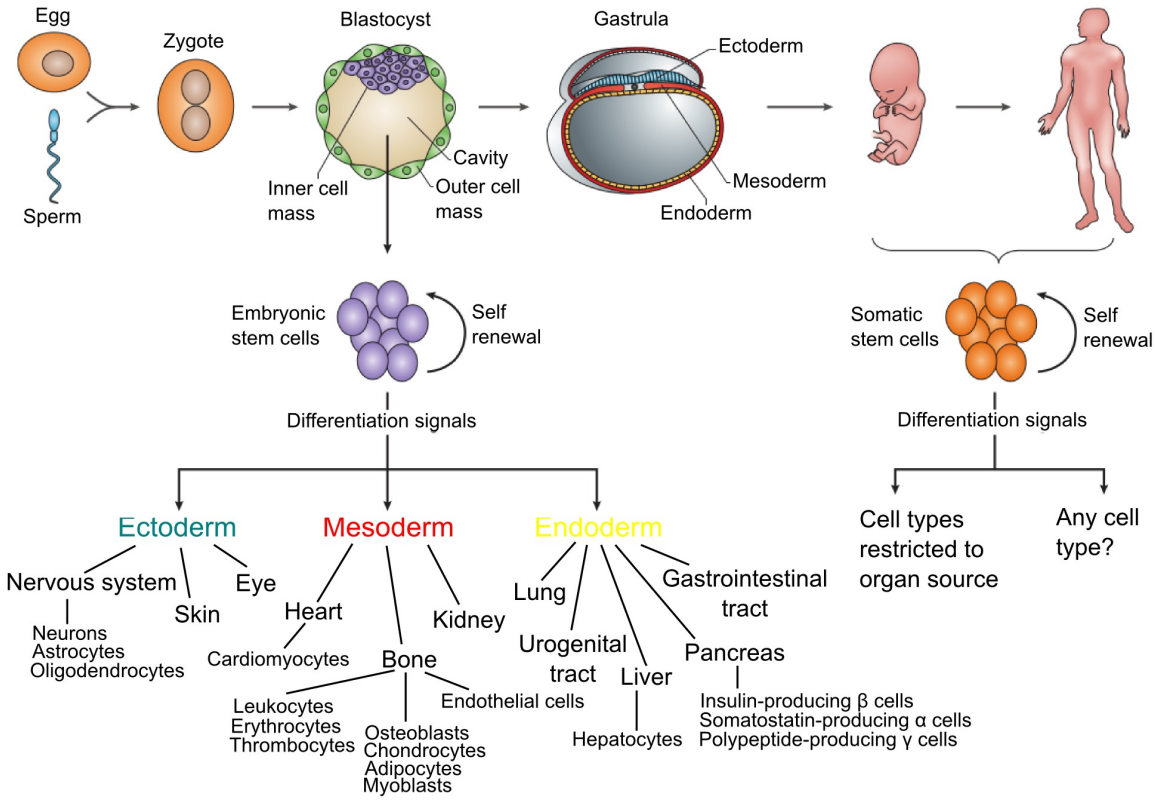

Figure 1.2.1. The source of different types of stem cells. Embryonic stem cells are derived from the inner cell mass of a blastocyst and possess the ability to differentiate into every cell type of all three germ layers under appropriate conditions. Different tissues from fetuses and adults contain somatic stem cells that can differentiate into various cell types from the organ from which they originate, but their extent to differentiate into cell types from other lineages is still being explored. Figure created from Mimeault, Batra 2006 and O'Connor, Crystal 2006.

propagated indefinitely while preserving a primitive embryonic state; they are capable to spontaneously differentiate into all derivatives of three primary germ layers, both in teratomas after grafting and *in vitro* under specific conditions; they can give rise to every cell type of a body when introduced into a host blastocyst (Pera et al. 2000). Although human ESCs have a great capacity for forming the basis of future therapies, their ability to form teratomas (benign tumors composed of different somatic cell types usually representing all three germ layers), when injected into immunodeficient mice (Thomson et al. 1998), is a major safety concern in their potential use (Goldring et al. 2011). Another obstacle hampering an extensive use of ESCs in clinical applications is ethical issues. Since they are obtained from human pre-implantation embryos which are destroyed during the process, it rises the debate regarding ontological and moral status of the pre-implantation embryos. This discussion is still ongoing and each country has its own political laws regulating the field of ESC research (de Wert, Mummery 2003). Nevertheless, the latest clinical study from United States of America (USA) shows the long-term safety of human ESC transplants to treat forms of macular degeneration. In this study the ESCs were firstly differentiated into retinal pigment epithelial cells and then transplanted into patients. No evidence of adverse proliferation, rejection, or serious ocular or systemic safety issues related to the transplanted tissue was found after a median follow-up of 22 months (Schwartz et al. 2015).

During the past decade another type of SCs that in many ways resembles ESCs and is called induced pluripotent stem cells (iPSCs) has revolutionized the field of SC research.

They were discovered in 2006 by showing that simultaneously enforced expression of four transcription factors: Oct4, Sox2, Klf4, and c-Myc can generate SCs with similar properties to those of ESCs from mouse fibroblasts (Takahashi, Yamanaka 2006). A year later this finding was replicated using human somatic cells and above-mentioned factors (Takashi et al. 2007), as well as combination of OCT4, SOX2, NANOG, and LIN28 (Yu et al. 2007). This work was awarded the Nobel Prize in Physiology or Medicine in 2012 shared by Sir John B. Gurdon and Shinya Yamanaka "for the discovery that mature cells can be reprogrammed to become pluripotent" (nobelprize.org). The published observations suggesting similarities between ESCs and iPSCs are just as many as those which show their differences (Narsinh et al. 2011, Puri, Nagy 2012). It seems that this controversy arises from variations among ESC and iPSC clones that are being analysed in every given study. This degree of variation emerges from different technical variables and, in the case of iPSCs, stochastic events during reprogramming (Yamanaka 2012). Although iPSCs promise availability of patient-specific pluripotent SC therapy, *in vitro* disease modeling, drug development, and disease-specific pharmacological treatment testing without the need of creation of human embryos (Puri, Nagy 2012), a great scientific effort is still needed to understand the mechanism of reprogramming to pluripotency in order to improve the efficiency of the current methodology (at the moment, maximum 10% of cells undergo complete reprogramming) and facilitate their medical applications (Plath, Lowry 2011). Recently the first clinical study on humans using iPSCs has been launched in Japan. The patient's skin cells were used to produce iPSCs that were afterwards differentiated into retinal pigment epithelium cells. Then a sheet of retinal pigment epithelium cells was transplanted into an eye of a woman to treat age-related macular degeneration (Cyranoski 2014).

Fetal stem cells (FSCs) can be isolated from fetal tissues obtained from cadaveric fetuses after elective abortion, spontaneous abortion, stillbirth, and ectopic pregnancy (Ishii, Eto 2014). They can be isolated from such fetal tissues as liver, bone marrow, pancreas, spleen, kidney, and blood (Abdulrazzak et al. 2010), as well as such extra-embryonic tissues as placenta, amniotic membrane, amniotic fluid, and Wharton's jelly (Marcus, Woodbury 2008). It is generally thought that a differentiation potential of FSCs is somewhere between ESCs and adult SCs (Abdulrazzak et al. 2010). Unlike ESCs, FSCs do not form teratomas *in vivo* and have low rejection reactions after transplanting, when obtained from fetuses up to 12 weeks old (Mimeault, Batra 2006). While only few ethical reservations exist over the use of extra-embryonic tissues as a source of FSCs, the exploitation of cadaveric fetal tissues is a subject of significant public and political debate (Ishii, Eto 2014). Yet, clinical trials using FSCs are actively conducted, mostly in USA and United Kingdom, and show promising results. However, full caution must be taken since a brain tumor of non-host origin was detected in a patient four years after the fetal neural SC therapy. The analysis showed that the tumor is derived from at least two donors emerging from the transplanted SCs (Amariglio et al. 2009). FSC transplantation has been used to treat neurological diseases (amyotrophic lateral sclerosis, cerebral palsy, cerebral atrophy, Huntington's disease, Parkinson's disease), central nervous system injuries, heart failure, diabetes, skin wounds, and *osteogenesis imperfecta* (Ishii, Eto 2014).

An umbilical cord (UC) could also serve as a very attractive source of SCs and its use is not limited by ethical issues, as the UC is discarded as biowaste after a childbirth. Not only Wharton's jelly within the UC, but also endothelial/subendothelial layer of umbilical vein, UC blood, and UC amniotic membrane (cord lining) contain SCs (Lim, Phan 2014). Cord lining can be used to obtain mesenchymal cells (Kita et al. 2010) and epithelial cells (Huang et al. 2011) that can differentiate into mesenchymal tissues, such as bone, cartilage, muscle, and epithelial tissues, such as skin and cornea, respectively. Both types of cord lining SCs can resist rejection after transplantation and have been proved effective in different clinical applications (Lim, Phan 2014). Since 1989 when the first successful UC blood transplantation

in a child with Fanconi anemia has been performed (Gluckman et al. 1989), the use of UC blood as a source of HSCs has remarkably increased leading to more than 20 000 cord blood transplants worldwide (Gluckman 2009). Currently there are at least 635 000 UC blood units stored in more than 100 UC blood banks (bmdw.org). The main advantage of UC blood over bone marrow or mobilized peripheral blood transplantation is a higher acceptable degree of human leukocyte antigen (HLA) mismatch between a donor and a recipient, as UC blood only require to be matched at four of six HLA class I and II molecules in order to keep a risk of developing severe GVHD at minimum. This benefit is likely caused by the low amount of T cells and immunologically naïve state of lymphocytes in UC blood (Rao et al. 2012). Additionally, UC blood SC superiorities include the ability to form more colonies in culture, higher cell cycle rate, autocrine production of growth factors, and longer telomeres (Gluckman et al. 1997). Furthermore, few studies have reported capacity of UC blood SCs under special culture conditions *in vitro* and *in vivo* to differentiate not only into cells of haematopoietic lineage, but also into dendritic cells, neural cell progenitors, hepatocytes, pancreatic cells, and endothelium (Mimeault, Batra 2006), but these controversial findings are not widely accepted (Gupta 2012). However, the biggest obstacle to the UC blood transplants is relatively small number of haematopoietic progenitor cells and haematopoietic SCs in UC blood leading to delayed engraftment, increased transplant related mortality, and reduced survival (Rocha, Gluckman 2006). This is the reason why UC blood transplants have been mostly performed in children, as recipients with weight higher than 50 kg need UC blood from more than one donor to ensure prompt engraftment (Rao et al. 2012).

Adult SCs are isolated from mature tissues where they exist in specialized niches within the greater part of adult tissues or organs and play an important role in tissue repair and regeneration (Mimeault, Batra 2006). They show lower differentiation ability when compared to ESCs or FSCs and are usually referred to by their tissue origin, e.g., adipose-derived SCs, dental pulp SCs (Bindu, Srilatha 2011). Although most somatic SCs are believed to be lineage-restricted, compiling evidence shows their capacity to give rise to another cell types of unrelated tissue (Catacchio et al. 2013). The examples of adult SCs of endodermal origin include lung epithelial SCs (Volckaert, De Langhe 2014), gastrointestinal tract SCs (Mills, Shivdasani 2011), pancreatic SCs (Zulewski et al. 2001), and liver SCs (Matthews, Yeoh 2005). Bone marrow SCs (Pittenger et al. 1999), cardiac SCs (Beltrami et al. 2003), adipose tissue SCs (Zuk et al. 2001), and muscle SCs (Shi, Garry 2006) are of mesodermal origin. And such somatic SCs as neural SCs (Watts et al. 2005), epidermal and hair follicle SCs (Blanpain, Fuchs 2006), corneal (Takács et al. 2009) and retinal SCs (Tropepe et al. 2000) are of ectodermal origin.

1.3. Mesenchymal stem cells

In 1976 Friedenstein and colleagues discovered that BM contains fibroblast-like cells that adhere to plastic culture plates and form discrete colonies initiated by a single cell (colony-forming unit fibroblast) (Friedenstein et al. 1976 after Chamberlain et al. 2007). Following work revealed that progeny of these cells can give rise to bone, cartilage, adipose tissue, and fibrous tissue after transplantation (Friedenstein et al. 1990 after Bianco et al. 2008), but a worldwide interest was risen only later when similar work was published describing isolation, expansion and tri-lineage differentiation potential of human BM mesenchymal stem cells (MSCs) (Pittenger et al. 1999). Since then, cells exhibiting characteristics of MSCs have been isolated not only from BM, but also from many other adult tissues, e.g., adipose tissue, muscle, bone, cartilage, tendon, skin, dental tissues, salivary gland, foreskin, synovial fluid, synovial membrane, endometrium, amniotic fluid, amniotic membrane, menstrual blood, peripheral blood, and from different fetal tissues, such as spleen, lung, pancreas, kidneys, as well as from UC blood, placenta, UC, Wharton's jelly (Taléns-

Visconti et al. 2006, Lin et al. 2007, Secco et al. 2008, Ullah et al. 2015).

Initially these cells were termed osteogenic SCs or bone marrow stromal SCs (Bianco et al. 2008), but a term "mesenchymal stem cells" was introduced in 1991 to name hypothetical multipotent and self-renewing precursor cells derived from embryonic MSCs which were involved in maintaining homeostasis of skeletal tissues and repairing them during adulthood (Caplan 1991). The cells described by Friedenstein were promptly referred to as a prototype of MSCs, even though there were no experimental data regarding these cells that could strictly meet all the characteristics conveyed in the original term of MSCs. The analysis of biological properties of these multipotent progenitors has been done on *in vitro* expanded populations that may not reveal actual *in vivo* situation, and the existence of a common post-natal mesenchymal progenitor has been an issue of debate, since bone and muscle have different progenitors during embryogenesis and the ability of these progenitor cells to differentiate into muscle cells *in vivo* has not yet been convincingly demonstrated (Nombela-Arrieta et al. 2011). Nonetheless, the term "mesenchymal stem cells" has gained huge global usage to describe stromal precursors with the ability to differentiate into cell types of mesodermal origin (Bianco et al. 2008). Although the International Society for Cellular Therapy (ISCT) has recommended the use of the name "multipotent mesenchymal stromal cells" to refer to *in vitro* cultured fibroblast-like plastic-adherent cells, regardless of the tissue source from which they have been isolated, and the term "mesenchymal stem cells" should be used to designate cells that meet specified stem cell criteria (long-term self-renewing cells that can differentiate into multiple cell types *in vivo*) (Horwitz et al. 2005), investigators all over the world continue to use historical term "mesenchymal stem cells" or alternatively - "mesenchymal stem/stromal cells" (Phinney, Prockop 2007, Keating 2012).

To define MSCs, the ISCT has proposed following minimal criteria: firstly, these cells must be plastic-adherent when maintained in standard culture conditions, secondly, they must express such surface markers as CD105, CD73, and CD90, but must lack the expression of CD45, CD34, CD14 or CD11b, CD19 or CD79α, and HLA-DR markers, thirdly, they must be able to differentiate into adipocytes, osteoblasts, and chondroblasts *in vitro* (Dominici et al. 2006). The main issue regarding identification of MSCs according to their surface markers is a lack of one unique MSC marker that would allow to distinguish these cells. Therefore, a panel of positive and negative markers must be verified to identify MSCs. Additional positive markers: CD13, CD29, CD44, CD71, CD106, CD166, CD271, CD146, ICAM-1, Stro-1, and negative markers: CD31, CD117, CD80, CD86, CD40, CD18, CD56 have been reported for MSCs (Chamberlain et al. 2007, Kolf et al. 2007, Lv et al. 2014), but, unfortunately, MSCs obtained from various tissues show dissimilar expression pattern of above-mentioned markers (Chamberlain et al. 2007). Moreover, isolation procedure, culture conditions, cell confluence, certain growth factors, as well as disease conditions of a donor may influence phenotype of MSCs (Lv et al. 2014). Although MSCs are defined by their *in vitro* differentiation into adipocytes, osteoblasts, and chondroblasts, the experimental evidence shows their ability to differentiate into other cell types as well, e.g., myocytes (Gang et al. 2004), cardiomyocytes (Xu et al. 2004), neurons (Woodbury et al. 2000), endothelial cells (Cao et al. 2005), hepatocytes (Lee et al. 2004), and pancreatic cells (Gao et al. 2008).

Historically BM has been regarded as the main source of MSCs for experimental and clinical use. And, undoubtedly, most of the knowledge we have about MSCs has come from extensive studies of BM (Secco et al. 2008). However, the number, differentiation potential, and maximal life span of BM MSCs decrease significantly with age (D'Ippolito et al. 1999, Nishida et al. 1999, Mueller, Glowacki 2001). Moreover, the harvest of BM itself is highly invasive procedure that can cause infection, bleeding, and chronic pain (Secco et al. 2008) and frequently requires general or spinal anaesthesia (Zuk et al. 2001). It has been estimated that only 0,001 to 0,01% of all nucleated cells of BM are MSCs (Pittenger et al. 1999), but it has not hampered their broad applications.

The potential clinical use of MSCs includes treating bone disorders (*osteogenesis imperfecta*, bone healing, bone defect repairing), liver diseases, neurological diseases (traumatic brain injuries, spinal cord injuries, Parkinson's disease, multiple sclerosis), heart damages, as well as healing chronic wounds. Currently, the only type of SCs being routinely used in clinics is HSCs (Catacchio et al. 2013). They are able to give rise to all types of functional blood cells (Mimeault, Batra 2006) and are mostly employed for the treatment of haematological malignancies (Catacchio et al. 2013). At the moment there are 526 registered clinical trials throughout the world in different clinical phases evaluating the potential of MSC based therapy (Figure 1.3.1.). The biggest part of these trials are Phase I/II studies and only few of them are in Phase III/IV (clinicaltrials.gov). A considerable part of these trials is devoted to treat cardiovascular disorders followed by autoimmune disease, osteoarthritis, liver disorders and GVHD (Figure 1.3.2.) (Ullah et al. 2015).

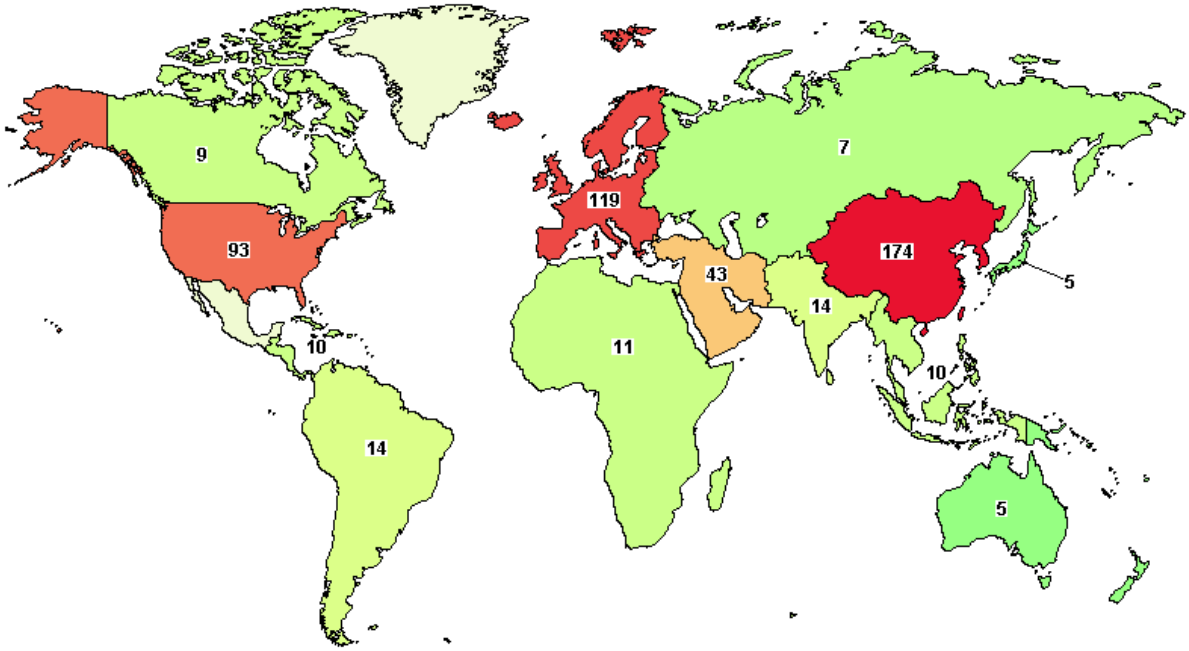

Figure 1.3.1. Registered clinical trials of mesenchymal stem cell-based therapy worldwide. Actual as of October 2015. Figure from clinicaltrials.gov.

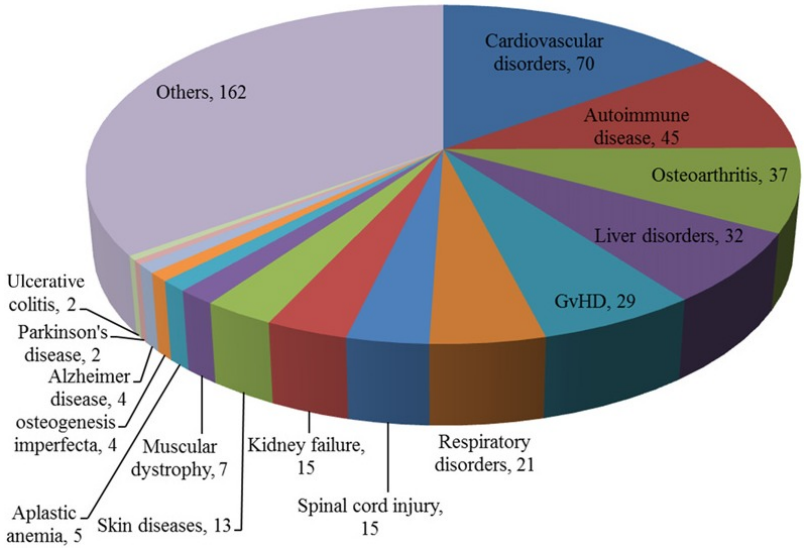

Figure 1.3.2. Number of various diseases registered for clinical trials of mesenchymal stem cell-based therapy. Figure from Ullah et al. 2015.

In the setting of allogeneic transplantation and prevention or treatment of GVHD MSCs may have a significant therapeutic potential since they do not induce considerable alloreactivity. It is known that MSCs express low levels of major histocompatibility complex (MHC) class I antigens and do not express MHC class II and co-stimulatory molecules, e.g., CD40, CD80, CD86. Therefore, MSCs are protected from alloreactive natural killer cell-mediated lysis (Sensebé et al. 2010). Furthermore, MSC populations display immunomodulatory capacities and their inhibitory effect on T cell proliferation has been studied extensively (Bartholomew et al. 2002, Di Nicola et al. 2002, Le Blanc et al. 2003, Tse et al. 2003). Although little is known about the molecular mechanisms underlying this phenomena, there is evidence of various factors such as transforming growth factor-β and hepatocyte growth factor (Di Nicola et al. 2002), prostaglandin E2 (Aggarwal, Pittenger 2005, Cui et al. 2007), indoleamine 2,3-deoxygenase (Meisel et al. 2004), heme oxygenase-1 (Chabannes et al. 2007), nitric oxide (Sato et al. 2007), interleukins - 6 and 10, human leukocyte antigen-G5 and matrix metalloproteinases (for reviews, see Abumaree et al. 2012, De Miguel et al. 2012) produced by MSCs that could mediate the suppression of T cell proliferation. In addition, MSCs express HLA-G antigen (non-classical MHC class I antigen with strong immune-inhibitory properties) that could contribute to inhibition of immune response (Nasef et al. 2007). It has been shown that MSCs can also inhibit the proliferation of T cells by blocking cyclin D2 expression and up-regulating p27Kip1 expression, thus arresting cells in the G1 phase of the cell cycle (Glennie et al. 2005). Other approaches that may be responsible for the ability of MSCs to modulate immune response is induction of CD8+ regulatory T cells (Djouad et al. 2003) or regulatory antigen-presenting cells (Beyth et al. 2005), as well as interference with dendritic cells (Aggarwal, Pittenger 2005) and inhibition of the formation of cytotoxic T cells (Rasmusson et al. 2003). In addition, human MSCs can also inhibit proliferation, differentiation, and chemotaxis of B cells (Corcione 2006).

1.4. Adipose-derived stem cells

Adipose tissue, like BM, is derived from mesoderm and serves as an excellent source of MSCs named adipose-derived stem/stromal cells. Other terms attributed to these cells can also be found in a scientific literature: adipose-derived adult stem (ADAS) cells, adipose-derived adult stromal cells (ADSCs), adipose stromal cells (ASCs), adipose mesenchymal stem cells (AdMSCs), processed lipoaspirate (PLA) cells. In order to minimize a confusion between all the existing names, the International Fat Applied Technology Society has suggested to use the term “adipose-derived stem cells” (ASCs) to identify the plastic-adherent, multipotent cell population isolated from adipose tissue (Gimble et al. 2007).

There are mainly two major types of adipose tissue – brown and white – that differ both morphologically and functionally (Tsuji et al. 2014). The brown adipose tissue (BAT) in humans is present and active in infants where it generates heat to sustain optimal body temperature without shivering (Nedergaard et al. 2007). This thermogenesis is sustained by uncoupling protein 1 (so named because it uncouples respiration from ATP synthesis leading to heat production, according to Enerbäck 2009), expressed in the inner membrane of mitochondria, and regulated by adrenergic signalling through sympathetic nervous system (Tsuji et al. 2014). Brown adipocytes have many small lipid vacuoles and large amount of mitochondria (Enerbäck 2009). This abundance of mitochondria together with a very high vascularization give the BAT its brown colour (Tsuji et al. 2014). It was generally accepted that BAT disappears within the first years of life and is absent in adults. However, since the year 2002 (although some evidence has been detected much earlier, but has been mostly ignored) this dogma has been challenged. BAT has been found in adults (Figure 1.4.1.) and is shown to be active. Still, not all adults have BAT, and estimated prevalence is in the range of

some dozens of percent (Nedergaard et al. 2007). Even though somatic SCs have been isolated from BAT (Silva et al. 2014), the low amount of BAT within a body does not make it a suitable source of ASCs.

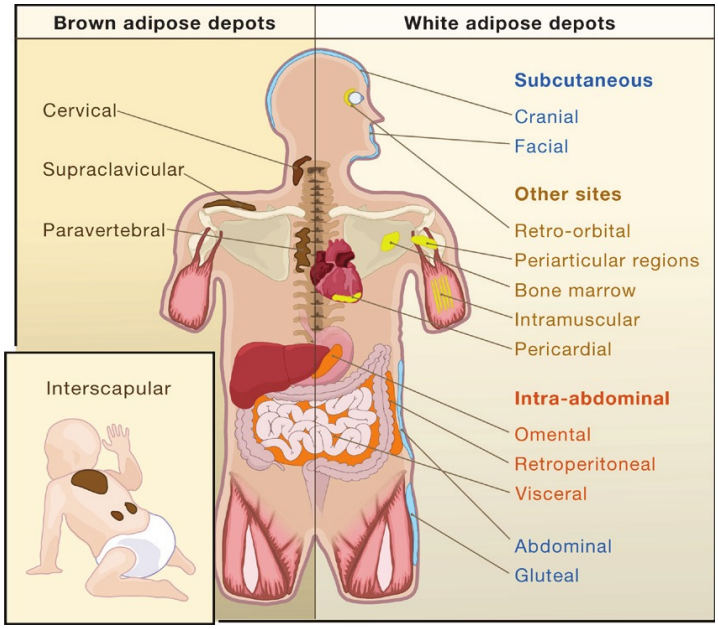

Figure 1.4.1. Figure and caption from Gesta et al. 2007: "Depots of white adipose tissue in humans are found in areas all over the body, with subcutaneous and intra-abdominal depots representing the main compartments for fat storage. Brown adipose tissue is abundant at birth and still present in adulthood but to a lesser extent."

The white adipose tissue (WAT), on the other hand, is found throughout a body (Figure 1.4.1.) (Gesta et al. 2007). It serves to store excess energy in the form of triglycerides and provides insulation. The colour of WAT is yellow or ivory (Tsuji et al. 2014). In contrast to brown adipocytes, the white adipocytes have few mitochondria and a single lipid droplet (Enerbäck 2009). ASCs are routinely isolated from stromal vascular fraction (SVF) of subcutaneous and intra-abdominal WAT and growing numbers of obese people around the world make WAT abundant and readily accessible source of ASCs. It is estimated that approximately 400 000 liposuction surgeries are performed every year in the USA alone and each of these procedures produce from 100 ml up to 3 l of lipoaspirate tissue that is regarded as medical waste (Gimble et al. 2007). Furthermore, 1 ml of adipose tissue holds 500-fold greater amount of stem cells than the same amount of BM (Fraser et al. 2006), but in contrast to BM MSCs, ASCs are easier to obtain and display lower donor site morbidity (Kakudo et al. 2007). One argument against the use of WAT could be its low amount in some patients, but even very small depots of fat might be sufficient for the isolation of ASCs due to their high frequency (Kern et al. 2006). Recent evidence shows that 1 g of WAT contains approximately 1-2x10^6 SVF cells from which 10% are ASCs (Pham 2014). It is known that SVF of adipose tissue contains a heterogeneous stromal cell population that includes not only ASCs, but also cells of haematopoietic lineage, e.g., granulocytes, monocytes, lymphocytes, erythrocytes, mast cells, as well as endothelial cells, fibroblasts, pericytes, and pre-adipocytes (Zuk et al. 2001, Bourin et al. 2013). Nevertheless, subsequent passaging of the initial SVF selects for a relatively homogeneous ASC population (Zuk et al. 2001).

Like MSCs from BM and other sources, ASCs are spindle-shaped cells with fibroblastoid morphology and normal karyotype that can be easily propagated *in vitro* (Zuk et al. 2001). It has been shown that ASCs bear high proliferative capacity and can undergo multilineage *in vitro* differentiation into adipocytes, osteoblasts, chondroblasts (Zuk et al.

2001, Kern et al. 2006), smooth muscle cells (Jeon et al. 2006), skeletal muscle cells (Zuk et al. 2002, Lee, Kemp 2006), cardiomyocytes (Planat-Bénard et al. 2004), neurons (Jang et al. 2010), endothelial cells (Cao et al. 2005), hepatocytes (Taléns-Visconti et al. 2006), and pancreatic cells (Chandra et al. 2011). Furthermore, their multi-lineage potential is not altered by freezing/thawing procedure (Rodriguez et al. 2005). ASCs are positive or negative for most of the cell surface markers defined for all types of MSCs, but recently the ISCT together with the International Federation for Adipose Therapeutics and Science have established minimal panel of surface markers to define ASCs. According to their statement, ASCs must be positive for such markers as CD13, CD29, CD44, CD73, CD90, CD105, (CD34 can also be present at variable levels and generally at early phase of culture), and negative for such markers as CD31, CD45, and CD235a. Additional positive: CD10, CD26, CD36, CD49d, CD49e, and negative: CD3, CD11b, CD49f, CD106, PODXL markers can be used for the characterization of ASCs (Bourin et al. 2013). This list can be extended with CD9, CD54, CD55, CD59, CD146, CD166 as positive and CD14, CD19, CD79α, CD80, CD117, CD133, CD144, c-kit as negative markers (Schäffler and Büchler 2007). In contrast to BM MSCs, ASCs express CD49d and CD36, but lack the expression of CD49f, CD104, and CD106 (Bourin et al. 2013, Ong, Sugii 2013). However, the expression of above-mentioned markers is not always consistent across scientific reports. This may be due to donor heterogeneity, methods and quality of ASC isolation, antibody sources, sensitivity of detection methods, and cell culture conditions (media composition, oxygen supply, cell confluency, passage number) (Ong, Sugii 2013). Additionally, there are differences in marker expression between cells of whole SVF and cultured ASCs that need to be taken into consideration (Cawthorn et al. 2012).

ASCs, similarly to BM MSCs, are immunoprivileged and suppress the proliferation of lymphocytes in a dose dependent manner (Yañez et al. 2006, Cui et al. 2007) making them effective donor cells in allogeneic setting, as well as reducing GVHD (Fraser et al. 2006). Likewise BM MSCs, ASCs also secrete various soluble factors, such as angiogenic factors (hepatocyte growth factor, vascular endothelial growth factor), haematopoietic factors (colony stimulating factors, interleukins-7, -12), proinflammatory factors (interleukins-1α, -6, -8, -11, tumor necrosis factor α), and anti-apoptotic factors (insulin-like growth factor 1) that promote tissue regeneration at the site of injury (Kilroy et al. 2007, Salgado et al. 2010). Additionally, ASCs can be effectively reprogrammed into iPSCs without a requirement for feeder cells (Sugii et al. 2010). All these characteristics make ASCs suitable for a broad spectrum of applications (Figure 1.4.2.) and there are currently 72 registered clinical trials around the

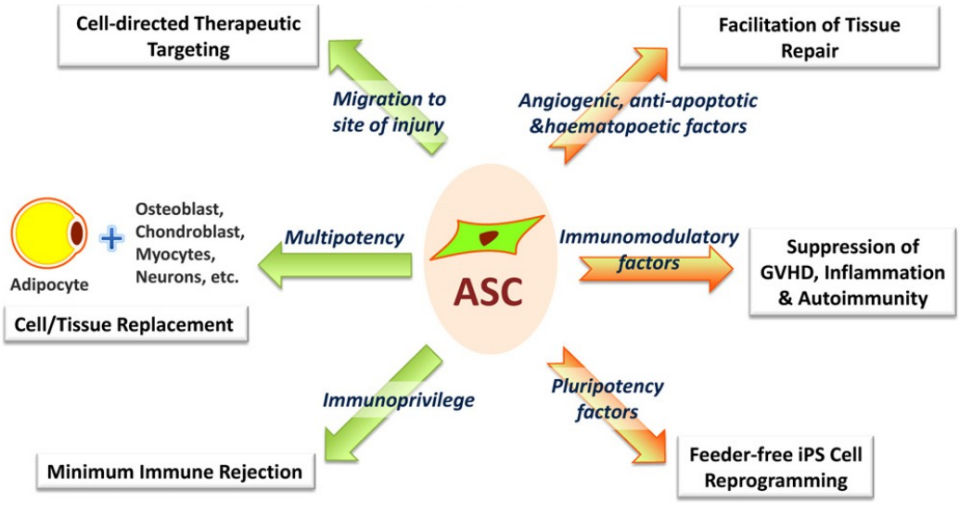

Figure 1.4.2. Figure and caption from Ong and Sugii 2013: "Biological properties and therapeutic potentials of ASCs. The right side summarizes secretome of the ASCs, and the left side summarizes multi-lineage differentiation capacity and immunobiology of the ASCs."

world exploring their potential (clinicaltrials.gov). Their efficacy in treating such conditions as type I and type II diabetes, liver cirrhosis, fistulas, GVHD, cardiovascular diseases, rheumatoid arthritis, Crohn's disease, ulcerous colitis, limb ischemia, multiple sclerosis, amyotrophic lateral sclerosis, bone repair, soft tissue augmentation, and lipodystrophy is being examined (Lindroos et al. 2011).

1.5. What is the difference between MSCs, fibroblasts, and pericytes?

In the past few years there has been a lot of discussion about a true identity of MSCs and their relation to fibroblasts and pericytes. Fibroblasts are widely considered to be terminally differentiated mesenchymal cells (Cappellesso-Fleury et al. 2010) that produce and remodel extracellular matrix and play a critical role in tissue development, differentiation, maintenance, and repair (Flavell et al. 2008). Since they are the most abundant cells of stroma (Flavell et al. 2008), they are considered to be the most frequent contaminating cell phenotype present in many cell cultures and, naturally, MSCs, that are localized in the stroma of tissue or organs, are no exception (Blasi et al. 2011). However, it is believed that successive passaging of the obtained cells serves as a purification of MSC culture (Horwitz et al. 2006).

Nevertheless, some researchers question the general assumption that MSCs are unique type of cells distinct from fibroblasts (Haniffa et al. 2009, Hematti 2012). Similarly to MSCs, fibroblasts exhibit spindle-shaped morphology, display comparable proliferation capability *in vitro* (Alt et al. 2011), and adhere to plastic (Flavell et al. 2008). Both MSCs and fibroblasts are positive for CD13, CD29, CD44, CD49e, CD71, CD73, CD90, CD105, CD166, STRO-1, and HLA class I markers and negative for CD14, CD31, CD34, CD45, CD80, CD86, CD133, glycophorin A, cadherin 5, and HLA class II markers (Jones et al. 2007, Covas et al. 2008, Lorenz et al. 2008, Alt et al. 2011, Blasi et al. 2011).

It is broadly accepted that a multipotent differentiation potential of the cells is one of the main criteria to define the identity of MSCs (Dominici et al. 2006). Therefore, it is no wonder that a true identity of MSCs is challenged when ability of fibroblasts to convert into other types of cells has been also shown. The dermal fibroblasts have been able to differentiate into adipocytes, osteocytes, chondrocytes (Lorenz et al. 2008, Alt et al. 2011, Blasi et al. 2011, Jääger et al. 2012), cardiomyocyte-like cells (Blasi et al. 2011), and even hepatocyte-like cells (Lysy et al. 2007). Human foreskin dermal fibroblasts gave rise to adipocytes, osteocytes and chondrocytes (Chen et al. 2007) and fibroblasts isolated from synovial membrane and human uterine tissues also could differentiate into adipocytes and osteocytes (Jones et al. 2007, Strakova et al. 2008). It has been discovered that ASCs and fibroblasts employ similar early mechanisms of differentiation into adipocytes and osteocytes, but exhibit distinct mechanisms of chondrogenic differentiation (Jääger et al. 2012). Contrary results have also been published, showing that human foreskin-derived dermal fibroblasts (Wagner et al. 2005) and dermal fibroblasts do not have differentiation potential (Brendel et al. 2005, Jones et al. 2007, Cappellesso-Fleury et al. 2010). However, it has been lately supposed that such reported evidence indicates that fibroblast preparations contain a heterogeneous cell population, including MSCs with various levels of differentiation potential and fibroblasts with no ability to convert into other cell types (Alt et al. 2011).

The observation that MSC populations display immunosuppressive effect on lymphocyte proliferation has been studied extensively (Bartholomew et al. 2002, Di Nicola et al. 2002, Le Blanc et al. 2003). This ability was attributed exclusively to MSCs, but it has been reported that fibroblasts could also inhibit the proliferation of lymphocytes (Haniffa et al. 2007, Jones et al. 2007, Cappellesso-Fleury et al. 2010). They act in a dose-dependent manner via soluble factors after initial cell contact has been made (Jones et al. 2007).

The above-mentioned similarities make it particularly complex to distinguish MSCs from fibroblasts in the same culture and to apply appropriate techniques for successful

elimination of fibroblasts (Blasi et al. 2011). The colony-forming capacity has been observed both in MSCs and dermal fibroblasts, but human embryonic lung fibroblasts do not form colonies (Alt et al. 2011). Recently CD106, CD146 and integrin alpha 11 were claimed as markers distinguishing BM MSCs from fibroblasts (Halfon et al. 2011). Different expression levels of CD10 and CD26 (Cappellesso-Fleury et al. 2010) could help discriminate between BM MSCs and fibroblasts. It may also be possible to evaluate their angiogenic and anti-inflammatory potential, since ASCs seems to be significantly more angiogenic and anti-inflammatory than dermal fibroblasts (Blasi et al. 2011).

These differences, although modest, show that MSCs and fibroblasts are not the same. It is still not absolutely clear, whether fibroblasts are more mature than MSCs (Blasi et al. 2011), but they are both part of a complex family of stromal cells with specialized niche functions (Haniffa et al. 2009). Some evidence indicates that MSCs are different from fibroblasts and more similar to pericytes (Blasi et al. 2011), as both MSCs and pericytes, but not fibroblasts, show high expression of CD146, while a fibroblast marker FSP-1 is only poorly expressed in MSCs and pericytes (Covas et al. 2008).

Pericytes are extensively branched cells of mesodermal origin that are located in the wall of non-muscular microvessels, capillaries, and postcapillary venules (Díaz-Flores et al. 1991) where they closely encircle endothelial cells that form the microvasculature (Crisan et al. 2008). Recently great popularity has been gained by a hypothesis that MSCs are situated throughout the body as pericytes and that the perivascular zone comprises the *in vivo* niche of MSCs (Crisan et al. 2008, da Silva Meirelles et al. 2008). This theory is supported by the fact that blood vessels are the only shared anatomical structure in the majority of solid tissues from which MSCs have been isolated (Lv et al. 2014). Pericytes share morphological appearance with MSCs (Crisan et al. 2008, Covas et al. 2008). Their immunophenotype profile is similar to MSCs since they are positive for the CD73, CD90, CD29, CD13, CD44, CD49e, CD54, STRO-1, CD146, CD166, HLA class I markers and negative for CD34, CD14, CD45, CD31, CD33, glycophorin A, cadherin 5, KDR, HLA class II markers (Covas et al. 2008). Furthermore, pericytes are able to differentiate into adipocytes, osteocytes, chondrocytes (Covas et al. 2008, Crisan et al. 2008), and myocytes (Crisan et al. 2008).

The perivascular origin of MSCs is further supported by an observation that perivascular cells natively, before culture, express surface antigens CD44, CD73, CD90, and CD105 that are used as markers for MSCs (Crisan et al. 2008). If MSCs would be the pericytes *in vivo*, they could be easily released from their niche and secrete immunoregulatory and bioactive factors upon tissue damage, effectively contributing to a physiological turnover throughout a body (Lv et al. 2014). More and more researchers tend to think that not all pericytes are MSCs, but all MSCs are pericytes, although some exceptions may exist (Caplan 2008).

However, this “perivascular niche” theory can not explain the fact that MSCs could be also found in avascular tissues, such as articular cartilage and *nucleus pulposus* (Lv et al. 2014). It is possible that pericytes are not the only cell lineage in our body that acts as a source of MSCs (Crisan et al. 2008, Feng et al. 2011). Evidence suggests that a contribution of pericyte-derived and non-pericyte-derived MSCs to cell differentiation in every tissue depends on the amount of blood vessels in that tissue and the kinetics of growth and repair (Feng et al. 2011).

1.6. Markers of pluripotency

1.6.1. OCT4

The human *OCT4* gene (official symbol *POU5F1*, also known as *OCT3*, *OCT4*, *OTF3*, *OTF4*) is located on chromosome 6p21.31 (Krishnan et al. 1995). It is a transcription factor known to be crucial to the establishment of pluripotency (Nichols et al. 1998). The human

OCT4 is expressed in totipotent and pluripotent stem cells starting from the unfertilized oocytes to the blastocyst (Wang X. et al. 2009). It is also highly expressed in human ESCs (Cauffman et al. 2006), embryonic germ cells (Goto et al. 1999), as well as in embryonic carcinoma cells (Jones et al. 2004). Its expression in stem cells is downregulated during differentiation (Hay et al. 2004).

The alternative splicing of *OCT4* gene results in three transcripts termed *OCT4A*, *OCT4B* (Takeda et al. 1992), and *OCT4B1* (Atlasi et al. 2008) (Figure 1.6.1.1.). All three transcript variants differ in their 5' termini, but are identical in 3' termini. *OCT4A* contains exons 1, 2b, 2d, 3, and 4, among which exon 1 is the unique part that distinguishes it from other two transcripts. *OCT4B* transcript is very similar to *OCT4A*, but it lacks the exon 1 which is replaced by exon 2a. *OCT4B1* transcript is highly identical to *OCT4B*, but it contains an additional exon 2c (Wang, Dai 2010).

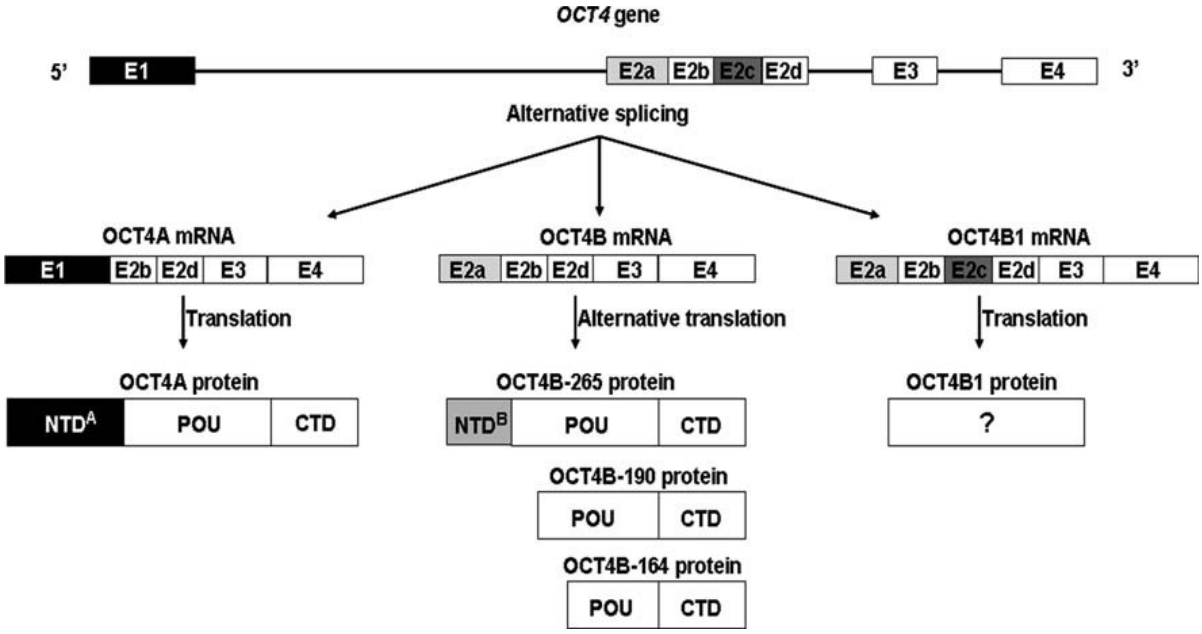

Figure 1.6.1.1. Figure and caption from Wang and Dai 2010: "The schematic structure of human *OCT4* gene. *OCT4* gene can generate three transcripts and four protein isoforms. The different regions of *OCT4* isoforms are indicated by different coloured boxes. The identical regions of *OCT4* isoforms are indicated by white boxes. CTD - C-transactivation domain; NTD - N-transactivation domain; POU – a DNA binding domain."

The *OCT4A* transcript (NCBI reference sequence NM_002701.5) produces a protein composed of 360 aa (Figure 1.6.1.2.) (Wang, Dai 2010). The OCT4A is a transcription factor belonging to POU family proteins that regulate the transcription of genes containing the conserved octamer motif (ATTTGCAT) in their promoter or enhancer regions. They bind to the octamer motif with their POU domain (Cauffman et al. 2006). The POU domain is build of two subdomains: a 75 aa amino-terminal POU specific (POU^S) region and a 60 aa carboxyl-terminal homeodomain (POU^H), which are connected by a variable linker of 15 to 56 aa (Pan et al. 2002). The POU domain is flanked by N-transactivation domain (133 aa) and C-transactivation domain (71 aa) (Wang, Dai 2010). The N-transactivation domain regulates a binding of OCT4A to target promoters and it distinguishes OCT4A from other OCT4 protein isoforms (Jez et al. 2014). The C-transactivation domain is subject to cell-type-specific regulation mediated by the POU domain (Brehm et al. 1997). The OCT4A protein localizes in the nucleus of ESCs, compacted embryo, and blastocyst (Cauffman et al. 2006). It is believed that only this isoform of OCT4 proteins contributes to maintenance of pluripotency and self-renewal (Cauffman et al. 2006, Lee et al. 2006).

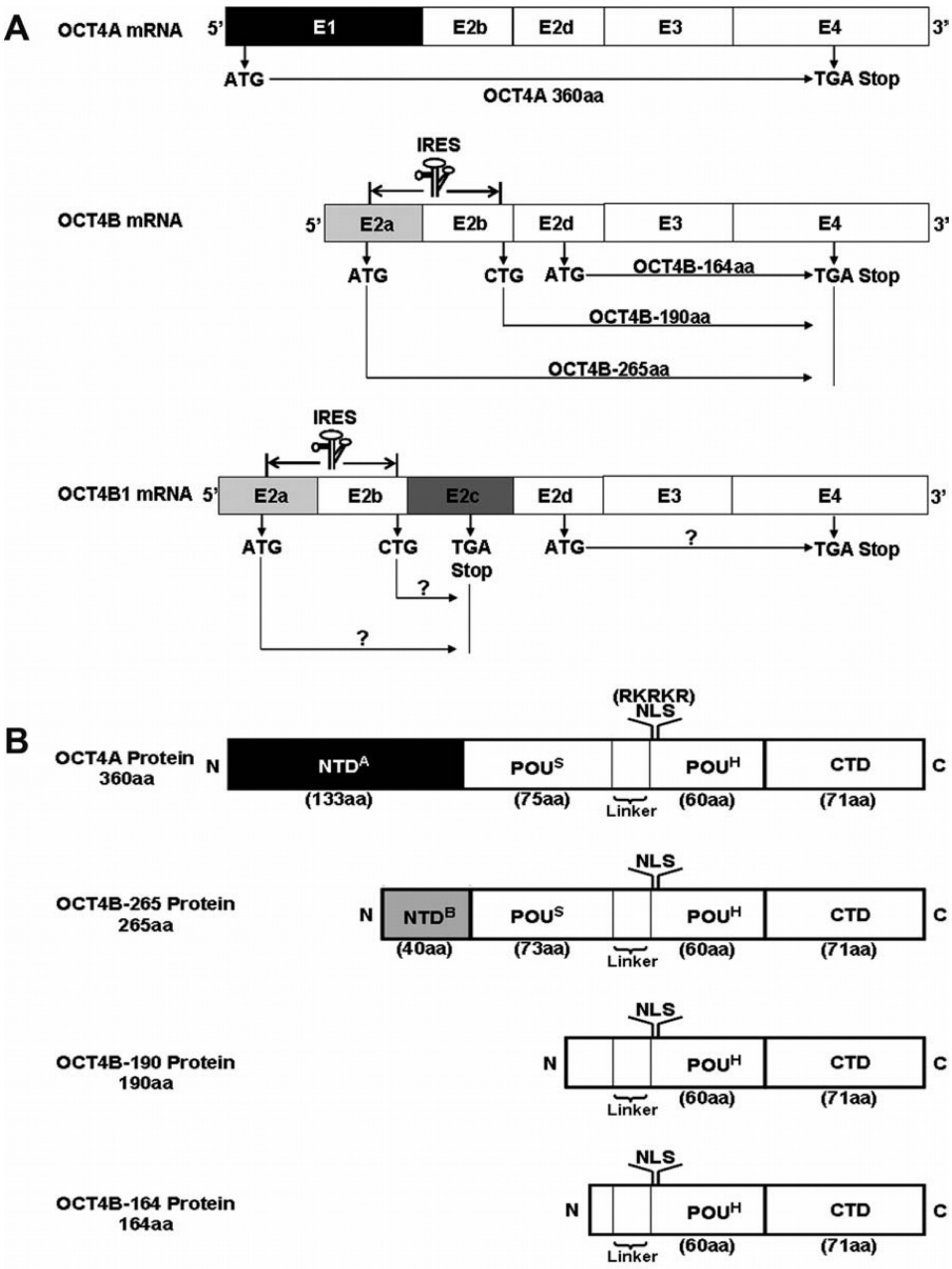

Figure 1.6.1.2. Figure and caption from Wang and Dai 2010: "(A) Schematic structure of OCT4 transcript isoforms. The translation start and stop sites and the putative internal ribosome entry site element on mRNA are indicated. (B) Schematic structure of OCT4 protein isoforms with their respective domains. CTD - C-transactivation domain; NTD - N-transactivation domain; IRES - internal ribosome entry site; POU^S - POU-specific region; POU^H - POU homeodomain; NLS – nuclear localization signal; aa – amino acids."

The *OCT4B* transcript (NCBI reference sequence NM_203289.5) encodes three protein isoforms termed OCT4B-265 (commonly referred to as simply OCT4B), OCT4B-190, and OCT4B-164 (Figure 1.6.1.2.) (Wang X. et al. 2009). The N-transactivation domain of the OCT4B-265 protein is 40 aa long and differs it from OCT4A isoform (Wang, Dai 2010). The rest 225 aa, comprising the POU domain and the C-transactivation domain, are identical in both OCT4B and OCT4A (Takeda et al. 1992). The OCT4B is mainly found in a cytoplasm of all cells throughout human preimplantation development from the four-cell stage onwards (Cauffman et al. 2006). Although the putative nuclear localization signal, identified in murine Oct4 as "RKRKR" (Pan et al. 2004), is present in all protein isoforms of OCT4 (Wang, Dai

2010), the cytoplasmic localization of OCT4B implies other biological function than that of OCT4A (Cauffman et al. 2006). It has been shown that OCT4B is upregulated under genotoxic stress in human ESCs and embryonic carcinoma (EC) cell lines and its overexpression can promote cell apoptosis in genotoxic stress response (Gao et al. 2012). The OCT4B-190 and OCT4B-164 proteins are diffusely localized both in cytoplasm and nucleus. The OCT4B-190 is upregulated under heat shock and oxidative stress in human ESC and tumor cell lines, and overexpression of OCT4B-190 increases the resistance to apoptosis induced by heat shock (Wang X. et al. 2009). The functional role of the OCT4B-164 protein has not yet been discovered (Gao et al. 2012).

The *OCT4B1* (GenBank accession number EU518650.1) mRNA has retained the intron 2 as an additional exon 2c, which contains an in-frame stop codon TGA (Figure 1.6.1.2.) (Atlasi et al. 2008). Therefore, it can not encode the full length protein isoforms of OCT4B-265 and OCT4B-190 and it is still not clear whether *OCT4B1* can generate the truncated proteins of those two isoforms. Until now the protein product of *OCT4B1* has not been identified (Wang, Dai 2010). An OCT4B1 construct has been created and expressed in human bladder cancer cell and unrestricted somatic stem cell lines with a help of lentiviral vectors. The results have shown that truncated OCT4B1 protein is produced and it localizes in a cytoplasm. The level of the transcript and protein rises under heat-stress stimulation, suggesting its potential role in mediating stress response (Yazd et al. 2011). It has been shown that *OCT4B1* could be spliced into *OCT4B* and encode its all three protein isoforms (Gao et al. 2010). The *OCT4B1* mRNA is highly expressed in human ESCs and EC cells and, like *OCT4A*, is downregulated upon differentiation (Atlasi et al. 2008). It could potentially serve as a marker of stemness (Papamichos et al. 2009). The expression of *OCT4B1* has been also reported in gastric cancer, where it could contribute to tumorigenesis process as an anti-apoptotic factor (Asadi et al. 2011).

In the last decade numerous studies have detected OCT4 in adult stem cells (Tai et al. 2005, Izadpanah et al. 2006, Greco et al. 2007, Kucia et al. 2007, Roche et al. 2007, Trivanović et al. 2015), and this has led to speculations that somatic stem cells may possess greater similarities to ESCs in terms of regulatory networks and potency than previously thought (Greco et al. 2007). The expression of OCT4 has been shown even in the human peripheral blood mononuclear cells that are terminally differentiated cells (Zangrossi et al. 2007). However, this observation was soon revisited by underlining that discrimination between OCT4A and OCT4B isoforms was not considered, and the authors have detected OCT4B which is not a marker of pluripotency (Kotoula et al. 2008). Designing the primers for RT-PCR or using antibodies within the region that is identical in both OCT4A and OCT4B isoforms have proved to be a banana skin for most of the studies that have claimed the expression of pluripotency marker OCT4 in adult stem cells (Liedtke et al. 2008). The reliable expression of OCT4A isoform in MSCs and somatic tumor cell lines has not been detected using specific primer pairs and antibodies for OCT4A. A positive signal has been only detected when primers for all three isoforms of OCT4 have been used, providing an evidence for the expression of OCT4B or OCT4B1 in these cells (Mueller et al. 2009). Additional scientific research using murine cells has shown that OCT4 is not essential for maintaining potency and self-renewal in the adult mammalian stem cells (Lengner et al. 2007). It is thought that albeit pluripotency markers can be observed at a basal level in adult stem cells, they may not have the same biological functions as in ESCs (Lengner et al. 2008).

Another possible pitfall that may be a cause of misinterpretation of the *OCT4A* expression in somatic stem cells is the existence of *OCT4* pseudogenes. The detection of *OCT4B* and *OCT4B1* isoforms at mRNA level is relatively easy, as no pseudogenes for these isoforms have been currently identified in the human genome (Wang, Dai 2010). But there are 6 known pseudogenes of *OCT4* (Pain et al. 2005), among which *OCT4P1*, *OCT4P3*, and *OCT4P4* share a high sequence homology, including the unique N-terminal coding sequence,

to *OCT4A* (Jez et al. 2014). Additionally there are at least 11 *OCT4* transcripts and *OCT4*-like sequences originating from chromosome 6 (Liedtke et al. 2007).

The *OCT4P1* was initially regarded as processed pseudogene with a complete ORF that can, theoretically, encode a protein that would be 1 aa shorter and have 14 mismatches when compared to OCT4A. It has been shown that the putative OCT4P1 protein, likewise OCT4A, localizes in a nucleus and even functions as a weak transcriptional activator (Panagopoulos et al. 2008). Since it may be a protein coding gene, it has been designated *POU5F1B* (NCBI reference sequence NM_001159542.1). BM MSCs and umbilical vein-derived stromal cells have been shown to express *POU5F1B*, *OCT4P3*, *OCT4P4*, and extremely low level of *OCT4A*, but neither of corresponding proteins have been detected (Kaltz et al. 2008). The expression of the same pseudogenes has been confirmed in different somatic cells, somatic tumor cell lines, and adult stem cells (Jez et al. 2014). It is known that in the human ESCs the OCT4A expression is downregulated during a differentiation (Hay et al. 2004), but, interestingly, the expression of above-mentioned OCT4 pseudogenes is increased in a parallel (Jez et al. 2014). It has been shown that haematopoietic stem cells derived from human umbilical cord blood express *OCT4P3*, *OCT4P4*, and *OCT4P5* (Redshaw, Strain 2010). The *OCT4P3* and *OCT4P4* have been observed in freshly isolated urothelium and urothelial carcinoma cell lines (Wezel et al. 2013), but *POU5F1B* and *OCT4P5* are transcribed in cancer cell lines and cancer tissues (Suo et al. 2005). A high level of *POU5F1B* expression is associated with aggressive phenotype and poor prognosis in gastric cancer patients (Hayashi et al. 2015).

To detect *OCT4A* alone, using RT-PCR method, the primers must lie in the 5' region of the *OCT4A* sequence, since the exon 1 is not found in other splice variants and it contains three unique polymorphisms (positions 48, 234, and 353, starting at the transcriptional start codon ATG), that can help in discriminating between parental *OCT4A* and pseudogenes (Liedtke et al. 2008). Human somatic stem cells, somatic tumor cells, and some adult cells may express *OCT4A* at a basal level, compared with pluripotent cells. However, the OCT4A protein has not been undoubtedly detected in non-pluripotent cells, and it is still unclear whether the basal level expression of OCT4A in non-pluripotent cells has a biological function (Wang, Dai 2010).

1.6.2. NANOG

The human *NANOG* gene (NCBI reference sequence NM_024865.3) consists of 8265 base pairs and is located on the short arm of chromosome 12 (12p13.31) (Schorle, Nettersheim 2012). It was named after the mythological Celtic land of the ever young – Tir nan Og (Chambers et al. 2003, Mitsui et al. 2003). There are four transcript variants that are encoded by *NANOG* gene. The mRNA variants *NANOG-001* and *NANOG-002* are translated into proteins with a length of 305 amino acids (aa) and 289 aa, respectively. A variant *NANOG-003* is known to undergo a nonsense-mediated decay, but a *NANOG-004* is putatively protein coding and its translation would result in a protein of 186 aa. The variant *NANOG-001* is commonly analysed and referred to as *NANOG* (Schorle, Nettersheim 2012). NANOG protein is a homeodomain (DNA-binding domain) containing transcription factor (Ambady et al. 2010) that plays an essential role in defining identity of ESCs and their self-renewal (Chambers et al. 2003, Mitsui et al. 2003). An equilibrium between monomeric and active dimeric forms of NANOG in murine ESCs helps to maintain their self-renewal (Mullin et al. 2008), and research suggests that homodimerization through the tryptophan rich region will be also required for human NANOG function (Chang et al. 2009). *NANOG* is expressed in pluripotent stem cells, such as ESCs and embryonic germ cells, and its expression is downregulated during cell differentiation (Chambers et al. 2003). Its presence is also observed in tumor cell lines, teratocarcinoma cell lines (Zhang et al. 2006), and somatic tumors such as

breast (Ezeh et al. 2005), prostate (Gu et al. 2007), cervical (Ye et al. 2008), and gastric cancer (Zhang et al. 2010).

The detection of *NANOG* gene in every human sample must be carefully verified since there are 11 pseudogenes known for *NANOG* in the complete human genome. *NANOG* pseudogene 1 (*NANOGP1*) is a duplication pseudogene since it contains regions homologous to the introns and exons of *NANOG* parent gene. *NANOGP2* to *NANOGP10* are processed pseudogenes as they lack introns and eight of them have in-frame stop codons, deletions, or frameshifts producing stop codons (Figure 1.6.2.1.). *NANOGP11* is found on a different chromosome and does not include sequence derived from the *NANOG* open reading frame (ORF) (Booth, Holland 2004). Among the pseudogenes, *NANOGP1*, *P2*, *P4*, *P7*, *P8*, *P9* and

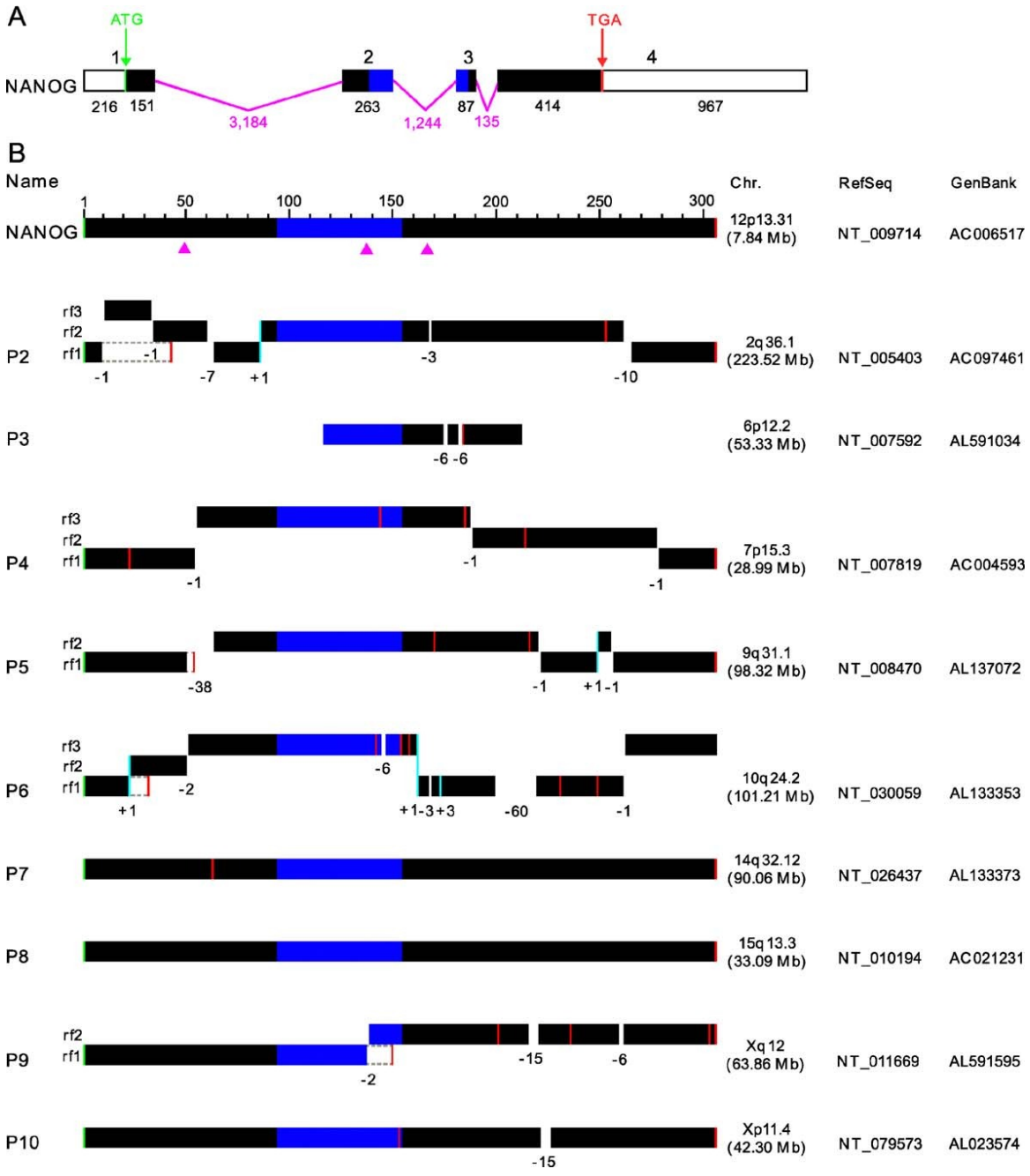

Figure 1.6.2.1. Figure and caption from Booth and Holland 2004: "(A) Human *NANOG* gene structure. The four exons (labelled 1–4) are represented by horizontal bars; the 5' and 3' UTRs are white and the protein coding region is black with the homeobox coloured blue. The three

introns are represented by pink lines. The length in nucleotides is written underneath each of the exons and introns. The start (ATG) and stop (TGA) codons are labelled and represented by a green and a red vertical line, respectively. (B) Nine processed pseudogenes compared to human NANOG protein. NANOGP11 is not shown, as it does not include sequence derived from the NANOG open reading frame. The NANOG protein is represented by a black horizontal bar with the homeodomain coloured blue. The start codon is represented by a green vertical line and the stop codon by a red vertical line. Intron positions are shown by pink triangles. For each pseudogene the black horizontal bar represents sequence similarity to the NANOG open reading frame, which can move between pseudogene reading frames (rf1, rf2, rf3) as a result of insertions and deletions. Insertions are represented by turquoise vertical lines and deletions by the absence of sequence similarity to NANOG. Below each insertion is a plus sign and below each deletion is a minus sign, followed by the number of nucleotide bases inserted/deleted at that point. Substitution mutations are not shown, except where these introduce stop codons into the reading frame homologous to NANOG. Red vertical lines indicate stop codons. These are shown when they occur in the reading frame homologous to NANOG or when they are the first stop codon encountered in rf1. In three of the pseudogenes (NANOGP2, P6, P9) insertions or deletions have caused reading-frame shifts before a stop codon was encountered in rf1. In these cases, the grey dashed lines indicate continuation of rf1 until the first stop codon is encountered."

P10 show more than 90% homology, and *NANOGP5* exhibits about 85% homology to the parent gene in their ORFs (Ambady et al. 2010). Most *NANOG* pseudogenes do not have the potential to produce functional proteins due to a critical mutations, but *NANOGP7* and *NANOGP8* are exceptions, since they do not contain insertions or deletions in the region that is homologous to the *NANOG* ORF. *NANOGP7* possesses an in-frame stop codon close to the start of the ORF, but *NANOGP8* has a complete ORF, extremely similar to original *NANOG* (Booth, Holland 2004).

NANOGP8 (NCBI reference sequence NC_000015.10) shows 99,5% homology to the original *NANOG* ORF (Ambady et al. 2010), but the exact amount of distinctive nucleotides between those two is ambiguous. Some comparison has shown differences at 5 positions in their ORF (Ambady et al. 2010), while most studies report 6 different nucleotides between *NANOG* and *NANOGP8* (Booth, Holland 2004, Zhang et al. 2006, Jeter et al. 2009). However, not all 6 identified nucleotide changes are identical to every study. Our sequence alignment of both ORFs shows 5 unique nucleotides distinguishing *NANOG* from *NANOGP8* (at the positions 47, 144, 246, 531, 759) (Appendix 4). These results indicate that there are modern polymorphisms within *NANOG* and *NANOGP8* that exist in actual reference sequences, thus leading to possible misidentification of RT-PCR products of *NANOG* or *NANOGP8* (Fairbanks et al. 2012). Naturally occurring variation in the *NANOG* sequence at the position 246 (relative to the ATG start codon), resulting in lysine substitution with asparagine, has been reported previously (Booth, Holland 2004). Further comparison of current and previous reference sequences has shown a high degree of modern polymorphisms within *NANOG* itself - 16 substituted and 27 deleted nucleotides within the 2115 nucleotides of the mRNA, six of which are in the ORF. It turns out that all but two (144 G > A, 759 G > C) variants between *NANOG* and *NANOGP8* ORFs detected in previous studies are modern polymorphisms. Only one of the fixed variants (759 G > C) between those two results in an aa change, thus making proteins encoded by *NANOG* and *NANOGP8* differ by only one fixed aa substitution (Fairbanks et al. 2012). Table 1.6.2.1. and Appendix 4 summarize all variants found between *NANOG* and *NANOGP8* ORFs, identifying fixed variants and modern polymorphisms in both of them.

Table 1.6.2.1. Table and caption partially from Fairbanks et al. 2012: "Variants between *NANOG* and *NANOGP8* ORF sequences detected by comparison of current primary and alternate reference assemblies and sequences obtained experimentally by Fairbanks et al. 2012. Polymorphic variants are indicated with a slash, separating the ancestral and derived variants, with the ancestral variant indicated first. All variants are polymorphic in either *NANOG* or *NANOGP8* except for two, indicated in red. Polymorphic variants not present in the comparison of primary and alternate reference assemblies of *NANOGP8* or in other studies, but observed in at least two individuals by Fairbanks et al. 2012 are indicated in blue. a - nucleotides in the reading frame are numbered relative to the first nucleotide in the ATG initiation codon; the symbol "=" denotes that a nucleotide substitution has no effect on the protein."

Variant in coding DNA[a]	Variant in protein[a]	*NANOG*	*NANOGP8*
47 C > A	Ala16Glu	C	C/A
126 T > C	=	T	T/C
144 G > A	**=**	**G**	**A**
165 T > C	=	T/C	T
190 G > T	Asp64Tyr	G	G/T
246 T > G	Asn82Lys	T/G	T
276 G > A	=	G/A	G
363 C > T	=	C/T	C
531 C > T	=	C/T	C
552 A > T	=	A	A/T
629 C > T	Thr210Ile	C	C/T
754 A > C	Met252Leu	A	A/C
759 G > C	**Gln253His**	**G**	**C**
798 C > T	=	C/T	C

NANOGP8 is transcriptionally active as a retrogene in several cancer cell lines and different types of cancer cells (Zhang et al. 2006, Jeter at al. 2009, Ambady et al. 2010, Ibrahim et al. 2012). Although *NANOG* gene and *NANOGP8* are both expressed in cancer cells, it seems that cancer cells mostly express *NANOGP8* and it promotes tumorigenesis more readily than NANOG (Fairbanks et al. 2012). Moreover, downregulation of *NANOG*/*NANOGP8* mRNA in cancer cells inhibits tumor development and clonal expansion of prostate, breast, and colon cancer cells, suggesting that its suppression may potentially be developed as a treatment for cancer (Jeter et al. 2009). *NANOGP8* expression has also been detected alongside with *NANOG* in human adult fibroblasts, umbilical vein endothelial cells, and total heart tissue, but smooth muscle cells express exclusively *NANOGP8* (Ambady et al. 2010). Research shows that recombinant NANOGP8 protein, like NANOG, localizes in a cell nucleus and promote an entry of cells into S-phase (Zhang et al. 2006). Further studies have verified this by showing that *NANOGP8* is translated into protein that exhibits predominantly nuclear localization and may play a functional role in the certain cell types. These observations suggest that low levels of expression of *NANOG* alongside with *NANOGP8* may be necessary for normal cell function even in differentiated cells (Ambady et al. 2010).

1.6.3. SOX2

The human *SOX2* gene (NCBI reference sequence NM_003106.3) is an intronless gene located on chromosome 3q26.3-q27. It belongs to the SOX family of transcription factors that has an important role in developmental and stem cell biology (Weina, Utikal 2014). These transcription factors contain a high-mobility group (HGM) box (Thiel 2013) that was originally identified in the sex-determining region on the chromosome Y and was termed SRY (Sinclair et al. 1990). The HMG domain allows precise DNA recognition and binding. The proteins that contain this domain with amino acid similarity of 50% or higher to the HMG domain of SRY are termed SOX (SRY-related HMG box) proteins (Sarkar, Hochedlinger 2013). These SOX proteins bind consensus sequence (A/T)ACAA(T/A) and interact with the minor DNA groove forcing the DNA helix apart in order to bend the target DNA up to 90 degrees. Additionally, the HMG box contains nuclear localization signals and calmodulin-binding site (Sekido, Lovell-Badge 2009). There are 20 different *SOX* genes expressed in mice and humans (Schepers et al. 2002). Based on the primary structure of their HMG box (the HMG domain sequence identity must be at least 80%), they are divided into groups termed A to H. *SOX2* belongs to the SOXB1 subgroup that also includes *SOX1* and *SOX3* (Sarkar, Hochedlinger 2013). The *SOX2* transcript encodes a 317 aa long protein which is composed of three domains: N-terminal, HMG, and C-terminal transactivation domain (Figure 1.6.3.1.) (Weina, Utikal 2014).

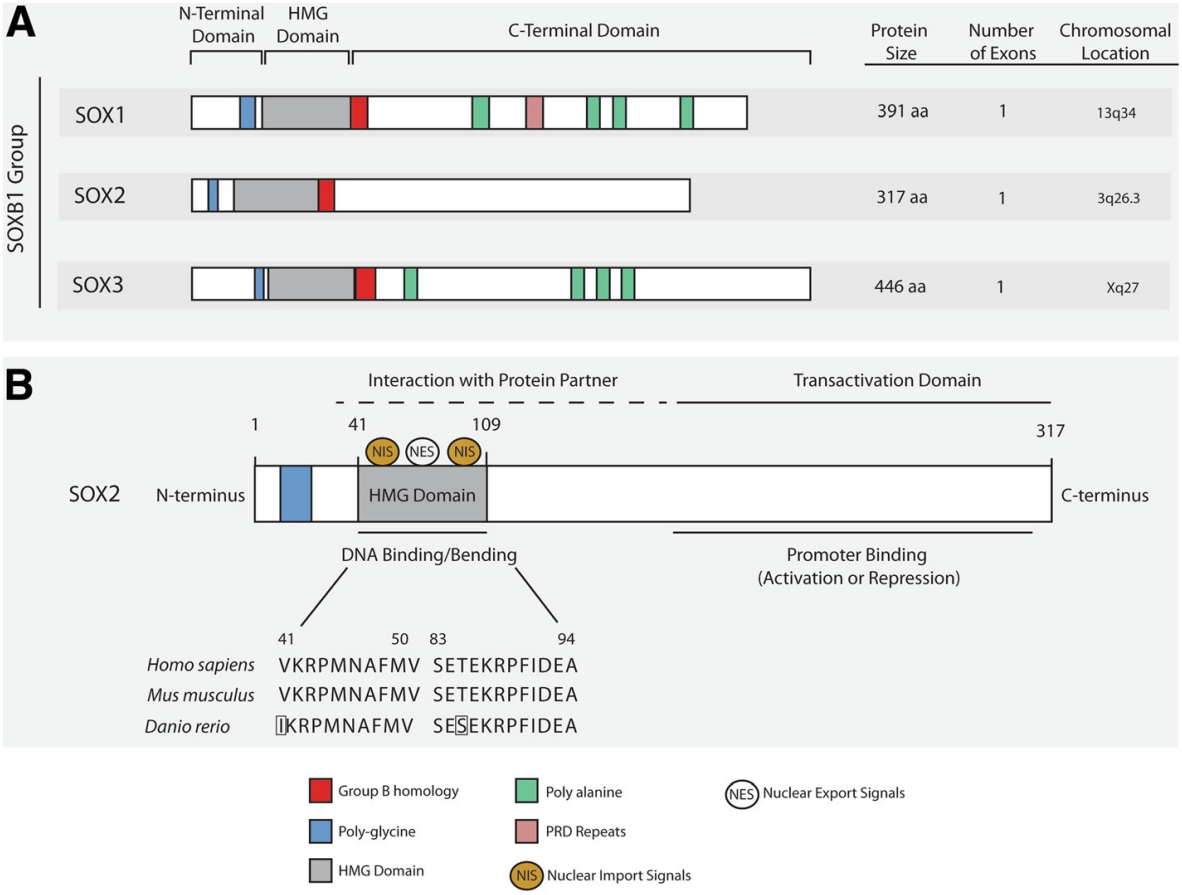

Figure 1.6.3.1. Figure and caption from Wiena and Utikal 2014: "SOX2 homology, structure, and protein function. (A) SOXB1 subgroup containing SOX1, SOX2, and SOX3 proteins that share large homology and contain three major domains: N-terminal, HMG, and C-terminal domain. (B) The HMG domain of SOX2 remains fairly conserved between Homo sapiens, Mus musculus and Danio rerio (Swiss-Prot: P48431, P48432, Q6P0E1). The HMG domain also serves as potential binding sites for protein partners. Moreover, nuclear import signals

(NIS) and nuclear export signals (NES) bind to the HMG domain regulating SOX2 itself. The transactivation domain functions as the region responsible for promoter binding, which in turn leads to activation or repression of target genes."

Developmental studies in mouse embryo have shown that murine Sox2 protein is initially present in ICM, epiblast, and germ cells, similarly to Oct4. However, unlike Oct4, Sox2 is also expressed in extra-embryonic ectoderm. Sox2 is essential for maintaining the cells of epiblast in an undifferentiated state, as in its absence they become trophectoderm or extra-embryonic endoderm. The lack of Sox2 results in early embryonic lethality (Avilion et al. 2003) because its signalling is critical for the formation of different endodermal and ectodermal tissues during fetal development, including nervous system, lens epithelium, anterior foregut endoderm and its derivatives, as well as sensory cells of a taste bud, inner ear, and retina (Arnold et al. 2011). Later in development, Sox2 is involved in specification and maintenance of neural stem cells during neurogenesis (Bylund et al. 2003, Graham et al. 2003), therefore it is a known marker for neural development, as it is expressed in undifferentiated precursor cells (Thiel 2013). It has been shown that Sox2 is involved in a branching of a bronchial tree and is necessary for differentiation of the epithelium of airways (Gontan et al. 2008). A forced expression of Sox2, or its paralogues Sox1 and Sox3, maintains neural progenitor cells in an undifferentiated state and prevents neuronal differentiation (Bylund et al. 2003).

Sox2 is also found in embryonic and adult neural stem cells (Thiel 2013). The silencing of this gene in ESCs by RNA interference leads to differentiation of these cells, indicating its critical role in the maintenance of ESC pluripotent state (Chew et al. 2005). Furthermore, Sox2 expression has also been detected in adult mammalian tissues, such as progenitors of brain and retina, trachea, tongue epithelium, dermal papilla of the hair follicle, putative progenitors of pituitary gland, testis, forestomach, glandular stomach, anus, cervix, lens, as well as glands associated with oral cavity, trachea, and cervix where it marks unipotent and multipotent stem cells (Arnold et al. 2011).

Aside from its crucial role in development and stem cell maintenance, SOX2 has been closely associated with cancer as well. It has been discovered that SOX2 is involved in many cancer-associated processes, such as cell proliferation (breast, prostate, pancreatic, and cervical cancers), evading apoptotic signals (prostate, gastric, and non-small cell lung cancers), and promoting invasion, migration, and metastasis (melanoma, glioma, colorectal, gastric, ovarian cancers, and hepatocellular carcinoma) (Weina, Utikal 2014). High expression of SOX2, as well as OCT4, proteins has been significantly associated with poorer clinical survival of esophageal squamous cancer patients (Wang Q. et al. 2009). SOX2 has also been proposed as a marker for pancreatic cancer stem cells which, based on cancer stem cell hypothesis, are the main cause of cancer progression, drug resistance, and recurrence (Herreros-Villanueva et al. 2013).

1.6.4. Interactions of OCT4, NANOG, and SOX2

Cellular pluripotency is defined as the ability of a cell to differentiate into every type of cell of ectodermal, mesodermal or endodermal origin. During mammalian development only specific group of cells in the early stage embryos is transiently endowed with pluripotency. ESCs are directly obtained from such pluripotent cell populations and can maintain this ability under special culture conditions *in vitro* (Niwa 2001). In the field of ESC research it is well-established practice to characterize these cells by the expression of particular pluripotency markers, that signify their ability to self renew and differentiate into each cell type within the organism, except extraembryonic tissues. OCT4, NANOG, and SOX2 are regarded as the central transcriptional regulators maintaining the pluripotency of ESCs (Boyer et al. 2005).

The interactions of these key pluripotency factors control a whole set of target genes, as well as each other, to sustain the properties of ESCs (Pan, Thomson 2007). It has been demonstrated that OCT4, NANOG, and SOX2 co-occupy the promoters of at least 353 target genes in human ESCs. Together they activate genes encoding components of key signalling pathways and repress the expression of genes that are essential to developmental processes, thus maintaining pluripotent state of ESCs (Boyer et al. 2005).

The exact molecular mechanisms that govern activity of OCT4, NANOG, and SOX2 are complex and not yet completely characterized (Lakatos et al. 2014). It is known that NANOG knock-down leads to differentiation of ESCs into the lineages of extraembryonic endoderm and trophectoderm (Hyslop et al. 2005), and removal of OCT4 also leads to differentiation into trophectoderm (Niwa et al. 2000). However, overexpression of NANOG enables a propagation of human ESCs without feeder cells or conditioned media and leads to the expression of markers specific to a primitive ectoderm (Darr et al. 2006), while upregulation of OCT4 induces commitment to primitive endoderm and mesoderm lineages (Niwa et al. 2000). The results from mouse ESCs indicate, that the primary function of OCT4 is to prevent differentiation of ESCs into trophectoderm, but NANOG inhibits differentiation into extraembryonic endoderm and actively maintains pluripotency (Mitsui et al. 2003).

Scientific observations suggest that OCT4 is different from many known transcription regulators, that seem to function in a binary on-off manner, because it controls the pluripotent state of the stem cells in a quantitative fashion (Pan et al. 2002). Only a specific level of OCT4 can maintain a stem cell renewal. 50% above or below the normal expression level in pluripotent stem cells trigger differentiation into endoderm/mesoderm or trophectoderm, respectively (Niwa et al. 2000). Similarly, SOX2 levels must also be maintained within narrow limits since increase in SOX2 protein reduces self-renewal and promotes differentiation of ESCs (Kopp et al. 2008). The expression pattern of NANOG is also unusual. Despite its crucial role in maintaining pluripotency, the expression of NANOG is heterogeneous in a population of ESCs. These cells can express different levels of NANOG and thus exhibit variable resistance to differentiation (Chambers et al. 2007). This heterogeneity is dynamically controlled, with individual cells exhibiting transient changes in expression levels (Lakatos et al. 2014). Furthermore, the expression of NANOG is mosaic in the inner cell mass of a blastocyst as well (Chazaud et al. 20006). The NANOG-positive cells give rise to epiblast, from which all three germ layers emerge, but NANOG-negative cells form the primitive endoderm, which contributes to extraembryonic tissues (Navarro et al. 2012).

To sustain pluripotency in ESCs, the target genes are regulated both by NANOG and OCT4 individually, and by NANOG and the combination of OCT4/SOX2, since OCT4 can heterodimerize with SOX2 in order to affect the expression of genes (Boyer et al. 2005). During the last decade several models have been suggested, describing the interactions between the key transcription factors OCT4, SOX2, and NANOG (Figure 1.6.4.1.).

The transcriptional network consisting of OCT4, SOX2, and NANOG behaves like a bistable switch resulting from several positive feedback loops. OCT4 and SOX2 regulate each other through the formation of a heterodimer. The OCT4/SOX2 heterodimer regulates NANOG, which feeds back to OCT4 and SOX2 (Figure 1.6.4.1.A). Through these feedback loops the expression of all three transcription factors can be collectively triggered or blocked by the input environmental signals. The switch stabilizes the expression of these three key genes and, by regulating their downstream target genes, leads to a binary decision: when OCT4, SOX2, and NANOG are expressed and the switch is ON, the self-renewal genes are ON and the genes involved in a differentiation process are OFF. When the switch is OFF, the opposite takes place, leading to the loss of pluripotency and initiation of a differentiation (Chickarmane et al. 2006).

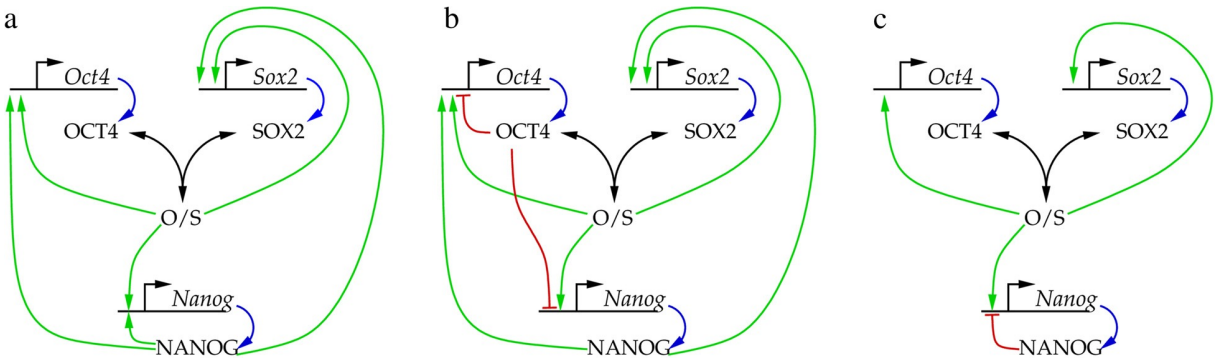

Figure 1.6.4.1. Figure and caption from Lakatos et al. 2014: "Suggested interactions of the OCT4-SOX2-NANOG core module of transcriptional embryonic stem cell regulation. (A) The symmetrical model considered by Chickarmane et al. 2006. (B) The model suggested by Pan, Thomson 2007, that includes negative feedback through OCT4. (C) The NANOG autoinhibitory circuit suggested by Navarro et al. 2012. Black arrows represent complex formation, green – transcriptional activation, red – repression, and blue – translation."

Additional research introduced a negative feedback loop formed by NANOG, OCT4, and another pluripotency factor FOXD3 (Pan et al. 2006). It was suggested, that OCT4 activates NANOG promoter, when expressed below normal level, but represses it, when its expression is above normal level in ESCs. When the expression of OCT4 rises above normal level, it represses its own promoter as well, thus keeping its expression level at a steady state (Figure 1.6.4.1.B). This negative feedback regulation loop is thought to explain the previous observations by Niwa et al. 2000, describing the dose dependencies of OCT4 in order to regulate the pluripotency of stem cells (Pan et al. 2006, Pan, Thomson 2007).

Previously it was widely accepted, that all three key pluripotency factors autoactivate themselves (Jaenisch, Young 2008), but later studies showed, that NANOG activity is autorepressive (Figure 1.6.4.1.C) (Navarro et al. 2012). Since the known fluctuations in a NANOG transcription occur within stem cells that express relatively uniform levels of OCT4 and SOX2 (Chambers et al. 2007), the discovered autorepression most likely takes part in controlling the dynamic transitions between NANOG transcription states. Furthermore, it turned out, that NANOG does not activate the expression of both OCT4 and SOX2 (Navarro et al. 2012).

The latest modelling approach showed that the model, suggested by Chickarmane et al. 2006, can not explain oscillations in NANOG expression. The direct OCT4 negative feedback on NANOG expression, proposed by Pan et al. 2006, is also unlikely to play an important role, since the feedback mechanism, that does not require changes in OCT4, is in accordance with its stable expression level (Chambers et al. 2007) and the observation, that changes in OCT4 expression levels trigger differentiation (Niwa et al. 2000). It is likely, that fluctuations in NANOG expression reflect individual cell-specific changes in parameters of an autocrine feedback loop, instead of changes in core regulatory cluster of OCT4-SOX2-NANOG itself. These external changes could result from modifications in ligand capture efficiency, receptor numbers, or the presence of crosstalks within MAPK signal pathway. Furthermore, the authors suggested, that NANOG fluctuations represent distinct sub-states within the ON state of the core NANOG switch, not transition states between the ON and OFF states, as proposed previously (Lakatos et al. 2014).

1.7. Stem cells for a treatment of type 1 diabetes

Diabetes mellitus or simply diabetes is called the epidemic of the 21st century and according to the International Diabetes Federation 387 million people had diabetes in 2014,

but there will be 592 million by 2035. Although type 2 diabetes (T2D) accounts for 85%-95% of all diabetes cases, the incidence of type 1 diabetes (T1D) is also increasing by approximately 3% each year. It is estimated that approximately 79 000 children under 15 years develop T1D each year. Worldwide there are approximately 497 000 children with T1D and 26% of them live in Europe (idf.org). There were 84 683 registered patients with diabetes in Latvia in 2014. Of these 4188 were T1D patients (spkc.gov.lv).

Diabetes is a group of complex metabolic diseases characterized by high blood sugar, i.e., hyperglycemia, resulting from insufficient amount of insulin, insulin resistance, or both. There are two main categories of diabetes: T1D and T2D. Additionally, gestational diabetes mellitus and other specific types of diabetes are also distinguished (Anonymous 2010). T2D (non-insulin-dependent diabetes) is characterized by a decline in pancreatic β cell function in combination with insulin resistance, or the inability to effectively use insulin in peripheral tissues. People with T2D must control their hyperglycemia by the means of healthy diet, increased exercise, blood glucose-lowering drugs, or daily insulin injections (Goldthwaite 2010). This type of diabetes usually occurs in adults and almost half of them is between 40 and 59 years old. More than 80% of T2D patients in this age group live in low- and middle-income countries. Lately, increasing number of children and adolescents are also diagnosed with T2D (idf.org).

T1D (insulin-dependent diabetes) results from autoimmune destruction of the pancreatic β cells leading to a lack of insulin secretion (Anonymous 2010). Therefore, people with T1D require daily insulin administration to survive (Goldthwaite 2010). Since this form of diabetes is usually diagnosed in children and young adults, although it can develop at any age (Anonymous 2010), the impact on a future quality of their life is more critical than of those with T2D. Even though insulin injections partly compensate the function of β cells, they are not able to regulate blood sugar as precisely as the endogenous insulin. This inaccurate control of blood glucose homoeostasis in a long run results into such complications as diabetic retinopathy, nephropathy, neuropathy, foot ulcers, and cardiovascular diseases (Zhong et al. 2012). The cause of T1D is still not fully understood, but it is thought to develop from interactions between genetic and environmental factors. For example, individuals with HLA DR3-DQ2/DR4-DQ8 genotype have approximately 20 times higher risk to develop T1D than general population. There are other HLA class II genotypes that bear moderately increased risk for T1D, but protective genotypes also exist (Nokoff et al. 2012). Non-HLA associated risk loci for T1D include the genes for INS, PTPN22, IL2RA, SH2B3 which influence immunity, ERBB3 which is involved in insulin production and metabolism, and many others (Concannon et al. 2009). Still unknown environmental factors are also thought to influence development of T1D since rising incidence, outbreaks, and a seasonal pattern could not be explained by genetics alone (Nokoff et al. 2012). An increasing environmental pressure has caused substantial changes in the distribution of T1D associated HLA genotypes, and this has resulted in a higher disease progression rate among individuals with protective HLA genotypes (Hermann et al. 2003). One of the most studied environmental factor in relation to T1D is enterovirus infection, and a recent meta-analysis has shown a significant association between those two (Yeung et al. 2011).

One of the main strategies for T1D treatment is pancreatic islet transplantation from two or more donors. Unfortunately, the lack of appropriate donors, damages of transplantable tissue, and use of immunosuppressive drugs limit the use of this method. Additionally, the function of pancreatic islets decreases relatively quickly after transplantation (Goldthwaite 2010). It has been shown that only 10% of islet transplant recipients maintain insulin independence five years after transplantation (Ryan et al. 2005). The use of SCs for T1D treatment is being explored as an alternative solution, as they could be injected into a patient, where they would migrate to the damaged pancreas and differentiate, replenishing β cells, or they could be employed *in vitro*, differentiating them into insulin-producing β cells and

afterwards introducing back into the patient (Goldthwaite 2010). However, the restoration of glucose-responsive and insulin-producing β cells is only one of two challenges that must be overcome to successfully cure T1D. The second obstacle manifests as a need to protect implanted β cells from repeated autoimmune destruction that caused the disease in the first place (Chhabra, Brayman 2013). This can be achieved by different immunosuppressive drugs, that is a common practice for most tissue transplants, or by alternative methods. These methods include the use of specific antibodies, fusion proteins, or oligonucleotides to eliminate the majority of the autoreactive cells, transplanting BM from a diabetes-resistant donor (Goldthwaite 2010), or exploiting immunoisolation. Using the immunoisolation technique, cells are enclosed in a semipermeable barrier device that allows the exchange of oxygen, nutrients, and insulin, but protects these cells from the immune system. Such materials as alginate, agarose, polyethylene glycol, chitosan, silica, and others have been tested to encapsulate pancreatic islets (O'Sullivan et al. 2011). Currently there are two companies: ViaCyte and BetaLogics that use encapsulation devices to shield cell transplants (Venkat et al. 2014). ViaCyte has developed a therapy called VC-01 which is made up of encapsulated pancreatic progenitor cells that have been differentiated from ESCs. These precursor cells are expected to differentiate into mature pancreatic cells, once implanted in the body. This product is currently being tested in Phase I/II human clinical trials (viacyte.com). In contrast, BetaLogics uses mature β-like cells, also differentiated from ESCs, that secrete insulin upon glucose stimulation. Animal studies have shown that these cells can reverse diabetes in approximately six weeks while progenitor cells used by ViaCyte could reach similar response after three to four month, as they need time to become mature and functional β cells. Despite the extra time needed for progenitor cells to fully differentiate, these cells can better survive hypoxic conditions after transplantation, they can give rise to other cell types of pancreatic islets, and their manufacturing is less costly (Venkat et al. 2014).

So far most of the research in this field has been carried out using ESCs due to their higher differentiation potential. The first proof of concept that ESCs can differentiate into insulin-producing cells was published fifteen years ago (Soria et al. 2000), and the first directed differentiation protocol, utilising five subsequent stages to obtain islet-like clusters composed of the cells positive for insulin, glucagon, and somatostatin, followed soon after (Lumelsky 2001). This protocol gained high popularity, but later it was discovered that the cells differentiated according to Lumelsky protocol was subjected to apoptosis or necrosis and the observed insulin release was most likely due to the uptake of significant amounts of insulin that was present in the differentiation medium rather than *de novo* synthesis (Hansson et al. 2004). Meanwhile, stepwise protocols that mimicked *in vivo* development of pancreas were starting to emerge. One of the most influential differentiation protocols simulating *in vivo* pancreatic organogenesis guided ESCs through stages of definitive endoderm, gut tube endoderm, and pancreatic endoderm leading to endocrine precursor cells that expressed endocrine hormones. Although obtained results suggested that generated cells may be more similar to immature fetal β cells than to adult β cells because of a very low insulin secretion in response to glucose stimulation and a coexpression of insulin and glucagon or insulin and somatostatin (D'Amour et al. 2006), this research set a course for future advancement in creation of insulin-producing cells. The protocol was later optimised (Kroon et al. 2008) by the same research group from ViaCyte company (at that time known as Novocell) and is now used as a base for their proposed VC-01 therapy to treat diabetes in the nearest future (viacyte.com). Different variations of this protocol and similar approaches have been reported with variable degrees of success (Jiang et al. 2007, Chen et al. 2009, Zhang et al. 2009, Kunisada et al. 2012). The main problems in the differentiation process are generation of cells with immature or abnormal phenotypes, production of various cell types from different germ layers and not pure monolineage culture, tumorigenic properties of undifferentiated ESCs and iPSCs (Cheng X. et al. 2012), and a low yield of insulin-positive cells (Hosoya 2012). As of

recently, the percentage of insulin-positive cells differentiated from ESCs or iPSCs were from 0,8% (Chen et al. 2009) to roughly 8% (D'Amour et al. 2006, Jiang et al. 2007, Kunisada et al. 2012), with the highest reported percentage being approximately 25% (Zhang et al. 2009). However, last year researchers from BetaLogics and their collaborators developed a protocol which can generate insulin-producing cells, similar to mature β cells, from ESCs with 50% efficiency that exhibit glucose-responsive insulin secretion and rapidly reverse diabetes after transplantation in mice (Rezania et al. 2014). Together with a report showing very similar results and offering differentiation protocol to generate large quantities of glucose-responsive β cells (Pagliuca et al. 2014) a treatment for diabetes has been definitely brought one step closer.

Despite attractiveness of the pluripotent SCs for such applications, ethical issues, the risk of teratoma development, and a need to find an appropriate donor limit their therapeutic use (Goldthwaite 2010). Therefore, adult SCs have been explored as a possible alternative. Experimental data show that SCs isolated from human UC blood (Sun B. et al. 2007, Hu et al. 2010), placenta (Chang et al. 2007), BM (Sun Y. et al. 2007, Tang et al. 2012), and adipose tissue (Timper et al. 2006, Lee et al. 2008, Okura et al. 2009, Chandra et al. 2011, Kang et al. 2011, Buang et al. 2012) are also able to differentiate into insulin-producing cells. Differentiation protocols used for somatic SCs usually include multiple stages, similarly to protocols employed for ESCs, and part of the extrinsic factors added to induction media is identical in both cases. Reported differentiation protocols for adult SCs last for few weeks on average, but there are protocols that require two to four months to obtain insulin-producing cells (Tang et al. 2012). On contrary, other researchers claim to differentiate MSCs into insulin-positive cells within 34 hours (Chen et al. 2004) or 3 days (Timper et al. 2006) only. However, these results are highly questionable, and an attempt to reproduce them has failed (Oishi et al. 2009). Since protocols for pluripotent SCs take approximately 20 days to complete and in the human fetal pancreas insulin-producing cells could be first detected only at around eight weeks of development (Naujok et al. 2011), it is very unlikely that an actual transdifferentiation of MSCs into insulin-producing cells could be achieved in such a short time span. Although several studies have demonstrated promising results (Chang et al. 2007, Sun Y. et al. 2007, Okura et al. 2009, Chandra et al. 2011), the problems, similar to those when using pluripotent SCs, must yet be overcome. The lack of an efficient standard method for functional insulin-producing cell generation, inability to consistently produce clinically significant amounts of insulin, and differentiation on a large scale will require further scientific efforts before adult SCs can be used for the treatment of diabetes (Wong 2011).

1.8. Differentiation of stem cells into insulin-producing cells

To successfully differentiate SCs into insulin-producing cells *in vitro*, it is crucial to understand the mechanisms that govern development of pancreas *in vivo*. The greatest part of our knowledge about pancreatic development comes from embryological studies of such model organisms as mouse, chicken, zebrafish (*Danio rerio*), or frog (*Xenopus laevis*). Although these vertebrates seem very distinctive, a development of pancreas is a highly conserved process, giving researchers the possibility to draw parallels with humans (Van Hoof et al. 2009).

According to the current scientific knowledge, pancreas emerges from the endoderm - the inner germ layer of an embryo. During the gastrulation endoderm precursors ingress in the anterior primitive streak forming a definitive endoderm (DE) (Grapin-Botton 2008) (Figure 1.8.1.). The DE initially consists of a flat sheet of cells with anterior-posterior pattern information. Afterwards, from this flat sheet a primitive gut tube with specified domains for various endoderm organ primordia is formed. Pancreas develops from the posterior foregut, emerging as buds from the dorsal and ventral sides of the gut tube. At this point the formation

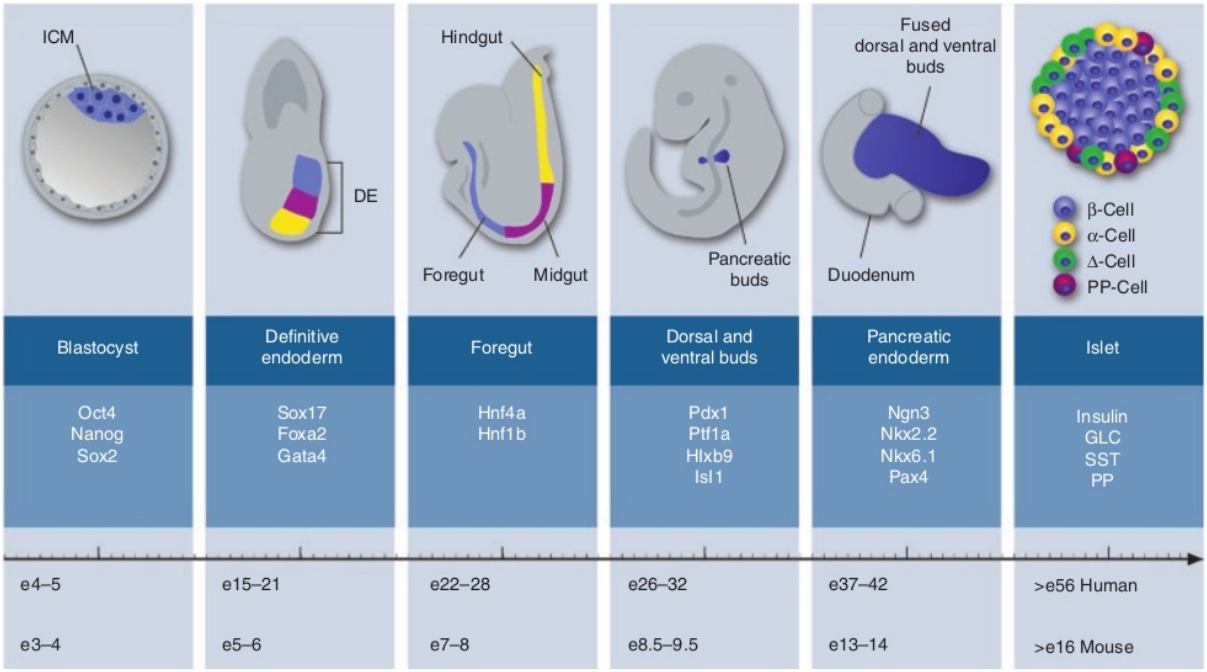

Figure 1.8.1. Figure and caption from Naujok et al. 2011: "Simplified schematic presentation of the pancreas development in mice. The inner cell mass (blue) of the blastocyst gives rise to the three germ layers in the process of gastrulation. The definitive endoderm is then formed by the recruitment of epiblast cells through the primitive streak via a mesendodermal progenitor with the latter cells of the foregut (blue), midgut (purple), and hindgut (yellow). Morphogenesis of the primitive gut is a result of an invagination movement by which the layered definitive endoderm becomes a tube structure. The pancreas formation begins with the independent budding of the dorsal and ventral buds at the posterior region of the foregut. These two buds grow into the surrounding mesenchyme, branch in a tree-like structure and eventually fuse after rotation of the gut to form the definitive pancreatic endoderm. This pre-differentiated epithelium grows in size with distinct endocrine and exocrine differentiation. The endocrine cells are organized in islets which are embedded in exocrine tissue and are composed of four major hormone-secreting cells types. Insulin is secreted by β cells (blue), glucagon by α cells (yellow), somatostatin by Δ cells (green), and pancreatic polypeptide by PP cells (purple). The timeline plots these key events for mouse. For comparison only, comparable stages of human β cell development have been mapped on the timeline. Several markers characteristic of each developmental step are listed. DE - definitive endoderm; GLC - glucagon; ICM - inner cell mass; PP - pancreatic polypeptide; SST – somatostatin."

of pancreas depends on retinoid signalling and on inhibition of hedgehog signalling (D'Amour et al. 2006). The developing pancreas consists of Pdx1 positive progenitors that will give rise to the islets, exocrine cells, and ductal cells (Gu et al. 2002). After the initial pancreatic bud formation, further morphogenesis, involving growth, branching, and differentiation, includes interactions between pancreatic epithelium and adjacent mesenchyme signals, e.g., fibroblast growth factor 10 (FGF10) (Bhushan et al. 2001). The specification of endocrine cells occurs in the next stage of pancreas development. Only Ngn3 positive pancreatic cells will give rise to all four types of endocrine islet cells (Gu et al. 2002), but the expression of *Ngn3* gene is permitted through the absence of Notch signalling (Wilson et al. 2003). The Ngn3 initiates the expression of such transcription factor genes as *Nkx2-2*, *Neurod1*, *Nkx6-1*, *Pax4*, *Pax6*, and *Isl1* that control endocrine cell differentiation. During this period the developing endocrine cells migrate from the branched epithelium into surrounding mesenchyme in order to form the islets of Langerhans. When hormone-expressing pancreatic cells have formed, they mature further to reach a fully functional state. For β cells it means that they acquire the ability to

release insulin in response to elevated glucose level (D'Amour et al. 2006). An example of the main intermediates in pancreatic endoderm differentiation *in vitro* using ESCs is depicted in Figure 1.8.2.

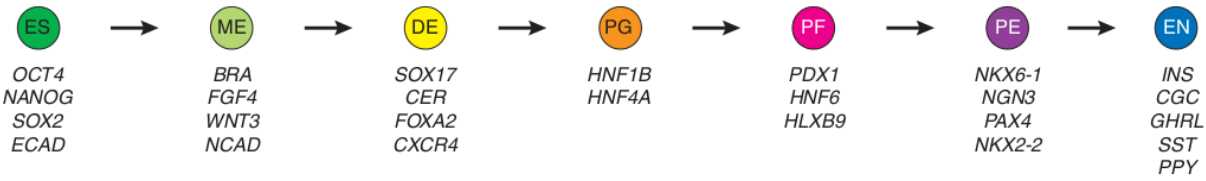

Figure 1.8.2. Schematic representation of the main intermediate states for *in vitro* differentiation of embryonic stem cells into hormone-expressing endocrine cells and key marker expression of each intermediate cell population. ES – embryonic stem cell; ME – mesendoderm; DE - definitive endoderm; PG - primitive gut tube; PF - posterior foregut endoderm; PE - pancreatic endoderm and endocrine precursor; EN - hormone-expressing endocrine cell. Figure from D'Amour et al. 2006.

For the SC differentiation into insulin-producing cells most of the protocols utilize addition and withdrawal of various extrinsic factors in a stepwise manner. Below are given the most common factors used in the induction protocols, as well as those factors or conditions which have shown significant impact on the course of SC differentiation into pancreatic β cells.

Activin A. The first step to successfully differentiate SCs into pancreatic endocrine cells is to induce DE differentiation. It is known that both Wnt/β-catenin and TGFβ signalling pathways are implicated in the formation of DE (Zorn et al. 1999). A member of the TGFβ superfamily, namely Nodal, is essential for endoderm specification in mice, and higher levels of Nodal signalling are required to form endoderm than mesoderm (Stainier 2002). Since a source of highly active Nodal protein is not readily available, it is possible to use activin instead. It is another TGFβ family member that binds practically the same receptors as Nodal and triggers similar signalling cascades. It has been demonstrated that high concentrations of activin A under an absence or low concentrations of serum facilitates the differentiation of human ESCs into definitive endoderm (D'Amour et al. 2005). If lower doses of activin A are used, differentiation into endocrine cells is considerably reduced (D'Amour et al. 2006). Additionally, suppression of phosphatidylinositol 3-kinase (PI3K) signalling and reduction of insulin/insulin-like growth factor signalling promotes the efficiency of DE differentiation. LY294002 has been often used as a potent inhibitor of PI3K signalling (McLean et al. 2007). For the last decade activin A has been included in most of the induction protocols, both for ESC and adult SC differentiation into DE, and the biggest part of studies claim positive results. However, others have found that stimulation of Nodal signalling with activin A is not sufficient to induce differentiation of DE from UC blood SCs (Filby et al. 2011).

CHIR99021. Since Wnt/β-catenin signalling is involved in the formation of DE (Zorn et al. 1999), fraction of induction protocols uses extrinsic factors to activate this pathway at the beginning of differentiation. The most commonly used is Wnt3a protein (D'Amour et al. 2006, Kroon et al. 2008, Chen et al. 2009). Its combination with activin A is expected to mimic coordinated expression of Wnt/β-catenin and Nodal signalling respectively, as it would be during the primitive streak formation (Hosoya 2012). Some of the effects of Wnt/β-catenin signalling can be reached by inhibition of glycogen synthase kinase 3 β (GSK3β) activity. CHIR99021 is a GSK3β and GSK3α-specific inhibitor, and it can be used instead of Wnt3a. It has been demonstrated that a combination of activin A and CHIR99021 induces DE more effectively than activin A and Wnt3. Moreover, the stability and cost of CHIR99021 makes it more attractive candidate for induction media than Wnt3a (Kunisada et al. 2012).

Sodium butyrate. Histone deacetylase inhibitors modulate gene expression by

increasing histone acetylation, thus regulating chromatin structure and activating gene transcription by rendering the target DNA more accessible to transcription factors (Li et al. 2008). Sodium butyrate is a known histone deacetylase inhibitor (Candido et al. 1978) that can inhibit proliferation, induce differentiation, and induce or repress gene expression in mammalian cell cultures (Davie 2003). It has been shown that sodium butyrate alone is mostly ineffective in inducing endoderm differentiation of ESCs, but its combination with activin A generates higher levels of *SOX17*, *FOXA2*, *HNF4A*, and *PDX1* gene expression (Jiang et al. 2007).

FGF10. Since one of the pathways involved in pancreatic development is fibroblast growth factor and their receptor signalling, such factors as basic FGF, FGF7, and FGF10 are frequently used in differentiation protocols (Hosoya 2012). FGF10 is a key signalling molecule engaged in the mesenchymal-epithelial interactions that are essential during the early stages of pancreatic development. Its main role is to regulate the proliferation of PDX1-positive progenitor cells and, therefore, the size of developing pancreas (Bhushan et al. 2001). Since persistent expression of FGF10 during embryogenesis activates Notch signalling, which inhibits the endocrine cell differentiation by blocking the expression of *NGN3* gene, it must be used only in the initial steps of differentiation (Hart et al. 2003).

Retinoic acid. It has been demonstrated that retinoic acid signalling is essential for specifying pancreas during development, and its role is conserved among vertebrates (Stafford et al. 2004). Retinoic acid stimulates the generation of *Pdx1*-positive cells that coexpress a transcription factor *Ptf1a*, an indicator of pancreatic commitment (Micallef et al. 2005). When used in combination with activin A during the initial steps of ESC differentiation protocol, induced cells express high levels of such pancreatic progenitor markers as *Pdx1*, *Hnf3B*, and *Hnf4A*. The obtained results suggest that retinoic acid facilitates the formation of pancreatic precursor cells and is critical for pancreatic β cell development and maturation (Shi et al. 2005). If retinoic acid is not added to the induction medium, noticeable levels of *NGN3*, *INS*, or *GCG* expression are not detected at later stages of differentiation, in spite of *PDX1* expression (D'Amour et al. 2006).

Nicotinamide. Already more than two decades ago nicotinamide has been shown to induce differentiation and maturation of human fetal pancreatic islet cells in culture (Otonkoski et al. 1993). More recently, many studies use it in the final stages of their differentiation protocols, as addition of nicotinamide results in sustained expression of *PDX1* gene, induction of β cell differentiation (Cho et al. 2008), increase of the insulin content (Vaca et al. 2003), and improvement of the yield of pancreatic endocrine cells (Jiang et al. 2007, Kunisada et al. 2012). Furthermore, nicotinamide is reported to protect cells from diminished sensitivity caused by prolonged exposure to high amounts of glucose present in differentiation medium, and it can be used to preserve viability and function of differentiated endocrine cells (Neshati et al. 2010).

Exendin-4. A hormone glucagon-like peptide-1 (GLP-1) is produced in the intestinal epithelial endocrine L-cells, and its main role is to stimulate insulin secretion and to inhibit glucagon secretion (Holst 2007). When GLP-1 is added to the endoderm precursor differentiation medium, the level of *PDX1* and *INS* transcription, as well as the amount of insulin-producing cells is slightly elevated. However, when sodium butyrate is used in early stages of differentiation followed by addition of GLP-1 in later stages, the expression of *PDX1* and later *NGN3* is significantly increased. This combination results in insulin-producing cell increase from 8% to 45% (Li et al. 2008). Since natural GLP-1 is rapidly degraded, it is possible to replace it by its long-acting analogue exendin-4 (Xu et al. 1999). Exendin-4 has been isolated from the venom of the lizard *Heloderma suspectum* (Eng et al. 1992), and it shares 53% sequence homology with GLP-1 and acts as a GLP-1 receptor agonist (Göke et al. 1993). It has been shown that exendin-4 stimulates differentiation of β cells from ductal progenitor cells and proliferation of β cells when given to rats (Xu et al.

1999). High amount of the protein increases the differentiation efficiency of mouse ESCs into β-like cells, their insulin synthesis and release (Li et al. 2010).

DAPT. To allow the expression of *NGN3* gene that is recognized as a regulator of pancreatic endocrine cell formation, the Notch signalling pathway must be blocked at later stages of differentiation. DAPT (N-[N-(3,5-difluorophenacetyl)-1-alanyl]-S-phenylglycine t-butyl ester) is a γ-secretase inhibitor that arrests Notch signalling and is often used in pancreatic induction protocols (Champeris Tsaniras, Jones 2010). However, other evidence suggests that the use of DAPT has only a slight positive effect on promoting endocrine differentiation (D'Amour et al. 2006).

Glucose. Fraction of induction protocols changes the glucose concentration at various stages of differentiation. Since it has been demonstrated that low concentrations of glucose (5 mM) increase insulin content in islet-like clusters, but higher concentrations (20-30 mM) increase replication of β cells *in vivo* and *in vitro* (Bonner-Weir et al. 1989 after Wong 2011), it is well founded to vary the glucose concentration to facilitate β cell replication and enhance insulin content and its secretion (Wong 2011). There are protocols that employ high concentrations of glucose at the beginning of differentiation and switch to low concentrations at later stages (Segev et al. 2004, Kang et al. 2011, Tang et al. 2012). Reduction of glucose concentration at the end of induction also helps to restore the sensitivity of cells to a glucose challenge, often performed after the differentiation has been completed (Tang et al. 2012). However, others use high concentrations of glucose throughout the differentiation (Sun Y. et al. 2007, Neshati et al. 2010). Evidence suggests that murine BM MSCs cultured under high-glucose for 2-4 months differentiate towards pancreatic endocrine cells (Tang et al. 2004). But exposure of mice to elevated blood glucose levels for only 3 days activates transcription of *Insulin* gene and produces proinsulin-positive cells in liver, adipose tissue, spleen, BM, and thymus suggesting that high levels of glucose could facilitate generation of insulin-producing cells from non-β cells (Kojima et al. 2004).

Oxygen. Low levels of oxygen (3% - 5%) have been shown to facilitate proliferation of SCs and maintain their undifferentiated state, while normoxic conditions (21% oxygen) tend to induce SC differentiation (Ezashi et al. 2005, D'Ippolito et al. 2006, Berniakovich, Giorgio 2013). The pancreatic islets are known for their high oxygen requirements, since they make up only 1% - 2% of the total number of cells of the pancreas, but use 25% of the pancreatic oxygen supply (Fraker et al. 2007). Additional research has demonstrated that high levels of oxygen (35% - 80%) stimulate differentiation of endocrine cells in murine pancreatic buds (Fraker et al. 2007, Heinis et al. 2010), as well as from mouse ESCs and human iPSCs (Hakim et al. 2014). This is achieved through suppression of hypoxia-inducible factor 1α (HIF-1α) activity. In normoxic conditions HIF-1α protein is rapidly degraded, but hypoxic conditions stabilize HIF-1α inducing its accumulation and, therefore, interaction with target genes (Berra et al. 2006). HIF-1α interacts with the intracellular domain of Notch, thus activating its signalling cascade (Gustafsson et al. 2005). On contrary, higher oxygenation would destabilize HIF-1α, thus inhibiting Notch signalling and, therefore, promoting endocrine differentiation. Furthermore, degradation of HIF-1α up-regulates Wnt/β-catenin signalling pathway that is critical for DE differentiation. Since HIF-1α is also known to interact with histone deacetylases leading to transcriptional repression, high levels of oxygen could act similarly to histone deacetylase inhibitors by eliminating HIF-1α (Fraker et al. 2009).

2. Materials and methods

2.1. Source of biological samples

The Latvian Central Medical Ethics Committee has approved the current research involving human participants (permit No.12). The human adipose tissue and blood were collected after written consent was obtained from the donors. Human abdominal subcutaneous adipose tissue and blood were derived during planned operations. Blood and tissue samples were processed in collaboration with "Cilmes Šūnu Tehnoloģijas" Ltd. within 3-5 hours after collection.

Most of the results described in this work have been obtained from an adipose-derived stem cell culture originating from one donor (donor No.4) and have been supplemented with the experimental data from four other donors (for more information, see Table 2.1.1.).

Table 2.1.1. Information about human donors used in the current study.

Donor code number	Type of adipose tissue collected	Age	Gender	State of health
No.3	abdominal subcutaneous	63	male	healthy
No.4	abdominal subcutaneous	40	male	healthy
No.5	abdominal subcutaneous	47	male	healthy
No.8	abdominal subcutaneous	30	female	Type 1 diabetes
No.9	abdominal subcutaneous	28	male	healthy

2.2. Preparation of autologous serum

Collected blood was allowed to clot for 1 hour at room temperature. The serum was collected, centrifuged at 2000 rpm for 30 min, filtered through 0,2 μm mesh, aliquoted, and stored at -20^{0}C.

2.3. Isolation and expansion of ASCs

2-5 ml of adipose tissue were scissored and treated with 0,3% pronase (EMD Millipore, USA) for 1 h at RT with gentle rotation followed by centrifugation for 7 min at 1000 rpm. The pellet was suspended, filtered through 40 μm mesh and centrifuged again for 5 min. Erythrocytes were lysed for 3 min at +37^{0}C using erythrocyte lysis buffer Hybri-Max (Sigma-Aldrich, Germany). Obtained cell pellet was suspended in a fresh cell culture medium (DMEM/F-12 (Life Technologies, UK) containing 10% autologous serum, 2 mM L-glutamine (Life Technologies, UK), 20 ng/ml basic fibroblast growth factor (BD, USA), 100 U/ml : 100 μg/ml penicillin - streptomycin (Life Technologies, UK)) and seeded onto a 75 cm^2 tissue culture flask (regarded as passage 0 (P0)). Cells were cultured at +37^{0}C, 5% CO_2.

Non adherent cells were removed on the next day by extensive washing with phosphate-buffered saline (PBS) (Life Technologies, UK). The remaining cells were cultivated in the medium supplemented with 10% AS for first 10 days and 5% AS afterwards. The cell culture medium was changed every third day. When the cells reached 80-90% confluence they were reseeded for the propagation purposes.

The methods of subsequent passaging and freezing of ASCs were done as follows. After the second passage, cells were frozen in DMEM/F12 supplemented with 10% dimethyl sulfoxide (Sigma-Aldrich, Germany) and 20% AS and stored in a liquid nitrogen. After

thawing ASCs were cultivated as previously through P3 to P8, freezing a fraction of cells before the each subsequent passage. After more than 4 years ASCs from passages 2 to 8 were thawed and used for the characterization.

2.4. Karyotyping

Karyotyping of ASCs (donor No.4) was performed at passage 3. The cells were treated with 10 μg/ml KaryoMAX Colcemid (Life Technologies, UK) for 30 min at +37^{0}C and detached using 0,25% trypsin/versen (Life Technologies, UK) solution for 5 min at +37^{0}C. To inactivate the trypsin AmnioMAX II Complete Medium (Life Technologies, UK) was added and the cell suspension was centrifuged for 5 min at 1000 rpm. Resulting cell pellet was exposed to pre-warmed 1% sodium citrate solution for 45 min at +37^{0}C. After centrifugation for 5 min at 1000 rpm the cells were fixed three times in cold methanol/acetic acid (3:1) for 20 min at -20^{0}C followed by repeated centrifugation as detailed above. 3 - 4 droplets of cell suspension in fixative was transferred to wet microscope slides, air-dried and heated for 1 h at +90^{0}C. Chromosomes were visualized by the standard GTG-banding technique using 0,005% trypsin/phosphate buffer (pH 6,8) solution for 1 min and 3% Giemsa stain for 5 min. This analysis was performed in the E. Gulbja laboratory (Latvia) by I.Grīviņa.

2.5. Immunocytochemistry

The immunocytochemistry method for the detection of cell surface markers was done as follows. After P3 ASCs were plated onto 8 well plastic chamber slides. After 48 h the cells were washed with PBS (+37^{0}C) and blocked in a 6% BSA (Sigma-Aldrich, Germany)/PBS solution for 1 h at RT. Primary antibodies (mouse monoclonal anti-CD34 (Abcam, UK), anti-CD45 (EMD Millipore, USA), anti-CD73 (Invitrogen, USA), anti-CD90 (EMD Millipore, USA) and anti-CD105 (EMD Millipore, USA)) were diluted in a 1% BSA/PBS (1:100) and incubated for 1,5 h at RT. After washing with 1% BSA/PBS, secondary antibodies (goat anti-mouse IgG (Fab specific; FITC) (Sigma-Aldrich, Germany) and anti-mouse IgM (Alexa Fluor 488) (Life Technologies, UK)) diluted in a 1% BSA/PBS (1:200) were applied in dark for 1 h at RT. The cells were washed with PBS and incubated with wheat germ agglutinin (Alexa Fluor®633 conjugated) (Life Technologies, UK) (10 μg/ml) for 10 min at RT. After repeated washing the cells were fixed with 3,7% formaldehyde (Sigma-Aldrich, Germany) for 20 min at +37^{0}C. Cell nuclei were counterstained with DAPI (4 μg/ml) (Sigma-Aldrich, Germany) for 7 min. The samples were mounted in ProLong Antifade reagent (Life Technologies, UK) and kept in dark for 12 h at +4^{0}C. Fluorescence microscope DM 6000B (Leica, Germany) and laser scanning confocal system TCS SP2 SE (Leica, Germany) were used for the analysis of obtained samples.

To identify the expression of intracellular pluripotency markers the ASCs from P4 were grown onto 13 mm uncoated glass coverslips. When adherent ASC bodies started to form, the immunocytochemistry was performed as follows: the coverslips were gently washed with prewarmed PBS, fixed in cold methanol (Sigma-Aldrich, Germany) for 10 min at -20^{0}C and 10 times dipped in ice cold acetone. After extensive washing with 1x Tris-buffered saline (TBS), cells were blocked in 1% BSA/TBS solution for 15 min at room temperature. Primary antibodies (mouse monoclonal anti-NANOG (Sigma-Aldrich, Germany) and anti-OCT4A (sc-5279) (Santa Cruz Biotechnology, USA)) were diluted in 1% BSA/TBS (1:100 and 1:75 respectively) and incubated overnight at 4^{0}C. In the next day cells were washed with 1x TBS and secondary goat anti-mouse Alexa Fluor 488 antibody (Life Technologies, UK), diluted in 1x TBS 1:300, was applied in dark for 40 min at room temperature. The samples were mounted in ProLong Gold Antifade reagent with DAPI (Life Technologies, UK) and analysed

after 12 hours using laser scanning confocal system TCS SP2 SE.

Additionally goat polyclonal anti-OCT4B (sc-8630) (Santa Cruz Biotechnology, USA) antibody (dilution 1:500) and rabbit polyclonal anti-NANOG (Santa Cruz Biotechnology, USA) antibody (dilution 1:150) with respective secondary rabbit anti-goat IgG Cy3 (Sigma-Aldrich, Germany) (dilution 1:400) and goat anti-rabbit IgG Cy3 (Sigma-Aldrich, Germany) (dilution 1:200) antibodies were used on monolayer ASC culture of the donor No.4.

To detect the intracellular markers confirming the differentiation of ASCs into a pancreatic lineage, the following immunocytochemistry method was used. The cells were fixed with 3,7% formaldehyde for 15 min at room temperature (for anti-SOX17, anti-INS, anti-GCG, anti-NGN3, anti-C-peptide and anti-SST antibodies) or with cold methanol for 10 min at -20^{0}C (for anti-PDX1 antibody). After double washing with 1x PBS, the cells were further incubated in 1x PBS for 15 min at room temperature. Formaldehyde fixed samples were additionally permeabilized in 0,25% Triton-X100 (Sigma-Aldrich, Germany)/PBS solution for 20 min at room temperature. For a blocking of all samples, a 6% BSA/PBS solution was used for 30 min at room temperature. Primary antibodies (rabbit polyclonal anti-SOX17, anti-PDX1, anti-NGN3 (Santa Cruz Biotechnology, USA), anti-C-peptide, anti-SST (Abcam, UK) and mouse monoclonal anti-INS (Santa Cruz Biotechnology, USA), anti-GCG (Abcam, UK)) were diluted in 1% BSA/PBS 1:100 and incubated overnight at +4^{0}C. In the next day cells were washed three times with 1x PBS and secondary goat anti-rabbit Alexa 594 or goat anti-mouse IgG (H+L) Alexa 488 antibodies (Life Technologies, UK), diluted in 1% BSA/PBS 1:200, were applied in dark for 60 min at room temperature. After extensive washing, the samples were mounted in ProLong Gold Antifade reagent with DAPI and analysed after 24 hours using fluorescence microscope DM 3000 (Leica, Germany).

For each immunocytochemical staining negative control sample with secondary antibody only was always performed, allowing to subtract possible background staining caused by secondary antibody.

2.6. Multi-colour flow cytometry

Flow cytometry was performed on ASCs of the donor No.4 at P2, P3, P4, P5, and P8. After more than 4 years of cryopreservation, ASCs of each passage were rapidly thawed, resuspended in 2 ml of PBS, centrifuged for 5 min at 600 x g and used for immunostaining. Fluorochrome-labeled anti-human monoclonal antibodies to HLA-DR-V450, CD14/CD19/CD45 cocktail-V500, CD29-PerCP-Cy5.5, CD44-APC-H7 (BD, USA) and CD34-FITC, CD105-PE, CD73-PE-Cy7, CD90-APC (eBioscience, USA) were used for 8-colour flow cytometric analysis. Corresponding isotype controls for gate setting were included in every experiment. In addition, cell viability in every sample was tested using Syto16 fluorescent nucleic acid stain (Life Technologies, UK) at FITC channel. Cells were stained as recommended by the manufacturers, washed with PBS, and analysed by 3-laser BD FACSCanto II flow cytometer (BD, USA) using FACSDiva v6.1.3 software. Obtained results were analysed and presented using Infinicyt v1.5.0 (Cytognos, Spain) software. The flow cytometry was performed by S.Ņikuļšins and U.Bērziņš.

2.7. Total RNA extraction

RNA was extracted from ASCs using TRI Reagent (Sigma-Aldrich, Germany) according to the manufacturer's instructions. Quantity and quality of the samples were assessed by measuring the concentration of total RNA and A260/A280 ratio using NanoDrop® ND-1000 spectrophotometer (Thermo Scientific, USA) as well as by visual evaluation in 1% TBE agarose gel.

2.8. DNase I treatment and cDNA synthesis

1 μg of total RNA of ASCs was treated with 1 U RNase-free DNase I (Thermo Scientific, Lithuania) for 30 min at +37^{0}C to remove traces of genomic DNA. After the measurement of concentration of DNase-treated sample with NanoDrop® ND-1000 spectrophotometer, 500 ng of RNA were reverse transcribed into cDNA with oligo(dT)$_{18}$ primers using RevertAid first strand cDNA synthesis kit (Thermo Scientific, Lithuania) in a total volume of 20 μl according to the manufacturer's instructions. Minus reverse transcriptase (RT) sample was also prepared in the same manner by omitting RT from the reaction.

To obtain cDNA from human pancreas, commercially available total RNA of normal adult pancreas (BioChain, USA) was used according to the above-mentioned method. Except in this case DNase I treatment was not performed, since it was already completed by manufacturer.

Commercially available cDNA of ESCs (from total RNA at 10 ng/μl) from Human ESC Germ Layer PCR Kit (EMD Millipore, USA) was exploited as a positive control for detection of pluripotency marker genes using RT-PCR.

2.9. Reverse transcription polymerase chain reaction (RT-PCR)

RT-PCR was performed to detect expression of a housekeeping gene *β-Actin* and pluripotency marker genes *OCT4A*, *NANOG*, and *SOX2*. Each RT-PCR reaction contained 1 μl of ASC cDNA template or 2,5 μl of ESC cDNA template to yield equal amount of input cDNA, primer pairs (synthesized at Metabion, Germany) at a final concentration of 400 nM (for *β-Actin*) or 200 nM (for *OCT4A*, *NANOG*, *SOX2*), 12,5 μl of 2x PCR Master Mix containing *Taq* DNA polymerase (Thermo Scientific, Lithuania) and nuclease-free water (Thermo Scientific, Lithuania) to 25 μl. The primer sequences used in RT-PCR are listed in Table 2.9.1. Reactions were carried out in a GeneAmp PCR System 9700 thermal cycler (Applied Biosystems, USA) under the following cycling conditions: 40 cycles (30 cycles for *β-Actin*) of 94^{0}C for 30 s, 60^{0}C - 65^{0}C (Table 2.9.1.) for 30 s and 72^{0}C for 30 s, with a final extension of 72^{0}C for 5 min. Minus RT controls as well as non-template control were run each time to inspect for possible contamination. PCR products were separated using a 3% TAE agarose gel electrophoresis method.

2.10. Purification and sequencing of RT-PCR products

In order to prepare RT-PCR products for sequencing, 3 μl of each RT-PCR product were incubated for 60 min at +37^{0}C with 0,5 μl of Exonuclease I (20 U/μl) (Thermo Scientific, Lithuania), 1 μl of Shrimp Alkaline Phosphatase (1 U/μl) (Thermo Scientific, Lithuania) and 2,5 μl of DEPC treated water (Thermo Scientific, Lithuania) followed by 15 min heating at +85^{0}C. 3 ng of the purified product were used for a direct sequencing in a 20 μl final reaction volume containing 4 μl of 5x sequencing buffer, 1 μl of ABI PRISM BigDye Terminator v.3.1 Ready Reaction Mix (Applied Biosystems, USA) and primer at a final concentration of 250 nM. The RT-PCR product identity was determined by 3130xl Genetic Analyser (Applied Biosystems, USA).

2.11. Quantitative real-time RT-PCR

Real-time RT-PCR was used to detect the expression of surface marker genes and genes involved in pancreatic differentiation. It was carried out using MiniOpticon Real-time PCR System (Bio-Rad, USA). Each reaction contained 1 μl of 9-fold diluted cDNA template,

Table 2.9.1. Primer sequences used in PCR analysis.

Analysis	Gene	Primer sequence (5' → 3')	Annealing temperature (^{0}C)	Reference
Housekeeping genes	β-Actin	Fw: GAGCTACGAGCTGCCTGAC Rw: GGATGCCACAGGACTCCATG	60	
	GUSB	Fw: CTGCATCACCACATGCAGGTG Rw: GAGTTGCTCACAAAGGTCACAGG	60	
	YWHAZ	Fw: CTACGACGTCCCTCAAACCTTG Rw: CAGGCTGCCATGTCATCATATCG	60	
Pluripotency genes	NANOG_1	Fw: CTTCCTCCATGGATCTGCTTATTCA Rw: CAGGTCTTCACCTGTTTGTAGCTGAG	60	
	NANOG_2	Fw: GCTTGCCTTGCTTTGAAGCA Rw: TTCTTGACCGGGACCTTGTC	60	EMD Millipore kit
	OCT4A	Fw: GATGGCGTACTGTGGGCCC Rw: TGGGACTCCTCCGGGTTTTG	65	Liedtke et al. 2007
	SOX2	Fw: GTACTGGCGAACCATCTCTGTG Rw: CCAACGGTGTCAACCTGCATG	65	
Surface marker genes	CD29	Fw: GAGAAGGATGTTGACGACTGTT Rw: CAGTGGGACACTCTGGATTCT	60	
	CD44	Fw: CCTCTGCAAGGCTTTCAATA Rw: CTTCTATGAACCCATACCTGC	60	
	CD73	Fw: CAGCATTCCTGAAGATCCAAG Rw: GATTGAGAGGAGCCATCCAG	60	
	CD90	Fw: GTCCTCTACTTATCCGCCTTC Rw: GACCAGTTTGTCTCTGAGCAC	58	
	CD105	Fw: CTCAAGACCAGGAAGTCCATA Rw: GATGAGGAAGGCACCAAAG	60	
Genes involved in pancreatic differentiation	WNT3	Fw: GCACGACTATCCTGGACCAC Rw: GAGGAAGTCACCGATGGCAC	60	
	SOX17	Fw: GCATGACTCCGGTGTGAATCT Rw: CACACGTCAGGATAGTTGCAGT	60	
	SOX17_C	Fw: AGGAAATCCTCAGACTCCTGGGTT Rw: CCCAAACTGTTCAAGTGGCAGACA	60	Chandra et al. 2011
	CK19	Fw: ATATGAGGTCATGGCCGAGCAGAA Rw: ACTGCAGCTCAATCTCAAGACCCT	60	Chandra et al. 2011
	FOXA2	Fw: GGGAGCGGTGAAGATGGA Rw: TCATGTTGCTCACGGAGGAGTA	60	D'Amour et al. 2006
	FOXA2	Fw: GCGACCCCAAGACCTACAG Rw: GGTTCTGCCGGTAGAAGGG	60	Lee et al. 2008
	CXCR4	Fw: CACCGCATCTGGAGAACCA Rw: GCCCATTTCCTCGGTGTAGTT	60	D'Amour et al. 2006
	HNF1B	Fw: GGAATGCAACAGGGCAGAATGT Rw: CAAACCAGTTGTAGACACGGAC	60	
	HNF1A	Fw: GAGTGCAATAGGGCGGAATG Rw: CAGTTGTAGACACGCACCTC	60	
	HNF4A	Fw: CTCGGAGCCACCAAGAGATC Rw: CTCGTCAAGGATGCGTATGGA	60	

Analysis	Gene	Primer sequence (5' → 3')	Annealing temperature (^{0}C)	Reference
Genes involved in pancreatic differentiation	PDX1	Fw: GATGAAGTCTACCAAAGCTCACGC Rw: GGAACTCCTTCTCCAGCTCTAGC	60	Jiang et al. 2007
	NKX6-1	Fw: CTGTACCCCTCATCAAGGATC Rw: GTTCGAAAGTCTTCTCCAGGG	60	
	PAX6	Fw: GTGAATGGGCGGAGTTATGAT Rw: GAACTGGAACTGACACACCAG	60	
	MNX1	Fw: CTCTGGAGCCGCCATTCTG Rw: CAGCAGTTTGAACGCTCGTG	60	
	INS	Fw: GGGAGGCAGAGGACCTG Rw: CCACAATGCCACGCTTCT	60	
	SST	Fw: CAGACTCCGTCAGTTTCTGC Rw: CATCATTCTCCGTCTGGTTGG	60	
	PPY	Fw: GGCCTAGGTATGGGAAAAGAC Rw: AGTCGTAGGAGACAGAAGGTG	60	
	ISL1	Fw: GTGGGCTGTTCACCAACTGTA Rw: GTGAATCTGATTGCCGCAACC	60	
	GCG	Fw: CTTGGTGCAGAAGTACAGAG Rw: CTGCTGTCTTCTGGTAGTGT	60	
	PTF1A	Fw: CAGAAGGTCATCATCTGCCATC Rw: AGTCCATGAGAGAGAGTGTCCT	60	

primer pairs (synthesized at Metabion, Germany) as listed in Table 2.9.1. at a final concentration of 400 nM, 12,5 µl 2x ABsolute Blue QPCR SYBR Green Low ROX Mix (Thermo Scientific, Lithuania) and nuclease-free water to 25 µl. PCR cycling conditions included a 95^{0}C heating step for 15 min to activate DNA polymerase, then 40 cycles of 95^{0}C for 30 s, 58^{0}C - 60^{0}C (Table 2.9.1.) for 30 s and 72^{0}C for 30 s. A melting curve was generated at the end of every run to ensure the amplification of a single product. Minus RT controls as well as non-template control were run each time to inspect for possible contamination. For the analysis of relative gene expression $2^{-\Delta C_T}$ method was used.

PCR efficiencies of each primer pair used to detect the expression of surface marker genes were obtained from standard curves using 3-fold dilution series of cDNA sample. PCR efficiencies of all primer pairs used in the experiment were in a range from 93% to 99%. Each reaction was run in triplicate.

For the samples obtained during pancreatic differentiation of ASCs only initial screening was performed, meaning that PCR efficiencies for each primer pair were not determined and no replicates were run. The differentiation samples were compared to human pancreas sample that served as a positive control.

2.12. Detection of alkaline phosphatase activity

Alkaline phosphatase activity was tested in the monolayer ASC culture and ASC bodies after the transfer to a new adherent plastic culture flask. The cell samples were fixed in 3,7% formaldehyde for 15 min at +4^{0}C, washed with distilled water and air-dried. To prepare a working solution, a Fast Blue BB salt (Lach-Ner, Czech Republic) was dissolved in a stock solution (58,3 mM naphthol AS phosphate (Lach-Ner, Czech Republic) dissolved in a dimethyl sulfoxide (final concentration 0,583 mM), 90 mM Tris-HCl (Sigma-Aldrich, Germany), pH 9,0-9,2, 5 mM $MgCl_2$ (Merck Millipore, Germany)) to a concentration of 1

mg/ml right before use. Addition of levamisole (Serva, Germany) to the working solution at a final concentration of 1 mM served as a negative control. After filtration the naphthol AS phosphate/Fast Blue BB working solution was added to the cells and incubated in dark for 25 min at room temperature followed by washing with distilled water.

2.13. *In vitro* differentiation of ASCs

To induce differentiation of ASCs into adipocytes, osteoblasts and chondroblasts, the ASCs were cultured in the appropriate induction medium at $+37^0$C, 5% CO_2. Non-induced cells were maintained in a control medium. Medium was changed every third day. Three replicates for each differentiation were always tested.

2.13.1. Adipogenic differentiation

For adipogenic differentiation, ASCs were cultured in DMEM (high glucose) (Life Technologies, UK) supplemented with 10% FBS (Life Technologies, UK), 2 mM L-glutamine, 10 μg/ml human insulin (Life Technologies, UK), 1 μM dexamethasone (Sigma-Aldrich, Germany), 100 μM indomethacin (Sigma-Aldrich, Germany), 0,5 mM isobutyl-methylxanthine (Sigma-Aldrich, Germany), and 5 μg/ml gentamicin (Life Technologies, UK). DMEM (high glucose) supplemented with 10% FBS, 2 mM L-glutamine, and 5 μg/ml gentamicin was used as a control medium. Differentiation was confirmed on day 16. Differentiated cells were fixed with 10% formaldehyde for 1 h at RT and washed with 60% isopropyl alcohol. After incubation in a 0,21% Oil Red O (Sigma-Aldrich, Germany) solution for 10 min at RT, the cells were counterstained with hematoxylin GILL No.3 (Sigma-Aldrich, Germany) for 3 min.

2.13.2. Osteogenic differentiation

To promote osteogenic differentiation, ASCs were treated with DMEM (low glucose, without L-glutamine and phenol red) (Life Technologies, UK) supplemented with 10% FBS, 2 mM L-glutamine, 10 mM glycerol-2-phosphate (Sigma-Aldrich, Germany), 0,1 μM dexamethasone, 50 μM L-ascorbic acid (Sigma-Aldrich, Germany), and 5 μg/ml gentamicin. Control medium consisting of DMEM (low glucose), 10% FBS, 2 mM L-glutamine, and 5 μg/ml gentamicin was used for non-induced cells in osteogenic, as well as chondrogenic differentiation. Osteogenesis was demonstrated on day 28 using Alizarin Red S (Sigma-Aldrich, Germany) to detect calcified extracellular matrix. Before staining cells were fixed with 3,7% formaldehyde for 1 h at RT followed by staining with 2% Alizarin Red S solution (pH 4,1 – 4,3) for 4 min.

2.13.3. Chondrogenic differentiation

For chondrogenic differentiation, 10 μl of ASCs suspension (concentration $8x10^6$ cells/ml) were allowed to attach to a plastic plate for 30 min at $+37^0$C, 5% CO_2. Then control medium or chondrogenic differentiation medium consisting of DMEM (low glucose, without L-glutamine, and phenol red) supplemented with 10% FBS, 2 mM L-glutamine, 1x insulin-transferrin-selenium-plus (BD, USA), 50 μM L-ascorbic acid, 40 μg/ml L-proline (Sigma-Aldrich, Germany), 0,1 μM dexamethasone, 10 ng/ml recombinant human transforming growth factor β3 (Life Technologies, UK), and 5 μg/ml gentamicin was added. After 29 days of chondrogenic induction, differentiated cells from P3 were fixed with 3,7% formaldehyde for 1 h at RT and then stained with 1% Alcian Blue (pH 2,5) (Sigma-Aldrich, Germany) for

30 min. When ASCs from P6 of the donor No.4, as well as ASCs of the donor No.5, were differentiated into chondrogenic lineage, the formed cell aggregates were collected, fixed in 10% formaldehyde overnight, embedded in paraffin, sectioned, and stained with 1% Alcian Blue in 0,1 N HCl (pH~1,3) for 30 min followed by washing with 0,1 N HCl.

2.13.4. Differentiation into insulin-producing cells

For the *in vitro* differentiation of ASCs into insulin-producing cells the following 5 protocols were used (for the overview, see Table 2.13.4.1.):

2.13.4.1. Protocol 1

The ASCs from the donor No.4 after P4 were seeded at a density of $3{,}125 \times 10^4$ cells per cm^2 and allowed to adhere for 24 h at $+37^0$C, 5% CO_2 in the cell culture medium containing 5% AS. On a next day the cells were washed with PBS to remove traces of serum and the first stage differentiation medium (DMEM/F12 containing 4 nM Activin A (Life Technologies, UK), 0,5 mM 2-mercaptoethanol (Life Technologies, UK), 1 mM sodium butyrate (Sigma-Aldrich, Germany), 2 mM L-glutamine, 100 U/ml : 100 μg/ml penicillin - streptomycin) and the first stage control medium (DMEM/F12 containing 2 mM L-glutamine, 100 U/ml : 100 μg/ml penicillin - streptomycin) were applied. After 3 days the second stage differentiation medium (DMEM/F12 containing 50 ng/ml recombinant human FGF10 (R&D Systems, UK), 1x B-27 supplement (Life Technologies, UK), 2 μM retinoic acid (Alfa Aesar, UK), 2 mM L-glutamine, 100 U/ml : 100 μg/ml penicillin - streptomycin) and the second stage control medium (DMEM/F12 containing 1x B-27 supplement, 2 mM L-glutamine, 100 U/ml : 100 μg/ml penicillin - streptomycin) were applied. The medium was changed every third day. After 9 days the third stage differentiation medium (DMEM/F12 containing 1x B-27 supplement, 10 mM nicotinamide (Sigma-Aldrich, Germany), 10 nM exendin-4 (Sigma-Aldrich, Germany), 1 μM DAPT (Sigma-Aldrich, Germany), 2 mM L-glutamine, 100 U/ml : 100 μg/ml penicillin - streptomycin) was applied. The third stage control medium was identical to the second stage control medium. After 21 days in the third stage differentiation medium the differentiation protocol was completed.

2.13.4.2. Protocol 2

The ASCs from the donor No.4 after P5 were grown at $+37^0$C, 5% CO_2 in the cell culture medium containing 5% AS until they reached 60% confluence. Before differentiation the cells were washed with PBS and grown in a pre-differentiation medium (DMEM/F12 containing 20 ng/ml recombinant human EGF (Sigma-Aldrich, Germany), 10 ng/ml bFGF, 2 mM L-glutamine, 100 U/ml : 100 μg/ml penicillin - streptomycin) for 2 days. Afterwards the first stage differentiation medium (DMEM/F12 containing 4 nM Activin A, 0,5 mM 2-mercaptoethanol, 1 mM sodium butyrate, 2 mM L-glutamine, 100 U/ml : 100 μg/ml penicillin - streptomycin) and the control medium (DMEM/F12 containing 2 mM L-glutamine, 100 U/ml : 100 μg/ml penicillin - streptomycin) were applied and the cells were further differentiated at $+37^0$C, 5% CO_2 and 60% O_2. To maintain such a high level of oxygen in a cell incubation chamber, the Xvivo System (BioSpherix, USA) was used for the whole differentiation process. The control medium throughout the Protocol 2 was identical. The medium was changed every third day. After 3 days the second stage differentiation medium (DMEM/F12 containing 50 ng/ml recombinant human FGF10, 2 μM retinoic acid, 2 mM L-glutamine, 100 U/ml : 100 μg/ml penicillin – streptomycin) was applied. After 6 days the third stage differentiation medium (DMEM/F12 containing 10 mM nicotinamide, 10 nM exendin-4, 1 μM DAPT, 2 mM L-glutamine, 100 U/ml : 100 μg/ml penicillin - streptomycin) was applied. The cell differentiation in the third stage differentiation medium was discontinued after 12 days due to a high rate of cell detachment.

Table 2.13.4.1. Overview of experimental protocols used to differentiate ASCs into insulin-producing cells.

Days	1	2	3	4	5	6	7	8	9	10	11	12	13	14	15	16	17	18	19	20	21	22	23	24	25	26	27	28	29	30	31	32	33	Reference
Protocol 1	Activin A 2-Mercaptoethanol Sodium butyrate			FGF10 B-27 Retinoic acid									B-27 Nicotinamide Exendin-4 DAPT																						
Protocol 2	EGF bFGF			Activin A 2-Mercaptoethanol Sodium butyrate 60% O_2						FGF10 Retinoic acid 60% O_2			Nicotinamide Exendin-4 DAPT 60% O_2																						
Protocol 3	Activin A bFGF Exendin-4			Activin A bFGF Exendin-4 FBS						Activin A Exendin-4 Nicotinamide FBS																									Kang et al. 2011
Protocol 4	Activin A BSA Insulin Transferrin Sodium butyrate 2-Mercaptoethanol bFGF			BSA Insulin Transferrin Taurine						BSA Insulin Transferrin Taurine Exendin-4 Nicotinamide Non-essential amino acids																									Chandra et al. 2011
Protocol 9	Activin A LY294002 CHIR99021 FBS Sodium butyrate 2-Mercaptoethanol			Activin A LY294002 FBS Sodium butyrate 2-Mercaptoethanol						B-27 Retinoic acid FGF10 FBS			B-27 Nicotinamide Exendin-4 Dexamethasone FBS																						

2.13.4.3. Protocol 3

The differentiation protocol was adapted from Kang et al. 2011. The ASCs from the donors No.3 and No.4 after P3 were seeded at a density of $5x10^4$ cells per well (6 well plates) and grown at $+37^0$C, 5% CO_2 in the cell culture medium (DMEM low glucose (Life Technologies, UK) containing 10% FBS (Life Technologies, UK), 20 ng/ml bFGF, 100 U/ml : 100 µg/ml penicillin - streptomycin) until they reached 80% confluence. The cells were grown in the first stage differentiation medium (DMEM high glucose (Life Technologies, UK) containing 4 nM Activin A, 20 ng/ml bFGF, 10 nM exendin-4, 100 U/ml : 100 µg/ml penicillin - streptomycin) and the first stage control medium (DMEM high glucose containing 100 U/ml : 100 µg/ml penicillin - streptomycin) for 3 days. Afterwards the second stage differentiation medium and the second stage control medium (both the same as in the first stage only each supplemented with 10% FBS) were applied. After 3 days the third stage differentiation medium (DMEM low glucose containing 4 nM Activin A, 10 mM nicotinamide, 10 nM exendin-4, 10% FBS, 100 U/ml : 100 µg/ml penicillin – streptomycin) and the third stage control medium (DMEM low glucose containing 10% FBS, 100 U/ml : 100 µg/ml penicillin – streptomycin) were applied. The medium was changed every third day. After 15 days in the third stage differentiation medium the differentiation protocol was completed.

2.13.4.4. Protocol 4

The differentiation protocol was adapted from Chandra et al. 2011. The ASCs from the donors No.3 and No.4 after P3 were seeded onto low attachment plates at a density of $7,5x10^5$ cells per well (6 well plates) and grown at $+37^0$C, 5% CO_2 in the first stage differentiation medium (DMEM/F12 containing 4 nM Activin A, 50 µM 2-mercaptoethanol, 1 mM sodium butyrate, 1% BSA (Sigma-Aldrich, Germany), 2 ng/ml bFGF, 5 µg/ml human recombinant insulin (Life Technologies, UK), 5 µg/ml human transferrin (Sigma-Aldrich, Germany), 100 U/ml : 100 µg/ml penicillin – streptomycin) or in the first stage control medium (DMEM/F12 containing 1% BSA, 100 U/ml : 100 µg/ml penicillin – streptomycin) for 3 days. Afterwards the second stage differentiation medium (DMEM/F12 containing 1% BSA, 5 µg/ml human recombinant insulin, 5 µg/ml human transferrin, 0,3 mM taurine (Sigma-Aldrich, Germany), 100 U/ml : 100 µg/ml penicillin – streptomycin) was applied. The second stage control medium was identical to the first stage control medium. After 3 days the third stage differentiation medium (DMEM/F12 containing 1,5% BSA, 5 µg/ml human recombinant insulin, 5 µg/ml human transferrin, 3 mM taurine, 100 nM exendin-4, 1 mM nicotinamide, 1x non-essential amino acids (Life Technologies, UK), 100 U/ml : 100 µg/ml penicillin – streptomycin) and the third stage control medium (DMEM/F12 containing 1,5% BSA, 100 U/ml : 100 µg/ml penicillin – streptomycin) were applied. The medium was changed every third day. After 15 days in the third stage differentiation medium the differentiation protocol was completed.

2.13.4.5. Protocol 9

The ASCs from the donors No.4 and No.8 after P3 were grown at $+37^0$C, 5% CO_2 in the cell culture medium (DMEM/F12 containing 10% FBS, 20 ng/ml bFGF, 2 mM L-glutamine, 100 U/ml : 100 µg/ml penicillin - streptomycin) until they reached 80% confluence. Afterwards the cells were grown in the first stage differentiation medium (DMEM/F12 containing 4 nM Activin A, 0,5 mM 2-mercaptoethanol, 1 mM sodium butyrate, 0,2% FBS, 50 µM LY294002 (Cayman Chemical, USA), 3 µM CHIR99021 (Cayman Chemical, USA), 100 U/ml : 100 µg/ml penicillin - streptomycin) or the first stage control medium (DMEM/F12 containing 0,2% FBS, 100 U/ml : 100 µg/ml penicillin - streptomycin) for 1 day. Then the second stage differentiation medium (DMEM/F12 containing 4 nM Activin A, 0,5 mM 2-mercaptoethanol, 1 mM sodium butyrate, 2% FBS, 50 µM LY294002, 100 U/ml : 100

μg/ml penicillin - streptomycin) and the second stage control medium (DMEM/F12 containing 2% FBS, 100 U/ml : 100 μg/ml penicillin – streptomycin) were applied. The control medium throughout the next stages of the Protocol 9 was identical to the second stage control medium. After 3 days the third stage differentiation medium (DMEM/F12 containing 1x B-27 supplement, 2 μM retinoic acid, 50 ng/ml FGF10, 2% FBS, 100 U/ml : 100 μg/ml penicillin - streptomycin) was applied. The medium was changed every third day. After 5 days the fourth stage differentiation medium (DMEM/F12 containing 1x B-27 supplement, 10 mM nicotinamide, 10 nM exendin-4, 10 μM dexamethasone, 2% FBS, 100 U/ml : 100 μg/ml penicillin – streptomycin) was applied. After 12 days in the fourth stage differentiation medium the differentiation protocol was completed.

2.13.5. Differentiation into cells of endodermal lineage

For the *in vitro* differentiation of ASCs into cells of endodermal lineage the ASCs from the donors No.4 and No.9 after P3 were grown at +37^{0}C, 5% CO_2 in the cell culture medium (DMEM/F12 containing 10% FBS, 20 ng/ml bFGF, 2 mM L-glutamine, 100 U/ml : 100 μg/ml penicillin - streptomycin) until they reached 80% confluence. Afterwards the following 4 protocols were used (for the overview, see Table 2.13.5.1.):

2.13.5.1. Protocol 5

The cells were grown in the first stage differentiation medium (DMEM/F12 containing 4 nM Activin A, 0,5 mM 2-mercaptoethanol, 1 mM sodium butyrate, 0,2% FBS, 50 μM LY294002, 3 μM CHIR99021, 100 U/ml : 100 μg/ml penicillin - streptomycin) or the first stage control medium (DMEM/F12 containing 0,2% FBS, 100 U/ml : 100 μg/ml penicillin - streptomycin) for 3 days. Then the second stage differentiation medium (DMEM/F12 containing 4 nM Activin A, 0,5 mM 2-mercaptoethanol, 1 mM sodium butyrate, 2% FBS, 50 μM LY294002, 100 U/ml : 100 μg/ml penicillin - streptomycin) and the second stage control medium (DMEM/F12 containing 2% FBS, 100 U/ml : 100 μg/ml penicillin - streptomycin) were applied. After 6 days in the second stage differentiation medium the differentiation protocol was completed.

2.13.5.2. Protocol 6

The differentiation protocol was adapted from Buang et al. 2012. The cells were grown in the first stage differentiation medium (DMEM high glucose containing 4 nM Activin A, 0,2% FBS, 10 mM nicotinamide, 10 nM exendin-4, 100 U/ml : 100 μg/ml penicillin - streptomycin) or the first stage control medium (DMEM/F12 containing 0,2% FBS, 100 U/ml : 100 μg/ml penicillin - streptomycin) for 3 days. For the next 4 days almost the same differentiation and control media were applied only 2% FBS was used instead of 0,2% FBS.

2.13.5.3. Protocol 7

The differentiation protocol was adapted from Gao et al. 2008. The cells were grown in the first stage differentiation medium (DMEM high glucose containing 10% FBS, 10 μM retinoic acid, 100 U/ml : 100 μg/ml penicillin – streptomycin) or in the first stage control medium (DMEM high glucose containing 10% FBS, 100 U/ml : 100 μg/ml penicillin - streptomycin) for 24 h. For the next 2 days the differentiation medium was replaced with the first stage control medium.

2.13.5.4. Protocol 8

The differentiation protocol was adapted from Sun Y. et al. 2007. The cells were grown in the first stage differentiation medium (DMEM high glucose containing 0,5 mM 2-mercaptoethanol, 100 U/ml : 100 μg/ml penicillin – streptomycin) or in the first stage control

medium (DMEM high glucose containing 100 U/ml : 100 µg/ml penicillin - streptomycin) for 2 days. Then the second stage differentiation medium (DMEM high glucose containing 1x non-essential amino acids, 20 ng/ml bFGF, 20 ng/ml EGF, 2x B-27 supplement, 2 mM L-glutamine, 100 U/ml : 100 µg/ml penicillin – streptomycin) or the second stage control medium (DMEM high glucose containing 2 mM L-glutamine, 100 U/ml : 100 µg/ml penicillin - streptomycin) were applied. After 8 days in the second stage differentiation medium the differentiation protocol was completed.

Table 2.13.5.1. Overview of experimental protocols used to differentiate ASCs into cells of endodermal lineage.

Days	1	2	3	4	5	6	7	8	9	10	Reference
Protocol 5	DMEM/F12 Activin A LY294002 CHIR99021 FBS Sodium butyrate 2-Mercaptoethanol			DMEM/F12 Activin A LY294002 FBS Sodium butyrate 2-Mercaptoethanol							
Protocol 6	DMEM high glucose Activin A FBS Nicotinamide Exendin-4										Buang et al. 2012
Protocol 7	DMEM high glucose FBS Retinoic acid	DMEM high glucose FBS									Gao et al. 2008
Protocol 8	DMEM high glucose 2-Mercaptoethanol		DMEM high glucose Non-essential amino acids bFGF EGF B-27								Sun Y. et al. 2007

3. Results and discussion

3.1. Characterization of ASC morphology and growth aspects

ASCs from fat tissue of the donor No.4 were isolated as described in section "Materials and Methods". Plastic-adherent cell population could be observed on the next day after isolation. Most of the cells were rounded, but few spindle-shaped cells with fibroblastoid morphology, characteristic to MSCs (Zuk et al. 2001, Romanov et al. 2005, Kern et al. 2006), were observed (Figure 3.1.1.A). A day later practically all cells exhibited typical MSC morphology (Figure 3.1.1.B) and after eight days of growth even monolayer of ASCs was formed (Figure 3.1.1.C). The first ten days ASCs were grown in a medium supplemented with 10% AS but this was reduced to 5% afterwards. In our study we substituted a FBS, which is routinely used to supplement most of the cell culture media, with an AS. Since ASCs have a significant therapeutic potential, all possible threats must be eliminated to ensure the safety of ASCs intended for the future clinical use. The greatest concerns arise about FBS. While dangers of prion diseases and zoonoses from the FBS are considered to be minimal (Doerr et al. 2003), it has been shown that 10^8 MSCs grown in the medium supplemented with 20% FBS would carry 7-30 mg of FBS proteins leading to possible autoimmune reaction against patient's own stem cells (Spees et al. 2004). To avoid this risk, we used AS instead and characterized various aspects of ASCs grown in such medium.

Figure 3.1.1. Morphology of ASCs from the donor No.4. (A) ASCs on the next day after isolation. (B) ASCs 2 days after isolation. (C) Monolayer of ASCs 8 days after isolation. Scale bar 100 μm (50 μm for Figure 3.1.1.A).

In order to characterize ASCs at subsequent passages, after the second passage cells were frozen and stored in a liquid nitrogen for two months. After thawing, ASCs were seeded onto tissue culture flasks (regarded as P3) and cultured as previously (Figure 3.1.2.A). When cells reached 80% confluence, they were trypsinized and subcultured, freezing a part of cells in parallel. During passaging the cells preserved their fibroblast-like morphology till inspected eighth passage (Figure 3.1.2.B, D), showing that ASCs could be easily and effectively cultured and propagated in the medium supplemented with 5% AS without the loss of their typical MSC morphology.

Figure 3.1.2. Morphology of ASCs from the donor No.4 at different passages. (A) ASCs at passage 3. (B) ASCs at passage 6. (C) ASCs at passage 8. Scale bar 100 μm.

To verify that obtained ASCs do not have any genetic abnormalities, karyotype analysis was performed after third passage for ASCs of the donor No.4. Karyotype of normal man (46, XY) was detected and changes in number or structure of chromosomes were not discovered (Figure 3.1.3.).

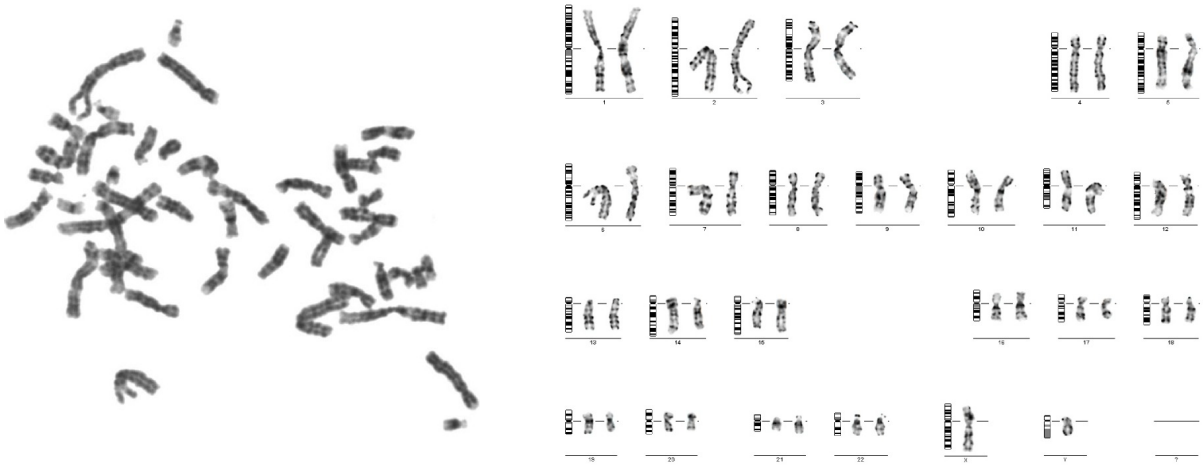

Figure 3.1.3. Karyotype of ASCs from the donor No.4 after the third passage. Number of metaphases analysed – 16. Author I.Grīviņa.

Under some presumed stress conditions the ASCs from the donor No.4 started to form cell aggregates. During a cultivation of ASCs from this donor we observed four different types of aggregates. The first and the most common type was plastic-adherent ASC aggregates (Figure 3.1.4.). The cells in a ASC monolayer started to congregate into clusters until all cells were assembled into distinct aggregates. The exact reason provoking this type of cell clustering is unknown. We assume that this was an ASC response to a stress caused by slight changes in the culture medium, growth environment or culture conditions. Similar plastic-adherent ASC aggregates were observed in the ASC cultures from few other donors, however, the occurrences and cell aggregate numbers were much lower.

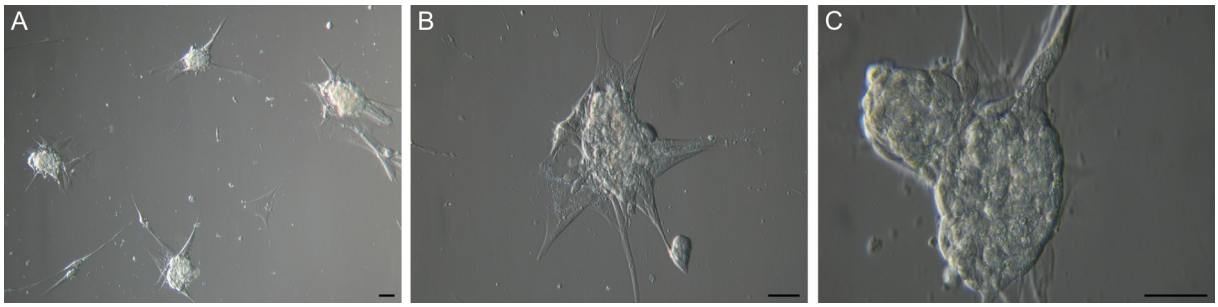

Figure 3.1.4. Plastic-adherent ASC aggregates of donor No.4 (A-C). Scale bar 50 µm.

The second type of ASC aggregates was detected only at early passages (P1-P3). Above the monolayer of ASCs, floating cell bodies were observed in the uppermost layer of the medium after each change of the fresh medium that also included a brief wash with a PBS. Initially they were detected as faint clumps (Figure 3.1.5.A) resembling dead cells. But the ASCs in these clusters continued to divide and grow (Figure 3.1.5.B) and started to form compact structures (Figure 3.1.5.C). These cell bodies began to congregate into clusters (Figure 3.1.5.D), eventually forming large aggregates of interconnected ASC bodies (Figure 3.1.5.E, F). Since the medium was changed every third day and the ASC bodies were removed together with the old medium, no more than 72 hours were needed for the formation of the observed large aggregates. Floating ASC aggregates in different sizes could be observed

simultaneously in each tissue culture flask. Both single bodies (Figure 3.1.6.A) and smaller or larger aggregates of ASC bodies (Figure 3.1.6.B, C) could be seen. Their dense structure and size made it possible to easily detect ASC aggregates even with a naked eye.

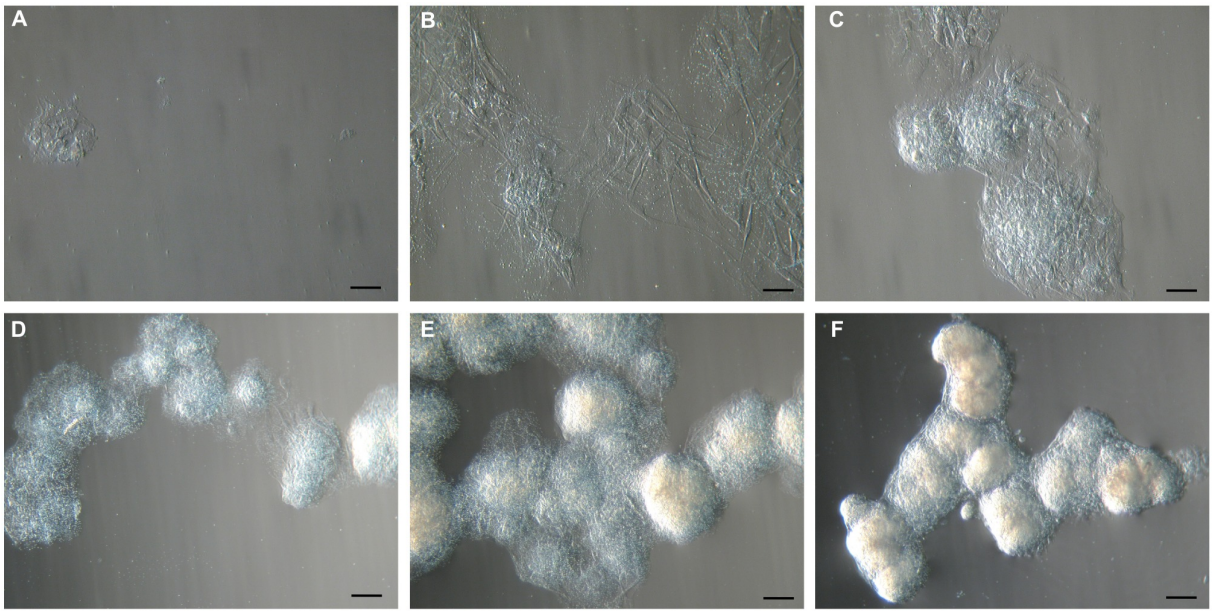

Figure 3.1.5. Formation of floating aggregates of ASC bodies. (A-F) Different stages of development of cell aggregates at P1. Scale bar 100 μm (50 μm for Figure 3.1.5.B).

Figure 3.1.6. Types of floating ASC bodies. (A) Single ASC body. (B) Small aggregate of ASC bodies. (C) Large aggregate of ASC bodies. Scale bar 100 μm (50 μm for Figure 3.1.6.A).

When individual floating ASC bodies were transferred onto new adherent plastic tissue culture flasks, they adhered to the surface within 24 hours. The new ASCs started to migrate out of the cell body soon after, ultimately covering the available growth surface and reducing the volume and density of initial ASC body (Figure 3.1.7.A-C). Since the size and compactness of original ASC bodies differed, it is not possible to precisely define the time needed for the ASC body to completely disappear forming new cell monolayer after transfer to the new tissue culture flask. Smaller ASC bodies can transform after a week, while bigger ASC bodies can still be observed after a month. This experiment showed that such culture medium where FBS is substituted with AS not only supports the formation of 3D bodies, but also facilitate growth of the new ASC monolayer after the body transfer onto new adherent culture flask.

In order to test the influence of medium on above-mentioned process, single floating ASC bodies were transferred onto new adherent plastic tissue culture flasks and cultivated in three different media. In one case the commercial medium MesenPRO RS™ (Life Technologies, UK) containing 2% FBS was used. For the other two experiments the cell

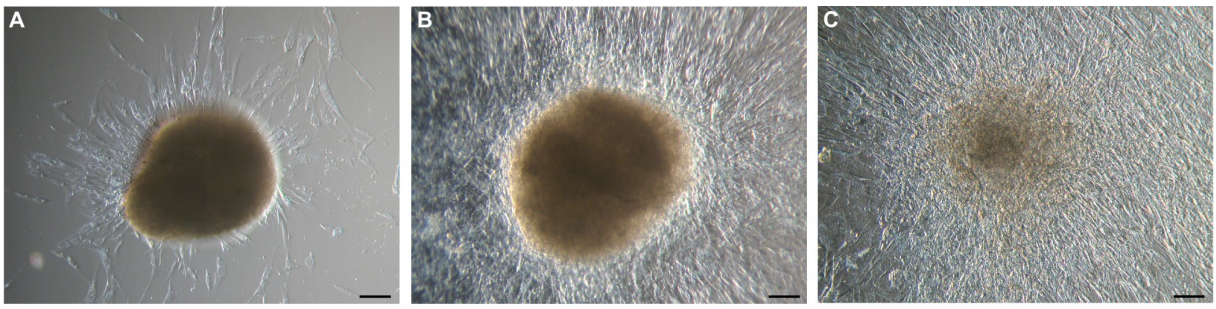

Figure 3.1.7. Cell growth after the transfer of single ASC bodies onto adherent cell culture plates. (A) ASC body after 3 days. (B) ASC body after 10 days. (C) ASC body after 30 days. Scale bar 100 μm.

growth medium was applied, but AS was substituted with 5% serum from different human donors (donors No.10 and No.11). After 48 hours most of the ASC bodies grown in the medium supplemented with human serum were attached to the surface and gradual expansion of spindle-shaped ASCs around the ASC body could be observed (Figure 3.1.8.A and D). In the MesenPRO RS™ medium none of the ASC bodies was adhered to the flask (Figure 3.1.8.G). Using commercial medium, four days were needed for few ASC bodies to attach to the surface and plastic-adherent cell growth (Figure 3.1.8.H), while in the medium containing human serum every ASC body was attached to the flask and dynamic expansion of cells could

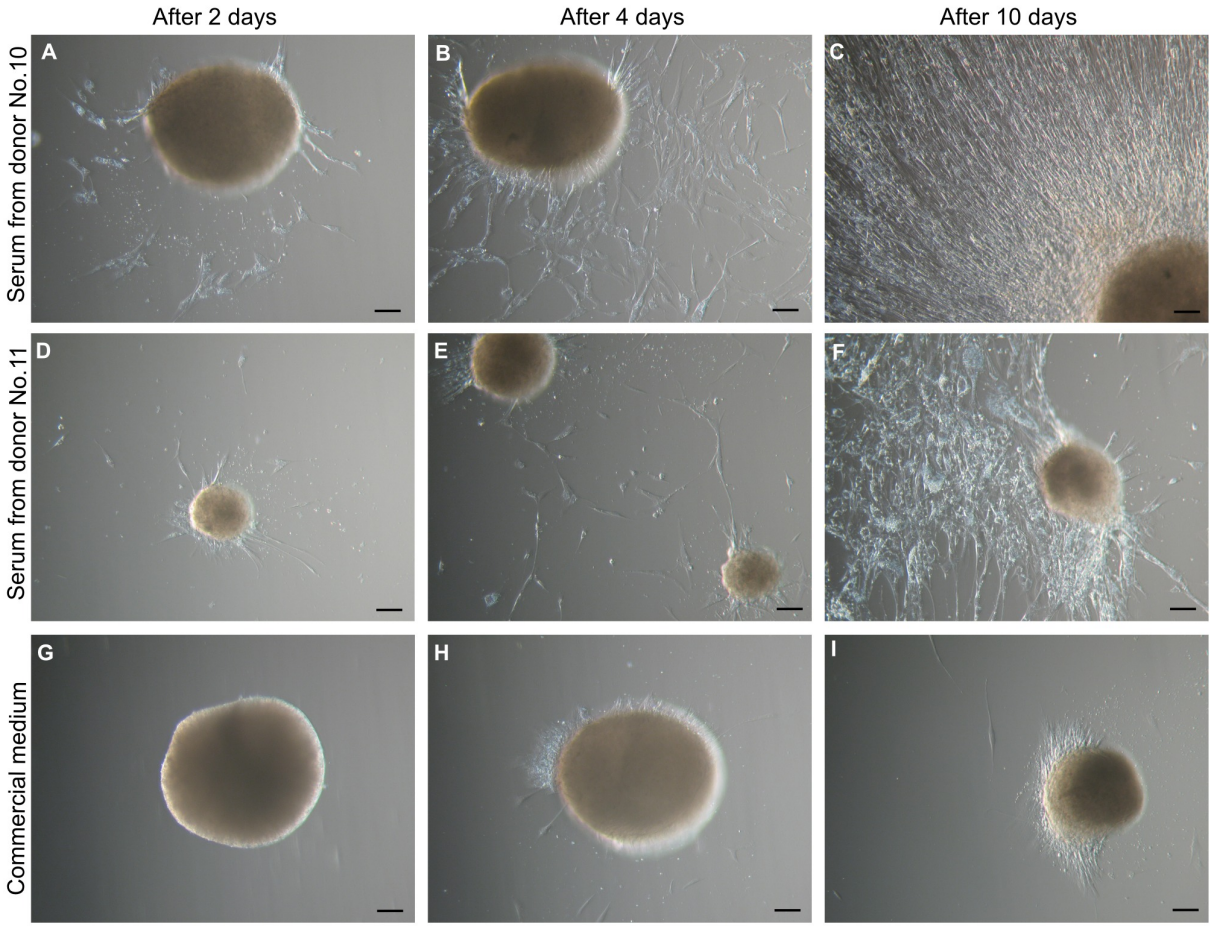

Figure 3.1.8. Cell growth in the different cell culture media after the transfer of ASC bodies onto adherent cell culture plates. (A-C) ASC body in the medium supplemented with 5% serum from donor No.10. (D-F) ASC body in the medium supplemented with 5% serum from donor No.11. (G-I) ASC body in the commercial medium MesenPRO RS™. Scale bar 100 μm.

be seen (Figure 3.1.8.B and E). After 10 days ASC bodies in the medium with 5% human serum were surrounded by extensive cell monolayer (Figure 3.1.8.C and F), whereas in the MesenPRO RS™ medium intense migration of ASCs out of the bodies was not observed (Figure 3.1.8.I) and few ASC bodies were still floating.

The third type of ASC aggregates was observed when ASCs were grown on an uncoated glass surface. In this case ASCs initially formed a monolayer and soon after started to cluster (Figure 3.1.9.A). More of the cells were huddled together creating an adherent ASC bodies (Figure 3.1.9.B). Eventually most of the ASCs were assembled into dense ASC bodies (Figure 3.1.9.C) that could remain adhered to the surface or detach and form floating ASC bodies. But contrary to the second type of ASC bodies, this type of floating bodies did not form aggregates.

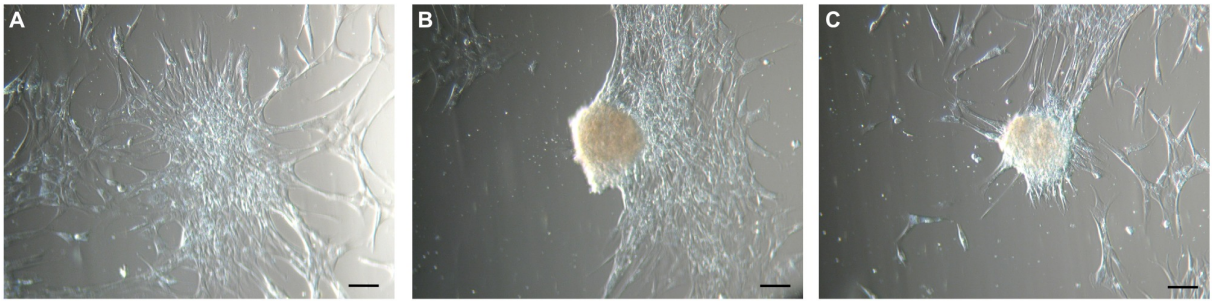

Figure 3.1.9. Formation of adherent ASC bodies onto a glass surface. (A) ASCs in a monolayer start to gather into clusters (day 2). (B) As more ASCs are congregated in the clusters, ASC bodies are formed (day 5). (C) Eventually most of the monolayer ASCs are clustered into dense bodies (day 8). Scale bar 100 μm.

The fourth type of ASC aggregates could be obtained when a cell culture medium was not changed for a prolonged time (7 – 10 days) (Figure 3.1.10.). Such stress conditions facilitated formation of floating ASC bodies, however, they differed from the floating ASC bodies observed during the early passages. In this case compact ASC bodies in different sizes were recognized in a medium, but different stages of development of cell bodies were not detected and they did not congregate into clusters and form large aggregates of interconnected ASC bodies. These ASC bodies could be easily collected and transferred onto new adherent plastic culture flask (Figure 3.1.11.A). Similarly to the second type of ASC aggregates, they rapidly adhered to the surface and within 12 hours new ASCs extensively migrated out of the cell body (Figure 3.1.11.B). 24 hours later most of the ASC aggregates had disappeared giving rise to a dense monolayer of ASCs (Figure 3.1.11.C).

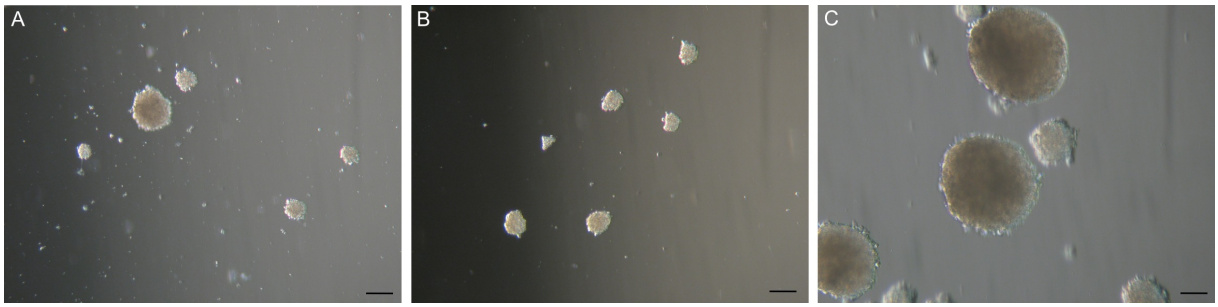

Figure 3.1.10. Floating ASC bodies formed after extended periods of not changing a cell medium. Scale bar 100 μm (50 μm for Figure 3.1.10.C). Author U.Bērziņš.

After a transfer onto new plastic tissue culture flasks spontaneously formed floating ASC bodies (the second and the fourth type), irrespective of their size, were capable to adhere to the surface and gradual spread of spindle-shaped ASCs out of the bodies was observed.

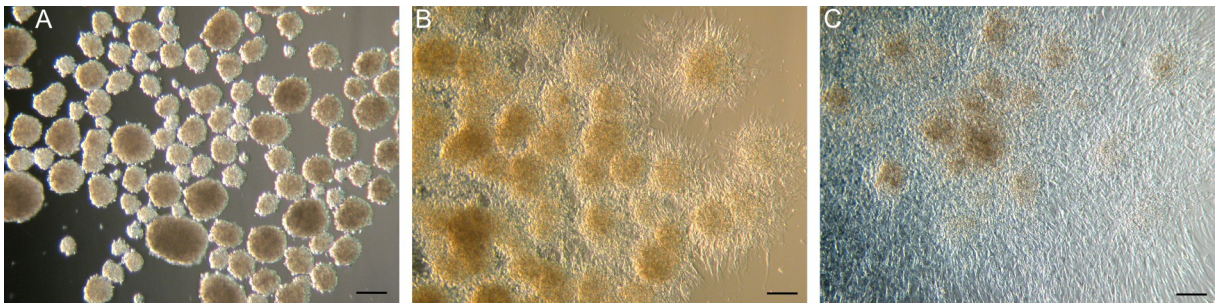

Figure 3.1.11. Cell growth after the transfer of floating ASC bodies onto new adherent cell culture plate. (A) ASC bodies immediately after the transfer. (B) ASC bodies after 12 hours. (C) ASC bodies after 36 hours. Scale bar 100 μm. Author U.Bērziņš.

This ability of three-dimensional (3D) spheroids to convert back to functional monolayer culture has been also described for MSC aggregates obtained by other methods (Kruse et al. 2004, Bartosh et al. 2010, Cheng N.C. et al. 2012). Our results regarding ASC bodies observed at early passages showed that even the replacement of autologous serum in the cell growth medium with allogeneic sera did not impede this process, while commercial medium MesenPRO RS™ delayed the attachment of ASC bodies to the surface and reorganization back to 2D culture (based on a visual assessment). It is known that the addition of FBS to MSC culture medium is essential for the attachment and proliferation of the cells (Lennon et al. 1996). Since the MesenPRO RS™ medium contains only 2% FBS and is adapted to the expansion of monolayer MSCs above clonal densities (according to manufacturer), it may not be suitable for the analysis of growth properties of ASC bodies.

When a cell growth after the transfer of ASC body onto new adherent cell culture plate is compared between the floating ASC bodies formed at early passages and ASC bodies formed after prolonged periods in an unchanged medium, the difference in time needed to reduce the volume of initial ASC body could be observed. The ASC bodies obtained after extended periods of not changing a cell medium adhered more quickly to the surface and formed uniform monolayer of ASCs within few days, while ASC bodies formed at early passages could still be detected after a month following the transfer onto new plate. Presumably this was related to a size and formation characteristics of the ASC bodies. The ASC bodies obtained when a cell culture medium was not changed for a prolonged time were comparatively smaller. Visual assessment indicated that a number of cells forming these ASC bodies was smaller and their arrangement was less dense when compared to the second type of ASC bodies. The organization of ASC bodies from early passages was more condensed, as during their assembly the cells were tightly interconnected forming a very solid structure. It is possible that compactness and a greater number of cells arranged in these ASC bodies did not favor their complete transformation back to monolayer culture as quickly as in the ASC bodies obtained after extended periods of unchanged cell medium.

We have obtained and propagated ASCs from 10 different human donors, but only in one case (donor No.4) have observed the spontaneous formation of herein described types of the ASC bodies (the experiments of ASC growth on a glass surface and without the change of a culture medium were not performed on ASCs from other donors). It seems that the cell aggregation in ASC bodies was triggered under various stress conditions that could not always be precisely determined. Since donor-to-donor variability in adult stem cell cultures covers diverse aspects of their characteristics (Siegel et al. 2013), it is possible that stress tolerance also varies between donors and the ASCs of donor No.4 are more sensitive. The first type of ASC bodies was most probably formed in the influence of stress caused by slight changes in the growth environment. A direct explanation for an aggregation of the second type of ASC bodies was not found. They appeared to form at early passages after each change of fresh medium that also included a brief wash with a PBS. Presumably a slight wash of ASCs from

this particular donor with PBS was sufficient to trigger a stress response in a form of cell aggregation. The third type of ASC bodies was apparently assembled in a response to stress created by unsuitable growth surface. Since ASCs are plastic adherent and their growth and morphological characteristics can be influenced when expanded on the untreated glass surface (Ho et al. 2006), it is feasible to suspect that reduced cell attachment ability caused the clustering of ASCs and their assembly into the bodies. The fourth type of ASC bodies was likely formed as a reaction to stress caused by altered composition of a culture medium due to a prolonged periods without a change of fresh medium.

In the last few years 3D culture method has become progressively acknowledged as a tool to increase differentiation properties and therapeutic potential of adult stem cells (Bartosh et al. 2010, Frith et al. 2010, Baraniak and McDevitt 2012, Cerwinka et al. 2012). This method has been commonly used in ESC cultures. When cultured in the absence of leukemia inhibitory factor or mouse embryonic fibroblasts, a spontaneous differentiation and formation of 3D aggregates of ESCs is observed. These aggregates are called embryoid bodies (EBs) (Kurosawa 2007). Over time EBs increase in cell number and complexity as they give rise to cells of all the three germ layers (Dang et al. 2002). The 3D culture method has also been widely exploited in neural stem cell studies to propagate, characterize and assay these cells by means of neurosphere system (Jensen, Parmar 2006) and in cancer research to simulate the tumor environment (Ivascu, Kubbies 2006). In order to obtain 3D adult stem cell aggregates, such methods as cell culture onto non-adherent surfaces, hanging drop technique, forced-aggregation, surface treatment, and microfabrication have been used (for review, see Sart et al. 2014). There is evidence that 3D culture methods facilitate higher cell-cell and cell-extracellular matrix interactions and are believed to hold a greater promise in mimicking *in vivo* environment than monolayer culture (Frith et al. 2010, Baraniak and McDevitt 2012). Such ASC aggregates show enhanced transdifferentiation capabilities not only into cells of mesodermal origin, but also into cells of endodermal and ectodermal origin (Cheng N.C. et al. 2012).

During our literature search we have not come across similar studies showing various types of spontaneously formed ASC aggregates. Cell aggregates comparable to herein described first type of ASC bodies have been reported in the course of pancreatic differentiation of MSCs (Sun et al. 2007, Neshati et al. 2010, Tang et al. 2012). The appearance of these aggregates is perceived as a successful sign of MSC differentiation into insulin-producing cells, because their morphology is similar to pancreatic islets. These islet-like structures often stain positive for dithizone as well, which is a selective stain for pancreatic β cells. However, there is a possibility that reported cell aggregation itself is not an evidence of MSC differentiation, but simply cell response to stress caused by suboptimal conditions of the differentiation.

Regarding the stress-caused aggregation of adult stem cells, it has been previously shown that adult human mesenchymal cell populations contain a specific type of stem cells, called Muse cells, able to form clusters in suspension culture after subjection to different stress conditions (Kuroda et al. 2010). It is possible to draw few parallels between our ASCs and Muse cells, but the formation of 3D aggregates is antipodal. While enduring and severe stress is the main criteria to isolate Muse cells from overall cell culture, our ASCs spontaneously formed 3D bodies even by a slightest stress that is normally considered routine (short wash with PBS between a change of medium).

3.2. Various marker expression in ASCs

3.2.1. Surface markers

One of the minimal criteria, set for the identification of MSCs, is the expression of such surface markers as CD105, CD73, CD90 and the lack of expression of CD45, CD34, CD14,

CD19, HLA-DR surface molecules (Dominici et al., 2006). To define ASCs, this list has been extended with CD9, CD10, CD13, CD29, CD44, CD54, CD55, CD59, CD106, CD146, CD166, HLA I as positive and CD31, CD80, CD117, CD133, CD144, c-kit, STRO-1 as negative markers (Schäffler and Büchler 2007). Each of above mentioned surface markers could be found on different types of cells and neither of them is unique to MSC. Currently there is a lack of specific marker that would allow to detect exclusively MSC, therefore a group of markers is needed to verify identity of isolated cell population (Lv et al. 2014).

Analysis of MSC surface markers was performed on ASCs of the donor No.4 after P3 using immunocytochemistry method. The obtained results showed that at least 95% (visual assessment) of the ASC population express CD73, CD90, and CD105, but lack expression of CD34 and CD45 (Figure 3.2.1.1.) that is consistent with previous reports (Zuk et al. 2002, Seo et al. 2005, Fraser et al. 2006, Kern et al. 2006, Taléns-Visconti et al. 2006). To verify that the detected MSC markers are indeed on the surface of the cells, a plasma membrane of ASCs was simultaneously labeled with wheat germ agglutinin (WGA) conjugated with Alexa Fluor®633. As shown in a Figure 3.2.1.2. the exact colocalization of surface markers and WGA can be observed indicating that CD73, CD90 and CD105 are found on the plasma membrane.

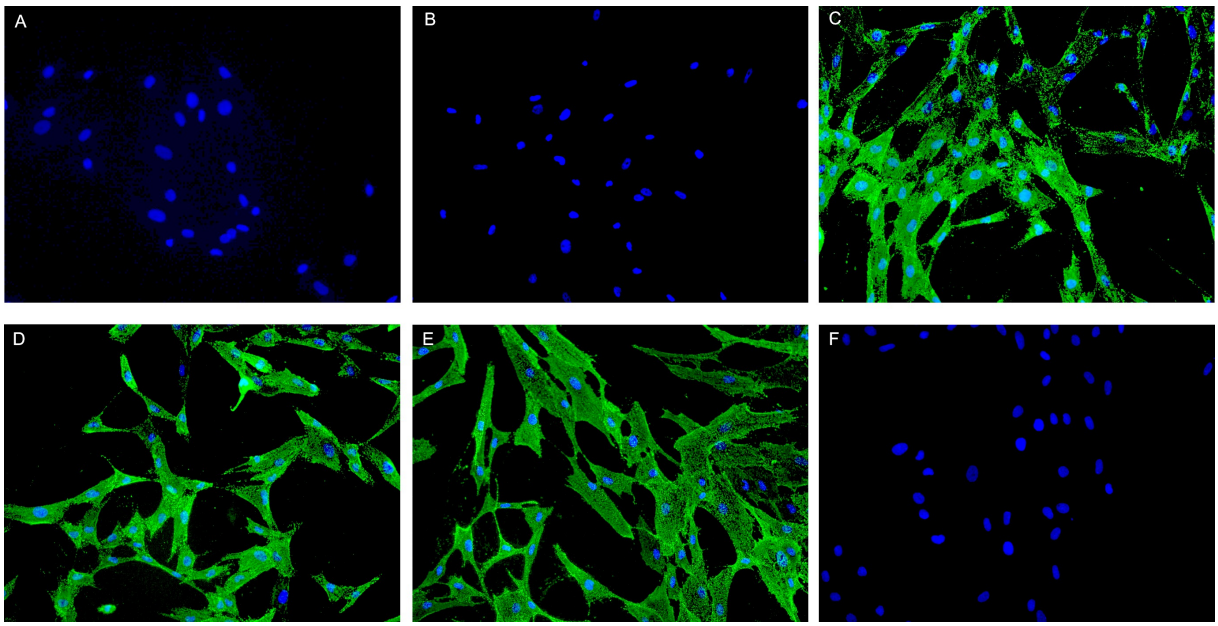

Figure 3.2.1.1. Expression of typical MSC surface markers on ASCs of the donor No.4 after the third passage. (A) CD34. (B) CD45. (C) CD73. (D) CD90. (E) CD105. (F) negative control, secondary antibody only. Cell nuclei stained with DAPI. Magnification 200x. Author R.Brūvere.

In order to obtain more accurate data on the amount of ASCs expressing MSC surface markers and their changes during the passages, a flow cytometric analysis was performed on ASCs of the donor No.4 cryopreserved after passages 2, 3, 4, 5, 8 and stored for more than 4 years. Here we have tested ASCs starting from P2. We have chosen this passage because from the 5 ml of fat tissue as an initial material we can harvest around 10^7 cells at the end of P2 that are frozen for a long term storage until the clinical necessity for the potential patient may arise. Fraction of the cryopreserved cells can be thawed, propagated and used for various assays based on potential patient's needs at any moment. We have determined that 5 ml of fat tissue yield approximately 10^9 ASCs at the end of P5 at our culture conditions using 5% AS. It is sufficient for 3-4 repeated injections of ASCs for a 90-100 kg patient using therapeutic dose of $3x10^6$ cells per kg of body weight.

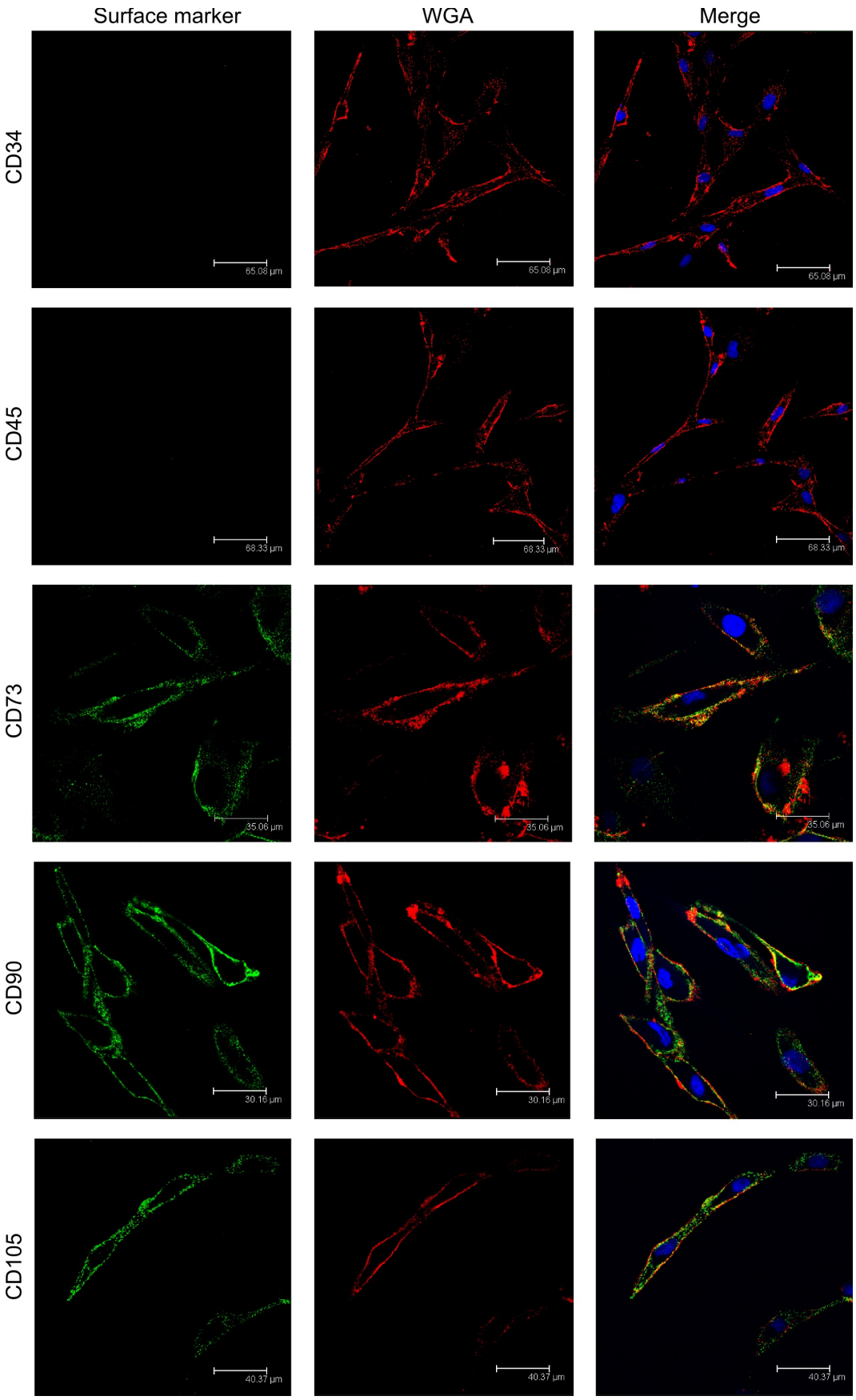

Figure 3.2.1.2. Colocalization of MSC surface markers CD34, CD45, CD73, CD90, CD105, and wheat germ agglutinin (WGA) on ASCs of the donor No.4 after the third passage; analysis of confocal laser scanning microscopy. Cell nuclei stained with DAPI. Author R.Brūvere.

When clinical need for the potential patient emerges, ASCs from P2 are thawed, expanded till P5 and frozen again. It is important because a) cellular properties must be tested again before injection at the given time point; b) the ability of potential patient to receive the therapy may not coincide with the time of readiness of ASCs; c) the planned time of injection may be delayed; d) preparation of ASC material can be performed remotely from a medical institution. We used flow cytometry analysis to determine the changes in cell surface marker expression at different passages of ASCs after more than 4 years of cryopreservation and double freezing immediately after thawing as it would be just before stem cell injection therapy.

Cell viability test (Syto 16 staining), which was carried out for each thawed vial, showed that concentration of live cells in all samples was at least 95%. 8-colour flow cytometry was used to test 10 different cell surface markers simultaneously on each cell. Obtained results showed that all the cells were positive for MSC markers CD29, CD44, CD73, CD90, CD105 and negative for such markers as HLA-DR, CD34 and a cocktail of CD14/CD19/CD45. While comparing mean fluorescence intensity of individual markers through different passages tested, an increase of marker fluorescence intensity in each subsequent passage was observed, except for a sharp decline in CD44 expression at P5 (Figure 3.2.1.3.). Since the ASC population remained phenotypically homogeneous, expressing CD29, CD44, CD73, CD90, and CD105 throughout all passages tested, the increase in fluorescence intensity may indicate the accumulation of protein expression with subsequent passaging. When fluorescence intensity was compared between markers, it can be seen that CD90 was the most abundant marker on the surface of ASCs followed by CD29 and CD73, but CD105 showed the lowest level of expression throughout all passages. Collected data suggest that the peak of protein expression for CD73 and CD44 markers can be observed at P5 or P4 respectively, but in case of CD29, CD90 and CD105 the increase until P8 can be detected.

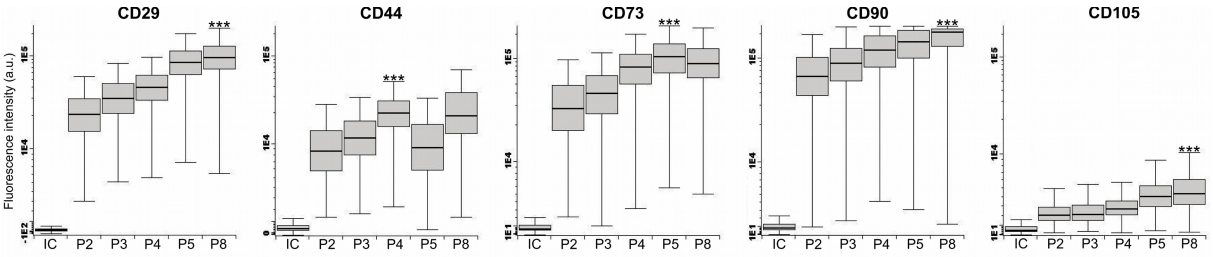

Figure 3.2.1.3. Fluorescence intensity analysis of cell surface marker expression on ASCs of the donor No.4 at different passages. Results are shown as box plots with median value (line), 25th and 75th percentiles as box and 10th and 90th percentiles as whiskers. Data analysis by Infinicyt software (v1.5.0). Asterisks at passage with the highest fluorescence intensity indicate statistically significant increase when compared to P2. *** $p < 0.001$. IC – isotype control; P – passage; a.u. - arbitrary units. Author S.Ņikuļšins.

To complement the flow cytometry data, the expression of positive MSC surface marker genes was analysed with real-time RT-PCR (Figure 3.2.1.4.). Obtained results showed that the expression of *CD29*, *CD44*, *CD73*, and *CD90* genes increased until P4 or P5 and reduced afterwards, but the highest level of *CD105* gene expression was detected at P2 followed by decline in subsequent passages.

The immunocytochemistry method gave us an insight into overall expression of each of the positive surface markers tested, but the 8-colour flow cytometry analysis allowed us to detect 10 cell surface markers simultaneously on each cell. The results showed that all ASCs, cultured in the medium containing AS, express typical MSC markers CD29, CD44, CD73, CD90, and CD105 concurrently irrespective of passage, demonstrating a very homogeneous

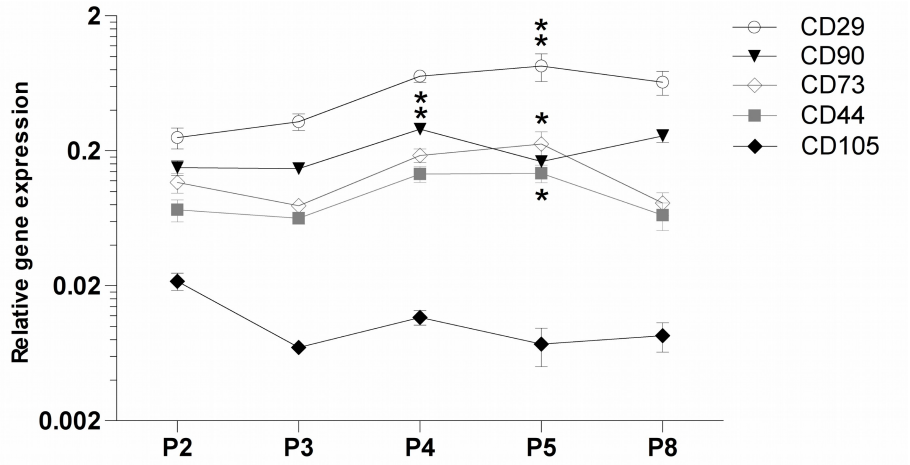

Figure 3.2.1.4. Comparison of relative expression level of positive MSC surface marker genes *CD29*, *CD44*, *CD73*, *CD90*, and *CD105* in ASCs of different passages by real-time RT-PCR (data normalized to *β-Actin*). Data represent the mean ± SD of triplicates. An asterisk at passage with the highest expression indicates statistically significant increase when compared to P2; *$p < 0.05$, **$p < 0.01$. P – passage.

cell population as of P2. However, median fluorescence intensity of positive cell surface markers increased with each subsequent passage. Negative markers such as HLA-DR, CD34, CD14, CD19, and CD45 were not detected. Other reports have demonstrated the incrementation of expression pattern of positive MSC surface markers with passages (Mitchell et al. 2006, Varma et al. 2007, Park and Patel 2010), while others have not detected the difference from P3 to P12 (Yang et al. 2011). The greatest disagreements exist over the expression of CD34 in ASCs. Few studies failed to detect CD34 (Zuk et al. 2002, Zhu et al. 2008), but others reported high levels of CD34 expression (Gronthos et al. 2001, Festy et al. 2005). It has been recently shown that cells in the SVF and early passages of ASCs express CD34, but the level of expression diminishes with further cell culturing (Mitchell et al. 2006, Astori et al. 2007, Varma et al. 2007), although contrary data have also been published showing not only increase of CD34 in later passages, but also accumulation of haematopoietic marker CD45 in ASCs (Park and Patel 2010). As possible reasons to these discrepancies researchers suggest factors secreted by adjacent cells in the early passages (Chamberlain et al. 2007), different cell culture conditions, donor-specific variability, choice in antibody labeling (Baer et al. 2013), and individual gating strategies used for flow cytometry (Astori et al. 2007). Since we have not tested the expression of the above mentioned surface markers at P0 or P1, we cannot speculate of whether ASCs, cultured in the presence of AS, express CD34 or CD45 at very early passages. But starting from P2, the cultured cells were homogeneously CD29, CD44, CD73, CD90, and CD105 positive demonstrating that culturing ASCs in the presence of AS do not influence the expression of characteristic MSC markers.

Since immunophenotype profile of MSCs is similar to fibroblasts and pericytes (Covas et al. 2008) and above-mentioned markers could not discriminate between those three, a possibility that tested cell population contains not only ASCs, but also fibroblasts and pericytes can not be entirely excluded. It has been long believed that successive passaging purifies MSC culture from other types of cells that can be present in the initial cell population immediately after isolation (Horwitz et al. 2006). However, some researchers question this theory, as well as the general assumption that MSCs are unique type of cells distinct from fibroblasts (Haniffa et al. 2009, Hematti 2012) and pericytes (Crisan et al. 2008).

Some evidence indicates that MSCs are different from fibroblasts and more similar to pericytes (Blasi et al. 2011). The hypothesis that MSCs are actually pericytes has also been postulated (Crisan et al. 2008, da Silva Meirelles et al. 2008). Additional research suggests

that both MSCs and pericytes express CD146 and it could be used as a marker to segregate them from fibroblasts which show no expression of this antigen (Covas et al. 2008). However, the current opinion is still in a disagreement as to whether ASCs express CD146, making it problematic to use it as a reliable marker and to claim that ASCs and pericytes are the same. Similarly, the lack of smooth muscle actin, which is a known pericyte marker, in most of the isolated ASC populations also argues against this hypothesis (Zuk 2013). Recently, CD106 and integrin alpha 11 were suggested as markers distinguishing BM MSCs from fibroblasts (Halfon et al. 2011), and different expression levels of CD10 and CD26 could also help to discriminate between BM MSCs and fibroblasts (Cappellesso-Fleury et al. 2010). Since no analogous studies have been published using ASCs, it is not clear whether these markers could be used for somatic SC populations isolated from fat tissue. Although the origin and true identity of ASCs is not absolutely understood, from a clinical perspective knowledge that such multipotent cells can be obtained from adipose tissue and exploited for the treatment of patients may be more important (Zuk 2013). While additional markers helping to separate ASCs from fibroblasts and pericytes were not included in this study, there is a great deal of evidence suggesting for their incorporation in our future work.

3.2.2. Pluripotency markers

One of the main criteria that allow to define pluripotent cells, such as ESCs, is the expression of specific pluripotency markers. That signifies their ability to self renew and differentiate into each cell type within the organism, except extraembryonic tissues. In the field of ESC research it is a well-established practice to characterize ESCs by the expression of OCT4, NANOG and SOX2 markers, as they are regarded as the central transcriptional regulators maintaining the pluripotency of ESCs (Boyer et al. 2005).

In the last decade numerous studies have detected OCT4 and other pluripotency markers in adult stem cells as well (Tai et al. 2005, Izadpanah et al. 2006, Greco et al. 2007, Kucia et al. 2007, Roche et al. 2007, Trivanović et al. 2015). To find out whether ASC culture of the donor No.4 also displays such pluripotency markers, polyclonal anti-OCT4 and anti-NANOG antibodies were used. Immunocytochemistry revealed the expression of OCT4 in most of the ASCs (Figure 3.2.2.1.). Although OCT4 is a transcription factor (Nichols et al. 1998) that must be expressed only in the nucleus, it was detected throughout the cell. More prominent granular nuclear staining was observed in some ASCs.

A transcription factor NANOG was mostly detected in the nuclei, but granular cytoplasmic staining was also observed and few ASCs demonstrated pronounced expression of NANOG in the nucleoli (Figure 3.2.2.2.). Since a polyclonal antibody (sc-33759) was used in this experiment, it may have caused some of the unspecific staining. The ASCs from two other donors, not described in this study, have also been tested for the expression of NANOG using the same antibody. These ASC cultures displayed predominant cytoplasmic staining and very weak nuclear staining (data not shown).

In the scientific literature, where similar experiments have been conducted, a cytoplasmic staining of pluripotency defining transcription factors can be also found (Tai et al. 2005, Carlin et al. 2006), but usually authors focus only on the nuclear staining and do not interpret the rest. Increasing amount of research tends to classify the ASCs (Izadpanah et al. 2006), BM MSCs (Moriscot et al. 2005, Tai et al. 2005), and umbilical cord blood MSCs (Tondreau et al. 2005) as pluripotent, based on the methods of immunofluorescence or PCR, where an expression of OCT4, NANOG or SOX2 is determined. Inaccurate conclusions may arise from the antibody used to determine the expression of pluripotency markers at the protein level. It has been shown that the intracellular distribution of these markers in adult stem cells varies significantly depending on the commercial antibody used. For example, different commercial anti-OCT4, anti-NANOG, and anti-SOX2 antibodies display

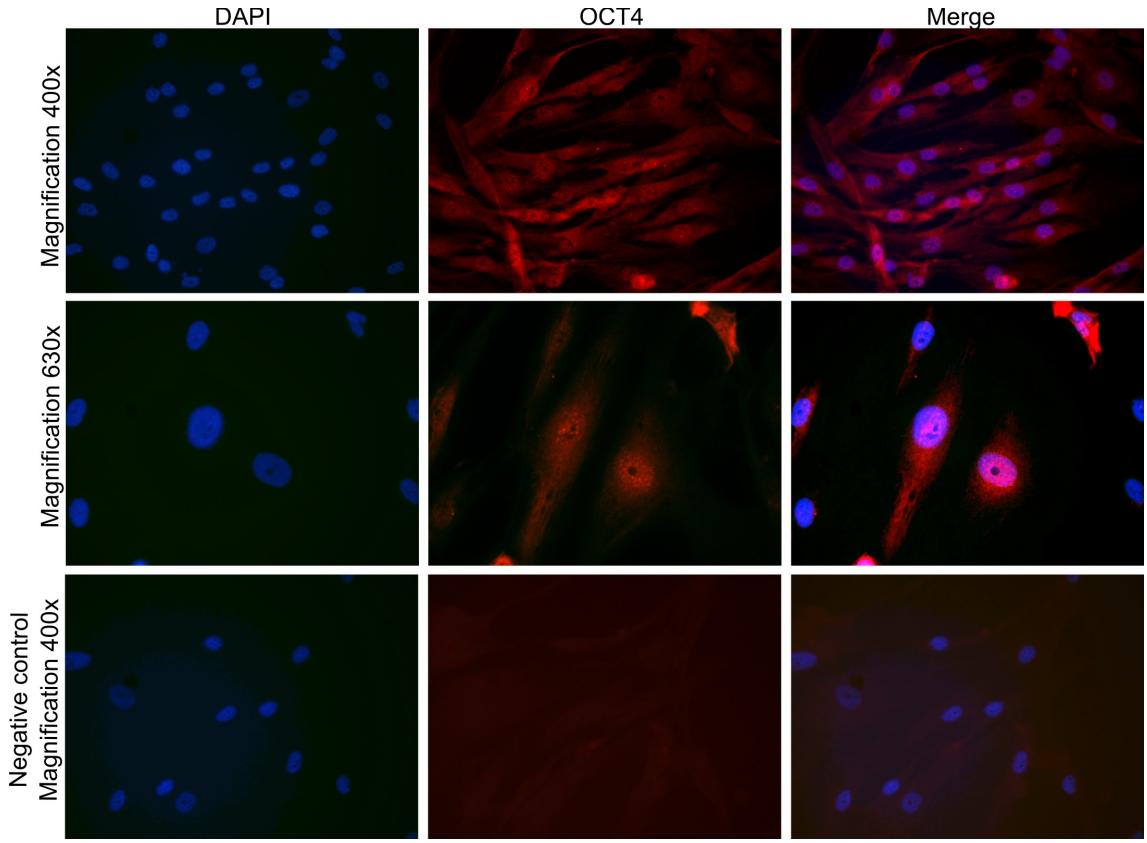

Figure 3.2.2.1. Expression of OCT4 in ASC culture of the donor No.4. Negative control – secondary antibody only. Cell nuclei stained with DAPI. Author R.Brūvere.

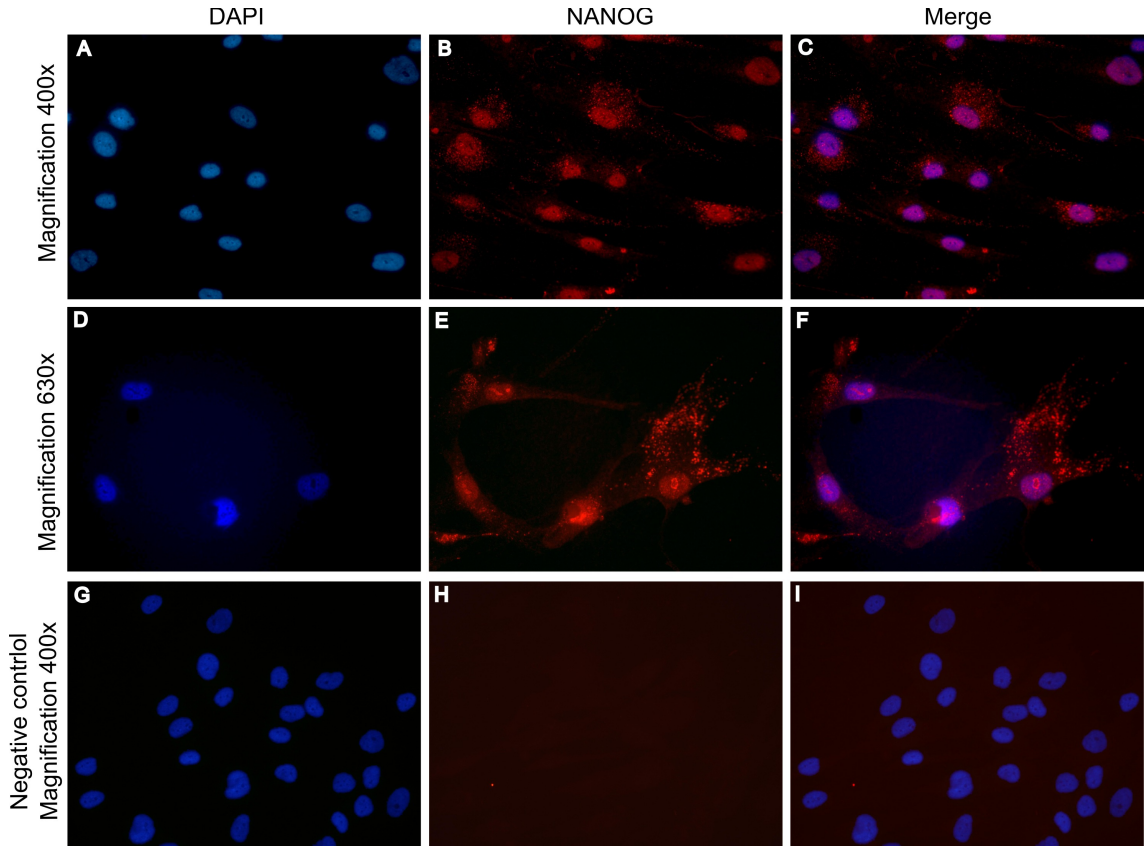

Figure 3.2.2.2. Expression of NANOG in ASC culture of the donor No.4. Negative control – secondary antibody only. Cell nuclei stained with DAPI. Author R.Brūvere.

cytoplasmic, nuclear or nucleolar staining respectively, or alternatively, no staining at all in ASCs and BM MSCs (Zuk 2009). Similarly, it is always a higher risk to obtain an unspecific staining when polyclonal antibodies are used, thus leading to incorrect interpretation of obtained data. Equally, a background staining from secondary antibody must be constantly taken into account.

There is one more factor that must be taken into consideration when anti-OCT4 antibodies are used. The alternative splicing of *OCT4* gene results in three different protein isoforms termed OCT4A, OCT4B (Takeda et al. 1992), and OCT4B1 (Atlasi et al. 2008). The OCT4A isoform is localized in a nucleus, but OCT4B is mainly found in a cytoplasm (Cauffman et al. 2006, Lee et al. 2006). The localization of OCT4B1 is not known, as the protein product of *OCT4B1* has not been identified yet (Wang, Dai 2010). It is believed that only OCT4A is responsible for maintenance of pluripotency and self-renewal (Lee et al. 2006), but biological function of OCT4B is still unclear (Gao et al. 2012). Research shows that OCT4B could be alternatively translated into three additional protein isoforms termed OCT4B-265, OCT4B-190, and OCT4B-164 (Wang X. et al. 2009). The OCT4B-190 and OCT4B-265 are both involved in a cell stress response (Wang X. et al. 2009, Gao et al. 2012), but a role of the OCT4B-164 has not yet been discovered. A very little is known about the biological function of the OCT4B1 isoform, but it has a probable role in stress response and apoptosis (Yazd et al. 2011). Most of the commercially available anti-OCT4 antibodies do not discriminate between isoforms of OCT4, as they are generated against C-terminus of OCT4 protein that is identical to all isoforms. This may explain the observed nuclear and cytoplasmic staining (Liedtke et al. 2008). Few antibodies, specific to only OCT4A isoform, are also available in the market, but they show only weak staining both in the nucleus and cytoplasm (Zuk 2009).

The anti-OCT4 antibody used in this study was a goat polyclonal antibody (sc-8630) that recognizes OCT4B isoform, but not the OCT4A isoform, according to manufacturer. This explains the staining pattern observed in our ASC culture, as OCT4B localizes mostly in a cytoplasm (Lee et al. 2006). The anti-OCT4 antibody that helps to identify the OCT4A isoform was also tested in our ASC culture. It was a mouse monoclonal antibody (sc-5279), raised against amino acids 1-134 of human origin, hence, non cross-reactive with OCT4B (according to manufacturer). Unfortunately, no expression was detected in the ASC culture (data not shown). This antibody has previously produced a weak staining in a nucleus and in a cytoplasm of ASCs and MSCs (Zuk 2009), but in our ASCs neither of them stained positive.

To test whether ASC aggregates also expressed pluripotency markers NANOG and OCT4, immunocytochemistry with monoclonal anti-NANOG and anti-OCT4A antibodies was employed on glass adherent ASC bodies. The obtained results showed the expression of NANOG in ASC bodies (Figure 3.2.2.3.A-C) and prominent NANOG positive nuclear staining was also observed in clustered ASCs where the formation of ASC bodies is initiated (Figure 3.2.2.3.D-F). Some cytoplasmic staining was also detected. The few monolayer ASCs neighbouring ASC bodies were NANOG negative. Similarly to monolayer ASCs tested previously, no positive signal was detected in ASC bodies using anti-OCT4A antibodies against N-terminus of OCT4 of human origin (data not shown).

The RT-PCR method was used to test an expression of pluripotency markers at the gene level. The expression of genes *OCT4A*, *NANOG*, and *SOX2* was detected in ASCs and plastic-adherent ASC aggregates (Figure 3.1.4.) of the donor No.4. Commercially available cDNA of ESCs was used as positive control (Figure 3.2.2.4.). The ASC aggregates were included in this analysis to test whether they differ from the monolayer ASCs in a way that may indicate a more primitive cell state. The expression of a housekeeping gene *β-Actin* was tested first to ascertain the same level of expression in all three samples to be compared. The obtained results regarding all three pluripotency marker genes showed a very weak expression in ASCs when compared to ESCs.

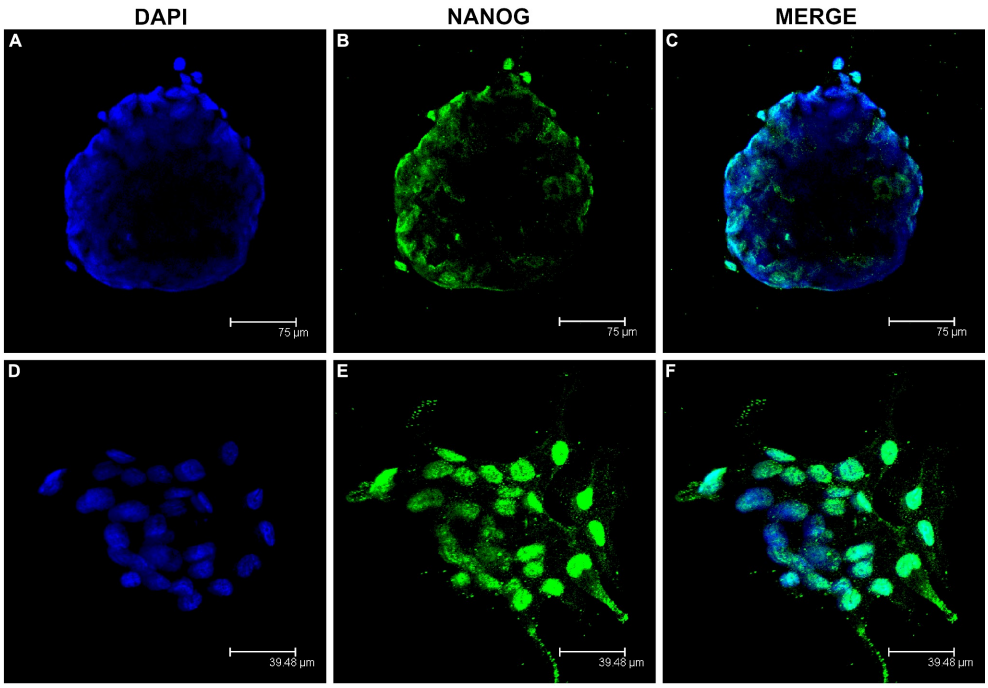

Figure 3.2.2.3. Expression of NANOG in adherent ASC bodies of the donor No.4 formed onto a glass surface at day 5. (A-C) Immunocytochemical localization of NANOG in completely organized ASC body. (D-F) Detection of NANOG in ASCs gathered into cluster triggering the first stage of ASC body formation. Cell nuclei stained with DAPI. Author D.Pjanova.

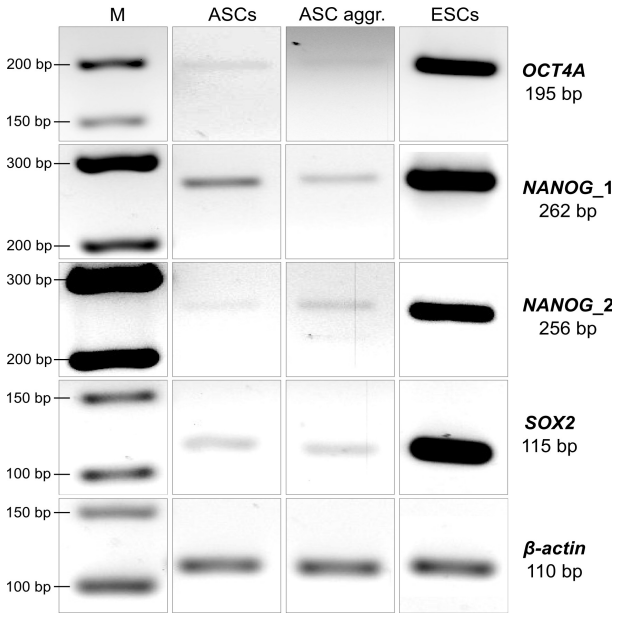

Figure 3.2.2.4. Expression of pluripotency marker genes *OCT4A*, *NANOG*, *SOX2* and housekeeping gene *β-Actin* in ASCs and ASC aggregates (ASC aggr.) of the donor No.4, and ESCs by RT-PCR. Analysis of RT-PCR products in 3% TAE agarose gel. NANOG_1 and NANOG_2 represent two different primer pairs tested. M – DNA ladder. bp – base pairs. ESCs – embryonic stem cells.

In the case of *OCT4* gene, the target was a mRNA of *OCT4A*, since only this isoform is involved in the maintenance of pluripotency (Lee et al. 2006). To detect exclusively *OCT4A*, the primers must lie in the 5' part of the *OCT4* sequence, as the exon 1 is not found in other splice variants (Figure 1.6.1.1.). Furthermore, the unique polymorphisms are located at

positions 48, 234, and 353 within exon 1, starting at the transcriptional start codon ATG, allowing to avoid amplification of false positive products derived from pseudogenes and *OCT4*-like sequences as well (Liedtke et al. 2008). In total, four different primer pairs were tested, but only the results obtained by one are shown herein. The exact primer sequences and a comparison of *OCT4A* gene product sequence, amplified with this primer pair, to three *OCT4* pseudogene sequences that closely resemble parental *OCT4A* gene can be found in the Appendix 1. All the primer pairs tested showed very low level of *OCT4A* expression both in ASCs and ASC aggregates of the donor No.4. No significant differences were found between the *OCT4A* expression in monolayer ASCs and ASC aggregates (Figure 3.2.2.4.). In contrast, the expression of *OCT4A* in the ESCs was very pronounced, verifying their pluripotent state. It must to be mentioned that the quantity of cDNA from both ASC samples used in a RT-PCR was twice the amount of ESC cDNA, emphasizing an even more modest expression of *OCT4A* in adult stem cells.

Similarly to *OCT4A*, detecting the expression of *NANOG* at the gene level is a tricky task. It is known that there are 11 human *NANOG* pseudogenes from whom *NANOGP8* is highly similar to the original *NANOG*, bearing only two fixed and twelve polymorphic nucleotide alternations within the ORF (Appendix 4) (Fairbanks et al. 2012). We have tested four different primer pairs for the detection of *NANOG* gene, but only two of them are described in this work. A comparison of *NANOG* gene product sequence, amplified with the two primer pairs, to 11 *NANOG* pseudogene sequences can be found in the Appendices 2 and 3. A higher expression level of *NANOG* in all samples was detected when NANOG_1 primer pair was used (Figure 3.2.2.4.). Similarly to *OCT4A* case, the level of *NANOG* expression in ASCs and ASC aggregates of the donor No.4 was much lower than that of ESCs, irrespective of the primer pair that was used. A difference in the amount of *NANOG* between ASCs and ASC aggregates was inconclusive, since the results for each primer pair were opposite.

Since there are no known pseudogenes or isoforms of *SOX2* (Ståhlberg et al. 2009), the detection of its expression by RT-PCR was more conclusive than that of *OCT4A* and *NANOG*. Similarly to the above-mentioned pluripotency markers, the level of *SOX2* expression in ASCs and ASC aggregates was equally low when compared to ESCs (Figure 3.2.2.4.).

A careful design of primers to specifically detect *OCT4A* isoform and *NANOG* gene does not fully guarantee the exclusion of false positive results. For this reason it is necessary to sequence the obtained RT-PCR products to make sure, that no amplification of pseudogenes has occurred. The same primer pairs used for the RT-PCR method were employed for the sequencing. Sequencing of RT-PCR products, amplified using OCT4A primer pair, confirmed the expression of *OCT4A* isoform both in adult stem cells of the donor No.4 and in ESCs. A comparison between original *OCT4A* gene fragment and sequencing result of respective RT-PCR products is shown in the Appendices 5, 6, 7, and 8. The sequencing with OCT4A forward primer has not been successful in the samples of ASCs and ASC aggregates, probably due to a improper sample quality caused by a very low level of *OCT4A* expression.

The obtained results from sequencing of RT-PCR products, amplified using NANOG_1 and NANOG_2 primer pairs, are summarized in Table 3.2.2.1. Within a sequence, amplified using NANOG_1 primer pair, are 5 positions that could help to distinguish *NANOG* from *NANOGP8*. Unfortunately, all of them are modern polymorphisms and not fixed variants. Nevertheless, sequencing results showed that ASCs of the donor No.4 express *NANOGP8* and not the original *NANOG* gene. From the sample of monolayer ASCs of the donor No.4 clear answer could not be obtained, as the critical nucleotides could indicate expression of both *NANOG* and *NANOGP8*. However, the results from aggregates of the same ASCs showed a variant T at the position 190, indicating the amplification of *NANOGP8*. In ESCs the expression of original *NANOG* was detected based on variants at the positions 276 and 363. A comparison between original *NANOG* gene fragment, amplified using NANOG_1 primer pair, and sequencing result of respective RT-PCR products is shown in the Appendices 9, 10, 11,

and 12.

Table 3.2.2.1. The sequencing results of RT-PCR products of ASCs and ASC aggregates of the donor No.4, and ESCs, amplified using NANOG_1 and NANOG_2 primer pairs. a - nucleotides in the reading frame are numbered relative to the first nucleotide in the ATG initiation codon; b – information based on Fairbanks et al. 2012; c – in order to make a comparison easier, the nucleotides on a reverse strand are converted into their respective complementary counterparts; NANOGP8 – NANOG pseudogene 8; F – forward primer; R – reverse primer; "-" - not applicable; X – sequence could not be determined at the respective position.

			NANOG_1				NANOG_2					
Position[a, b]	*NANOG*[b]	*NANOGP8*[b]	ASCs No.4 (F)	ASC aggr. (R)[c]	ESCs (F)	ESCs (R)[c]	ASCs No.4 (F)	ASCs No.4 (R)[c]	ASC aggr. (F)	ASC aggr. (R)[c]	ESCs (F)	ESCs (R)[c]
47.	**C**	**C/A**	-	-	-	-	X	C	X	C	X	C
126.	**T**	**T/C**	-	-	-	-	T	T	T	T	T	T
144.	**G**	**A**	-	-	-	-	X	A	X	X	G	G
165.	**T/C**	**T**	X	T	X	T	T	T	T	T	C	C
190.	**G**	**G/T**	X	T	X	G	T	T	T	X	G	G
246.	**T/G**	**T**	T	T	T	T	T	X	T	X	T	X
276.	**G/A**	**G**	X	G	A	A	G	X	G	X	G	X
363.	**C/T**	**C**	C	C	T	T	-	-	-	-	-	-

Within a sequence, amplified using NANOG_2 primer pair, are 7 positions (one fixed variant at the position 144 and 6 modern polymorphisms) distinguishing *NANOG* from *NANOGP8*. The same as using NANOG_1 primer pair, the expression of parent *NANOG* was detected in ESCs, according to observed variants at the positions 144 and 165. Unfortunately, the data regarding ASCs of the donor No.4 were inconclusive. In accordance with the variant T, detected at the position 190, these cells express *NANOGP8*. This conclusion was further supported by an identification of the variant A at the position 144 in one case out of four. The rest of three sequences were ambiguous due to sequencing artefacts near this position. Repeated efforts did not result in more precise data and for this reason it is likely that the very low level of the initial sample caused these artefacts. Within these sequencing chromatograms, around the position 144, specific peaks could not be observed, but two signal lines, representing the nucleotides G and A (as in *NANOG* and *NANOGP8* respectively), were always present. As the position 144 is of utmost importance, since it represents one of only two fixed variants that could help to distinguish *NANOG* from *NANOGP8*, it could undoubtedly prove the expression of one or another in ASCs of the particular donor. It is tempting to speculate that there is a possibility that ASCs of the donor No.4 express both *NANOG* and *NANOGP8,* as it has been a case in other types of cells (Ambady et al. 2010). It is probable that they dominantly express *NANOGP8* at low level and the expression of parent *NANOG* gene, at even more modest level, is also existent. Although the current evidence regarding *NANOG* expression in ASCs is questionable, the expression of *NANOGP8* in these cells has been clearly detected by both primer pairs used. A comparison between original *NANOG* gene fragment, amplified using NANOG_2 primer pair, and sequencing result of respective RT-PCR products is shown in the Appendices 13, 14, 15, 16, 17, and 18.

If the expression of *NANOGP8* was detected in ASCs of the donor No.4 and the expression of *NANOG* was doubtful, then a protein detected by anti-NANOG antibody most likely was NANOGP8, not NANOG. This leads to a conclusion that *NANOGP8* in ASCs of this donor is not only transcribed, but also translated into protein. Since the proteins encoded by *NANOG* and *NANOGP8* differ by only one fixed aa substitution and possibly few other, depending on modern polymorphisms in each individual (Table 1.6.2.1.) (Fairbanks et al. 2012), the anti-NANOG antibodies can not distinguish between the two. Therefore, the presence of positive signal detected by anti-NANOG antibodies could be due to translation of *NANOG*, *NANOGP8*, or both.

The NANOGP8 protein has been also detected in human smooth muscle cells, where it exhibits predominantly nuclear localization. Other cell types that express exclusively *NANOG* or transcripts of both *NANOG* and *NANOGP8*, show various staining patterns within the same cell culture (Ambady et al. 2010). The ASCs of the donor No.4 showed mainly nuclear staining and less prominent granular cytoplasmic staining. This was observed in monolayer ASC culture, as well as in ASC aggregates, using two different antibodies. The main difference between the two was a lack of any staining in ASCs adjacent to adherent ASC bodies or clustered ASCs. The results regarding the expression of *NANOGP8* in monolayer ASCs and their aggregates were obtained from cells grown on adherent plastic cell culture plates. The ASC aggregates, stained with anti-NANOG antibody, were formed on an uncoated glass surface. Therefore, we can not exclude the possibility, that different growth conditions have an influence on gene expression, leading to distinct expression patterns. We do not have a direct proof that ASCs grown on the glass surface also express *NANOGP8*. It is possible that such growth conditions facilitate the expression of parent *NANOG*, caused by more rapid clustering of ASCs, thus providing higher and more effective cell-cell and cell-extracellular matrix interactions. Furthermore, the monoclonal anti-NANOG antibody used on glass-adherent ASC aggregates may be more specific than polyclonal antibody used on monolayer ASCs.

The monolayer ASCs of the donor No.4 were also tested for an alkaline phosphatase (AP) activity using naphthol AS phosphate/Fast Blue BB solution. High activity of AP in human adult can be observed in small intestine, kidney, liver, placenta, bone and neutrophils (Butterworth 1983), but in embryo all tissues show strong AP activity at early stages of development (Bernstine 1973). Four isozymes of AP are discriminated in the humans: tissue-nonspecific (liver/bone/kidney), intestinal, placental and germ cell (Millán 2006). The tissue-nonspecific AP (TNAP) expression is a known marker for embryonic stem cells and osteoblast differentiation, but it has also been observed in undifferentiated BM MSCs (Kim et al. 2012). Separate ASCs in monolayer showed the AP activity detected by two types of blue colouring. Most of the cells, positive for AS, displayed uniform staining (Figure 3.2.2.5.A), while in the others granular staining was observed (Figure 3.2.2.5.B). Addition of levamisole

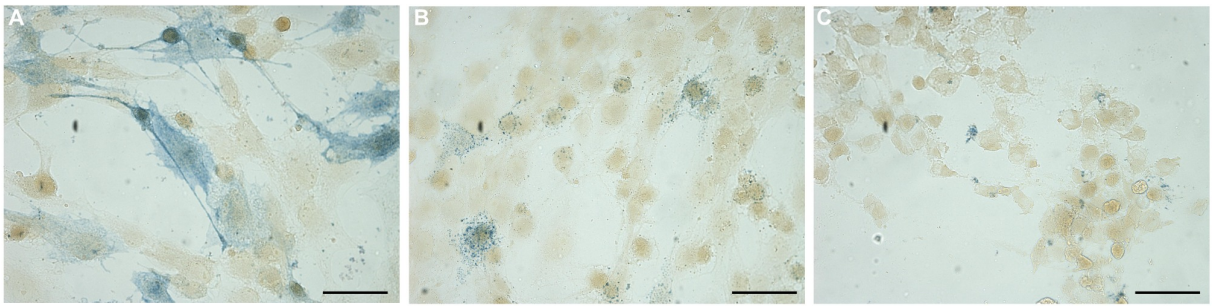

Figure 3.2.2.5. Detection of the alkaline phosphatase activity in ASCs of the donor No.4 at P3 using naphthol AS phosphate/Fast Blue BB solution. (A-B) ASCs positive for alkaline phosphatase activity (blue) demonstrating uniform and granular staining. (C) Inhibition of alkaline phosphatase activity by levamisole. Scale bar 50 μm. Author R.Brūvere.

to the naphthol AS phosphate/Fast Blue BB solution served as an evidence for the specificity of reaction, since the levamisole inhibits the AP activity (Van Belle 1976), resulting in a lack of blue colouring (Figure 3.2.2.5.C).

When ASC bodies, after the transfer to a new adherent plastic culture flasks (Figure 3.1.7.), were tested for an AP activity, the ASCs, assembled into bodies, did not stain positive for AP irrespective of their size. However, a large fraction of cells migrating out of the ASC bodies exhibited AP activity detected by blue staining (Figure 3.2.2.6.).

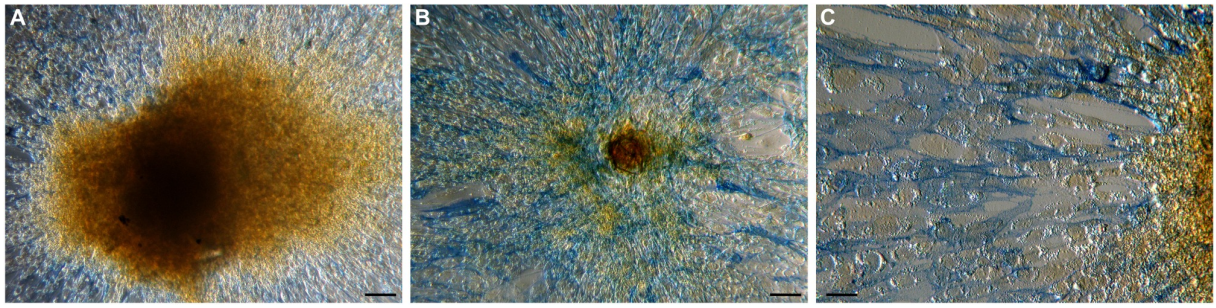

Figure 3.2.2.6. Detection of the alkaline phosphatase activity in ASC bodies of the donor No.4 9 days after the transfer onto adherent cell culture plates using naphthol AS phosphate/Fast Blue BB solution. (A) Absence of AP activity in large ASC body. (B) Lack of AP activity in small ASC body and evident AP activity (blue) in the cells surrounding the ASC body. (C) AP activity (blue) in the cells migrating out of the ASC body. Scale bar 100 μm (50 μm for Figure 3.2.2.6.C).

Few ASCs in monolayer and substantial part of cells migrating out of the ASC bodies after their transfer to a new adherent culture flask displayed AP activity. It has been previously shown that TNAP positive (TNAP+) BM MSCs possess lower multipotentiality than TNAP negative (TNAP-) cells and are prone to differentiate into osteoblasts more often than into adipocytes or chondrocytes. TNAP+ BM MSCs also show lower proliferation rates and diminished expression of pluripotency marker genes *NANOG* and *REX-1* when compared to TNAP- BM MSCs (Kim et al. 2012). Since ASCs share most of their characteristics with BM MSCs, it could be possible that ASCs in monolayer, staining positive for AP, represented more mature cells, while the major part of the monolayer ASCs were AP negative, hence illustrating their multipotentiality. As ASC bodies after the transfer onto new adherent surface did not show the AP activity, but significant part of the surrounding cells were AP positive, the ASCs forming 3D bodies may indicate more primitive cells than ASCs migrating out of the bodies. These observations suggest that particular stress conditions can cause the spontaneous formation of 3D ASC bodies (described in section 3.1.) that may represent more primitive cell subpopulation within the individual ASC culture.

Numerous studies have detected OCT4 and other pluripotency markers in adult stem cells in the last decade (Tai et al. 2005, Izadpanah et al. 2006, Ambady et al. 2010, Trivanović et al. 2015). These findings have led to speculations that somatic stem cells may possess greater similarities to ESCs in terms of regulatory networks and potency than previously thought (Greco et al. 2007). However, additional scientific research contrasts this hypothesis by evidence that OCT4 is not essential for maintaining potency and self-renewal in the adult mammalian stem cells (Lengner et al. 2007). It is thought that albeit pluripotency markers can be observed at a basal level in adult stem cells, they may not have the same biological functions as in ESCs (Lengner et al. 2008). Indeed, our results showed the expression of all three pluripotency determining key transcription factors *OCT4*, *NANOG*, and *SOX2* in ASCs, but the detected level of expression was much lower than that of ESCs. It turned out that the detected expression of *NANOG* in ASCs was not the expression of parental *NANOG* gene, but its pseudogene 8. The data showed that a sequencing of RT-PCR products is the only reliable

method to distinguish *NANOG* from *NANOGP8*. Despite of the numerous *NANOG*, as well as *OCT4* pseudogenes (Booth, Holland 2004, Liedtke et al. 2007) that can easily confuse researchers and result into misleading conclusions regarding pluripotency of adult stem cells (Lengner et al. 2008), part of the published research still overlooks this aspect.

3.3. Differentiation ability of ASCs

3.3.1. Differentiation of ASCs into cells of mesodermal lineage

To test whether ASCs cultured in the medium supplemented with AS exhibit multilineage potential, they were differentiated into adipocytes, osteocytes, and chondrocytes using a lineage-specific induction factors. At first, the ASCs from the donor No.4 at P3 were subjected to the differentiation into cells of above-mentioned mesodermal lineages. After more than 4 years of cryopreservation these cells were examined for ability to maintain their potential of differentiation in even later passages such as P6.

When ASCs were treated with adipogenic induction medium, the fibroblastoid morphology in the fraction of cells changed already during the first week of differentiation. These cells flattened and broadened and a significant accumulation of intracellular lipid droplets was also observed. Throughout the differentiation the amount of such cells and the size and the quantity of intracellular lipid-filled vacuoles increased rapidly. Adipogenic differentiation was confirmed after 28 (for P3) or 16 (for P6) days by Oil Red O staining (Figure 3.3.1.1.A and G). The Oil Red O staining was also performed on differentiated cells of P3 after 14 days of differentiation, but since the amount of mature adipocytes was modest, the process of differentiation was continued. Intracellular lipid droplets of differentiated cells accumulated Oil Red O indicating the phenotype of mature adipocytes. Cells cultivated in a control medium did not show the signs of adipogenic differentiation (Figure 3.3.1.1.D and J).

To differentiate ASCs into osteocytes, the cells were cultivated in osteogenic medium for 28 days. No visible signs of the differentiation could be observed without the use of specific dye. Osteogenic induction of ASCs was assessed by Alizarin Red S. It is a dye that stains calcium deposits within mineralized extracellular matrix produced by osteoblasts (Tapp et al. 2009). A red staining was detected around a small portion of differentiated ASCs from P3 (Figure 3.3.1.1.B) and only in few spots of differentiated cells from P6 (Figure 3.3.1.1.H). Two types of Alizarin Red S staining were observed in differentiated cells from P3. One part of the cells had lighter and smoother staining, but other cells were surrounded by dense, intensive and circular stain. This difference may point to distinct stages of differentiation. In the control cells from both passages red staining was not observed (Figure 3.3.1.1.E and K).

Chondrogenic differentiation was induced using micromass culture technique. High-density micromass culture ensures effective condensation of cells, considered to be a critical stage in the initiation of chondrogenic differentiation (Handschel et al. 2007). Micromass culture of ASCs resulted in the formation of a dense aggregate of cells. After an incubation for three days in a chondrogenic medium, new cells started to grow out of the initially formed nodule. During the chondrogenic differentiation these cells proliferated rapidly and started to condense, forming new, smaller cell aggregates. After 28 days of differentiation the cells were stained with Alcian Blue under acidic conditions to detect sulphated glycosaminoglycans that are characteristic to extracellular matrix of chondrocytes (Lev and Spicer 1964, Zuk et al. 2001).

Differentiated aggregates of cells from P3 were fixed and stained with 1% Alcian Blue (pH 2,5) directly in the cell culture dish (Figure 3.3.1.1.C). The initial and newly formed cell aggregates in the chondrogenic medium were Alcian Blue positive, indicating the presence of sulfated proteoglycans within the extracellular matrix. However, the Alcian Blue staining of the initial cell aggregate was comparatively weak. It was most probably due to the compactness and size of the aggregate. The dense structure of the nodule possibly hindered a

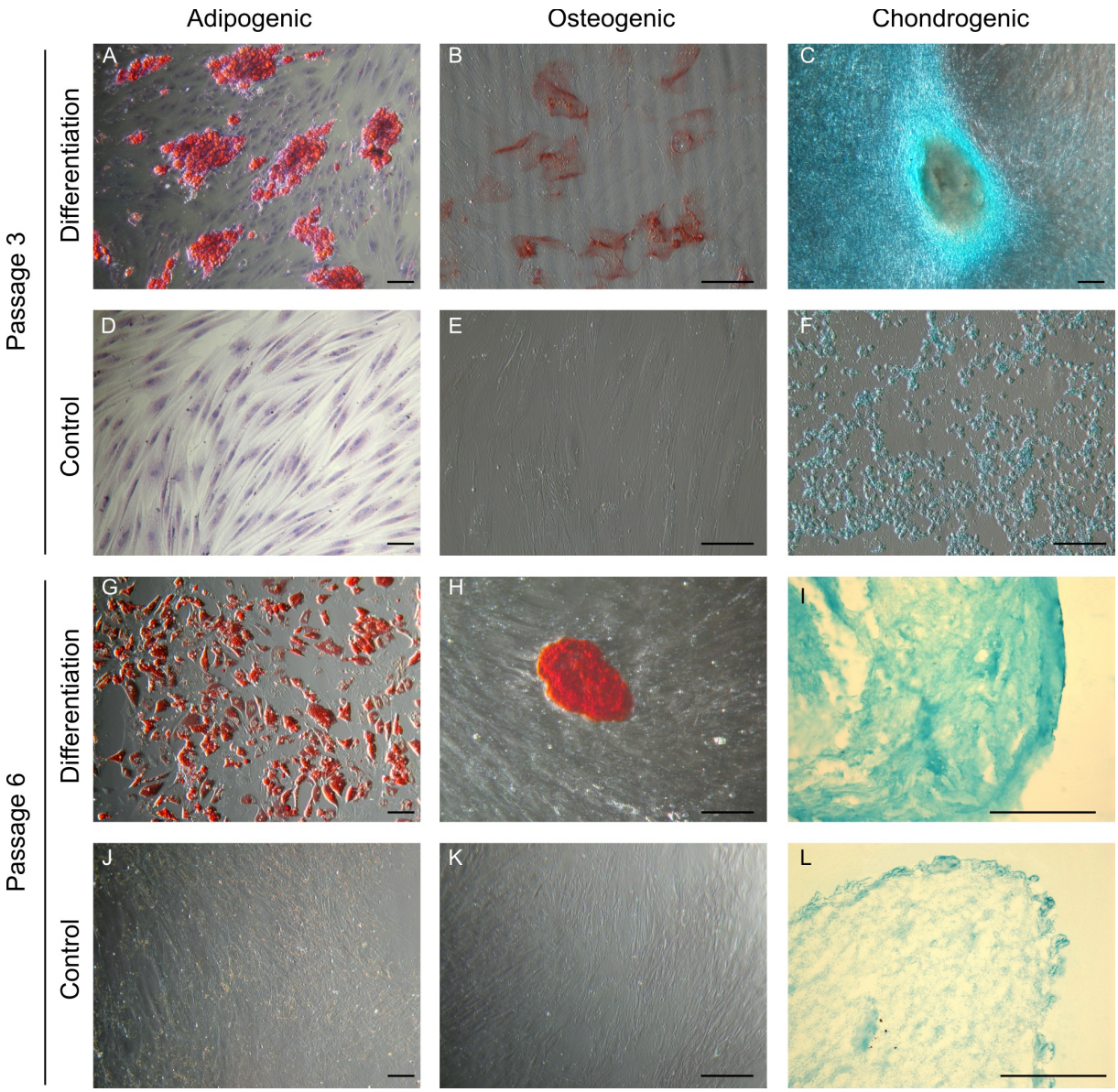

Figure 3.3.1.1. ASCs of the donor No.4 from the third and the sixth passages differentiated towards adipogenic, osteogenic, and chondrogenic lineages. (A, D, G, J) Oil Red O staining of differentiated and control cells. (B, E, H, K) Alizarin Red S staining of differentiated and control cells. (C, F, I, L) Alcian Blue staining of differentiated and control cells. In the Figures 3.3.1.1. A and D the cells are counterstained with hematoxylin. Scale bar 100 µm.

penetration of the Alcian Blue during a relatively short dyeing time. Different approach was used to confirm chondrogenic differentiation of the ASCs from P6. The formed cell aggregates were collected, fixed, embedded in paraffin, sectioned, and only then stained with 1% Alcian Blue (pH 1,3) (Figure 3.3.1.1.I). The lower pH of the dyeing solution was also introduced, since at pH 2,5 not only sulphated, but also carboxyl groups containing glycosaminoglycans stain with Alcian Blue (Lev and Spicer, 1964).

In a control medium cells from P3 did not form aggregates and intense cell growth and condensation was not detected. Weak Alcian Blue staining was also observed in the control medium although the morphology of the cells radically differed from the cells subjected to the chondrogenic differentiation (Figure 3.3.1.1.F). The ASCs from P6 initially formed the cell aggregate in the control medium. Similarly to the differentiation samples, new cells started to grow out of the initially formed nodule and a formation of smaller cell aggregates was observed. But in contrast to the differentiation samples, reduction of the volume and density

of the initial cell aggregate was detected. The paraffin-embedded sections of control samples were stained with Alcian Blue, but in spite of low pH of the dyeing solution, a light blue staining was also detected in the control (Figure 3.3.1.1.L).

ASC ability to differentiate into other cell types of mesodermal origin is a key for verifying their identity. Obtained results showed that ASCs cultured in the presence of AS can be effectively differentiated into adipocytes and chondrocytes not only at P3, but also at P6. However ASC differentiation into osteocytes was weak at P3 and obtained data suggest that it may have decreased even more at P6. Comparison of the differentiation samples from P3 and P6 was done by visual assessment, and the aim of *in vitro* differentiation was to evaluate the potency of ASCs from various passages to differentiate into other cell types of mesodermal origin as such, not to directly compare the extent of each differentiation between P3 and P6. In the case of osteogenic differentiation the weak formation of calcified extracellular matrix was observed in all triplicates at P3, but Alizarin Red S staining was detected only in one triplicate at P6. As this most likely represents a characteristic of the ASC donor, since the same protocol of differentiation has yielded reliable results with ASCs from different donors, for example, the donor No.5 (Figure 3.3.1.2.), it is impossible to state that the ability of ASCs, cultured in AS, to differentiate into osteogenic lineage diminishes in later passages. Others show that differential capacity of ASCs, when cultured in the standard media, is preserved through 10 to 13 passages (Wall et al. 2007, Gruber et al. 2012), but decreases at P25 (Zhu et al. 2008).

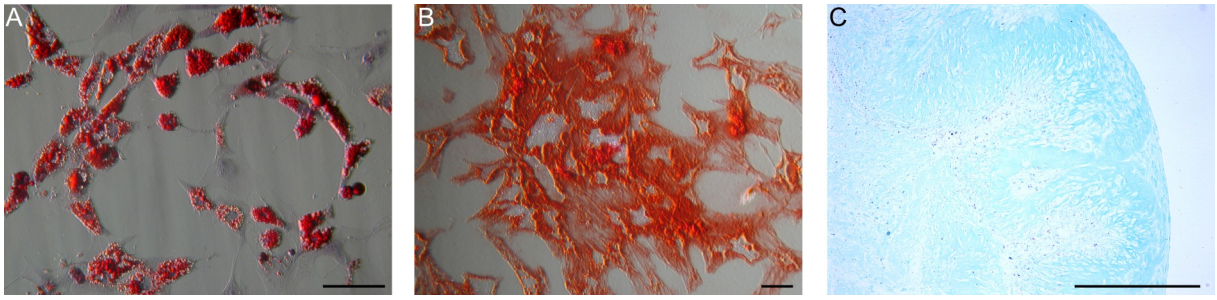

Figure 3.3.1.2. ASCs of the donor No.5 at P4 differentiated towards adipogenic, osteogenic, and chondrogenic lineages. (A) Detection of lipids with Oil Red O. (B) Detection of calcified extracellular matrix with Alizarin Red S. (C) Detection of sulfated proteoglycans with Alcian Blue. In the Figure 3.3.1.2. A the cells are counterstained with hematoxylin. Scale bar 100 μm.

One could argue that the observed differentiation could represent the presence of various lineage-committed progenitor cells or other multipotent cells, such as pericytes or BM MSCs from peripheral blood, and not the multipotentiality of ASCs (Zuk et al. 2001). Since SVF contains preadipocytes that can differentiate into mature fat cells, it would be feasible to suspect their possible contribution to adipogenic differentiation. However, only 0,02% of human adipose tissue are adipocyte precursor cells (Pettersson et al. 1984) and such a low overall occurrence could not constitute for the detected level of adipogenic differentiation. The possibility that osteogenic or chondrogenic progenitor cells could be found in SVF due to disruption of blood vessels in adipose tissue is very low as well. Even if circulating blood carries such progenitor cells, their amount in peripheral blood is likely negligible. The same could be said about BM MSCs, as there is not enough evidence supporting their presence in peripheral blood (Zuk et al. 2001). And since only 0,001 to 0,01% of all nucleated cells of BM are MSCs (Pittenger et al. 1999), their amount in circulating blood is bound to be even lower, thus making their possible contamination of SVF insignificant (Zuk et al. 2001). However, the possibility that fibroblasts and pericytes could be present in SVF may not be entirely excluded. Since their immunophenotype profile is very similar to ASCs (Covas et al.

2008) and the surface markers exploited in this study could not discriminate between them and ASCs, and considering the ability of both fibroblasts (Lorenz et al. 2008, Blasi et al. 2011) and pericytes (Covas et al. 2008, Crisan et al. 2008) to differentiate into adipocytes, osteocytes, and chondrocytes, it is probable that observed differentiation is partly due to their presence in ASC culture.

3.3.2.Differentiation of ASCs into insulin-producing cells

3.3.2.1. Protocol 1

The ASCs from the donor No.4 at P5 were subjected to the differentiation Protocol 1. This protocol was composed from analysis of literature covering production of pancreatic hormone-expressing cells from ESCs, since these differentiation protocols are more detailed than those described for somatic SCs and majority of the extrinsic factors added to induction media is identical in both cases. For the first 3 days the cells were deprived of serum, as an absence or low concentrations of serum in the presence of high concentrations of activin A facilitates the differentiation of human ESCs into definitive endoderm (D'Amour et al. 2005). After the first stage of differentiation the cells started to enlarge and an accumulation of intracellular granules as well as clustering of ASCs were observed (Figure 3.3.2.1.1.).

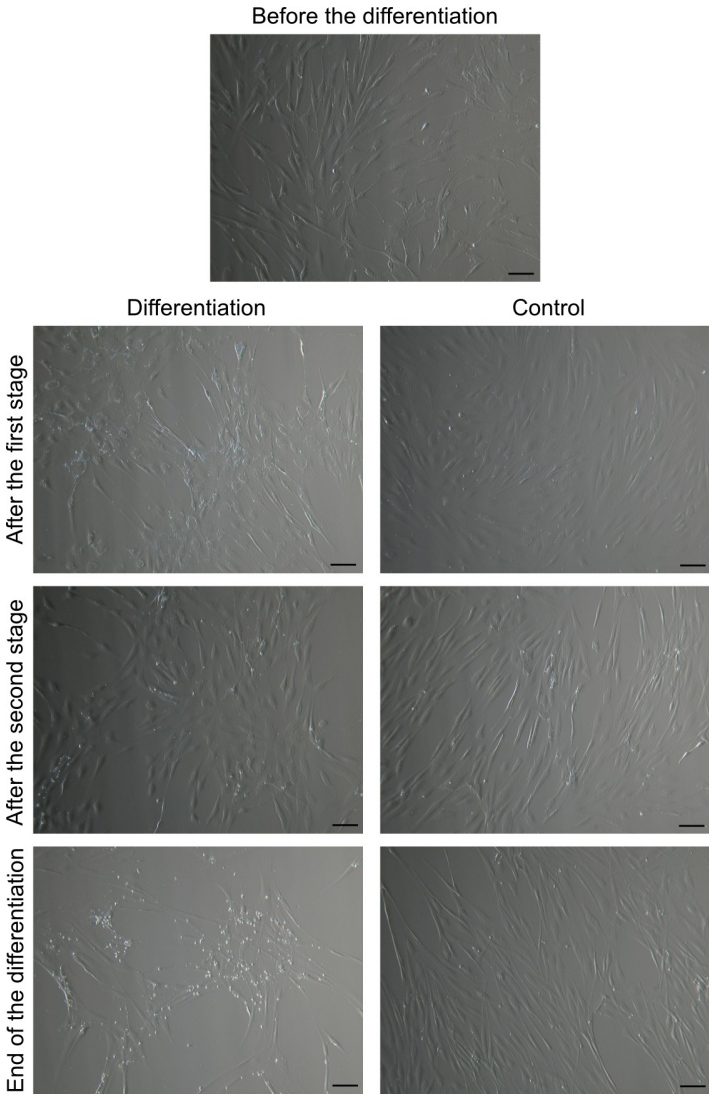

Figure 3.3.2.1.1. Morphological changes in ASCs during their differentiation into insulin-producing cells using the Protocol 1. Scale bar 100 μm.

During the second stage of differentiation the cells lost their intracellular granules, but the clustering became more prominent. At the end of this stage few rounded granules, attached to a cell surface, were detected. The amount of these granules increased during the third stage of differentiation. The granules were considered cell debris or dead cells although they could not be effectively removed by washing with PBS. Since the cell death became more pronounced, the DAPT was omitted from the third stage differentiation medium after few days to exclude a possible cell death by elevated DMSO (used as a solvent for DAPT) concentration in the medium. At the end of the differentiation the remaining monolayer cells were gathered into clusters and covered with cell debris. In the control medium discrete cell clustering and slight amount of cell debris were observed.

To test the course of differentiation, an immunocytochemistry method was used. After the first stage of differentiation the cells in differentiation and control media were stained using anti-SOX17 antibody. As the SOX17 is a transcription factor, it should be located in a nucleus. The results revealed notable nuclear staining as well as slight cytoplasmic staining in both differentiation and control samples (Figure 3.3.2.1.2.). No substantial difference was found between these two samples tested.

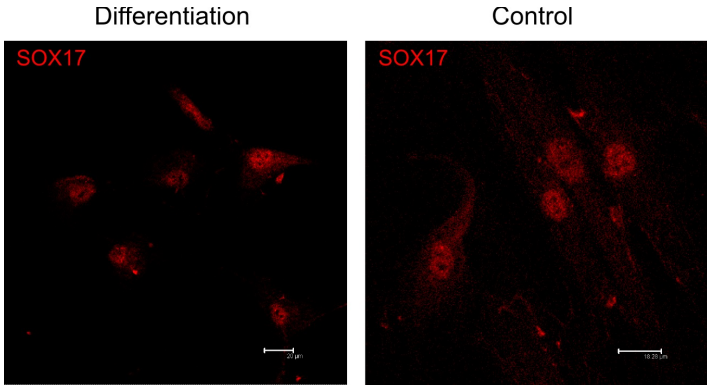

Figure 3.3.2.1.2. Expression of SOX17 in ASCs after the first stage of differentiation into insulin-producing cells using the Protocol 1. Analysis of confocal laser scanning microscopy. Author R.Brūvere.

After the second stage of differentiation the differentiation and control samples were stained using anti-PDX1 antibody. Likewise SOX17, PDX1 is also the transcription factor and should be expressed in a nucleus. Obtained immunocytochemistry data showed exclusive staining of nucleoli and an other cell organelle, likely a Golgi complex (Figure 3.3.2.1.3.). No prominent difference in a staining pattern was found between differentiation and control samples, however the staining intensity in the control sample was reduced in comparison to the differentiation sample (based on a visual assessment).

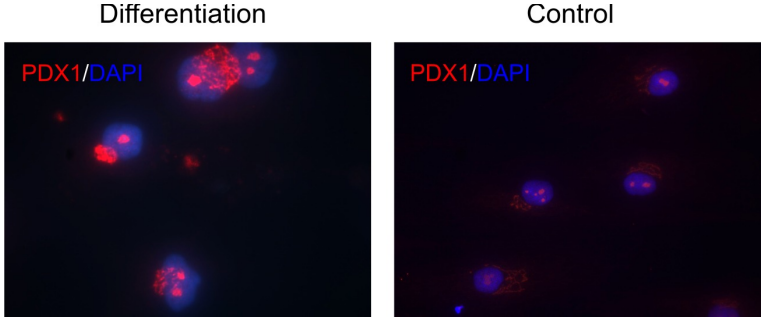

Figure 3.3.2.1.3. Expression of PDX1 in ASCs after the second stage of differentiation into insulin-producing cells using the Protocol 1. Cell nuclei stained with DAPI. Magnification 1000x for the differentiation image and 630x for the control image. Author R.Brūvere.

At the end of the differentiation Protocol 1 a double staining immunocytochemistry method was used on the differentiation samples. Anti-C-PEPT, anti-NGN3, and anti-SST antibodies were co-stained with anti-INS or anti-GCG antibodies which were tested on cryosections of mouse pancreas beforehand to verify their reactivity (Appendix 27). The obtained results from the differentiation Protocol 1 demonstrated that INS was weakly expressed in a cytoplasm and, although it is a cytoplasmic protein, distinctly found in the nuclei (Figure 3.3.2.1.4.). The C-PEPT was found only in the cytoplasm and it showed a colocalization with cytoplasmic staining of INS. The NGN3, which is the transcription factor, was mainly detected in the nuclei and probably the Golgi complex, as the staining pattern of this organelle was similar to that observed using the anti-PDX1 antibody. The exact colocalization was found between INS and SST. Even though the SST is the cytoplasmic protein, an apparent nuclear staining was also discovered likewise in the case of INS. The GCG was expressed in the cytoplasm and showed colocalization with C-PEPT and cytoplasmic parts of staining of NGN3 and SST (Figure 3.3.2.1.5.).

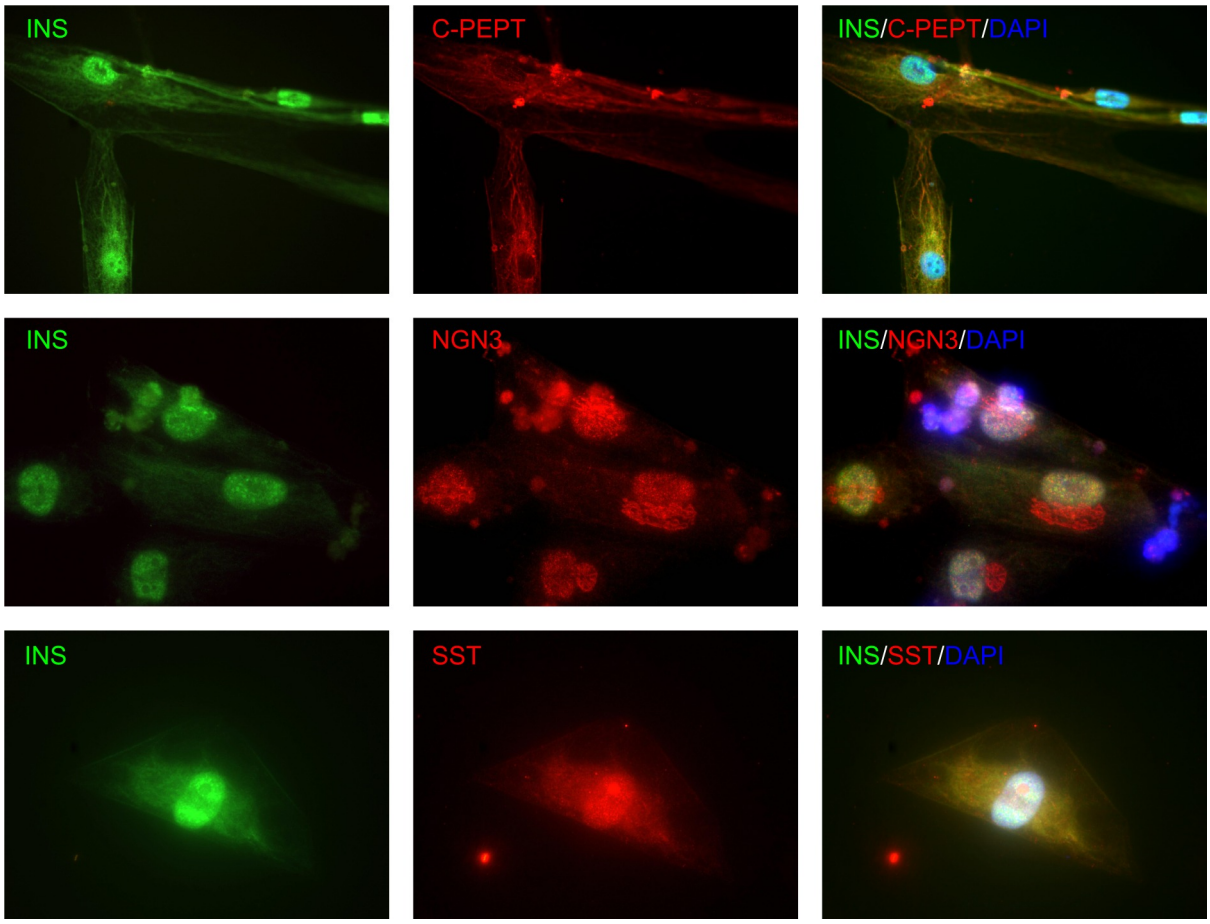

Figure 3.3.2.1.4. Expression of INS, C-PEPT, NGN3 and SST in ASCs after their differentiation into insulin-producing cells using the Protocol 1. Cell nuclei stained with DAPI. Magnification 1000x. Author R.Brūvere.

The dead cells, broadly observed during the third stage of differentiation, were also detected after the immunocytochemical analysis (Figure 3.3.2.1.4. in the INS/NGN3 image and Figure 3.3.2.1.5. in the GCG/NGN3 and GCG/SST images). They were recognized as small, rounded cells with very bright staining of DAPI and all the antibodies tested, probably caused by an unspecific binding due to the damaged membranes.

After each stage of differentiation part of the cells was collected in order to obtain total RNA and perform quantitative real-time RT-PCR analysis. Unfortunately a yield of RNA from

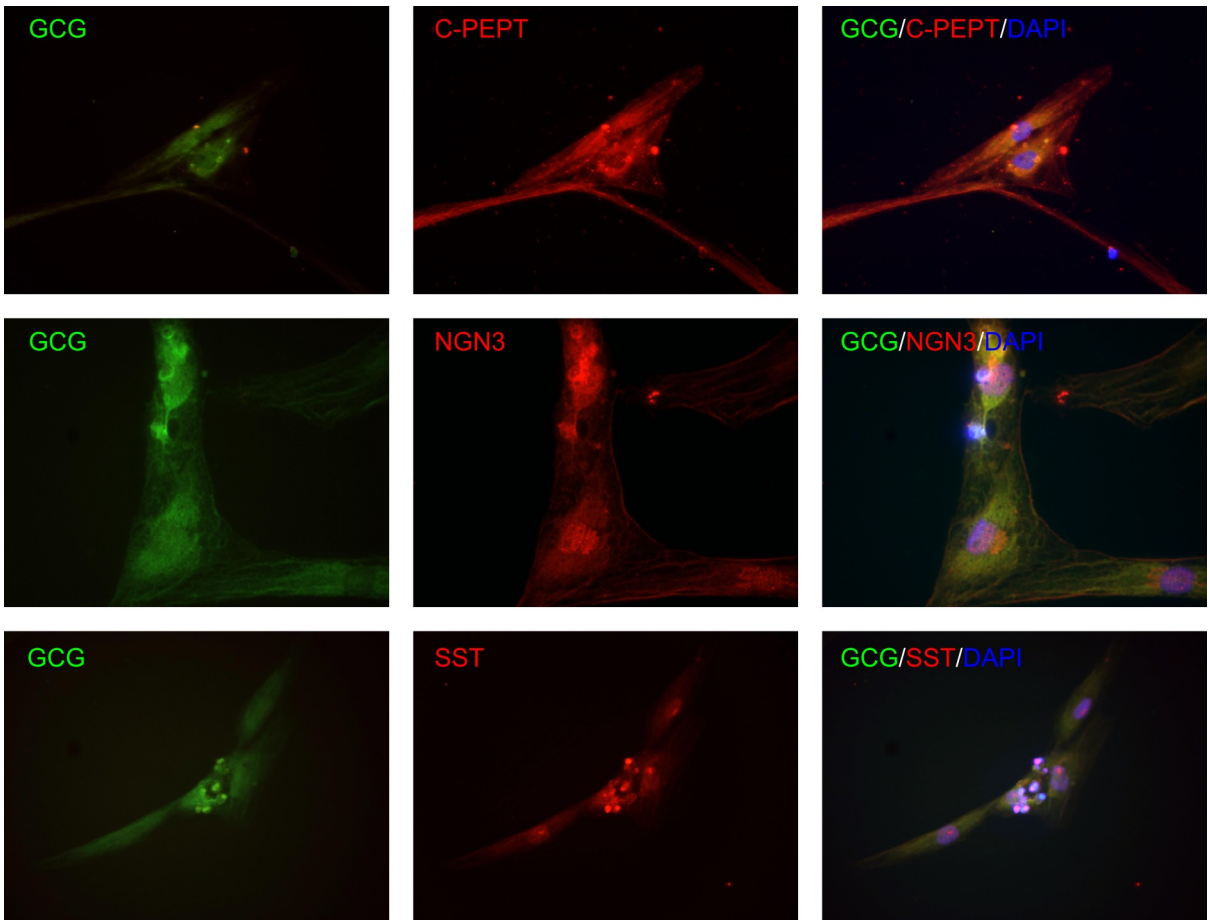

Figure 3.3.2.1.5. Expression of GCG, C-PEPT, NGN3 and SST in ASCs after their differentiation into insulin-producing cells using the Protocol 1. Cell nuclei stained with DAPI. Magnification 400x for the GCG/C-PEPT and GCG/SST images and 630x for the GCG/NGN3 image. Author R.Brūvere.

all gathered samples was very low due to a chosen extraction method and resulting RNA was not suitable for effective PCR analysis. We were able to perform an initial analysis of the expression of genes *PDX1*, *MNX1*, and *INS* using a cDNA synthesised from the scarce RNA samples. None of the samples from all stages of differentiation or control showed the expression of above-mentioned genes (data not shown).

Since the expression of genes *PDX1* and *INS* was not detected and the observed staining pattern of respective antibodies was also inconclusive, it is likely that ASCs were not able to differentiate into insulin-producing cells using above-tested protocol. Firstly, their initial differentiation into DE was uncertain, as immunocytochemistry results using anti-SOX17 antibody showed no difference between the differentiation and control samples. It is doubtful that undifferentiated ASCs express SOX17 which is a marker of endoderm (Grapin-Botton 2008). Even if so, it could not be much higher than a background level and there should be considerable upregulation visible in the differentiation sample after the first stage of the Protocol 1. Activin A, which was used during the first stage of differentiation, is known to facilitate the differentiation of human ESCs into DE (D'Amour et al. 2005). It has also been successfully used in the differentiation protocols of MSCs (Sun Y. et al. 2007, Chandra et al. 2011), although other research has showed that the use of activin A is insufficient to induce differentiation of DE from UC blood SCs (Filby et al. 2011). Secondly, the posterior foregut marker PDX1 was not detected after the second stage of differentiation at gene level and immunocytochemistry data did not show its expected staining pattern. It inclines to suggest that even if the detected positive signal of SOX17 represented the cells that were prone to

endodermal differentiation, the further process of differentiation has been hampered. However, immunocytochemical analysis at the end of the differentiation demonstrated that the cells stained positive for INS, GCG, C-PEPT, NGN3, and SST. Nevertheless, their staining pattern did not entirely match the staining of positive control (mouse pancreas). Additionally, the transition states of ASCs were not detected neither using SOX17 nor PDX1 antibodies, and it is highly unlikely that such differentiation would happen directly, without gradual transformation that could be followed. The lack of *INS* gene detection by real-time RT-PCR analysis is in further support of unspecific binding of used antibodies rather than actual expression of tested antigens. Together these results suggest that ASCs were not able to differentiate into insulin-producing cells using Protocol 1.

3.3.2.2. Protocol 2

The ASCs from the donor No.4 at P6 were subjected to the differentiation Protocol 2. This protocol was based on the Protocol 1, but with few alterations. First, before the differentiation the ASCs were grown in the serum-free pre-differentiation medium containing EGF and bFGF for 2 days. This step has been successfully used in hepatogenic differentiation protocol (Taléns-Visconti et al. 2006). Since it is believed that pancreas and liver share a common precursor (Zaret 2001), this step could facilitate the chosen differentiation protocol. Second, starting from the first stage of differentiation the cells were grown at 60% O_2 level, as elevated levels of oxygen could favor the pancreatic differentiation (Fraker et al. 2009, Heinis et al. 2010). Third, B-27 supplement was omitted from the differentiation protocol, since it contains human recombinant insulin that can give false positive result in the immunocytochemical analysis with anti-INS antibody (Hansson et al. 2004).

The ASCs, used for the experiment, showed an accumulation of intracellular granules from the beginning of differentiation probably due to a late cell passage and became more prominent during the course of differentiation (Figure 3.3.2.2.1.). Until the end of the second stage no difference between the control and experimental samples was observed. Part of the cells lost their spindle-shaped appearance and shifted to more rounded and flattened look. At the third stage of differentiation the cells in the differentiation medium started to detach from the surface due to apoptosis or necrosis. After the twelfth day in the third stage differentiation medium the experiment was discontinued due to the high rate of cell death. In the control medium the detachment of the cells was also detected, but not in such a great scale as in the differentiation medium.

The cells in the differentiation medium after the first and second stages of differentiation were stained with anti-SOX17 and anti-PDX1 antibodies respectively (Figure 3.3.2.2.2.). Obtained results revealed similarities with the staining pattern observed in the cells differentiated using the Protocol 1. The SOX17 was detected in the nuclei and only slightly in the cytoplasm. The PDX1 was identified for the most part in the nucleoli, but distinct staining of probable Golgi complex, as in the cells differentiated after the Protocol 1, was not observed. Instead, a weak cytoplasmic staining could be seen throughout the cytoplasm.

At the end of the differentiation Protocol 2 a double staining immunocytochemistry method was also tried on the differentiation samples. Since most of the cells were lost during the last stage of differentiation and in a fraction of remaining cells a fragmentation of a nucleus was observed (from DAPI staining; data not shown) signalling of undergoing necrosis or apoptosis, the obtained results could not be considered reliable. This makes a competent analysis of tested markers impossible. The examples of acquired INS, C-PEPT and SST staining are given in the Figure 3.3.2.2.3.

The same concern applies to an extraction of total RNA. The cells from the third stage of differentiation do not represent a healthy cell culture hence rendering the gene analysis meaningless. The real-time RT-PCR analysis was carried out on the cDNA samples of

differentiation and control cells from the first and second stages, but no expression of genes *PDX1*, *MNX1*, *HNF4A*, *NKX6-1*, and *INS* was detected (data not shown).

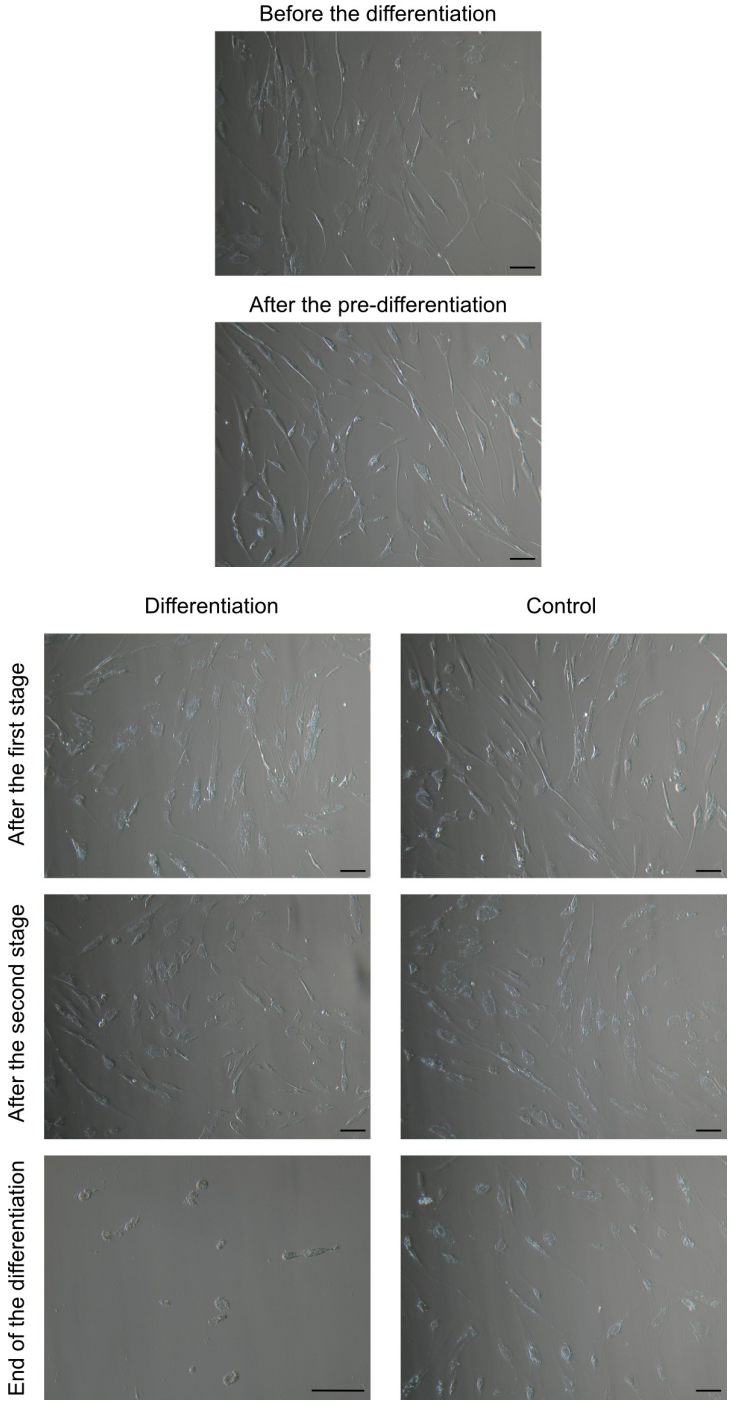

Figure 3.3.2.2.1. Morphological changes in ASCs during their differentiation into insulin-producing cells using the Protocol 2. Scale bar 100 μm.

Because of the prominent loss of cells during the last stage of differentiation rendering any possible further analysis unnecessary, the Protocol 2 was considered unsuccessful. The exact cause of cell necrosis or apoptosis was not fully identified. Since this differentiation protocol was very similar to the Protocol 1, but cell detachment at such scale was not observed during the differentiation Protocol 1, it is plausible to suspect that the cell death was caused by few novelties introduced in the Protocol 2. The pre-differentiation stage could not have induced the cell necrosis or apoptosis, as the cell death was not detected until the third

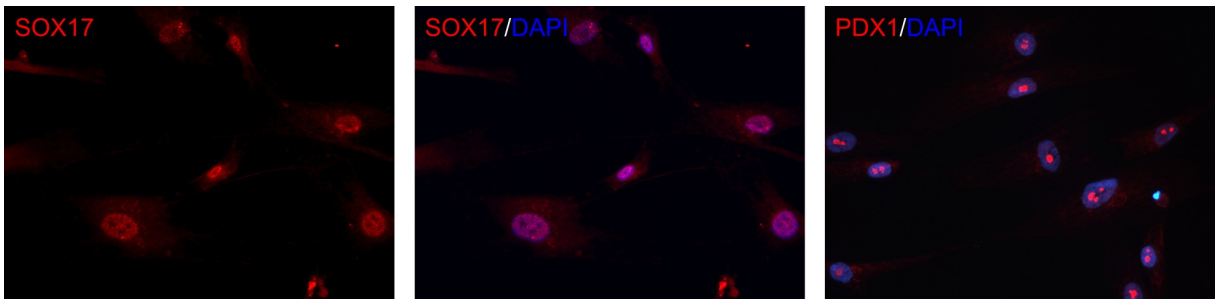

Figure 3.3.2.2.2. Expression of SOX17 and PDX1 in ASCs after the first (for SOX17) and the second (for PDX1) stages of differentiation into insulin-producing cells using the Protocol 2. Cell nuclei stained with DAPI. Magnification 400x.

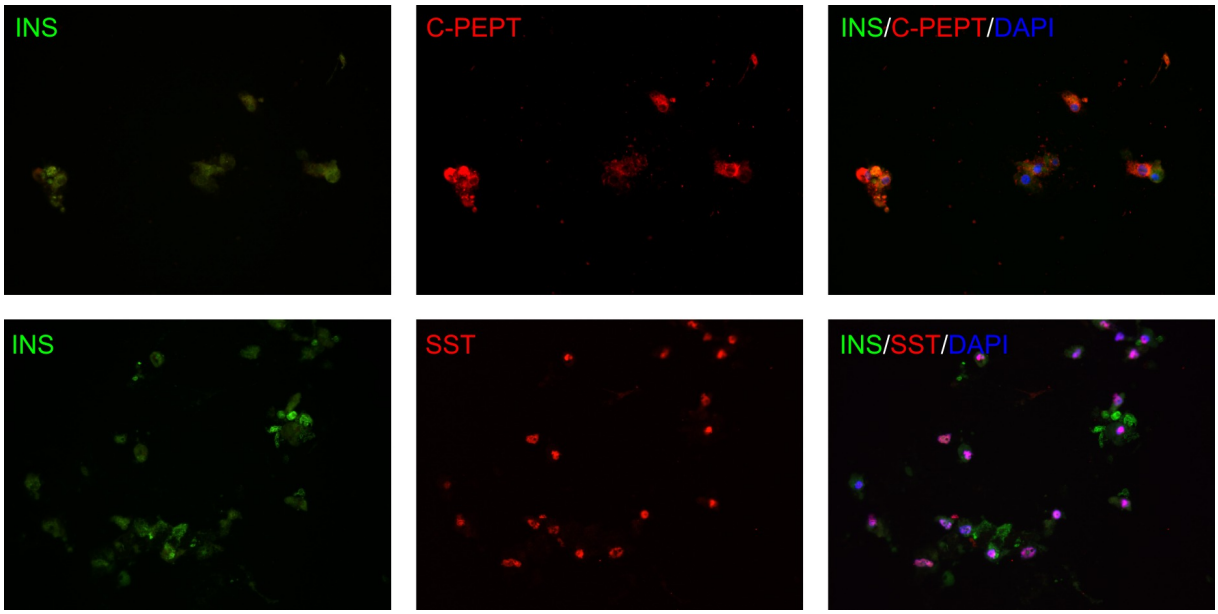

Figure 3.3.2.2.3. Expression of INS, C-PEPT, and SST in ASCs after their differentiation into insulin-producing cells using the Protocol 2. Cell nuclei stained with DAPI. Magnification 400x.

stage. Similarly, discontinued use of B-27 supplement can not have any impact on the survival of cells. That leaves the change of growth conditions, since the differentiation Protocol 2 was performed at 60% O_2 instead of 21% O_2, as usually accepted. Although oxygen is critical for the normal growth of mammalian cells, concentrations higher than 200 μM have been shown to obstruct the growth and metabolism of various types of cells. Normally cells are cultured at 21% gas-phase O_2 where they are exposed to dissolved O_2 concentrations of 200 μM or less (saturation of the air with water vapor at 37^{0}C reduces the concentration of oxygen to approximately 190 μM). Research shows that a human β cell line TK6 can grow normally at 40% O_2 (approximately 380 μM dissolved oxygen) and continued exponential cell growth can be observed up to O_2 concentration of 540 μM (Oller et al. 1989). Mouse ESCs and human iPSCs can be more efficiently differentiated into insulin-producing cells at 60% O_2 (Hakim et al. 2014), and murine pancreatic buds cultured at 80% O_2 show much higher β cell differentiation when compared to cultures at 21% O_2 (Heinis et al. 2010). Since, to our knowledge, there have not been any published data about impact of high levels of oxygen on the growth, differentiation, or survival of MSCs, one can only speculate about its influence during the differentiation Protocol 2. As ASCs in a control medium were cultured under the same conditions, but exhibited much lower cell death rate, the elevated level of O_2 could not be the only cause of observed cell necrosis or apoptosis. However, the cells in the control

medium at the end of differentiation were more flattened and their spindle-shaped appearance was partly lost, not speaking in favor of ASC cultivation at 60% O_2 for prolonged periods. Experiments with mouse ESCs have shown that culturing at high levels of O_2 starting from the first day of their differentiation into insulin-producing cells diminishes survival of cells. To avoid this, mouse ESCs are subjected to 60% O_2 starting from the third day of differentiation. Additionally, their culturing at high levels of O_2 during the early stages of differentiation has the biggest effect on the efficiency of differentiation (Hakim et al. 2014). It is possible that similar approach to use 60% O_2 only during the first two stages of differentiation and to apply it few days after the initiation of differentiation would have yielded better results and reduced the cell death. There is also a slight probability that a later cell passage used for this differentiation has influenced the failure of this protocol. It is hard to say why, because the ASCs from the donor No.4 at P6 have been successfully differentiated into adipocytes, osteocytes, and chondrocytes. Since no data is available on MSC differentiation or survival under high levels of oxygen depending on cell passage, this possibility can not be entirely excluded.

3.3.2.3. Protocol 3

The ASCs from the donors No.3 and No.4 at P4 were subjected to the differentiation Protocol 3. Since differentiation of ASCs into insulin-producing cells using previous two protocols composed by ourselves was not successful, we chose to test the differentiation protocol described by Kang et al. 2011. We incorporated small changes into their protocol by substituting a glucagon-like peptide 1 (GLP-1) by an exendin-4 and excluding a FBS for the first 3 days. Since natural GLP-1 is rapidly degraded, it is possible to use its long-acting analogue exendin-4 (Suen et al. 2006). And since activin A stimulates the differentiation more effectively when the FBS is absent or in low concentrations (D'Amour et al. 2005), we decided to eliminate it at the beginning of the differentiation.

Throughout the differentiation ASCs from both donors preserved their spindle-shaped appearance and no morphological changes were detected in differentiated cells when compared to control cells (Figure 3.3.2.3.1.). In the course of the differentiation a formation of cell clusters was observed both in differentiation and control cells, but it was caused by a rapid cell growth in the differentiation and control media and a limited growth space rather than a ASC differentiation itself. Since a cell growth of both donors was practically identical, only morphology of ASCs of the donor No. 3 during the differentiation is presented herein.

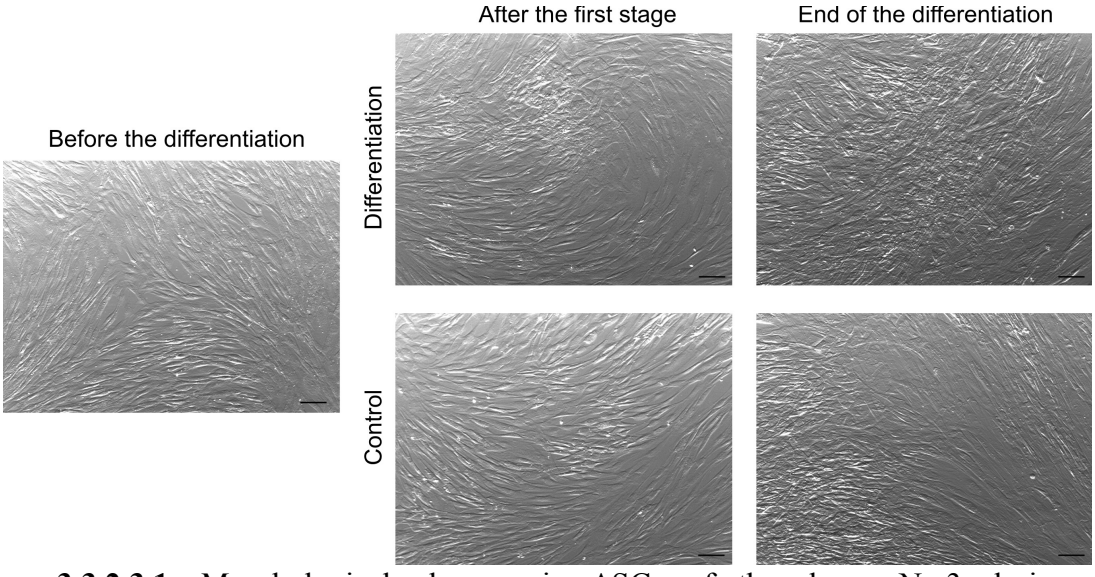

Figure 3.3.2.3.1. Morphological changes in ASCs of the donor No.3 during their differentiation into insulin-producing cells using the Protocol 3. Scale bar 100 μm.

For this protocol immunocytochemistry method was not performed. After the first stage and at the end of differentiation the cells were collected for total RNA isolation. A reversely transcribed cDNA was used to detect expression of housekeeping genes *GUSB* and *YWHAZ* as well as genes *SOX17*, *FOXA2*, *CK19*, *PDX1*, *INS*, *SST*, *PPY*, *ISL1*, and *GCG* involved in the differentiation into insulin-producing cells by quantitative real-time RT-PCR analysis. After the initial screening of the genes critical to successful differentiation, only *SOX17*, *FOXA2*, *CK19, SST*, and *PPY* were detected in some of the examined samples (data not shown). Since those genes were detected both in differentiation and control samples from both donors, but no visible trend was detected throughout tested samples, the differentiation into insulin-producing cells using Protocol 3 was considered unsuccessful. This protocol has been used to differentiate ASCs from human eyelid into insulin-secreting cells with considerable achievement. Even without extra addition of insulin-like growth factor 2 to the induction medium, after three weeks of differentiation the cells expressed such genes as *ISL1*, *NGN3*, *NKX2.2*, *PDX1*, *NKX6.1*, and *INS* among others β cell-related genes, as well as secreted insulin in a glucose-dependent manner (Kang et al. 2011). As probable reasons for the inability of used protocol to induce differentiation of herein studied ASCs could be suggested different source of ASCs, donor-to-donor variability, or alterations made to differentiation medium.

3.3.2.4. Protocol 4

In parallel with the Protocol 3 the ASCs from the donors No.3 and No.4 at P4 were also subjected to the differentiation protocol published by Chandra et al. 2011. This study used low adherence cell culture dishes to achieve cell differentiation via aggregation. The same as in the Protocol 3, a GLP-1 was replaced with an exendin-4. In addition, sodium selenite was omitted.

The use of low attachment cell culture plates resulted in the formation of ASC aggregates soon after the beginning of the differentiation Protocol 4. On the next day the ASCs were congregated into irregular aggregates of different sizes that freely floated into a medium (Figure 3.3.2.4.1.). After the first stage of the differentiation most of the cell aggregates became rounded in shape, but their size still differed greatly. After the second stage a considerable part of smaller aggregates had disappeared, and this pattern was observed also throughout the third stage of the differentiation. The main reason for the cell loss during the differentiation process was disintegration of formed ASC aggregates. It seemed that cell to cell interactions within the small-scale aggregates were not strong enough, causing their decomposition. Towards the end of the differentiation, even the larger aggregates started to disintegrate. The cells at the outer edge of aggregates became swollen and gradually loosened. This process together with a mechanical loss of the cells during the medium changes, that included collection and centrifugation of ASC aggregates, resulted in a very few large aggregates at the end of the differentiation Protocol 4.

After the first stage and at the end of differentiation a total RNA was isolated and the same set of gene expression as after the Protocol 3 was tested by quantitative real-time RT-PCR. Similarly to that protocol, only *SOX17*, *CK19, SST*, and *PPY* were detected in some of the examined samples, but without a coherent trend (data not shown). Although cell aggregation into 3D clusters has been successfully employed on ASCs leading to their differentiation into physiologically functional islet-like cell aggregates (Chandra et al. 2011), this method was not effective in our experience. Observations during the differentiation process suggested that ASCs cultivation on low adherence cell culture plates did not give the expected result. Quite the opposite, disintegration of 3D aggregates and subsequent loss of cells gave no opportunity to evaluate the efficiency of the tested protocol itself, since such culture conditions were not optimal for ASCs survival, let alone differentiation.

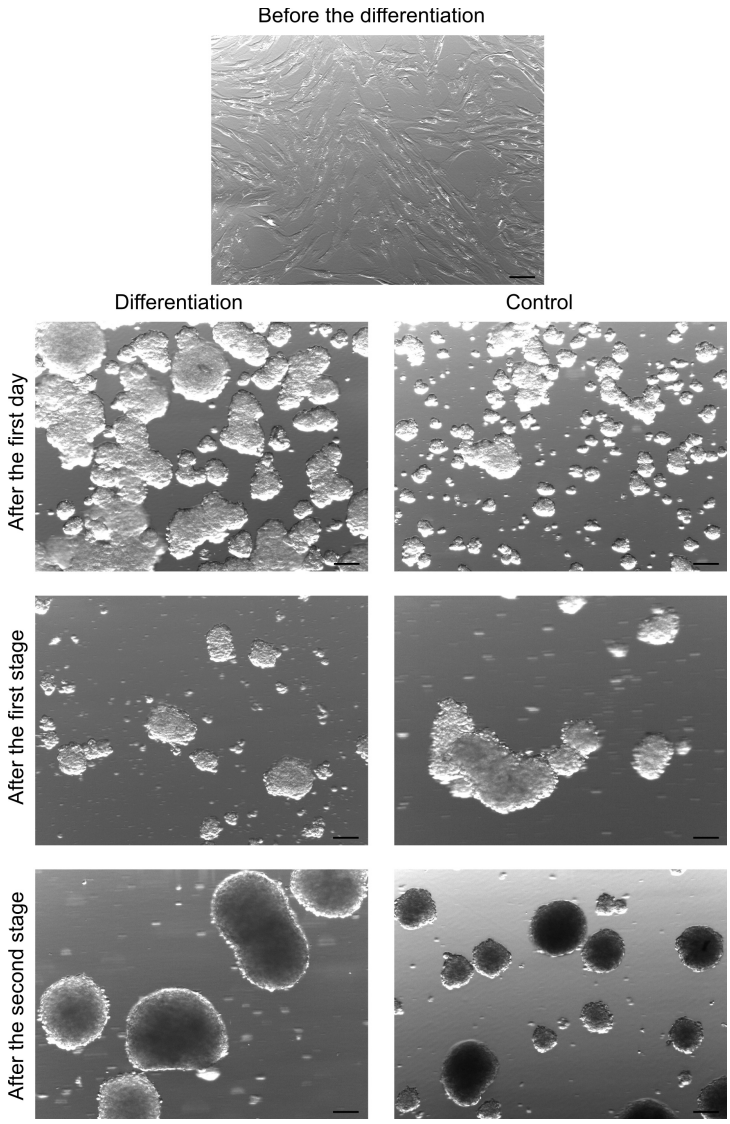

Figure 3.3.2.4.1. Morphological changes in ASCs of the donor No.3 during their differentiation into insulin-producing cells using the Protocol 4. Scale bar 100 μm.

3.3.2.5. Protocols 5-8

Since previously examined 4 protocols did not result in a successful differentiation of ASCs into insulin-producing cells, we decided to test whether ASCs are at least able to differentiate into cells of endodermal origin. This is usually achieved after the second stage of differentiation into insulin-producing cells and is the most important turning-point in the process of this differentiation. We chose three previously published studies that have shown notable differentiation of MSCs into insulin-producing cells and followed the first two stages of their differentiation protocols that should result into the differentiation of cells with endodermal characteristics according to their results. Additionally we included the fourth protocol to test a role of small molecules in the differentiation process. The ASCs from the donors No.4 and No.9 at P4 were subjected to the differentiation. The ASCs from both donors showed morphological differences before a start of the differentiation. ASCs of the donor No.4 were spindle-shaped like classical MSCs (Figure 3.3.2.5.1.) whereas part of the ASCs of the donor No.9 were larger, more flattened, and exhibited more rounded shape (Figure 3.3.2.5.2.).

Protocol 5 was based on the observations that two small molecules LY294002 and CHIR99021 can facilitate differentiation into endodermal lineage (McLean et al. 2007, Kunisada et al. 2012). After the first stage of the differentiation the cells from both donors

were finely spindle-shaped (Figures 3.3.2.5.1. and 3.3.2.5.2.), but the cells of the donor No.9 showed elevated cell death rate. At the end of the differentiation protocol almost all cells of the donor No.9 were lost. The cells of the donor No.4 turned out to be more tolerant as approximately 50% of the cells remained after the differentiation has been finished. The ASCs of both donors in a control medium did not show any changes throughout the differentiation.

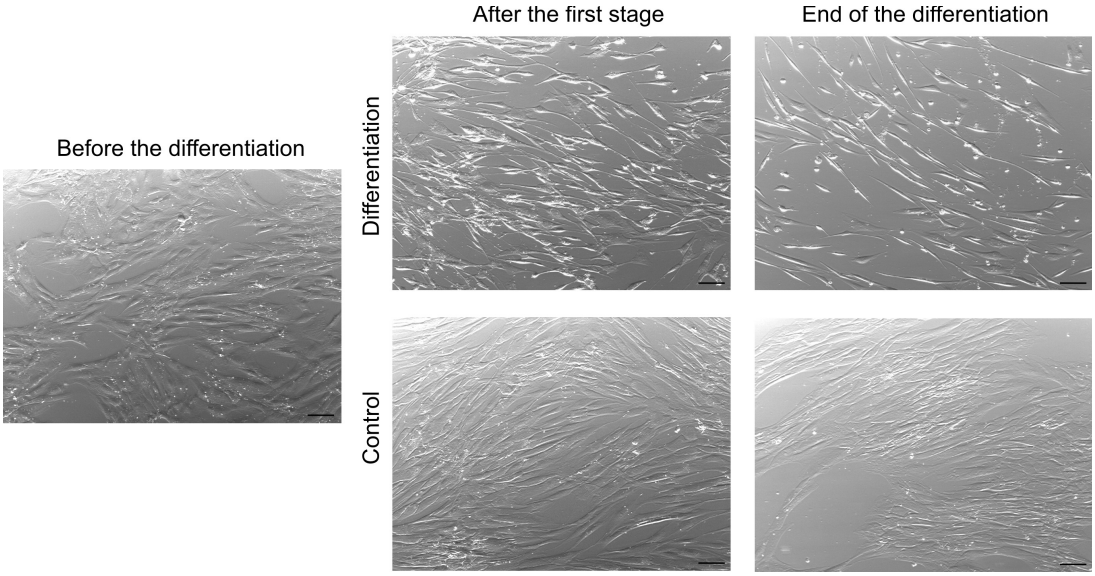

Figure 3.3.2.5.1. Morphological changes in ASCs of the donor No.4 during their differentiation into cells of endodermal lineage using the Protocol 5. Scale bar 100 μm.

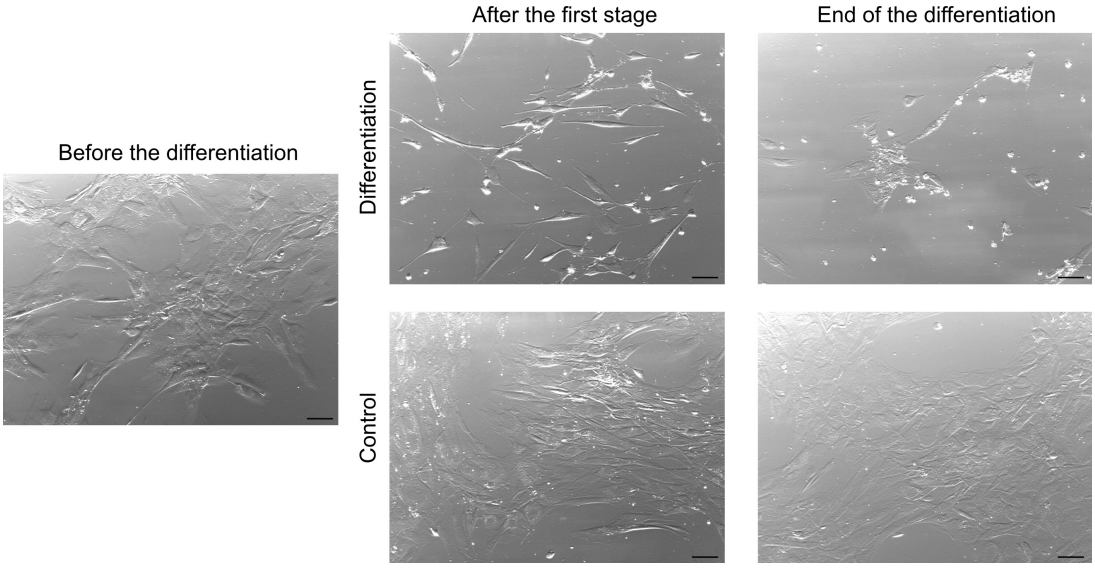

Figure 3.3.2.5.2. Morphological changes in ASCs of the donor No.9 during their differentiation into cells of endodermal lineage using the Protocol 5. Scale bar 100 μm.

Since all the components of the differentiation medium used in the Protocol 5, except LY294002 and CHIR99021, have been tested previously and have not shown such cell death rate, it is feasible to suspect the role of those two small molecules in the observed process. CHIR99021 is a highly selective inhibitor of GSK3β and GSK3α and its effect on other cell signalling processes would be very low (Kunisada et al. 2012), thus diminishing its potential effect on observed cell death. Although there is no information about its influence on ASC cultures, it has been shown that UC blood SCs can be cultured in the presence of CHIR99021 at least for a week with increasing cell numbers (Huang et al. 2012). On the other hand,

LY294002 is not only a strong inhibitor of PI3K signalling, but also a potent inhibitor of other proteins. And considering the crucial role of PI3K signalling in growth, proliferation, metabolism, and survival of cells (Gharbi et al. 2007), its long-term inhibition alone could lead to elevated cell death. It is known that LY294002 at higher concentrations than 50 μM causes human ESC death in a concentration-dependent manner, but its action in DE formation is safe and effective at concentrations between 20 and 50 μM (McLean et al. 2007). Although in this protocol LY294002 was used at 50 μM concentration that should be safe for ESCs, its influence on ASCs is unknown. As observed during this differentiation Protocol 5, there was a significant difference between ASCs from both donors regarding their tolerance for used induction protocol, most likely caused by impact of LY294002. The exposure time of LY294002 is another crucial issue in ESC differentiation into DE. Sustained inhibition of PI3K for 4 to 5 days is necessary for successful differentiation of ESCs (McLean et al. 2007), and since differentiation potential of somatic SCs is considered lower than that of ESCs, the treatment with LY294002 was prolonged in our protocol. It is possible that the detected increase in cell death was due to a role of PI3K in cell survival processes, and blockade of its signalling for more than 5 days turned out to be critical for examined ASC cultures. However, ASCs of the donor No.9 were more susceptible and even 3 days in the presence of LY294002 caused their death. The observed change in cell morphology of both donors was also likely the result of LY294002 action, as it has been observed in human ESCs and is associated with downregulation of the cell adhesion molecule E-cadherin (McLean et al. 2007).

Protocol 6 was based on the manuscript by Buang et al. 2012. The original manuscript described a generation of insulin-producing cells from human ASCs in three weeks. We repeated the first stage of their protocol substituting only a glucagon-like peptide 1 (GLP-1) by an exendin-4 and changing a concentration of FBS. The authors used 10% FBS for the differentiation medium, but we applied 0,2% FBS for the first 3 days and 2% FBS afterwards. We decided to reduce the concentration of FBS, as their protocol included addition of activin A and it is known to be more effective in the presence of low concentrations of FBS (D'Amour et al. 2005). During the differentiation ASCs did not change their morphology and no difference was observed between differentiation and control cells in neither of donors (Figures 3.3.2.5.3. and 3.3.2.5.4.). A transformation of cell growth pattern of both donors was

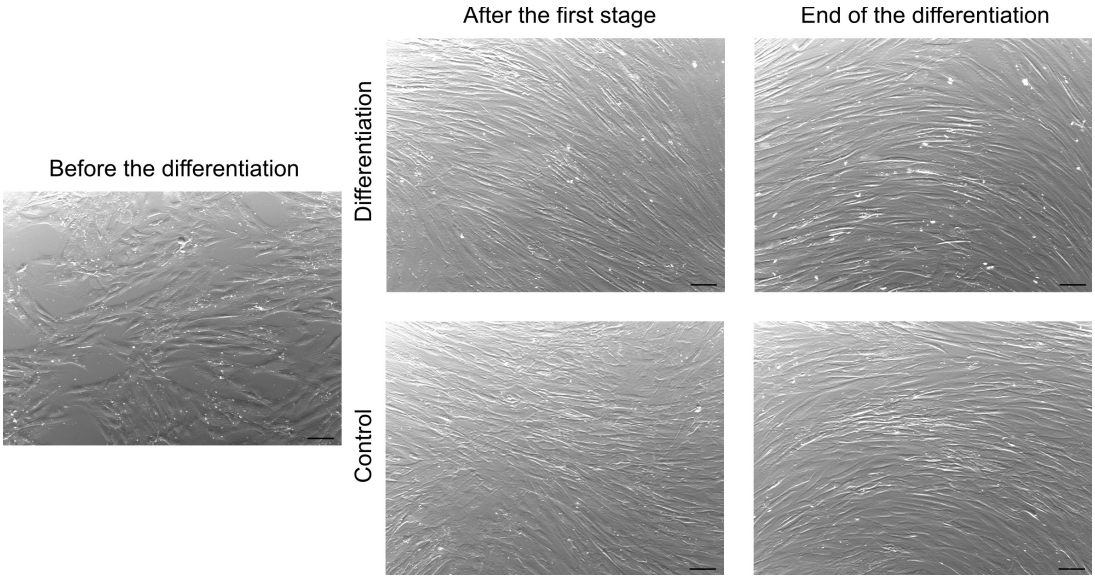

Figure 3.3.2.5.3. Morphological changes in ASCs of the donor No.4 during their differentiation into cells of endodermal lineage using the Protocol 6. Scale bar 100 μm.

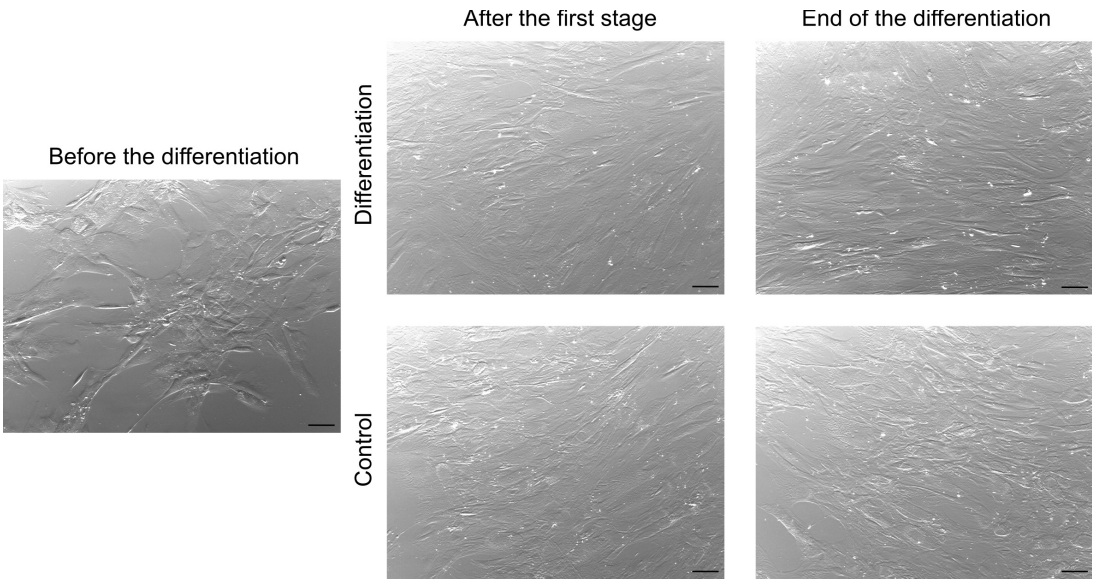

Figure 3.3.2.5.4. Morphological changes in ASCs of the donor No.9 during their differentiation into cells of endodermal lineage using the Protocol 6. Scale bar 100 μm.

detected, as active cell growth continued throughout the differentiation process. This is in compliance with published data, since during the first stage of differentiation continuous cell expansion is observed and morphological changes could be detected only during the following stage (Buang et al. 2012).

Protocol 7 was based on the manuscript by Gao et al. 2008. The first stage of this differentiation protocol lasts only three days during which UC blood SCs show no changes in their morphology, but the expression of *NGN3* and *PDX1* genes could be already detected according to the authors (Gao et al. 2008). During these three days of differentiation the ASCs continued to actively proliferate and no significant changes in a cell morphology were

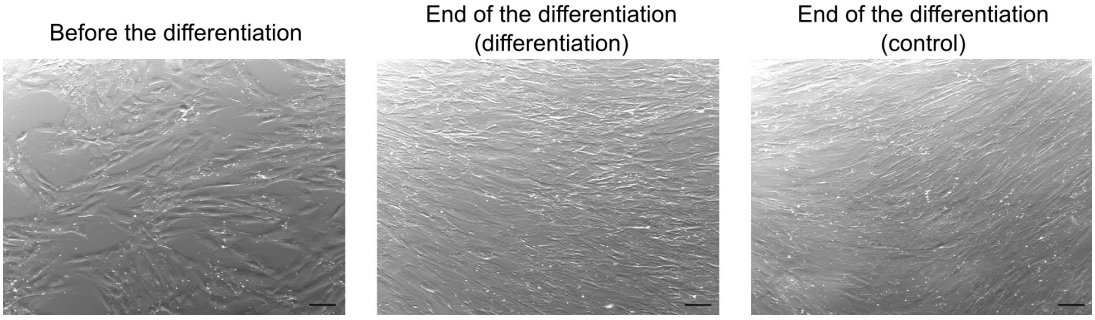

Figure 3.3.2.5.5. Morphological changes in ASCs of the donor No.4 during their differentiation into cells of endodermal lineage using the Protocol 7. Scale bar 100 μm.

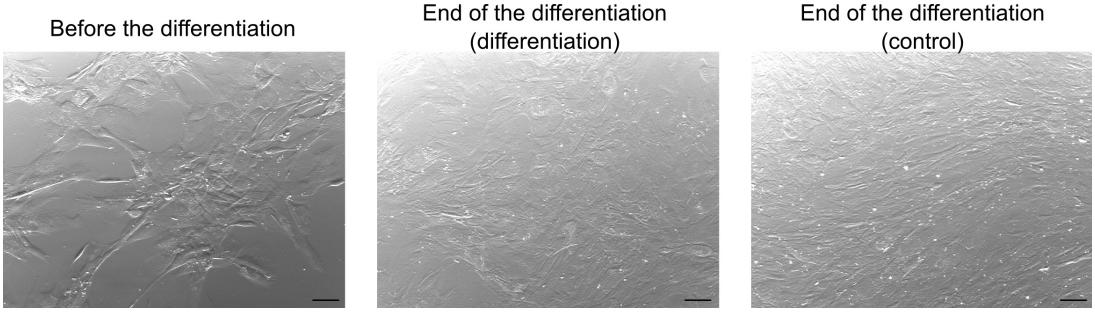

Figure 3.3.2.5.6. Morphological changes in ASCs of the donor No.9 during their differentiation into cells of endodermal lineage using the Protocol 7. Scale bar 100 μm.

observed in both donors (Figures 3.3.2.5.5. and 3.3.2.5.6.). Similarly no difference was detected between differentiation and control samples.

Protocol 8 was based on the manuscript by Sun Y. et al. 2007. After a two stage differentiation protocol lasting for 10 days authors observed changes in BM MSC morphology and formation of cell aggregates, as well as showed the expression of genes *Nestin*, *PDX1*, *NGN3*, *PAX4*, *INS*, and *GCG* (Sun Y. et al. 2007). Likewise using the Protocol 7, no transformations in ASC morphology were noticed in the course of differentiation Protocol 8 in the cells of both donors, and the cells under differentiation conditions did not differ from the control cells (Figures 3.3.2.5.7. and 3.3.2.5.8.).

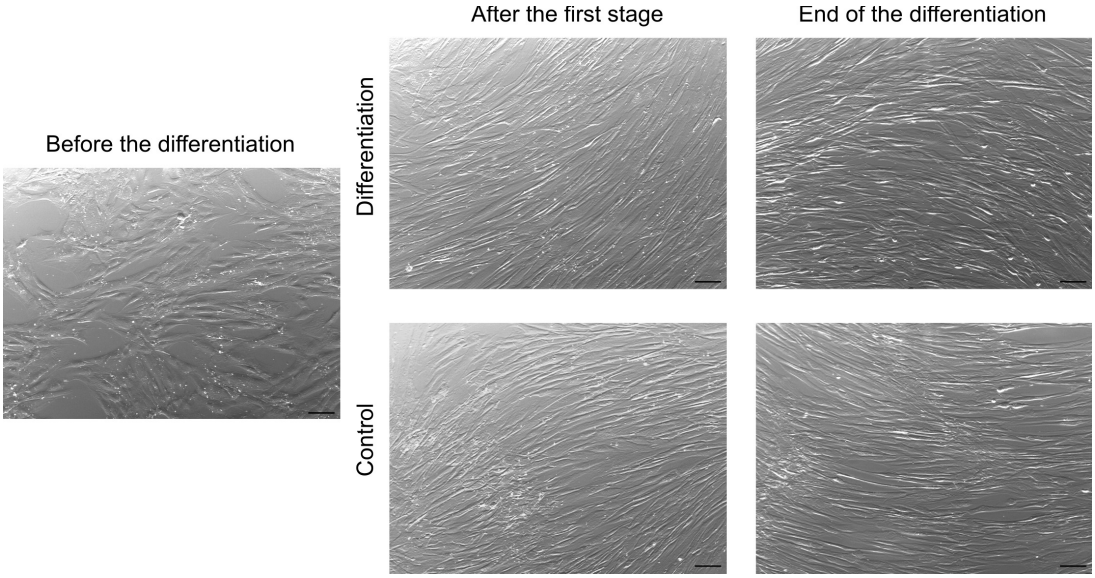

Figure 3.3.2.5.7. Morphological changes in ASCs of the donor No.4 during their differentiation into cells of endodermal lineage using the Protocol 8. Scale bar 100 μm.

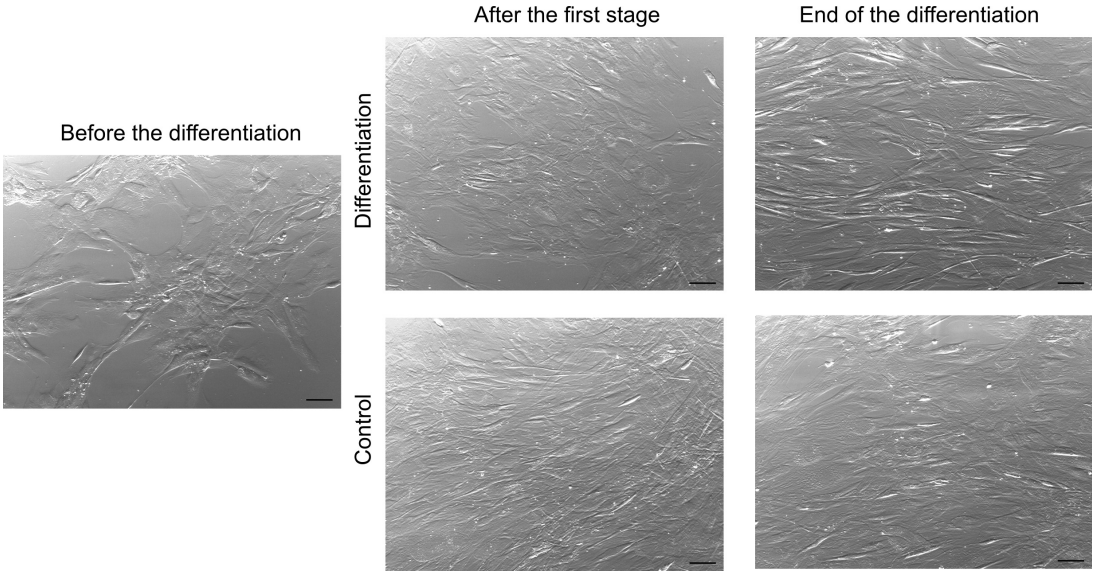

Figure 3.3.2.5.8. Morphological changes in ASCs of the donor No.9 during their differentiation into cells of endodermal lineage using the Protocol 8. Scale bar 100 μm.

At the end of the every differentiation the cells were stained with anti-SOX17 and anti-PDX1 antibodies to detect pancreatic progenitors. The nuclear staining of SOX17 was identified along with cytoplasmic staining in both the differentiated and control cells using the

Protocols 6, 7, and 8 (Appendices 20, 21, 22). When the Protocol 5 was employed, the SOX17 was observed throughout the differentiated cells, but distinct staining of the nuclei was not recognized, although control cells displayed more pronounced nuclear staining (Appendix 19). The staining intensity of SOX17 antibody was weak in all cases, except in the differentiated cells of the Protocol 5. This increase was most likely caused by the evident cell death in these samples and hence compromised cell membranes leading to more unspecific antibody binding. The PDX1 staining was observed in the same pattern as in the Protocols 1 and 2. The definite staining of nucleoli and probable Golgi complex was detected both in the differentiated cells and in the control cells using all four differentiation protocols (Appendices 23, 24, 25, 26). No significant differences in the SOX17 or PDX1 staining manner were observed between the cells of both donors, although the definite motive of the PDX1 staining in some protocols was less marked in the cells of the donor No.4 due to the smaller and more spindle-shaped cells.

After the differentiation the cells were collected and total RNA was obtained. Suitable RNA sample from the differentiated cells of donor No.9 from Protocol 5 was not acquired due to a high cell death during the differentiation protocol. The obtained RNA samples were reversely transcribed into cDNA and real-time RT-PCR was performed to detect expression of genes *GUSB, YWHAZ*, *β-Actin* (housekeeping genes), *SOX17*, *FOXA2*, *PDX1*, and *CXCR4*. For the genes *SOX17* and *FOXA2* two primer pairs were tested. The human pancreas served as a positive control. Additionally a sample of ASCs of donor No.4 before a start of the differentiation was analysed. The initial screening of the above-mentioned genes showed no expression of the genes *FOXA2* and *PDX1* in any of the samples examined, except the positive control (data not shown). The genes *SOX17* and *CXCR4* were detected both in few differentiation and some control samples from both donors, but no apparent coherence was observed between those two (Figure 3.3.2.5.9.). No similar pattern was also found between the expression of *SOX17* gene detected by two different primer sets. Since the initial screening showed no visible difference among all four differentiation protocols tested, nor between differentiation and control samples or both donors, further and more extensive gene analysis was not performed.

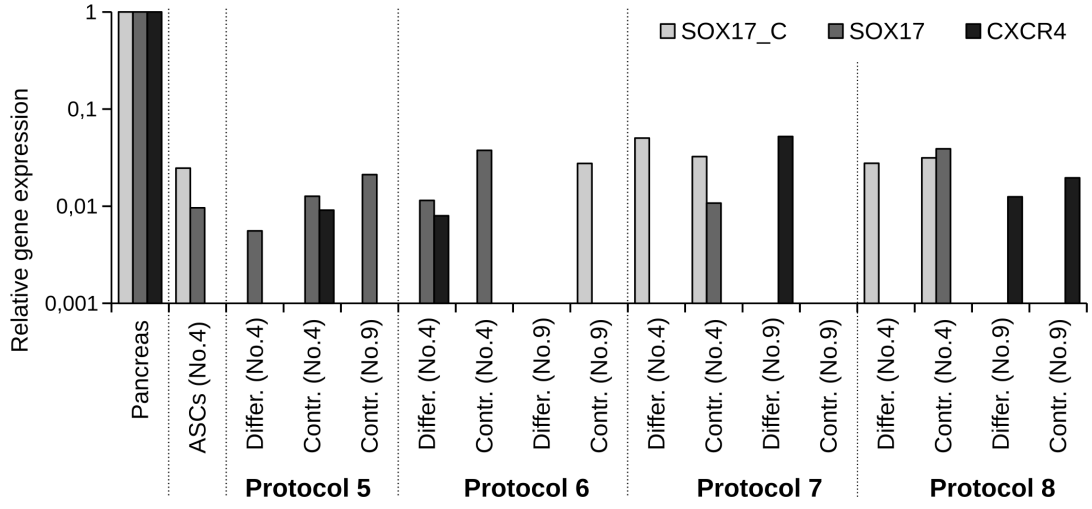

Figure 3.3.2.5.9. Comparison of relative expression level of genes *SOX17* and *CXCR4* in the differentiated and control cells of donors No.4 and No.9 by real-time RT-PCR (data normalized to *GUSB*). For the detection of *SOX17* gene expression two primer pairs were used: SOX17_C and SOX17. Protocols 5-8 - different protocols used to differentiate ASCs into cells of endodermal lineage. No.4 – donor No.4; No.9 – donor No.9; ASCs – adipose-derived stem cells before the differentiation; Differ. - differentiated cells; Contr. - cells grown in a control medium.

The overall results from four above-described protocols showed no solid evidence of tested ASC ability to differentiate into cells of endodermal origin. It is unclear whether the chosen protocols have been unsuitable for the tested ASC cultures, the ASCs of both donors are incapable of differentiation into types of cells that do not have mesodermal origin, or published protocols for MSC differentiation into endodermal cells are not universal and can not be successfully repeated in a slightly altered setting.

3.3.2.6. Protocol 9

The ASCs from the donors No.4 and No.8 (diabetic donor) at P4 were subjected to the differentiation Protocol 9. The first two stages were identical to the Protocol 5 followed by two additional stages of differentiation. Although a differentiation of ASCs into cells of endodermal origin using the Protocol 5 was not successful and high rate of cell death was observed, we decided to test the effects of CHIR99021 and LY294002 by reducing the time of differentiation in the presence of these small molecules.

After the first stage of differentiation the cells of both donors in the differentiation medium started to gather into clusters (Figures 3.3.2.6.1. and 3.3.2.6.2.). During the second

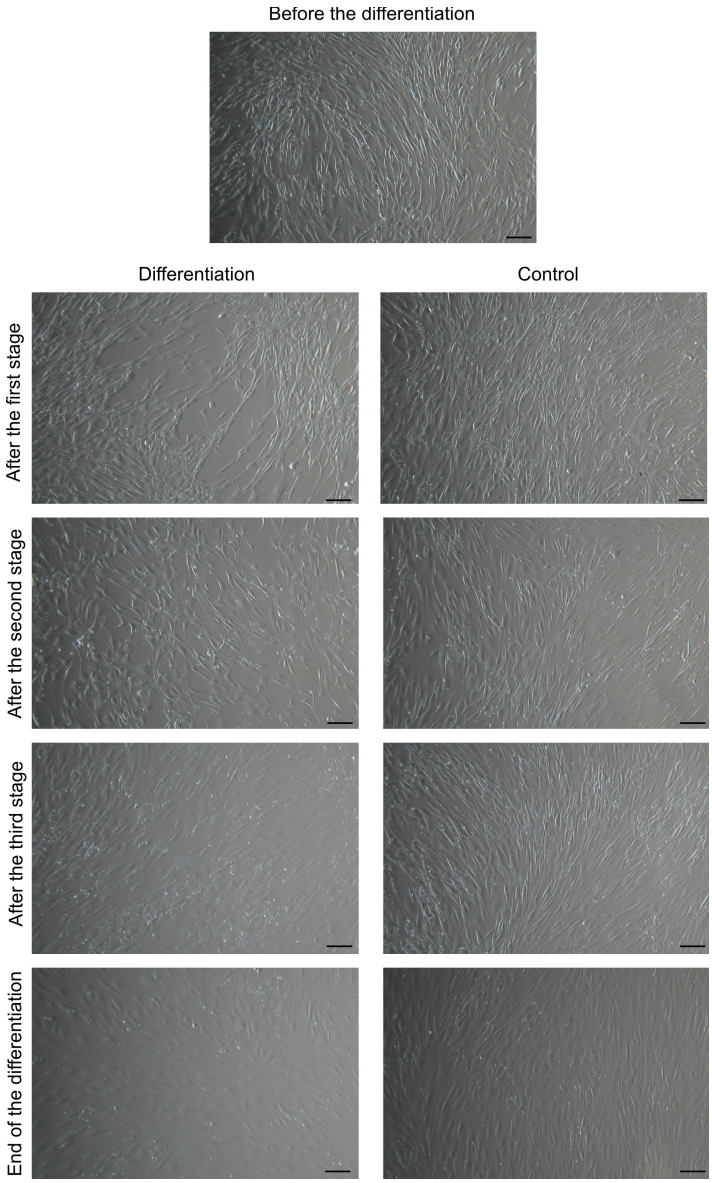

Figure 3.3.2.6.1. Morphological changes in ASCs of the donor No.4 during their differentiation into insulin-producing cells using the Protocol 9. Scale bar 100 μm.

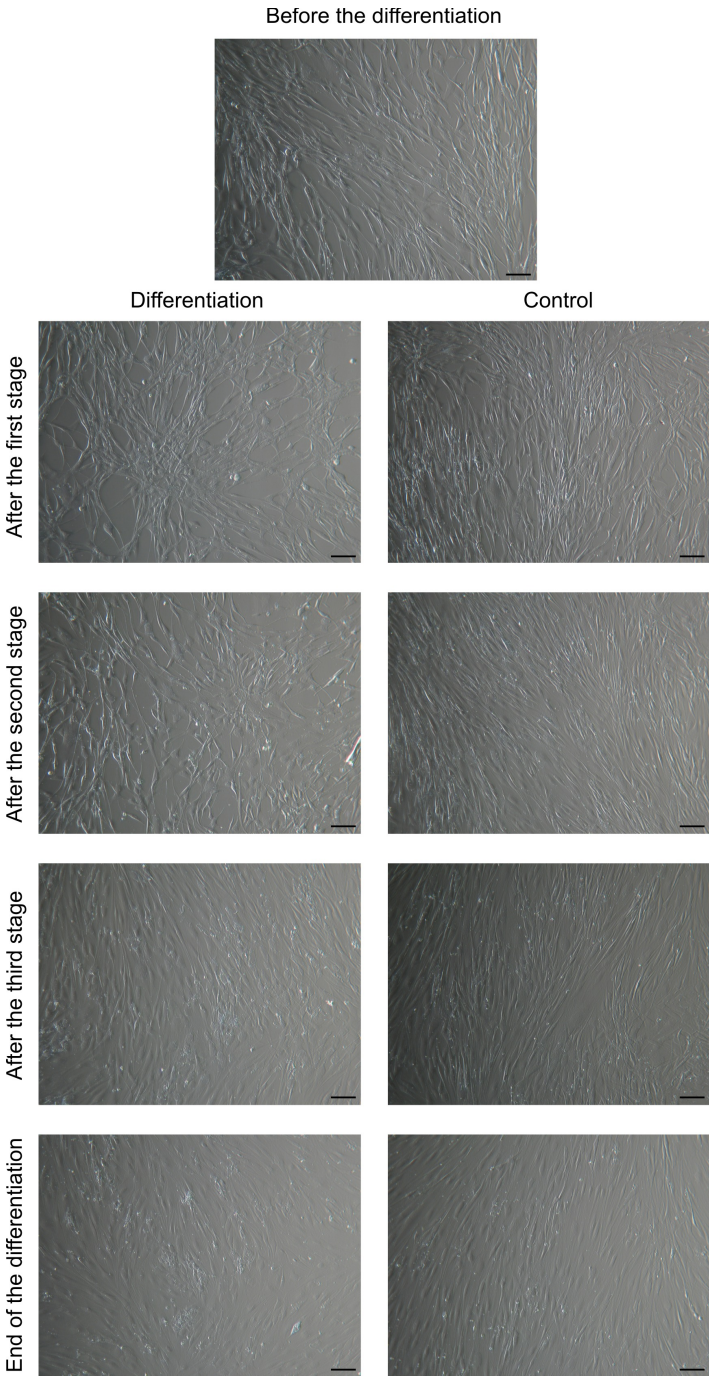

Figure 3.3.2.6.2. Morphological changes in ASCs of the donor No.8 during their differentiation into insulin-producing cells using the Protocol 9. Scale bar 100 μm.

stage of differentiation further clustering was not observed although the previously formed groups of cells were still evident. In the course of the first two stages of differentiation slightly elevated cell death was detected, but it did not impede the differentiation. Throughout the third stage of differentiation part of the cells started to lose their spindle-shaped appearance and became more flattened. These cells were usually clustered together in small groups. Furthermore, accumulation of intracellular granules was identified in the altered cells. During the last stage of differentiation cell flattening became more apparent and was also observed in small amounts in the control cells. Similarly, the small clusters of cells were detected in the control samples at the end of differentiation. No difference was discovered between the cells of both donors throughout the differentiation process.

At the end of the differentiation Protocol 9 a double staining immunocytochemistry

method was used on both the differentiation and control samples. Anti-C-PEPT, anti-NGN3, anti-PDX1, and anti-SST antibodies were co-stained with anti-INS and anti-GCG antibodies in the same manner as for the differentiated samples in the Protocols 1 and 2. Although the expression of PDX1 is usually tested earlier in the course of differentiation to detect pancreatic precursors, it can still be found in restricted parts of adult pancreas (Stoffers et al. 1997). Our obtained results demonstrated that a staining pattern of PDX1 is practically the same as in all previous protocols tested. The distinct staining of nucleoli and probable Golgi complex was detected both in the differentiated cells and in the control cells, but more marked nuclear staining was observed in part of the cells when compared to former protocols (Figure 3.3.2.6.3.).

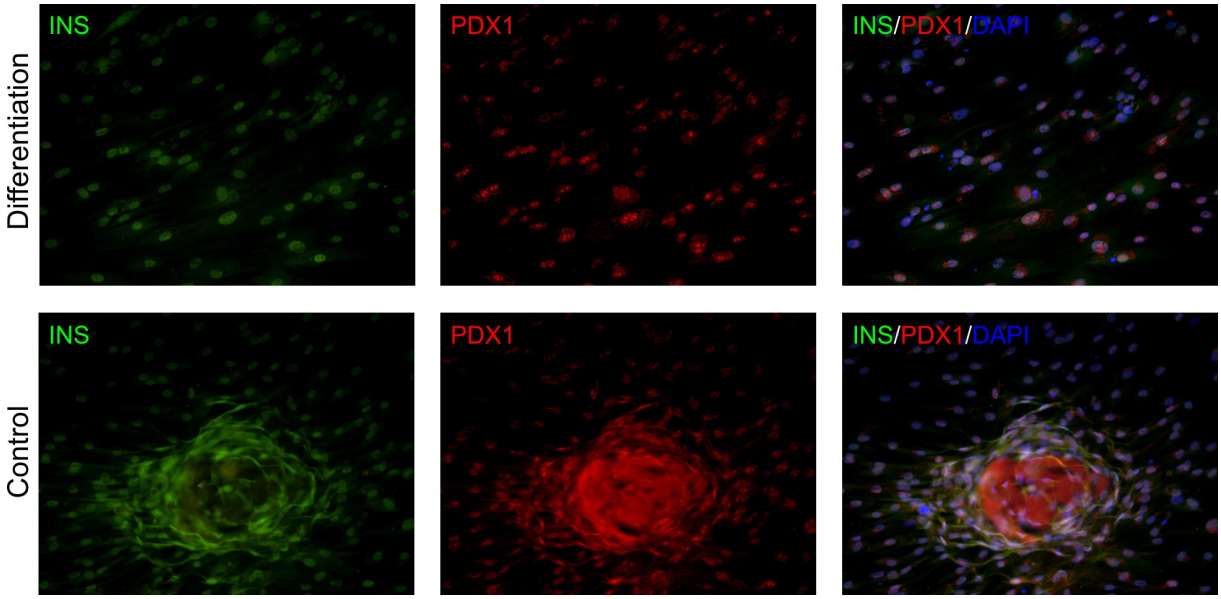

Figure 3.3.2.6.3. Expression of INS and PDX1 in ASCs of donor No.8 after their differentiation into insulin-producing cells using the Protocol 9. Cell nuclei stained with DAPI. Magnification 200x.

The INS staining pattern was also almost identical to earlier protocols – distinct staining of nuclei and weak expression in a cytoplasm (Figures 3.3.2.6.3. - 3.3.2.6.6.). However, few cells with more pronounced cytoplasmic staining were observed in the differentiation samples (Figure 3.3.2.6.4.). The C-PEPT was found only in the cytoplasm and it showed a colocalization with cytoplasmic staining of INS, but no difference was detected between the differentiation and control sample (Figure 3.3.2.6.4.).

The staining of NGN3 was very weakly identified solely in the nuclei of both differentiated and control cells (Figure 3.3.2.6.5.). The observed expression of SST in the cell nuclei was almost at the background level and could not be considered as positive signal (Figure 3.3.2.6.6.). The expected cytoplasmic staining was not observed, although it is impossible to distinguish the exact staining pattern of the examined protein in a cluster of cells. Most likely the visible colouring in the centre of cell clusters shown in the Figures 3.3.2.6.3., 3.3.2.6.5., and 3.3.2.6.6. is a staining artefact because no actual cells could be seen amidst of these clusters.

The double immunocytochemistry staining with GCG antibodies is not presented in this work because a GCG signal was only slightly above the background level in all samples tested and therefore was not considered as positive. Other antibody staining showed identical results to those presented above. The same applies to the immunocytochemistry results from the cells of donor No.4. Since obtained data from both donors were indistinguishable, only one set of the results was described herein.

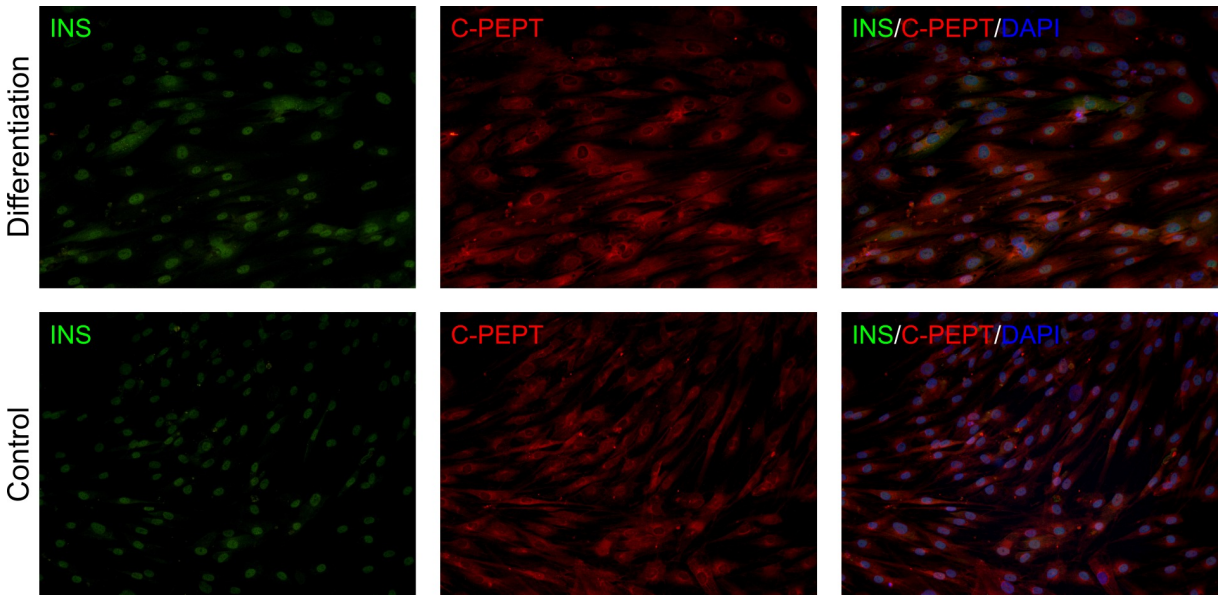

Figure 3.3.2.6.4. Expression of INS and C-PEPT in ASCs of donor No.8 after their differentiation into insulin-producing cells using the Protocol 9. Cell nuclei stained with DAPI. Magnification 200x.

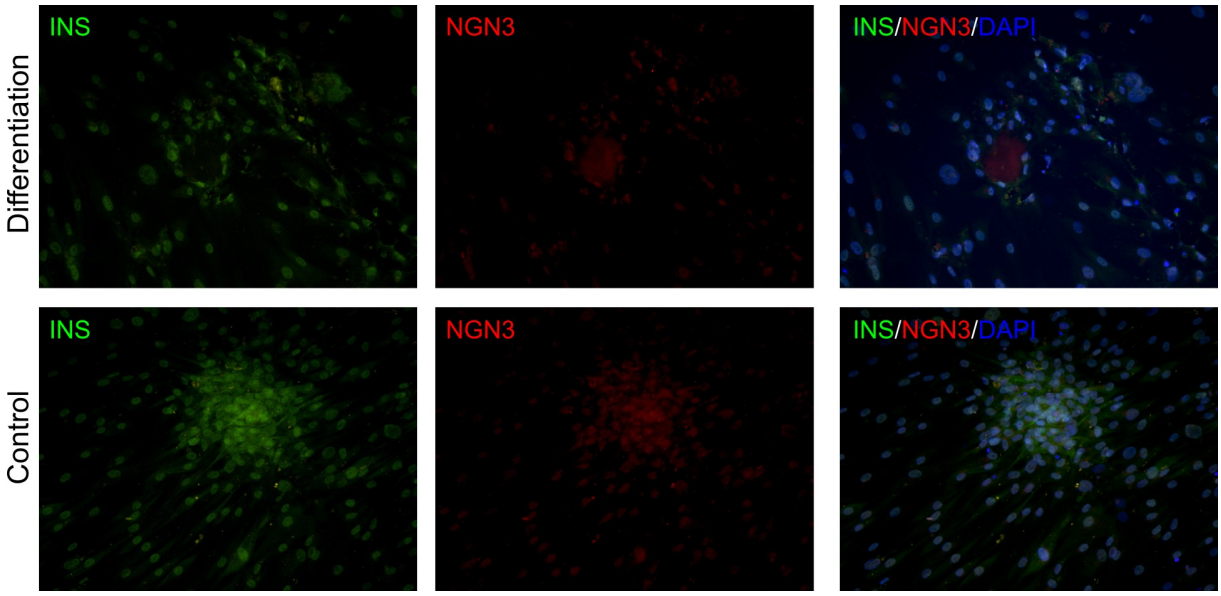

Figure 3.3.2.6.5. Expression of INS and NGN3 in ASCs of donor No.8 after their differentiation into insulin-producing cells using the Protocol 9. Cell nuclei stained with DAPI. Magnification 200x.

The total RNA was obtained from differentiation and control samples after the second stage of differentiation and at the end of the Protocol 9. The RNA samples were reversely transcribed into cDNA and real-time RT-PCR was performed to detect expression of genes *GUSB*, *β-Actin* (housekeeping genes), *SOX17*, *FOXA2*, *PDX1*, *WNT3*, *CXCR4*, *CK19*, *INS*, *PPY*, *SST*, *HNF1A*, *HNF1B*, *HNF4A*, *GCG*, *PAX6*, *NKX6-1*, *MNX1*, and *PTF1A*. The human pancreas served as a positive control. The initial screening of the above-mentioned genes showed no expression of the genes *PDX1*, *HNF1A*, *HNF1B*, *PTF1A*, *INS* and *GCG* in any of the samples examined, except the positive control (data not shown). The expression of the genes *SOX17*, *FOXA2*, *WNT3*, *CK19*, *PPY*, *SST*, *PAX6*, and *NKX6-1* was found in most of the samples tested, both in differentiation and control, but no visible trend of increase or decrease of the gene expression during the differentiation was observed (data not shown). Only the

expression of the genes *CXCR4* and *MNX1* followed a detectable trend (Figure 3.3.2.6.7.).

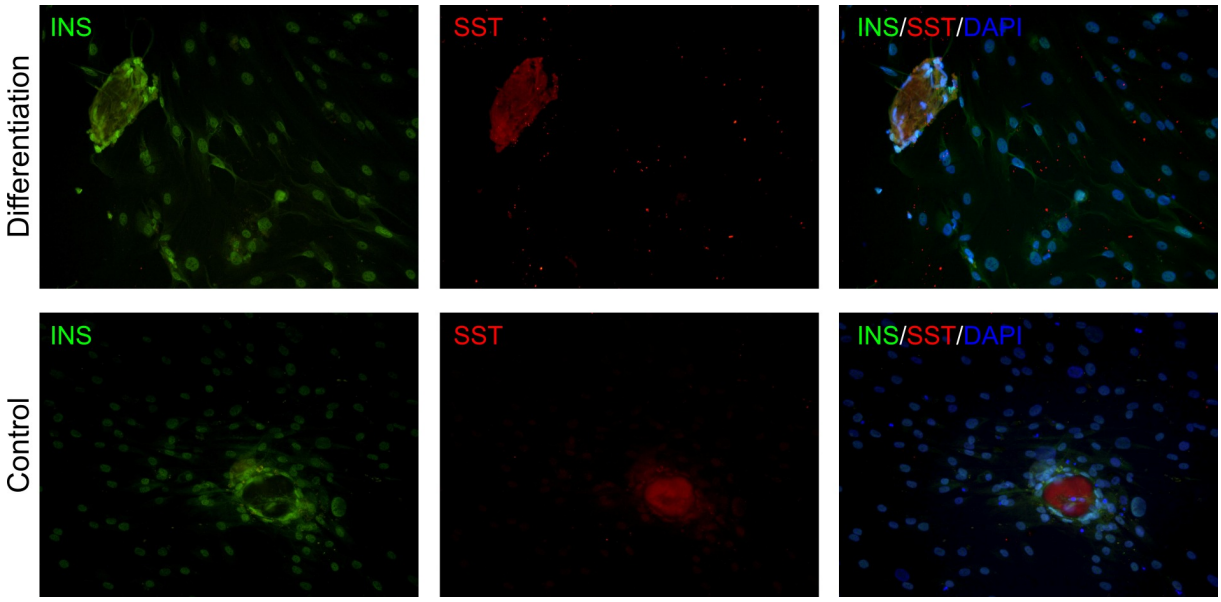

Figure 3.3.2.6.6. Expression of INS and SST in ASCs of donor No.8 after their differentiation into insulin-producing cells using the Protocol 9. Cell nuclei stained with DAPI. Magnification 200x.

The expression of the gene *CXCR4* was detected only in the samples of the donor No.8. It was found at a low level already in undifferentiated ASCs. After the second stage of the differentiation, the expression of *CXCR4* in the differentiation sample was tenfold higher when compared to ASCs before the differentiation. The expression in control sample was almost doubled. At the end of the differentiation the *CXCR4* was not detected in any of the samples tested. The expression of the gene *MNX1* was observed at a very low level only after the second stage of the differentiation, both in differentiation samples of the donors No.4 and the donor No.8. The expression of both above-mentioned genes was much lower than in a human pancreas, indicating a modest degree of efficiency of the chosen differentiation protocol or a low level of ASCs submitted to this differentiation.

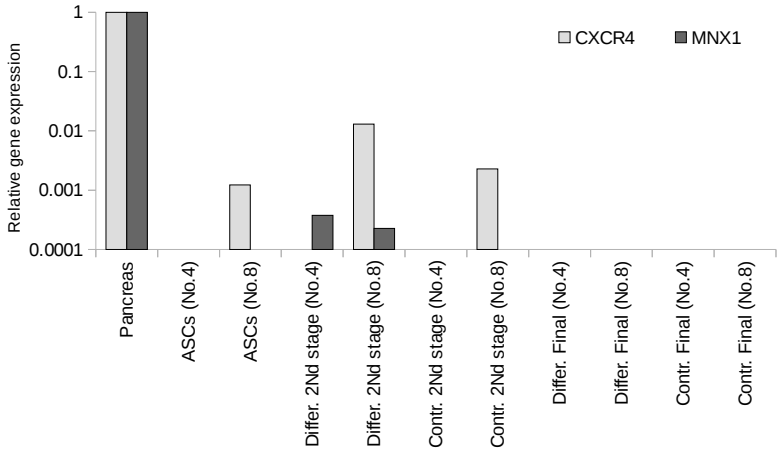

Figure 3.3.2.6.7. Comparison of relative expression level of genes *CXCR4* and *MNX1* in the differentiated and control cells of donors No.4 and No.8 after the second stage (2nd stage) of the differentiation Protocol 9 and at the end of it (Final) by real-time RT-PCR (data normalized to *GUSB*). No.4 – donor No.4; No.8 – donor No.8; ASCs – adipose-derived stem cells before the differentiation; Differ. - differentiated cells; Contr. - cells grown in a control medium.

CXCR4 (chemokine (C-X-C motif) receptor 4) is a chemokine receptor, and together with its ligand, stromal derived factor 1α, is critical for differentiation of numerous tissues during development. It is an essential component of pancreatic ductal cell survival, proliferation, and migration throughout pancreatic organogenesis, as well as regeneration (Kayali et al. 2003). It has been used as a marker of pancreatic endocrine progenitors and has been suggested as one of the possible markers that could help to identify putative pancreatic SCs (Koblas et al. 2007). In the course of *in vitro* pancreatic cell differentiation CXCR4 is considered as a marker of definitive endoderm (D'Amour et al. 2005, D'Amour et al. 2006, Jiang et al. 2007, Zhang et al. 2009).

MNX1 (motor neuron and pancreas homeobox 1) (also known as HLXB9) is a transcription factor which is expressed at the early stages of pancreatic development and also later in differentiated β cells (Riley and Gannon 2014). It is required for dorsal pancreatic bud development and differentiation of endocrine cell types (Grapin-Botton et al. 2001). In zebrafish model loss of *Mnx1* provokes the differentiation of β cell precursors into α cells, suggesting that *Mnx1* promotes β and suppresses α cell fate (Dalgin et al. 2011). Its expression coincide with such gut endoderm patterning genes as *PDX1* and *PTF1A* (Riley and Gannon 2014).

Since only initial screening of samples was performed, meaning that PCR efficiencies for each primer pair were not determined and no replicates were run, no definite conclusions can be drawn from the obtained results. However, it gives an insight into success of used differentiation protocol. One could speculate that a combination of activin A, sodium butyrate, LY294002, and CHIR99021 has stimulated differentiation of ASCs into DE and further into the posterior foregut, indicated by the detection of an increase in *CXCR4* expression in the samples of donor No.8, as well as expression of *MNX1* in both donors. All of these components and their combinations have been previously shown to effectively induce endoderm differentiation in ESCs and iPSCs (D'Amour et al. 2005, Jiang et al. 2007, McLean et al. 2007, Kunisada et al. 2012) and may have proven useful in the setting of adult SCs as well. At this stage of pancreatic differentiation *PDX1* expression is regarded as a turning point of successful differentiation as PDX1-positive cells will give rise to the islets, exocrine cells, and ductal cells (Gu et al. 2002). *PDX1* expression usually coincide with the expression of *PTF1A* and *MNX1* genes (Riley and Gannon 2014). Since only expression of *MNX1* was detected, but PDX1 was not observed neither at gene nor at protein level, it may not be enough to suggest efficient ASC differentiation into posterior foregut. Even if ASCs of both donors have been able to transdifferentiate into endodermal cells at some level, their further differentiation into insulin-producing cells has been impeded as no solid evidence has been collected to suggest otherwise.

Published results show that not only ASCs (Timper et al. 2006, Lee et al. 2008, Okura et al. 2009, Chandra et al. 2011, Kang et al. 2011, Buang et al. 2012), but also SCs isolated from human UC blood (Sun B. et al. 2007, Hu et al. 2010), placenta (Chang et al. 2007), and BM (Sun Y. et al. 2007, Tang et al. 2012) can be differentiated into insulin-producing cells. Unfortunately, we have not been able to differentiate any of our tested ASC cultures into insulin-positive cells. Even attempts to obtain cells expressing endodermal markers have not produced any reliable results. Since the lack of an efficient standard method for functional insulin-producing cell generation *in vitro* forces every researcher to create individual differentiation protocol, it does not come as a surprise that part of those protocols can not be reproduced neither by us, nor by others (Oishi et al. 2009). An optimization of the timing and combination of chemical factors to activate or suppress the key signalling pathways during pancreatic development is critical to positive outcome. However, the mechanisms and pathways that govern the required changes in cell phenotype to reach the desired cell type are not fully understood. This makes a controlled and highly reproducible differentiation much harder to design. We do believe that ASC differentiation into insulin-producing cell can be

achieved and our lack of success is only due to unsuitable protocols. Our results suggest that herein used protocols that have been originally designed for BM MSC or UC blood SC differentiation can not be directly employed on ASCs. Even those that have been tested on ASCs can probably produce non-identical results if the site of adipose tissue or the method of their acquirement differs. During our work we have seen diversity of ASC morphology, proliferative capacity, and differential capacity among various donors (unpublished results). In this work morphological differences were observed between ASCs of the donors No.4 and No.9. Differentiation ability into osteocytes was also unequal in ASCs of the donors No.4 and No.5. Also the 3D aggregate formation in the ASC culture of the donor No.4 was likewise unique. This donor-to-donor variability is another problem hampering the design of effective differentiation protocols. Nevertheless, the further exploration of chemical, as well as physiological and mechanical factors regulating the process of differentiation is continuing, and it will require a great deal of scientific efforts before somatic SCs can be effectively differentiated into insulin-producing cells for diabetes treatment.

4. Conclusions

1. Human ASCs can be effectively cultured and expanded in the medium supplemented with autologous serum. Such culture conditions do not influence their morphology, expression of characteristic MSC surface markers and the ability to differentiate into adipocytes, osteocytes, and chondrocytes.

2. ASCs from the second passage to the eighth passage, cultured in the presence of autologous serum, represent a highly homogeneous cell population showing simultaneous expression of such surface markers as CD29, CD44, CD73, CD90, and CD105, but lacking the expression of HLA-DR, CD14, CD19, CD34, and CD45. The accumulation of positive surface proteins increases with each subsequent passage and is preserved after double cell freezing and more than 4 years of cryopreservation.

3. The observed ASC aggregation into three-dimensional bodies may represent a response mechanism triggered by various stress conditions, such as alterations in the culture medium, growth environment, culture conditions, or growth surface, since the formation of different types of bodies was detected after changes in one or more of these factors.

4. The floating ASC bodies that have spontaneously formed at early passages may represent more primitive cell subpopulation within the individual ASC culture due to their ability to form such three-dimensional aggregates and lack of alkaline phosphatase activity.

5. The expression of pluripotency marker genes *OCT4A* and *SOX2* is very low in ASCs. The OCT4A protein can not be detected neither in monolayer culture of ASCs nor in glass adherent ASC bodies.

6. ASCs show the expression of *NANOG* pseudogene 8, but the level of transcription is very modest. The parental *NANOG* gene is detected in ESCs, but its presence in ASCs is inconclusive.

7. It is possible that *NANOG* pseudogene 8 is translated into protein in the tested ASCs and the presence of positive signal detected by anti-NANOG antibodies could be due to translation of *NANOG* pseudogene 8, *NANOG*, or both.

8. ASCs cultured in the medium containing autologous serum can differentiate into adipocytes, osteocytes, and chondrocytes at least until the sixth passage. ASCs from different donors show various degree of differentiation towards osteogenic lineage.

9. ASC cultures of four donors could not be differentiated into cells of endodermal lineage or insulin-producing cells employing the nine differentiation protocols tested in this study.

5. Theses for defence

1. The fetal bovine serum in a conventional adult stem cell culture medium can be substituted with the autologous serum without affecting the characteristics and abilities of the cells.

2. To avoid false positive results that lead to attribution of pluripotent cell characteristics to adult stem cells, an accurate and complex approach is required to confirm the expression of pluripotency markers OCT4 and NANOG in human stem cells.

3. *NANOG* pseudogene 8 is not only transcribed in the tested ASC culture, but it may also be translated into protein.

4. The differentiation of ASC into cells of endodermal lineage or insulin-producing cells could not be achieved using the commonly described protocols for adult stem cells, because the chemical, as well as physiological and mechanical factors regulating the process of such differentiation are weakly understood and each published protocol is highly adapted for individual case.

Acknowledgements

I would like to express sincere gratitude to my supervisor Dr. Tatjana Kozlovska for her guidance and encouragement throughout my scientific work at her research group. I am grateful for her trust in my judgements and freedom she has given me to seek my own place in science.

I am also very thankful to Uldis Bērziņš who accepted me as his associate on his newly started work with adult stem cells. He gave me a remarkable opportunity to participate in the development of this completely new field of research in the Latvian Biomedical Research and Study Centre. He always regarded me as equal, relied on my opinion, and provided all the materials needed to continue our journey on exploring stem cells.

My gratitude goes to Dr. Baiba Niedre-Otomere who introduced me into everyday life of laboratory work and thought me a great deal of scientific methods and ability to organize, plan, and analyse my experiments.

I would also like to thank Prof. Pauls Pumpēns for his endless optimism, scientific passion, and genuine interest in every person he meets. It was a great honour to be welcomed as an undergraduate student in his laboratory ten years ago and I am pleased to be acquainted with such admirable scientist.

I am deeply grateful to Prof. Viesturs Baumanis who always profoundly cared for his students at the Department of Molecular Biology, Faculty of Biology, University of Latvia. He often believed in us, students, even more than we believed in ourselves and served as an excellent role model for new scientists.

I am thankful to Dr. Rūta Brūvere for her tireless help with microscopy and most appreciated advice on immunofluorescence technique, Natālija Gabruševa for teaching me methods of immunocytochemistry and histology, Dr. Dace Pjanova for her assistance with confocal microscopy, Irena Timofejeva for helping and consulting on matters of cell culturing, Dr. Jekaterina Ērenpreisa for sharing her deep scientific knowledge, as well as kind lending of various materials and reagents, Sergejs Ņikuļšins for flow cytometry analysis, Ilona Mandrika and Ramona Petrovska for the great opportunity to work with them on cell differentiation, Angelina Pismennaja for teaching me method of paraffin embedding, and Dr. Ligija Ignatoviča for sequencing.

Many thanks go to my colleagues from our group who have always helped me to solve any problems and questions I have had and created pleasant atmosphere to work in. I would especially like to thank Aleksandra Vežāne for her friendship and ability to hear me out on every matter of life.

I appreciate my former students Irina Bankovska (Djačkova) and Agnese Ezerta who have helped me greatly during my research and respected me as their supervisor while I have been only learning myself.

Last, but not least, I would like to thank my family who has always supported and encouraged me throughout my whole life. My deepest gratitude goes to my beloved husband Jānis who has been there for me every day for the last twelve years. He has been both my biggest supporter and critic. Not one of my countless pieces of writing has escaped his editing, proofreading, and approval, and this has meant a lot to me. None of this would be possible without his love and devotion.

This research was financially supported by a grant from the TOP 07-27 project of the Ministry of Education and Science, Republic of Latvia, by the grants from project No. 09.1283 and project No.10.0014 of the Latvian Council of Science, by the European Regional Development Fund grant 2010/0230/2DP/2.1.1.1.0/10/APIA/VIAA/075, Cilmes Šūnu Tehnoloģijas Ltd., and by the European Social Fund within the project “Support for Doctoral Studies at University of Latvia”.

References

Abdulrazzak H., Moschidou D., Jones G., Guillot P.V. Biological characteristics of stem cells from foetal, cord blood and extraembryonic tissues. *J R Soc Interface* 2010, 7(Suppl 6): S689-S706.

Abumaree M., Al Jumah M., Pace R.A., Kalionis B. Immunosuppressive Properties of Mesenchymal Stem Cells. *Stem Cell Rev* 2012, 8(2): 375-392.

Aggarwal S., Pittenger M.F. Human mesenchymal stem cells modulate allogeneic immune cell responses. *Blood* 2005, 105(4): 1815-1822.

Amariglio N., Hirshberg A., Scheithauer B.W., Cohen Y., Loewenthal R., Trakhtenbrot L., Paz N., Koren-Michowitz M., Waldman D., Leider-Trejo L., Toren A., Constantini S., Rechavi G. Donor-derived brain tumor following neural stem cell transplantation in an ataxia telangiectasia patient. *PloS Med* 2009, 6(2): e1000029.

Ambady S., Malcuit C., Kashpur O., Kole D., Holmes W.F., Hedblom E., Page R.L., Dominko T. Expression of NANOG and NANOGP8 in a variety of undifferentiated and differentiated human cells. *Int J Dev Biol* 2010, 54(11-12): 1743-1754.

Anonymous. American Diabetes Association. Diagnosis and classification of diabetes mellitus. *Diab Care* 2010, 33(Suppl 1): S62-S69.

Alt E., Yan Y., Gehmert S., Song Y.H., Altman A., Gehmert S., Vykoukal D., Bai X. Fibroblasts share mesenchymal phenotypes with stem cells, but lack their differentiation and colony-forming potential. *Biol Cell* 2011, 103(4): 197-208.

Arnold K., Sarkar A., Yram M.A., Polo J.M., Bronson R., Sengupta S., Seandel M., Geijsen N., Hochedlinger K. Sox2(+) adult stem and progenitor cells are important for tissue regeneration and survival of mice. *Cell Stem Cell* 2011, 9(4): 317-329.

Asadi M.H., Mowla S.J., Fathi F., Aleyasin A., Asadzadeh J., Atlasi Y. OCT4B1, a novel spliced variant of OCT4, is highly expressed in gastric cancer and acts as an antiapoptotic factor. *Int J Cancer* 2011, 128(11): 2645-2652.

Astori G., Vignati F., Bardelli S., Tubio M., Gola M., Albertini V., Bambi F., Scali G., Castelli D., Rasini V., Soldati G., Moccetti T. "In vitro" and multicolor phenotypic characterization of cell subpopulations identified in fresh human adipose tissue stromal vascular fraction and in the derived mesenchymal stem cells. *J Transl Med* 2007, 5: 55.

Atlasi Y., Mowla S.J., Ziaee S.A.M., Gokhale P.J., Andrews P.W. Oct4 spliced variants are differentially expressed in human pluripotent and nonpluripotent cells. *Stem Cells* 2008, 26(12): 3068-3074.

Avilion A.A., Nicolis S.K., Pevny L.H., Perez L., Vivian N., Lovell-Badge R. Multipotent cell lineages in early mouse development depend on SOX2 function. *Genes Dev* 2003, 17(1): 126-140.

Baer P.C., Kuçi S., Krause M., Kuçi Z., Zielen S., Geiger H., Bader P., Schubert R. Comprehensive phenotypic characterization of human adipose-derived stromal/stem cells and their subsets by a high throughput technology. *Stem Cells Dev* 2013, 22(2): 330-339.

Baraniak P.R., McDevitt T.C. Scaffold-free culture of mesenchymal stem cell spheroids in suspension preserves multilineage potential. *Cell Tissue Res* 2012, 347(3): 701-711.

Bartholomew A., Sturgeon C., Siatskas M., Ferrer K., McIntosh K., Patil S., Hardy W., Devine S., Ucker D., Deans R., Moseley A., Hoffman R. Mesenchymal stem cells suppress lymphocyte proliferation in vitro and prolong skin graft survival in vivo. *Exp Hematol* 2002, 30(1): 42-48.

Bartoov-Shifman R., Hertz R., Wang H., Wolheim C.B., Bar-Tana J., Walker M.D. Activation of the insulin gene promoter through a direct effect of hepatocyte nuclear factor 4 alpha. *J Biol Chem* 2002, 277(29): 25914-25919.

Bartosh T.J., Ylöstalo J.H., Mohammadipoor A., Bazhanov N., Coble K., Claypool K., Lee R.H., Choi H., Prockop D.J. Aggregation of human mesenchymal stromal cells (MSCs) into 3D spheroids enhances their antiinflammatory properties. *Proc Natl Acad Sci U S A* 2010,

107(31): 13724-13729.
Beltrami A.P., Barlucchi L., Torella D., Baker M., Limana F., Chimenti S., Kasahara H., Rota M., Musso E., Urbanek K., Leri A., Kajstura J., Nadal-Ginard B., Anversa P. Adult cardiac stem cells are multipotent and support myocardial regeneration. *Cell* 2003, 114(6): 763-776.
Berniakovich I., Giorgio M. Low oxygen tension maintains multipotency, whereas normoxia increases differentiation of mouse bone marrow stromal cells. *Int J Mol Sci* 2013, 14(1): 2119-2134.
Bernstine E.G., Hooper M.L., Grandchamp S., Ephrussi B. Alkaline phosphatase activity in mouse teratoma. *Proc Natl Acad Sci U S A* 1973, 70(12): 3899-3903.
Berra E., Ginouvès A., Pouysségur J. The hypoxia-inducible-factor hydroxylases bring fresh air into hypoxia signalling. *EMBO Rep* 2006, 7(1): 41-45.
Beyth S., Borovsky Z., Mevorach D., Liebergall M., Gazit Z., Aslan H., Galun E., Rachmilewitz J. Human mesenchymal stem cells alter antigen-presenting cell maturation and induce T-cell unresponsiveness. *Blood* 2005, 105(5): 2214-2219.
Bhushan A., Itoh N., Kato S., Thiery J.P., Czernichow P., Bellusci S., Scharfmann R. Fgf10 is essential for maintaining the proliferative capacity of epithelial progenitor cells during early pancreatic organogenesis. *Development* 2001, 128(24): 5109-5117.
Bianco P., Robey P.G., Simmons P.J. Mesenchymal stem cells: revisiting history, concepts, and assays. *Cell Stem Cell* 2008, 2(4): 313-319.
Bindu H.A., Srilatha B. Potency of various types of stem cells and their transplantation. *J Stem Cell Res Ther* 2011, 1: 115.
Blanpain C., Fuchs E. Epidermal Stem Cells of the Skin. *Annu Rev Cell Dev Biol* 2006, 22: 339-373.
Blasi A., Martino C., Balducci L., Saldarelli M., Soleti A., Navone S.E., Canzi L., Cristini S., Invernici G., Parati E.A., Alessandri G. Dermal fibroblasts display similar phenotypic and differentiation capacity to fat-derived mesenchymal stem cells, but differ in anti-inflammatory and angiogenic potential. *Vasc Cell* 2011, 3(1): 5.
Booth H.A.F., Holland P.W.H. Eleven daughters of NANOG. *Genomics* 2004, 84(2): 229-238.
Bourin P., Bunnell B.A., Casteilla L., Dominici M., Katz A.J., March K.L., Redl H., Rubin J.P., Yoshimura K., Gimble J.M. Stromal cells from the adipose tissue-derived stromal vascular fraction and culture expanded adipose tissue-derived stromal/stem cells: a joint statement of the International Federation for Adipose Therapeutics and Science (IFATS) and the International Society for Cellular Therapy (ISCT). *Cytotherapy* 2013, 15(6): 641-648.
Boyer L.A., Lee T.I., Cole M.F., Johnstone S.E., Levine S.S., Zucker J.P., Guenther M.G., Kumar R.M., Murray H.L., Jenner R.G., Gifford D.K., Melton D.A., Jaenisch R., Young R.A. Core transcriptional regulatory circuitry in human embryonic stem cells. *Cell* 2005, 122(6): 947-956.
Brehm A., Ohbo K., Schöler H. The carboxy-terminal transactivation domain of Oct-4 acquires cell specificity through the POU domain. *Mol Cell Biol* 1997, 17(1): 154-162.
Brendel C., Kuklick L., Hartmann O., Kim T.D., Boudriot U., Schwell D., Neubauer A. Distinct gene expression profile of human mesenchymal stem cells in comparison to skin fibroblasts employing cDNA microarray analysis of 9600 genes. *Gene Expr* 2005, 12(4-6): 245-257.
Buang M.M.L., Seng H.K., Chung L.H., Saim A.B., Idrus R.B. In vitro generation of functional insulin-producing cells from lipoaspirated human adipose tissue-derived stem cells. *Arch Med Res* 2012, 43(1): 83-88.
Butterworth PJ. Alkaline phosphatase. Biochemistry of mammalian alkaline phosphatases. *Cell Biochem Funct* 1983, 1(2): 66-70.
Bylund M., Andersson E., Novitch B.G., Muhr J. Vertebrate neurogenesis is counteracted by Sox1-3 activity. *Nat Neurosci* 2003, 6(11): 1162-1168.
Candido E.P., Reeves R., Davie J.R.. Sodium butyrate inhibits histone deacetylation in cultured

cells. *Cell* 1978, 14(1): 105-113.
Cao, Y; Sun, Z; Liao, L; Meng, Y; Han, Q; Zhao, RC. Human adipose tissue-derived stem cells differentiate into endothelial cells in vitro and improve postnatal neovascularization in vivo. *Biochem Biophys Res Commun* 2005, 332(2) :370-379.
Caplan A.I. All MSCs are pericytes? *Cell Stem Cell* 2008, 3(3): 229-230.
Caplan A.I. Mesenchymal stem cells. *J Orthop Res* 1991, 9(5): 641-650.
Cappellesso-Fleury S., Puissant-Lubrano B., Apoil P.A., Titeux M., Winterton P., Casteilla L., Bourin P., Blancher A. Human fibroblasts share immunosuppressive properties with bone marrow mesenchymal stem cells. *J Clin Immunol* 2010, 30(4): 607-619.
Carlin R., Davis D., Weiss M., Schultz B., Troyer D. Expression of early transcription factors Oct-4, Sox-2 and Nanog by porcine umbilical cord (PUC) matrix cells. *Reprod Biol Endocrinol* 2006, 4: 8.
Catacchio I., Berardi S., Reale A., De Luisi A., Racanelli V., Vacca A., Ria R. Evidence for bone marrow adult stem cell plasticity: properties, molecular mechanisms, negative aspects, and clinical applications of hematopoietic and mesenchymal stem cells transdifferentiation. *Stem Cells Int* 2013, 2013: 589139.
Cauffman G., Liebaers I., Van Steirteghem A., Van de Velde H. POU5F1 isoforms show different expression patterns in human embryonic stem cells and preimplantation embryos. *Stem Cells* 2006, 24(12): 2685-2691.
Cawthorn W.P., Scheller E.L., MacDougald O.A. Adipose tissue stem cells meet preadipocyte commitment: going back to the future. *J Lipid Res* 2012, 53(2): 2217-246.
Cerwinka W.H., Sharp S.M., Boyan B.D., Zhau H.E., Chung L.W.K., Yates C. Differentiation of human mesenchymal stem cell spheroids under microgravity conditions. *Cell Regen* 2012, 1: 2.
Chabannes D., Hill M., Merieau E., Rossignol J., Brion R., Soulillou P., Anegon I., Cuturi M.C. A role for heme oxygenase-1 in the immunosuppressive effect of adult rat and human mesenchymal stem cells. *Blood* 2007, 110(10): 3691-3694.
Chamberlain G., Fox J., Ashton B., Middleton J. Concise review: mesenchymal stem cells: their phenotype, differentiation capacity, immunological features, and potential for homing. *Stem Cells* 2007, 25(11): 2739-2749.
Chambers I., Colby D., Robertson M., Nichols J., Lee S., Tweedie S., Smith A. Functional expression cloning of Nanog, a pluripotency sustaining factor in embryonic stem cells. *Cell* 2003, 113(5): 643-655.
Chambers I., Silva J., Colby D., Nichols J., Nijmeijer B., Robertson M., Vrana J., Jones K., Grotewold L., Smith A. Nanog safeguards pluripotency and mediates germline development. *Nature* 2007, 450(7173): 1230-1234.
Champeris Tsaniras S., Jones P.M. Generating pancreatic beta-cells from embryonic stem cells by manipulating signaling pathways. *J Endocrinol* 2010, 206(1): 13-26.
Chandra V., Swetha G., Muthyala S., Jaiswal A.K., Bellare J.R., Nair P.D., Bhonde R.R. Islet-like cell aggregates generated from human adipose tissue derived stem cells ameliorate experimental diabetes in mice. *PloS ONE* 2011, 6(6): e20615.
Chang C.M., Kao C.L., Chang Y.L., Yang M.J., Chen Y.C., Sung B.L., Tsai T.H., Chao K.C., Chiou S.H., Ku H.H. Placenta-derived multipotent stem cells induced to differentiate into insulin-positive cells. *Biochem Biophys Res Commun* 2007, 357(2): 414-420.
Chang D.F., Tsai S.C., Wang X.C., Xia P., Senadheera D., Lutzko C. Molecular characterization of the human NANOG protein. *Stem Cells* 2009, 27(4): 812-821.
Chazaud C., Yamanaka Y., Pawson T., Rossant J. Early lineage segregation between epiblast and primitive endoderm in mouse blastocysts through the Grb2-MAPK pathway. *Dev Cell* 2006, 10(5): 615-624.
Chen F.G., Zhang W.J., Bi D., Liu W., Wei X., Chen F.F., Zhu L., Cui L., Cao Y. Clonal analysis of nestin(-) vimentin(+) multipotent fibroblasts isolated from human dermis. *J Cell Sci* 2007, 120(16): 2875-2883.

Chen L.B., Jiang X.B., Yang L. Differentiation of rat marrow mesenchymal stem cells into pancreatic islet beta-cells. *World J Gastroenterol* 2004, 10(20): 3016-3020.

Chen S., Borowiak M., Fox J.L., Maehr R., Osafune K., Davidow L., Lam K., Peng L.F., Schreiber S.L., Rubin L.L., Melton D. A small molecule that directs differentiation of human ESCs into the pancreatic lineage. *Nat Chem Biol* 2009, 5(4): 258-265.

Cheng N.C., Wang S., Young T.H. The influence of spheroid formation of human adipose-derived stem cells on chitosan films on stemness and differentiation capabilities. *Biomaterials* 2012, 33(6): 1748-1758.

Cheng X., Ying L., Lu L., Galvão A.M., Mills J.A., Lin H.C., Kotton D.N., Shen S.S., Nostro M.C., Choi J.K., Weiss M.J., French D.L., Gadue P. Self-renewing endodermal progenitor lines generated from human pluripotent stem cells. *Cell Stem Cell* 2012, 10(4): 371-384.

Chew J.L., Loh Y.H., Zhang W., Chen X., Tam W.L., Yeap L.S., Li P., Ang Y.S., Lim B., Robson P., Ng H.H. Reciprocal transcriptional regulation of Pou5f1 and Sox2 via the Oct4/Sox2 complex in embryonic stem cells. *Mol Cell Biol* 2005, 25(14): 6031-6046.

Chhabra P., Brayman K.L. Stem cell therapy to cure type 1 diabetes: from hype to hope. *Stem Cells Transl Med* 2013, 2(5): 328-336.

Chickarmane V., Troein C., Nuber U.A., Sauro H.M., Peterson C. Transcriptional dynamics of the embryonic stem cell switch. *PloS Comput Biol* 2006, 2(9): e123.

Cho Y.M., Lim J.M., Yoo D.H., Kim J.H., Chung S.S., Park S.G., Kim T.H., Oh S.K., Choi Y.M., Moon S.Y., Park K.S., Lee H.K. Betacellulin and nicotinamide sustain *PDX1* expression and induce pancreatic β-cell differentiation in human embryonic stem cells. *Biochem Biophys Res Commun* 2008, 366(1): 129-134.

Concannon P., Rich S.S., Nepom G.T. Genetics of type 1A diabetes. *N Engl J Med* 2009, 360(16): 1646-1654.

Corcione A., Benvenuto F., Ferretti E., Giunti D., Cappiello V., Cazzanti F., Risso M., Gualandi F., Mancardi G.L., Pistoia V., Uccelli A. Human mesenchymal stem cells modulate B-cell functions. *Blood* 2006, 107(1): 367-372.

Covas D.T., Panepucci R.A., Fontes A.M., Silva W.A.Jr., Orellana M.D., Freitas M.C., Neder L., Santos A.R., Peres L.C., Jamur M.C., Zago M.A. Multipotent mesenchymal stromal cells obtained from diverse human tissues share functional properties and gene-expression profile with CD146+ perivascular cells and fibroblasts. *Exp Hematol* 2008, 36(5): 642-654.

Crisan M., Yap S., Casteilla L., Chen C.W., Corselli M., Park T.S., Andriolo G., Sun B., Zheng B., Zhang L., Norotte C., Teng P.N., Traas J., Schugar R., Deasy B.M., Badylak S., Buhring H.J., Giacobino J.P., Lazzari L., Huard J., Péault B. A perivascular origin for mesenchymal stem cells in multiple human organs. *Cell Stem Cell* 2008, 3(3): 301-313.

Cui L., Yin S., Liu W., Li N., Zhang W., Cao Y. Expanded adipose-derived stem cells suppress mixed lymphocyte reaction by secretion of prostaglandin E2. *Tissue Eng* 2007, 13(6): 1185-1195.

Cyranoski D. 2014. Japanese woman is first recipient of next-generation stem cells. Nature/News. http://www.nature.com/news/japanese-woman-is-first-recipient-of-next-generation-stem-cells-1.15915

Dalgin G., Ward A.B., Hao L.T., Beattie C.E., Nechiporuk A., Prince V.E. Zebrafish mnx1 controls cell fate choice in the developing endocrine pancreas. *Development* 2011, 138(21): 4597-4608.

D'Amour K.A., Agulnick A.D., Eliazer S., Kelly O.G., Kroon E., Baetge E.E. Efficient differentiation of human embryonic stem cells to definitive endoderm. *Nat Biotechnol* 2005, 23(12): 1534-1541.

D'Amour K.A., Bang A.G., Eliazer S., Kelly O.G., Agulnick A.D., Smart N.G., Moorman M.A., Kroon E., Carpenter M.K., Baetge E.E. Production of pancreatic hormone-expressing endocrine cells from human embryonic stem cells. *Nat Biotechnol* 2006, 24(11): 1392-1401.

Dang S.M., Kyba M., Perlingeiro R., Daley G.Q., Zandstra P.W. Efficiency of embryoid body formation and hematopoietic development from embryonic stem cells in different culture systems. *Biotechnol Bioeng* 2002, 78(4): 442-453.

Darr H., Mayshar Y., Benvenisty N. Overexpression of NANOG in human ES cells enables feeder-free growth while inducing primitive ectoderm features. *Development* 2006, 133(6): 1193-1201.

da Silva Meirelles L., Caplan A.I., Nardi N.B. In search of the in vivo identity of mesenchymal stem cells. *Stem Cells* 2008, 26(9): 2287-2299.

Davie J.R. Inhibition of histone deacetylase activity by butyrate. *J Nutr* 2003, 133(7 Suppl): 2485S-2493S.

De Miguel M.P., Fuentes-Julián S., Blázquez-Martínez A., Pascual C.Y., Aller M.A., Arias J., Arnalich-Montiel F. Immunosuppressive Properties of Mesenchymal Stem Cells: Advances and Applications. *Curr Mol Med* 2012, 12(5): 574-591.

de Wert G., Mummery C. Human embryonic stem cells: research, ethics and policy. *Hum Reprod* 2003, 18(4): 672-682.

Díaz-Flores L., Gutiérrez R., Varela H., Rancel N., Valladares F. Microvascular pericytes: a review of their morphological and functional characteristics. *Histol Histopathol* 1991, 6(2): 269-286.

Di Nicola M., Carlo-Stella C., Magni M., Milanesi M., Longoni P.D., Matteucci P., Grisanti S., Gianni A.M. Human bone marrow stromal cells suppress T-lymphocyte proliferation induced by cellular or nonspecific mitogenic stimuli. *Blood* 2002, 99(10): 3838-3843.

D'Ippolito G., Diabira S., Howard G.A., Roos B.A., Schiller P.C. Low oxygen tension inhibits osteogenic differentiation and enhances stemness of human MIAMI cells. *Bone* 2006, 39(3): 513-522.

D'Ippolito G., Schiller P.C., Ricordi C., Roos B.A., Howard G.A. Age-related osteogenic potential of mesenchymal stromal stem cells from human vertebral bone marrow. *J Bone Miner Res* 1999, 14(7): 1115-1122.

Djouad F., Plence P., Bony C., Tropel P., Apparailly F., Sany J., Noël D., Jorgensen C. Immunosuppressive effect of mesenchymal stem cells favors tumor growth in allogeneic animals. *Blood* 2003, 102(10): 3837-3844.

Doerr H.W., Cinatl J., Stürmer M., Rabenau H.F. Prions and orthopedic surgery. *Infection* 2003, 31(3): 163-171.

Dominici M., Le Blanc K., Mueller I., Slaper-Cortenbach I., Marini F.C., Krause D.S., Deans R., Keating A., Prockop D.J., Horwitz E.M. Minimal criteria for defining multipotent mesenchymal stromal cells. The International Society for Cellular Therapy position statement. *Cytotherapy* 2006, 8(4): 315-317.

Dzierzak E., Enver T. Stem cell researchers find their niche. *Development* 2008, 135(9): 1569-1573.

Enerbäck S. The origins of brown adipose tissue. *N Engl J Med* 2009, 360(19): 2021-2023.

Eng J., Kleinman W.A., Singh L., Singh G., Raufman J.P. Isolation and characterization of exendin-4, an exendin-3 analogue, from Heloderma suspectum venom. *J Biol Chem* 1992, 267(11): 7402-7405.

Ezashi T., Das P., Roberts R.M. Low O_2 tensions and the prevention of differentiation of hES cells. *Proc Natl Acad Sci U S A* 2005, 102(13): 4783-4788.

Ezeh U.I., Turek P.J., Reijo R.A., Clark A.T. Human embryonic stem cell genes OCT4, NANOG, STELLAR, and GDF3 are expressed in both seminoma and breast carcinoma. *Cancer* 2005, 104(10): 2255-2265.

Fairbanks D.J., Fairbanks A.D., Ogden T.H., Parker G.J., Maughan P.J. NANOGP8: evolution of a human-specific retro-oncogene. *G3 (Bethesda)* 2012, 2(11): 1447-1457.

Feng J., Mantesso A., De Bari C., Nishiyama A., Sharpe P.T. Dual origin of mesenchymal stem cells contributing to organ growth and repair. *Proc Natl Acad Sci U S A* 2011, 108(16): 6503-6508.

Festy F., Hoareau L., Bes-Houtmann S., Péquin A.M., Gonthier M.P., Munstun A., Hoarau J.J., Césari M., Roche R. Surface protein expression between human adipose tissue-derived stromal cells and mature adipocytes. *Histochem Cell Biol* 2005, 124(2): 113-121.

Filby C.E., Williamson R., von Kooy P., Pébay A., Dottori M., Elwood N.J., Zaibak F. Stimulation of Activin A/Nodal signaling is insufficient to induce definitive endoderm formation of cord blood-derived unrestricted somatic stem cells. *Stem Cell Res Ther* 2011, 2(2): 16.

Flavell S.J., Hou T.Z., Lax S., Filer A.D., Salmon M., Buckley C.D. Fibroblasts as novel therapeutic targets in chronic inflammation. *Br J Pharmacol* 2008, 153(Suppl 1): S241-S246.

Fraker C.A., Álvarez S., Papadopoulos P., Giraldo J., Gu W., Ricordi C., Inverardi L., Domínguez-Bendala J. Enhanced oxygenation promotes cell differentiation in vitro. *Stem Cells* 2007, 25(12): 3155-3164.

Fraker C.A., Ricordi C., Inverardi L., Domínguez-Bendala J. Oxygen: a master regulator of pancreatic development? *Biol Cell* 2009, 101(8): 431-440.

Fraser J.K., Wulur I., Alfonso Z., Hedrick M.H. Fat tissue: an underappreciated source of stem cells for biotechnology. *Trends Biotechnol* 2006, 24(4): 150-154.

Frith J.E., Res M., Thomson B., Genever P.G. Dynamic three-dimensional culture methods enhance mesenchymal stem cell properties and increase therapeutic potential. *Tissue Eng Part C Methods* 2010, 16(4): 735-749.

Fuchs E., Tumbar T., Guasch G. Socializing with the neighbors: stem cells and their niche. *Cell* 2004, 116(6): 769-778.

Gang E.J., Jeong J.A., Hong S.H., Hwang S.H., Kim S.W., Yang I.H., Ahn C., Han H., Kim H. Skeletal myogenic differentiation of mesenchymal stem cells isolated from human umbilical cord blood. *Stem Cells* 2004, 22(4): 617-624.

Gao F., Wu D.Q., Hu Y.H., Jin G.X. Extracellular matrix gel is necessary for in vitro cultivation of insulin producing cells from human umbilical cord blood derived mesenchymal stem cells. *Chin Med J* 2008, 121(9): 811-818.

Gao Y., Wang X., Han J., Xiao Z., Chen B., Su G., Dai J. The novel OCT4 spliced variant OCT4B1 can generate three protein isoforms by alternative splicing into OCT4B. *J Genet Genomics* 2010, 37(7): 461-465.

Gao Y., Wei J., Han J., Wang X., Su G., Zhao Y., Chen B., Xiao Z., Cao J., Dai J. The novel function of OCT4B isoform-265 in genotoxic stress. *Stem Cells* 2012, 30(4): 665-672.

Gesta S., Tseng Y.H., Kahn C.R. Developmental origin of fat: tracking obesity to its source. *Cell* 2007, 131(2): 242-256.

Gharbi S.I., Zvelebil M.J., Shuttleworth S.J., Hancox T., Saghir N., Timms J.F., Waterfield M.D. Exploring the specificity of the PI3K family inhibitor LY294002. *Biochem J* 2007, 404(1): 15-21.

Gimble J.M., Katz A.J., Bunnell B.A. Adipose-derived stem cells for regenerative medicine. *Circ Res* 2007, 100(9): 1249-1260.

Glennie S., Soeiro I., Dyson P.J., Lam E., Dazzi F. Bone marrow mesenchymal stem cells induce division arrest anergy of activated T cells. *Blood* 2005, 105(7): 2821-2827.

Gluckman E. History of cord blood transplantation. *Bone Marrow Transpl* 2009, 44: 621-626.

Gluckman E., Broxmeyer H.A., Auerbach A.D., Friedman H.S., Douglas G.W., Devergie A., Esperou H., Thierry D., Socie G., Lehn P., Cooper S., English D., Kurtzberg J., Bard J., Boyse E.A. Hematopoietic reconstitution in a patient with Fanconi's anemia by means of umbilical-cord blood from an HLA-identical sibling. *N Engl J Med* 1989, 321(17): 1174-1178.

Gluckman E., Rocha V., Boyer-Chammard A., Locatelli F., Arcese W., Pasquini R., Ortega J., Souillet G., Ferreira E., Laporte J.P., Fernandez M., Chastang C. Outcome of cord-blood transplantation from related and unrelated donors. *N Engl J Med* 1997, 337(6): 373-381.

Goldring C.E., Duffy P.A., Benvenisty N., Andrewa P.W., Ben-David U., Eakins R., French N.,

Hanley N.A., Kelly L., Kitteringham N.R., Kurth J., Ladenheim D., Laverty H., McBlane J., Narayanan G., Patel S., Reinhardt J., Rossi A., Sharpe M., Park B.K. Assessing the safety of stem cell therapeutics. *Cell Stem Cell* 2011, 8(6): 618-628.

Goldthwaite C.A.Jr. 2010. Are stem cells the next frontier for diabetes treatment? http://stemcells.nih.gov/info/Regenerative_Medicine/Pages/2006Chapter7.aspx

Gontan C., de Munck A., Vermeij M., Grosveld F., Tibboel D., Rottier R. Sox2 is important for two crucial processes in lung development: branching morphogenesis and epithelial cell differentiation. *Dev Biol* 2008, 317(1): 296-309.

González-Reyes A. Stem cells, niches and cadherins: a view from Drosophila. *J Cell Sci* 2003, 116(Pt 6): 949-954.

Goto T., Adjaye J., Rodeck C.H., Monk M. Identification of genes expressed in human primordial germ cells at the time of entry of the female germ line into meiosis. *Mol Hum Reprod* 1999, 5(9): 851-860.

Göke R., Fehmann H.C., Linn T., Schmidt H., Krause M., Eng J., Göke B. Exendin-4 is a high potency agonist and truncated exendin-(9-39)-amide an antagonist at the glucagon-like peptide 1-(7-36)-amide receptor of insulin-secreting β-cells. *J Biol Chem* 1993, 268(26): 19650-19655.

Graham V., Khudyakov J., Ellis P., Pevny L. SOX2 functions to maintain neural progenitor identity. *Neuron* 2003, 39(5): 749-765.

Grapin-Botton A. 2008. Endoderm specification. http://www.stembook.org/node/524

Grapin-Botton A., Majithia A.R., Melton D.A. Key events of pancreas formation are triggered in gut endoderm by ectopic expression of pancreatic regulatory genes. *Genes Dev* 2001, 15(4): 444-454.

Greco S.J., Liu K., Rameshwar P. Functional similarities among genes regulated by Oct4 in human mesenchymal and embryonic stem cells. *Stem Cells* 2007, 25(12): 3143-3154.

Gronthos S., Franklin D.M., Leddy H.A., Robey P.G., Storms R.W., Gimble J.M. Surface protein characterization of human adipose tissue-derived stromal cells. *J Cell Physiol* 2001, 189(1): 54-63.

Gruber H.E., Somayaji S., Riley F., Hoelscher G.L., Norton H.J., Ingram J., Hanley E.N.Jr. Human adipose-derived mesenchymal stem cells: serial passaging, doubling time and cell senescence. *Biotech Histochem* 2012, 87(4): 303-311.

Gu G., Dubauskaite J., Melton D.A. Direct evidence for the pancreatic lineage: NGN3+ cells are islet progenitors and are distinct from duct progenitors. *Development* 2002, 129(10): 2447-2457.

Gu G., Yuan J., Wills M., Kasper S. Prostate cancer cells with stem cell characteristics reconstitute the original human tumor in vivo. *Cancer Res* 2007, 67(10): 4807-4815.

Gupta R. 2012. Cord blood stem cells: current uses and future challenges. http://www.eurostemcell.org/factsheet/cord-blood-stem-cells-current-uses-and-future-challenges

Gustafsson M.V., Zheng X., Pereira T., Gradin K., Jin S., Lundkvist J., Ruas J.L., Poellinger L., Lendahl U., Bondesson M. Hypoxia requires Notch signaling to maintain the undifferentiated cell state. *Dev Cell* 2005, 9(5): 617-628.

Hakim F., Kaitsuka T., Raeed J.M., Wei F.Y., Shiraki N., Akagi T., Yokota T., Kume S., Tomizawa K. High oxygen condition facilitates the differentiation of mouse and human pluripotent stem cells into pancreatic progenitors and insulin-producing cells. *J Biol Chem* 2014, 289(14): 9623-9638.

Halfon S., Abramov N., Grinblat B., Ginis I. Markers distinguishing mesenchymal stem cells from fibroblasts are downregulated with passaging. *Stem Cells Dev* 2011, 20(1): 53-66.

Handschel J.G.K., Depprich R.A., Kübler N.R., Wiesmann H.P., Ommerborn M., Meyer U. Prospects of micromass culture technology in tissue engineering. *Head Face Med* 2007, 3: 4.

Haniffa M.A., Collin M.P., Buckley C.D., Dazzi F. Mesenchymal stem cells: the fibroblasts' new

clothes? *Haematologica* 2009, 94(2): 258-263.
Haniffa M.A., Wang X.N., Holtick U., Rae M., Isaacs J.D., Dickinson A.M., Hilkens C.M., Collin M.P. Adult human fibroblasts are potent immunoregulatory cells and functionally equivalent to mesenchymal stem cells. *J Immunol* 2007, 179(3): 1595-1604.
Hansson M., Tonning A., Frandsen U., Petri A., Rajagopal J., Englund M.C.O., Heller R.S., Håkansson J., Fleckner J., Sköld H.N., Melton D., Semb H., Serup P. Artifactual insulin release from differentiated embryonic stem cells. *Diabetes* 2004, 53(10): 2603-2609.
Hart A., Papadopoulou S., Edlund H. Fgf10 maintains notch activation, stimulates proliferation, and blocks differentiation of pancreatic epithelial cells. *Dev Dyn* 2003, 228(2): 185-193.
Hay D.C., Sutherland L., Clark J., Burdon T. Oct-4 knockdown induces similar patterns of endoderm and trophoblast differentiation markers in human and mouse embryonic stem cells. *Stem Cells* 2004, 22(2): 225-235.
Hayashi H., Arao T., Togashi Y., Kato H., Fujita Y., De Velasco M.A., Kimura H., Matsumoto K., Tanaka K., Okamoto I., Ito A., Yamada Y., Nakagawa K., Nishio K. The OCT4 pseudogene POU5F1B is amplified and promotes an aggressive phenotype in gastric cancer. *Oncogene* 2015, 34(2): 199-208.
Hayhurst G.P., Lee Y.H., Lambert G., Ward J.M., Gonzalez F.J. Hepatocyte nuclear factor 4alpha (nuclear receptor 2A1) is essential for maintenance of hepatic gene expression and lipid homeostasis. *Mol Cell Biol* 2001, 21(4): 1393-1403.
Heinis M., Simon M.T., Ilc K., Mazure N.M., Pouysségur J., Scharfmann R., Duvillié B. Oxygen tension regulates pancreatic β-cell differentiation through hypoxia-inducible factor 1α. *Diabetes* 2010, 59(3): 662-669.
Hematti P. Mesenchymal stromal cells and fibroblasts: a case of mistaken identity? *Cytotherpy* 2012, 14(5): 516-521.
Hermann R., Knip M., Veijola R., Simell O., Laine A.P., Akerblom H.K., Groop P.H., Forsblom C., Pettersson-Fernholm K., Ilonen J. Temporal changes in the frequencies of HLA genotypes in patients with type 1 diabetes - indication of an increased environmental pressure? *Diabetologia* 2003, 46(3): 420-425.
Herreros-Villanueva M., Zhang J.S., Koenig A., Abel E.V., Smyrk T.C., Bamlet W.R., de Narvajas A.A., Gomez T.S., Simeone D.M., Bujanda L., Billadeau D.D. SOX2 promotes dedifferentiation and imparts stem cell-like features to pancreatic cancer cells. *Oncogenesis* 2013, 2: e61.
Ho M., Yu D., Davidsion M.C., Silva G.A. Comparison of standard surface chemistries for culturing mesenchymal stem cells prior to neural differentiation. *Biomaterials* 2006, 27(24): 4333-4339.
Holst J.J. The physiology of glucagon-like peptide 1. *Physiolo Rev* 2007, 87(4): 1409-1439.
Horwitz E.M., Andreef M., Frassoni F. Mesenchymal stromal cells. *Curr Opin Hematol* 2006, 13(6): 419-425.
Horwitz E.M., Le Blanc K., Dominici M., Mueller I., Slaper-Cortenbach I., Marini F.C., Deans R.J., Krause D.S., Keating A. Clarification of the nomenclature for MSC: The International Society for Cellular Therapy position statement. *Cytotherapy* 2005, 7(5): 393-395.
Hosoya M. Preparation of pancreatic β-cells from human iPS cells with small molecules. *Islets* 2012, 4(3): 249-252.
Hsu Y.C., Fuchs E. A family business: stem cell progeny join the niche to regulate homeostasis. *Nat Rev Mol Cell Biol* 2012, 13(2): 103-114.
Hsu Y.C., Li L., Fuchs E. Transit-amplifying cells orchestrate stem cell activity and tissue regeneration. *Cell* 2014, 157(4): 935-949.
Hu Y.H., Wu D.Q., Gao F., Li G.D., Zhang X.C. Notch signaling: a novel regulating differentiation mechanism of human umbilical cord blood-derived mesenchymal stem cells into insulin-producing cells in vitro. *Chin Med J* 2010, 123(5): 606-614.
Huang J., Nguyen-McCarty M., Hexner E.O., Danet-Desnoyers G., Klein P.S. Maintenance of

hematopoietic stem cells through regulation of Wnt and mTOR pathways. *Nat Med* 2012, 18(12): 1778-1785.

Huang L., Wong Y.P., Gu H., Cai Y.J., Ho Y., Wang C.C., Leung T.Y., Burd A. Stem cell-like properties of human umbilical cord lining epithelial cells and the potential for epidermal reconstitution. *Cytotherapy* 2011, 13(2): 145-155.

Hyslop L., Stojkovic M., Armstrong L., Walter T., Stojkovic P., Przyborski S., Herbert M., Murdoch A., Strachan T., Lako M. Downregulation of NANOG induces differentiation of human embryonic stem cells to extraembryonic lineages. *Stem Cells* 2005, 23(8): 1035-1043.

Ibrahim E.E., Babaei-Jadidi R., Saadeddin A., Spencer-Dene B., Hossaini S., Abuzinadah M., Li N., Fadhil W., Ilyas M., Bonnet D., Nateri A.S. Embryonic NANOG activity defines colorectal cancer stem cells and modulates through AP1- and TCF-dependent mechanisms. *Stem Cells* 2012, 30(10): 2076-2087.

Ishii T., Eto K. Fetal stem cell transplantation: Past, present, and future. *World J Stem Cells* 2014, 6(4): 404-420.

Ivascu A., Kubbies M. Rapid generation of single-tumor spheroids for high-throughput cell function and toxicity analysis. *J Biomol Screen* 2006, 11(8): 922-932.

Izadpanah R., Trygg C., Patel B., Kriedt C., Dufour J., Gimble J.M., Bunnell B.A. Biologic properties of mesenchymal stem cells derived from bone marrow and adipose tissue. *J Cell Biochem* 2006, 99(5): 1285-1297.

Jaenisch R., Young R. Stem cells, the molecular circuitry of pluripotency and nuclear reprogramming. *Cell* 2008, 132(4): 567-582.

Jang S., Cho H.H., Cho Y.B., Park J.S., Jeong H.S. Functional neural differentiation of human adipose tissue-derived stem cells using bFGF and forskolin. *BMC Cell Biol* 2010, 11: 25.

Jääger K., Islam S., Zajac P., Linnarsson S., Neuman T. RNA-Seq analysis reveals different dynamics of differentiation of human dermis- and adipose-derived stromal stem cells. *PloS ONE* 2012, 7(6): e38833.

Jensen J.B., Parmar M. Strengths and limitations of the neurosphere culture system. *Mol Neurobiol* 2006, 34(3): 153-161.

Jeon E.S., Moon H.J., Lee M.J., Song H.Y., Kim Y.M., Bae Y.C., Jung J.S., Kim J.H. Sphingosylphosphorylcholine induces differentiation of human mesenchymal stem cells into smooth-muscle-like cells through a TGF-β-dependent mechanism. *J Cell Sci* 2006, 119(Pt 23): 4994–5005.

Jeter C.R., Badeaux M., Choy G., Chandra D., Patrawala L., Liu C., Calhoun-Davis T., Zaehres H., Daley G.Q., Tang D.G. Functional evidence that the self-renewal gene NANOG regulates human tumor development. *Stem Cells* 2009, 27(5): 993-1005.

Jez M., Ambady S., Kashpur O., Grella A., Malcuit C., Vilner L., Rozman P., Dominko T. Expression and differentiation between OCT4A and its Pseudogenes in human ESCs and differentiated adult somatic cells. *PloS One* 2014, 9(2): e89546.

Jiang J., Au M., Lu K., Eshpeter A., Korbutt G., Fisk G., Majumdar A.S. Generation of insulin-producing islet-like clusters from human embryonic stem cells. *Stem Cells* 2007, 25(8): 1940-1453.

Jones S., Horwood N., Cope A., Dazzi F. The antiproliferative effect of mesenchymal stem cells is a fundamental property shared by all stromal cells. *J Immunol* 2007, 179(5): 2824-2831.

Jones T.D., Ulbright T.M., Eble J.N., Baldridge L.A., Cheng L. OCT4 staining in testicular tumors: a sensitive and specific marker for seminoma and embryonal carcinoma. *Am J Surg Pathol* 2004, 28(7): 935-940.

Kakudo N., Shimotsuma A., Kusumoto K. Fibroblast growth factor-2 stimulates adipogenic differentiation of human adipose-derived stem cells. *Biochem Biophys Res Commun* 2007, 359(2): 239-244.

Kaltz N., Funari A., Hippauf S., Delorme B., Noël D., Riminucci M., Jacobs V.R., Häupl T., Jorgensen C., Charbord P., Peschel C., Bianco P., Oostendorp R.A. In vivo osteoprogenitor

potency of human stromal cells from different tissues does not correlate with expression of POU5F1 or its pseudogenes. *Stem Cells* 2008, 26(9): 2419-2424.

Kang H.M., Park S., Kim H. Insulin-like growth factor 2 enhances insulinogenic differentiation of human eyelid adipose stem cells via the insulin receptor. *Cell Prolif* 2011, 44(3): 254-263.

Kayali A.G., Van Gunst K., Campbell I.L., Stotland A., Kritzik M., Liu G., Flodström-Tullberg M., Zhang Y.Q., Sarvetnick N. The stromal cell–derived factor-1α/CXCR4 ligand–receptor axis is critical for progenitor survival and migration in the pancreas. *J Cell Biol* 2003, 163(4): 859-869.

Keating A. Mesenchymal stromal cells: new directions. *Cell Stem Cell* 2012, 10(6): 709-716.

Kern S., Eichler H., Stoeve J., Klüter H., Bieback K. Comparative Analysis of Mesenchymal Stem Cells from Bone Marrow, Umbilical Cord, or Adipose Tissue. *Stem Cells* 2006, 24(5): 1294-1301.

Kilroy G.E., Foster S.J., Wu X., Ruiz J., Sherwood S., Heifetz A., Ludlow J.W., Stricker D.M., Potiny S., Green P., Halvorsen Y.D., Cheatham B., Storms R.W., Gimble J.M. Cytokine profile of human adipose-derived stem cells: expression of angiogenic, hematopoietic, and pro-inflammatory factors. *J Cell Physiol* 2007, 212(3): 702-709.

Kim Y.H., Yoon D.S., Kim H.O., Lee J.W. Characterization of different subpopulations from bone marrow-derived mesenchymal stromal cells by alkaline phosphatase expression. *Stem Cells Dev* 2012, 21(16): 2958-2968.

Kita K., Gauglitz G.G., Phan T.T., Herndon D.N., Jeschke M.G. Isolation and characterization of mesenchymal stem cells from the sub-amniotic human umbilical cord lining membrane. *Stem Cells Dev* 2010, 19(4): 491-502.

Koblas T., Zacharovová K., Berková Z., Mindlová M., Girman P., Dovolilová E., Karasová L., Saudek F. Isolation and characterization of human CXCR4-positive pancreatic cells. *Folia Biol (Praha)* 2007, 53(1): 13-22.

Kojima H., Fujimiya M., Matsumura K., Nakahara T., Hara M., Chan L. Extrapancreatic insulin-producing cells in multiple organs in diabetes. *Proc Natl Acad Sci U S A* 2004, 101(8): 2458-2463.

Kolf C.M., Cho E., Tuan R.S. Mesenchymal stromal cells. Biology of adult mesenchymal stem cells: regulation of niche, self-renewal and differentiation. *Arthritis Res Ther* 2007, 9(1): 204.

Kopp J.L., Ormsbee B.D., Desler M., Rizzino A. Small increases in the level of Sox2 trigger the differentiation of mouse embryonic stem cells. *Stem Cells* 2008, 26(4): 903-911.

Kotoula V., Papamichos S.I., Lambropoulos A.F. Revisiting OCT4 expression in peripheral blood mononuclear cells. *Stem Cells* 2008, 26(1): 290-291.

Krishnan B.R., Jamry I., Chaplin D.D. Feature mapping of the HLA class I region: localization of the POU5F1 and TCF19 genes. *Genomics* 1995, 30(1): 53-58.

Kroon E., Martinson L.A., Kadoya K., Bang A.G., Kelly O.G., Eliazer S., Young H., Richardson M., Smart N.G., Cunningham J., Agulnick A.D., D'Amour K.A., Carpenter M.K., Baetge E.E. Pancreatic endoderm derived from human embryonic stem cells generates glucose-responsive insulin-secreting cells in vivo. *Nat Biotechnol* 2008, 26(4): 443-452.

Kruse C., Birth M., Rohwedel J., Assmuth K., Goepel A., Wedel T. Pluripotency of adult stem cells derived from human and rat pancreas. *Appl Phys A* 2004, 79(7): 1617-1624.

Kucia M., Halasa M., Wysoczynski M., Baskiewicz-Masiuk M., Moldenhawe S., Zuba-Surma E., Czajka R., Wojakowski W., Machalinski B., Ratajczak M.Z. Morphological and molecular characterization of novel population of CXCR4+ SSEA-4+ Oct-4+ very small embryonic-like cells purified from human cord blood: preliminary report. *Leukemia* 2007, 21(2): 297-303.

Kunisada Y., Tsubooka-Yamazoe N., Shoji M., Hosoya M. Small molecules induce efficient differentiation into insulin-producing cells from human induced pluripotent stem cells. *Stem Cell Res* 2012, 8(2): 274-284.

Kuroda Y., Kitada M., Wakao S., Nishikawa K., Tanimura Y., Makinoshima H., Goda M., Akashi H., Inutsuka A., Niwa A., Shigemoto T., Nabeshima Y., Nakahata T., Nabeshima Y., Fujiyoshi Y., Dezawa M. Unique multipotent cells in adult human mesenchymal cell populations. *Proc Natl Acad Sci U S A* 2010,107(19): 8639-8643.

Kurosawa H. Methods for inducing embryoid body formation: in vitro differentiation system of embryonic stem cells. *J Biosci Bioeng* 2007, 103(5): 389-398.

Lakatos D., Travis E.D., Pierson K.E., Vivian J.L., Czirok A. Autocrine FGF feedback can establish distinct states of Nanog expression in pluripotent stem cells: a computational analysis. *BMC Syst Biol* 2014, 8: 112.

Le Blanc K. Tammik L., Sundberg B., Haynesworth S.E., Ringdén O. Mesenchymal stem cells inhibit and stimulate mixed lymphocyte cultures and mitogenic responses independently of the major histocompatibility complex. *Scand J Immunol* 2003, 57(1): 11-20.

Lee D.H., Chung H.M. Differentiation into endoderm lineage: pancreatic differentiation from embryonic stem cells. *Int J Stem Cells* 2011, 4(1): 35-42.

Lee J., Han D.J., Kim S.C. In vitro differentiation of human adipose tissue-derived stem cells into cells with pancreatic phenotype by regenerating pancreas extract. *Biochem Biophys Res Commun* 2008, 375(4): 547-551.

Lee J., Kim H.K., Rho J.Y., Han Y.M., Kim J. The human OCT-4 isoforms differ in their ability to confer self-renewal. *J Biol Chem* 2006, 281(44): 33554-33565.

Lee J.H., Kemp D.M. Human adipose-derived stem cells display myogenic potential and perturbed function in hypoxic conditions. *Biochem Biophys Res Commun* 2006, 341(3): 882-88.

Lee K.D., Kuo T.K., Whang-Peng J., Chung Y.F., Lin C.T., Chou S.H., Chen J.R., Chen Y.P., Lee O.K. In vitro hepatic differentiation of human mesenchymal stem cells. *Hepatology* 2004, 40(6): 1275-1284.

Lengner C.J., Camargo F.D., Hochedlinger K., Welstead G.G., Zaidi S., Gokhale S., Scholer H.R., Tomilin A., Jaenisch R. Oct4 expression is not required for mouse somatic stem cell self-renewal. *Cell Stem Cell* 2007, 1(4): 403-415.

Lengner C.J., Welstead G.G., Jaenisch R. The pluripotency regulator Oct4: a role in somatic stem cells? *Cell Cycle* 2008, 7(6): 725-728.

Lennon D.P., Haynesworth S.E., Bruder S.P., Jaiswal N., Caplan A.I. Human and animal mesenchymal progenitor cell from bone marrow: identification of serum for optimal selection and proliferation. *In Vitro Cell Dev Biol – Animal* 1996, 32(10): 602-611.

Lev R., Spicer S.S. Specific staining of sulphate groups with alcian blue at low pH. *J. Histochem Cytochem* 1964, 12(4): 309.

Li H., Lam A., Xu A.M., Lam K.S., Chung S.K. High dosage of Exendin-4 increased early insulin secretion in differentiated beta cells from mouse embryonic stem cells. *Acta Pharmacol Sin* 2010, 31(5): 570-577.

Li L., Lili R., Hui Q., Min W., Xue W., Xin S., Jing L., Yan L., Yeqiang L., Fenrong H., Furong L., Guanxin S. Combination of GLP-1 and sodium butyrate promote differentiation of pancreatic progenitor cells into insulin-producing cells. *Tissue Cell* 2008, 40(6): 437-445.

Liedtke S., Enczmann J., Waclawczyk S., Wernet P., Kögler G. Oct4 and its pseudogenes confuse stem cell research. *Cell Stem Cell* 2007, 1(4): 364-366.

Liedtke S., Stephan M., Kögler G. Oct4 expression revisited: potential pitfalls for data misinterpretation in stem cell research. *Biol Chem* 2008, 389(7): 845-850.

Lim I.J., Phan T.T. Epithelial and mesenchymal stem cells from the umbilical cord lining membrane. *Cell Transplant* 2014, 23(4-5): 497-503.

Lin T.M., Chang H.W., Wang K.H., Kao A.P., Chang C.C., Wen C.H., Lai C.S., Lin S.D. Isolation and identification of mesenchymal stem cells from human lipoma tissue. *Biochem Biophys Res Commun* 2007, 361(4): 883-889.

Lindroos B., Suuronen R., Miettinen S. The potential of adipose stem cells in regenerative medicine. *Stem Cell Rev* 2011, 7(2): 269-291.

Lorenz K., Sicker M., Schmelzer E., Rupf T., Salvetter J., Schulz-Siegmund M., Bader A. Multilineage differentiation potential of human dermal skin-derived fibroblasts. *Exp Dermatol* 2008, 17(11): 925-932.

Lumelsky N., Blondel O., Laeng P., Velasco I., Ravin R., McKay R. Differentiation of embryonic stem cells to insulin-secreting structures similar to pancreatic islets. *Science* 2001, 292(5520): 1389-1394.

Lv F.J., Tuan R.S., Cheung K.M., Leung V.Y. Concise review: the surface markers and identity of human mesenchymal stem cells. *Stem Cells* 2014, 32(6): 1408-1419.

Lysy P.A., Smets F., Sibille C., Najimi M., Sokal E.M. Human skin fibroblasts: From mesodermal to hepatocyte-like differentiation. *Hepatology* 2007, 46(5): 1574-1585.

Maehr R., Chen S., Snitow M., Ludwig T., Yagasaki L., Goland R., Leibel R.L., Melton D.A. Generation of pluripotent stem cells from patients with type 1 diabetes. *Proc Natl Acad Sci U S A* 2009, 106(37): 15768-15773.

Marcus A.J., Woodbury D. Fetal stem cells from extra-embryonic tissues: do not discard. *J Cell Mol Med* 2008, 12(3): 730-742.

Martin G.R. Isolation of a pluripotent cell line from early mouse embryos cultured in medium conditioned by teratocarcinoma stem cells. *Proc Natl Acad Sci U S A* 1981, 78(12): 7634-7638.

Matthews V.B., Yeoh G.C. Liver stem cells. *IUBMB Life* 2005, 57(8): 549-553.

McLean A.B., D'Amour K.A., Jones K.L., Krishnamoorthy M., Kulik M.J., Reynolds D.M., Sheppard A.M., Liu H., Xu Y., Baetge E.E., Dalton S. Activin a efficiently specifies definitive endoderm from human embryonic stem cells only when phosphatidylinositol 3-kinase signaling is suppressed. *Stem Cells* 2007, 25(1): 29-38.

Meisel R., Zibert A., Laryea M., Göbel U., Däubener W., Dilloo D. Human bone marrow stromal cells inhibit allogeneic T-cell responses by indoleamine 2,3-dioxygenase-mediated tryptophan degradation. *Blood* 2004, 103(12): 4619-4621.

Micallef S.J., Janes M.E., Knezevic K., Davis R.P., Elefanty A.G., Stanley E.G. Retinoic acid induces Pdx1-positive endoderm in differentiating mouse embryonic stem cells. *Diabetes* 2005, 54(2): 301-305.

Millán J.L. Alkaline phosphatases: structure, substrate specificity and functional relatedness to other members of a large superfamily of enzymes. *Purinergic Signal* 2006, 2(2): 335-341.

Mills J.C., Shivdasani R.A. Gastric epithelial stem cells. *Gastroenterology* 2011, 140(2): 412-424.

Mimeault M., Batra S.K. Concise review: recent advances on the significance of stem cells in tissue regeneration and cancer therapies. *Stem Cells* 2006, 24(11): 2319-2345.

Mitchell J.B., McIntosh K., Zvonic S., Garrett S., Floyd Z.E., Kloster A., Di Halvorsen Y., Storms R.W., Goh B., Kilroy G., Wu X., Gimble J.M. Immunophenotype of human adipose-derived cells: temporal change in stromal-associated and stem cell–associated markers. *Stem Cells* 2006, 24(2): 376-385.

Mitsui K., Tokuzawa Y., Itoh H., Segawa K., Murakami M., Takahashi K., Maruyama M., Maeda M., Yamanaka S. The homeoprotein Nanog is required for maintenance of pluripotency in mouse epiblast and ES cells. Cell 2003, 113(5): 631-642.

Moriscot C., de Fraipont F., Richard M.J., Marchand M., Savatier P., Bosco D., Favrot M., Benhamou P.Y. Human bone marrow mesenchymal stem cells can express insulin and key transcription factors of the endocrine pancreas developmental pathway upon genetic and/or microenvironmental manipulation in vitro. *Stem Cells* 2005, 23(4): 594-603.

Morrison S.J., Kimble J. Asymmetric and symmetric stem-cell divisions in development and cancer. *Nature* 2006, 441(7097): 1068-1074.

Mueller S.M., Glowacki J. Age-related decline in the osteogenic potential of human bone marrow cells cultured in three-dimensional collagen sponges. *J Cell Biochem* 2001, 82(4): 583-590.

Mueller T., Luetzkendorf J., Nerger K., Schmoll H.J., Mueller L.P. Analysis of OCT4 expression

in an extended panel of human tumor cell lines from multiple entities and in human mesenchymal stem cells. *Cell Mol Life Sci* 2009, 66(3): 495-503.
Mullin N.P., Yates A., Rowe A.J., Nijmeijer B., Colby D., Barlow P.N., Walkinshaw M.D., Chambers I. The pluripotency rheostat Nanog functions as a dimer. *Biochem J* 2008, 411(2): 227-231.
Narsinh K.H., Plews J., Wu J.C. Comparison of human induced pluripotent and embryonic stem cells: fraternal or identical twins? *Mol Ther* 2011, 19(4): 635-638.
Nasef A., Mathieu N., Chapel A., Frick J., François S., Mazurier C., Boutarfa A., Bouchet S., Gorin N.C., Thierry D., Fouillard L. Immunosuppressive effects of mesenchymal stem cells: involvement of HLA-G. *Transplantation* 2007, 84(2): 231-237.
Naujok O., Burns C., Jones P.M., Lenzen S. Insulin-producing surrogate β-cells from embryonic stem cells: are we there yet? *Mol Ther* 2011, 19(10): 1759-1768.
Navarro P., Festuccia N., Colby D., Gagliardi A., Mullin N.P., Zhang W., Karwacki-Neisius V., Osorno R., Kelly D., Robertson M., Chamber I. OCT4/SOX2-independent Nanog autorepression modulates heterogeneous Nanog gene expression in mouse ES cells. *EMBO J* 2012, 31(24): 4547-4562.
Naveiras O., Daley G.Q. Stem cells and their niche: a matter of fate. *Cell Mol Life Sci* 2006, 63(7-8): 760-766.
Nedergaard J., Bengtsson T., Cannon B. Unexpected evidence for active brown adipose tissue in adult humans. *Am J Physiol Endocrinol Metab* 2007, 293(2): E444-E452.
Neshati Z., Matin M.M., Bahrami A.R., Moghimi A. Differentiation of mesenchymal stem cells to insulin-producing cells and their impact on type 1 diabetic rats. *J Physiol Biochem* 2010, 66(2): 181-187.
Nichols J., Zevnik B., Anastassiadis K., Niwa H., Klewe-Nebenius D., Chambers I., Schöler H., Smith A. Formation of pluripotent stem cells in the mammalian embryo depends on the POU transcription factor Oct4. *Cell* 1998, 95(3): 379-391.
Nishida S., Endo N., Yamagiwa H., Tanizawa T., Takahashi H.E. Number of osteoprogenitor cells in human bone marrow markedly decreases after skeletal maturation. *J Bone Miner Metab* 1999, 17(3): 171-177.
Niwa H. Molecular mechanism to maintain stem cell renewal of ES cells. *Cell Struct Funct* 2001, 26(3): 137-148.
Niwa H., Miyazaki J., Smith A.G. Quantitative expression of Oct-3/4 defines differentiation, dedifferentiation or self-renewal of ES cells. *Nat Genet* 2000, 24(4): 372-376.
Nokoff N.J., Rewers M., Cree Green M. The interplay of autoimmunity and insulin resistance in type 1 diabetes. *Discov Med* 2012, 13(69): 115-122.
Nombela-Arrieta C., Ritz J., Silberstein L.E. The elusive nature and function of mesenchymal stem cells. *Nat Rev Mol Cell Biol* 2011, 12(2): 126-131.
O'Connor T.P., Crystal R.G. Genetic medicines: treatment strategies for hereditary disorders. *Nat Rev Genet* 2006, 7(4): 261-276.
Oishi K., Noguchi H., Yukawa H., Hayashi S. Differential ability of somatic stem cells. *Cell Transplant* 2009, 18(5): 581-589.
Okura H., Komoda H., Fumimoto Y., Lee C.M., Nishida T., Sawa Y., Matsuyama A. Transdifferentiation of human adipose tissue-derived stromal cells into insulin-producing clusters. *J Artiff Organs* 2009, 12(2): 123-130.
Oller A.R., Buser C.W., Tyo M.A., Thilly W.G. Growth of mammalian cells at high oxygen concentrations. J Cell Sci 1989, 94(Pt 1): 43-49.
Ong W.K., Sugii S. Adipose-derived stem cells: fatty potentials for therapy. *Int J Biochem Cell Biol* 2013, 45(6): 1083-1086.
O'Sullivan E.S., Vegas A., Anderson D.G., Weir G.C. Islets transplanted in immunoisolation devices: a review of the progress and the challenges that remain. *Endocr Rev* 2011, 32(6): 827-844.
Otonkoski T., Beattie G.M., Mally M.I., Ricordi C., Hayek A. Nicotinamide is a potent inducer

of endocrine differentiation in cultured human fetal pancreatic cells. *J Clin Invest* 1993, 92(3): 1459-1466.

Pagliuca F.W., Millman J.R., Gürtler M., Segel M., Van Dervort A., Ryu J.H., Peterson Q.P., Greiner D., Melton D.A. Generation of functional human pancreatic β cells in vitro. *Cell* 2014, 159(2): 428-439.

Pain D., Chirn G.W., Strassel C., Kemp D.M. Multiple retropseudogenes from pluripotent cell-specific gene expression indicates a potential signature for novel gene identification. *J Biol Chem* 2005, 280(8): 6265-6268.

Pan G., Li J., Zhou Y., Zheng H., Pei D. A negative feedback loop of transcription factors that controls stem cell pluripotency and self-renewal. *FASEB J* 2006, 20(10): E1094-E1102.

Pan G., Thomson J.A. Nanog and transcriptional networks in embryonic stem cell pluripotency. *Cell Res* 2007, 17(1): 42-49.

Pan G., Qin B., Liu N., Schöler H.R., Pei D. Identification of a nuclear localization signal in OCT4 and generation of a dominant negative mutant by its ablation. *J biol Chem* 2004, 279(35): 37013-37020.

Pan G.J., Chang Z.Y., Schöler H.R., Pei D. Stem cell pluripotency and transcription factor Oct4. *Cell Res* 2002, 12(5-6): 321-329.

Panagopoulos I., Möller E., Collin A., Mertens F. The POU5F1P1 pseudogene encodes a putative protein similar to POU5F1 isoform 1. *Oncol Rep* 2008, 20(5): 1029-1033.

Papamichos S.I., Kotoula V., Tarlatzis B.C., Agorastos T., Papazisis K., Lambropoulos A.F. OCT4B1 isoform: the novel OCT4 alternative spliced variant as a putative marker of stemness. *Mol Hum Reprod* 2009, 15(5): 269-270.

Park E., Patel A.N. Changes in the expression pattern of mesenchymal and pluripotent markers in human adipose-derived stem cells. *Cell Biol Int* 2010, 34(10): 979-984.

Pera M.F., Dottori M. Stem cells and their developmental potential. In: Bongso A., Lee E.H. Stem cells: from bench to bedside. Singapore: *World Scientific Publishing Co. Pte. Ltd.* 2005, 55-70.

Pera M.F., Reubinoff B., Trounson A. Human embryonic stem cells. *J Cell Sci* 2000, 113, 5-10.

Pettersson P., Cigolini M., Sjöström L., Smith U., Björntorp P. Cells in human adipose tissue developing into adipocytes. *Acta Med Scand* 1984, 215(5): 447-451.

Pham P.V. Adipose stem cells in the clinic. *Biomed Res Ther* 2014, 1(2): 57-70.

Phinney D.G., Prockop D.J. Concise review: mesenchymal stem/multipotent stromal cells: the state of transdifferentiation and modes of tissue repair - current views. *Stem Cells* 2007, 25(11): 2896-2902.

Pittenger M.F., Mackay A.M., Beck S.C., Jaiswal R.K., Douglas R., Mosca J.D., Moorman M.A., Simonetti D.W., Craig S., Marshak D.R. Multilineage potential of adult human mesenchymal stem cells. *Science* 1999, 284(5411): 143-147.

Planat-Bénard V., Menard C., André M., Puceat M., Perez A., Garcia-Verdugo J.M., Pénicaud L., Casteilla L. Spontaneous cardiomyocyte differentiation from adipose tissue stroma cells. *Circ Res* 2004, 94(2): 223-229.

Plath K., Lowry W.E. Progress in understanding reprogramming to the induced pluripotent state. *Nat Rev Genet* 2011, 12(4): 253-265.

Puri M.C., Nagy A. Concise review: Embryonic stem cells versus induced pluripotent stem cells: the game is on. *Stem Cells* 2012, 30(1): 10-14.

Rao M., Ahrlund-Richter L., Kaufman D.S. Concise review: Cord blood banking, transplantation and induced pluripotent stem cell: success and opportunities. *Stem Cells* 2012, 30(1): 55-60.

Rasmusson I., Ringdén O., Sundberg B., Le Blanc K. Mesenchymal stem cells inhibit the formation of cytotoxic T lymphocytes, but not activated cytotoxic T lymphocytes or natural killer cells. *Transplantation* 2003, 76(8): 1208-1213.

Redshaw Z., Strain A.J. Human haematopoietic stem cells express Oct4 pseudogenes and lack the ability to initiate Oct4 promoter-driven gene expression. *J Negat Results Biomed* 2010,

9(1): 2.
Rezania A., Bruin J.E., Arora P., Rubin A., Batushansky I., Asadi A., O'Dwyer S., Quiskamp N., Mojibian M., Albrecht T., Yang Y.H.C., Johnson J.D., Kieffer T.J. Reversal of diabetes with insulin-producing cells derived in vitro from human pluripotent stem cells. *Nat Biotechnol* 2014, 32(11): 1121-1133.
Riley K.G., Gannon M. Pancreas development and regeneration. In: Moody S.A. Principles of developmental genetics. 2nd edition. USA: *Academic Press* 2014, 571-572.
Rocha V., Gluckman E. Clinical use of umbilical cord blood hematopoietic stem cells. *Biol Blood Marrow Transplant* 2006, 12(1 Suppl 1): 34-41.
Roche S., Richard M.J., Favrot M.C. Oct-4, Rex-1, and Gata-4 expression in human MSC increase the differentiation efficiency but not hTERT expression. *J Cell Biochem* 2007, 101(2): 271-280.
Rodriguez A.M., Elabd C., Amri E.Z., Ailhaud G., Dani C. The human adipose tissue is a source of multipotent stem cells. *Biochimie* 2005, 87(1): 125-128.
Romanov Y.A., Darevskaya A.N., Merzlikina N.V., Buravkova L.B. Mesenchymal Stem Cells from Human Bone Marrow and Adipose Tissue: Isolation, Characterization, and Differentiation Potentialities. *Bull Exp Biol Med* 2005, 140(1): 138-143.
Ryan E.A., Paty B.W., Senior P.A., Bigam D., Alfadhli E., Kneteman N.M., Lakey J.R., Shapiro A.M. Five-year follow-up after clinical islet transplantation. *Diabetes* 2005, 54(7): 2060-2069.
Salgado A.J., Reis R.L., Sousa N.J., Gimble J.M. Adipose tissue derived stem cells secretome: soluble factors and their roles in regenerative medicine. *Curr Stem Cell Res Ther* 2010, 5(2): 103-110.
Sarkar A., Hochedlinger K. The Sox family of transcription factors: versatile regulators of stem and progenitor cell fate. *Cell Stem Cell* 2013, 12(1): 15-30.
Sart S., Tsai A.C., Li Y., Ma T. Three-dimensional aggregates of mesenchymal stem cells: cellular mechanisms, biological properties, and applications. *Tissue Eng Part B Rev* 2014, 20(5): 365-380.
Sato K., Ozaki K., Oh I., Meguro A., Hatanaka K., Nagai T., Muroi K., Ozawa K. Nitric oxide plays a critical role in suppression of T-cell proliferation by mesenchymal stem cells. *Blood* 2007, 109(1): 228-234.
Schäffler A., Büchler C. Concise review: adipose tissue-derived stromal cells – basic and clinical implications for novel cell-based therapies. *Stem Cells* 2007, 25(4): 818-27.
Schepers G.E., Teasdale R.D., Koopman P. Twenty pairs of sox: extent, homology, and nomenclature of the mouse and human sox transcription factor gene families. *Dev Cell* 2002, 3(2): 167-170.
Schorle H., Nettersheim D. NANOG (Nanog homeobox). *Atlas Genet Cytogenet Oncol Haematol* 2012, 16(10): 727-731.
Schwartz S.D., Regillo C.D., Lam B.L., Eliott D., Rosenfeld P.J., Gregori N.Z., Hubschman J.P., Davis J.L., Heilwell G., Spirn M., Maguire J., Gay R., Bateman J., Ostrick R.M., Morris D., Vincent M., Anglade E., Del Priore L.V., Lanza R. Human embryonic stem cell-derived retinal pigment epithelium in patients with age-related macular degeneration and Stargardt's macular dystrophy: follow-up of two open-label phase 1/2 studies. *Lancet* 2015, 385(9967): 509-516.
Secco M., Zucconi E., Vieira N.M., Fogaça L.L.Q., Cerqueira A., Carvalho M.D.F., Jazedje T., Okamoto O.K., Muotri A.R., Zatz M. Multipotent stem cells from umbilical cord: cord is richer than blood! *Stem Cells* 2008, 26(1): 146-150.
Segev H., Fishman B., Ziskind A., Shulman M., Itskovitz-Eldor J. Differentiation of human embryonic stem cells into insulin-producing clusters. *Stem Cells* 2004, 22(3): 265-274.
Sekido R., Lovell-Badge R. Sex determination and SRY: down to a wink and a nudge? *Trends Genet* 2009, 25(1): 19-29.
Sensebé L., Krampera M., Schrezenmeier H., Bourin P., Giordano R. Mesenchymal stem cells

for clinical application. *Vox Sang* 2010, 98(2): 93-107.
Seo M.J., Suh S.Y., Bae Y.C., Jung J.S. Differentiation of human adipose stromal cells into hepatic lineage in vitro and in vivo. *Biochem Biophys Res Commun* 2005, 328(1): 258-264.
Shahriyari L., Komarova N.L. Symmetric vs. asymmetric stem cell divisions: an adaptation against cancer? *PloS ONE* 2013, 8(10): e76195.
Shi X., Garry D.J. Muscle stem cells in development, regeneration, and disease. *Genes Dev* 2006, 20(13): 1692-1708.
Shi Y., Hou L., Tang F., Jiang W., Wang P., Ding M., Deng H. Inducing embryonic stem cells to differentiate into pancreatic β cells by a novel three-step approach with activin A and all-trans retinoic acid. *Stem Cells* 2005, 23(5): 656-662.
Siegel G., Kluba T., Hermanutz-Klein U., Bieback K., Northoff H., Schäfer R. Phenotype, donor age and gender affect function of human bone marrow-derived mesenchymal stromal cells. *BMC Med* 2013, 11: 146.
Silva F.J., Holt D.J., Vargas V., Yockman J., Boudina S., Atkinson D., Grainger D.W., Revelo M.P., Sherman W., Bull D.A., Patel A.N. Metabolically active human brown adipose tissue derived stem cells. *Stem Cells* 2014, 32(2): 572-581.
Sinclair A.H., Berta P., Palmer M.S., Hawkins J.R., Griffiths B.L., Smith M.J., Foster J.W., Frischauf A.M., Lovell-Badge R., Goodfellow P.N. A gene from the human sex-determining region encodes a protein with homology to a conserved DNA-binding motif. *Nature* 1990, 346(6281): 240-244.
Soria B., Roche E., Berná G., León-Quinto T., Reig J.A., Martín F. Insulin-secreting cells derived from embryonic stem cells normalize glycemia in streptozotocin-induced diabetic mice. *Diabetes* 2000, 49(2): 157-162.
Spees J.L., Gregory C.A., Singh H., Tucker H.A., Peister A., Lynch P.J., Hsu S.C., Smith J., Prockop D.J. Internalized antigens must be removed to prepare hypoimmunogenic mesenchymal stem cells for cell and gene therapy. *Mol Ther* 2004, 9(5): 747-756.
Stafford D., Hornbruch A., Mueller P.R., Prince V.E. A conserved role for retinoid signaling in vertebrate pancreas development. *Dev Genes Evol* 2004, 214(9): 432-441.
Stainier D.Y. A glimpse into the molecular entrails of endoderm formation. *Genes Dev* 2002, 16(8): 893-907.
Ståhlberg A., Bengtsson M., Hemberg M., Semb H. Quantitative transcription factor analysis of undifferentiated single human embryonic stem cells. *Clin Chem* 2009, 55(12): 2162-2170.
Stoffers D.A., Thomas M.K., Habener J.F. Homeodomain protein IDX-1: a master regulator of pancreas development and insulin gene expression. *Trends Endocrinol Metab* 1997, 8(4): 145-151.
Strakova Z., Livak M., Krezalek M., Ihnatovych I. Multipotent properties of myofibroblast cells derived from human placenta. *Cell Tissue Res* 2008, 332(3): 479-488.
Suen P.M., Li K., Chan J.C.N., Leung P.S. In vivo treatment with glucagon-like peptide 1 promotes the graft function of fetal islet-like cell clusters in transplanted mice. *Int J Biochem Cell Biol* 2006, 38(5-6): 951-960.
Sugii S., Kida Y., Kawamura T., Suzuki J., Vassena R., Yin Y.Q., Lutz M.K., Berggren W.T., Izpisúa Belmonte J.C., Evans R.M. Human and mouse adipose-derived cells support feeder-independent induction of pluripotent stem cells. *Proc Natl Acad Sci U S A* 2010, 107(8): 3558-3563.
Sun B., Roh K.H., Lee S.R., Lee Y.S., Kang K.S. Induction of human umbilical cord blood-derived stem cells with embryonic stem cell phenotypes into insulin producing islet-like structure. *Biochem Biophys Res Commun* 2007, 354(4): 919-923.
Sun Y., Chen L., Hou X.G., Hou W.K., Dong J.J., Sun L., Tang K.X., Wang B., Song J., Li H., Wang K.X. Differentiation of bone marrow-derived mesenchymal stem cells from diabetic patients into insulin-producing cells in vitro. *Chin Med J* 2007, 120(9): 771-776.
Suo G., Han J., Wang X., Zhang J., Zhao Y., Zhao Y., Dai J. Oct4 pseudogenes are transcribed in

cancers. *Biochem Biophys Res Commun* 2005, 337(4): 1047-1051.
Tai M.H., Chang C.C., Olson L.K., Trosko J.E. Oct4 expression in adult human stem cells: evidence in support of the stem cell theory of carcinogenesis. *Carcinogenesis* 2005, 26(2): 495-502.
Takahashi K., Tanabe K., Ohnuki M., Narita M., Ichisaka T., Tomoda K., Yamanaka S. Induction of pluripotent stem cells from adult human fibroblasts by defined factors. *Cell* 2007, 131(5): 861-872.
Takahashi K., Yamanaka S. Induction of pluripotent stem cells from mouse embryonic and adult fibroblast cultures by defined factors. *Cell* 2006, 126(4): 663-676.
Takács L., Tóth E., Berta A., Vereb G. Stem cells of the adult cornea: from cytometric markers to therapeutic applications. *Cytometry A* 2009, 75(1): 54-66.
Takeda J., Seino S., Bell G.I. Human Oct3 gene family: cDNA sequences, alternative splicing, gene organization, chromosomal location, and expression at low levels in adult tissues. *Nucleic Acids Res* 1992, 20(17): 4613-4620.
Taléns-Visconti R., Bonora A., Jover R., Mirabet V., Carbonell F., Castell J.V., Gómez-Lechón M.J. Hepatogenic differentiation of human mesenchymal stem cells from adipose tissue in comparison with bone marrow mesenchymal stem cells. *World J Gastroenterol* 2006, 12(36): 5834-5845.
Tang D.Q., Cao L.Z., Burkhardt B.R., Xia C.Q., Litherland S.A., Atkinson M.A., Yang L.J. In vivo and in vitro characterization of insulin-producing cells obtained from murine bone marrow. *Diabetes* 2004, 53(7): 1721-1732.
Tang D.Q., Wang Q, Burkhardt B.R., Litherland S.A., Atkinson M.A., Yang L.J. In vitro generation of functional insulin-producing cells from human bone marrow-derived stem cells, but long-term culture running risk of malignant transformation. *Am J Stem Cells* 2012, 1(2): 114-127.
Tapp H., Hanley E.N., Patt J.C., Gruber H.E. Adipose-Derived Stem Cells: Characterization and Current Application in Orthopaedic Tissue Repair. *Exp Biol Med* 2009, 234(1): 1-9.
Thiel G. How Sox2 maintains neural stem cell identity. *Biochem J* 2013, 450(3): e1-e2.
Thomson J.A., Itskovitz-Eldor J., Shapiro S.S., Waknitz M.A., Swiergiel J.J., Marshall V.S., Jones J.M. Embryonic stem cell lines derived from human blastocysts. *Science* 1998, 282(5391): 1145-1147.
Timper K., Seboek D., Eberhardt M., Linscheid P., Christ-Crain M., Keller U., Müller B., Zulewski H. Human adipose tissue-derived mesenchymal stem cells differentiate into insulin, somatostatin, and glucagon expressing cells. *Biochem Biophys Res Commun* 2006, 341(4): 1135-1140.
Tocci A., Forte L. Mesenchymal stem cells: use and perspectives. *Hematol J* 2003, 4(2): 92-96.
Tondreau T., Meuleman N., Delforge A., Dejeneffe M., Leroy R., Massy M., Morties C., Bron D., Lagneaux L. Mesenchymal stem cells derived from CD133-positive cells in mobilized peripheral blood and cord blood: proliferation, Oct4 expression, and plasticity. *Stem Cells* 2005, 23(8): 1105-1112.
Trivanović D., Jauković A., Popović B., Krstić J., Mojsilović S., Okić-Djordjević I., Kukolj T., Obradović H., Santibanez J.F., Bugarski D. Mesenchymal stem cells of different origin: Comparative evaluation of proliferative capacity, telomere length and pluripotency marker expression. *Life Sci* 2015, 141: 61-73.
Tropepe V., Coles B.L., Chiasson B.J., Horsford D.J., Elia A.J., McInnes R.R., van der Kooy D. Retinal stem cells in the adult mammalian eye. *Science* 2000, 287(5460): 2032-2036.
Tse W.T., Pendleton J.D., Beyer W.M., Egalka M.C., Giunan E.C. Suppression of allogeneic T-cell proliferation by human marrow stromal cells: implications in transplantation. *Transplantation* 2003, 75(3): 389-397.
Tsuji W., Rubin J.P., Marra K.G. Adipose-derived stem cells: Implications in tissue regeneration. *World J Stem Cells* 2014, 6(3): 312-321.
Ullah I., Subbarao R.B., Rho G.J. Human mesenchymal stem cells - current trends and future

prospective. *Biosci Rep* 2015, 35(2): art:e00191.
Vaca P., Berná G., Martín F., Soria B. Nicotinamide induces both proliferation and differentiation of embryonic stem cells into insulin-producing cells. *Transplant Proc* 2003, 35(5): 2021-2023.
Van Belle H. Alkaline phosphatase. I. Kinetics and inhibition by levamisole of purified isoenzymes from humans. *Clin Chem* 1976, 22(7): 972-976.
Van Hoof D., D'Amour K.A., German M.S. Derivation of insulin-producing cells from human embryonic stem cells. *Stem Cell Res* 2009, 3(2-3): 73-87.
Varma M.J.O., Breuls R.G.M., Schouten T.E., Jurgens W.J.F.M., Bontkes H.J., Schuurhuis G.J., van Ham S.M., van Milligen F.J. Phenotypical and functional characterization of freshly isolated adipose tissue-derived stem cells. *Stem Cells Dev* 2007, 16(1): 91-104.
Venkat M., Wolf A., Deming H. 2014. What is the discussion on stem cells and diabetes all about? A guide to the hope and the hype. *http://diatribe.org/issues/71/learning-curve/diabetes-stem-cell*
Volckaert T., De Langhe S. Lung epithelial stem cells and their niches: Fgf10 takes center stage. *Fibrogenesis Tissue Rapair* 2014, 7: 8.
Wagner W., Wein F., Seckinger A., Frankhauser M., Wirkner U., Krause U., Blake J., Schwager C., Eckstein V., Ansorge W., Ho A.D. Comparative characteristics of mesenchymal stem cells from human bone marrow, adipose tissue, and umbilical cord blood. *Exp Hematol* 2005, 33(11): 1402-1416.
Wall M.E., Bernacki S.H., Loboa E.G. Effects of serial passaging on the adipogenic and osteogenic differentiation potential of adipose-derived human mesenchymal ste cells. *Tissue Eng* 2007, 13(6): 1291-1298.
Wang H., Maechler P., Antinozzi P.A., Hagenfeldt K.A., Wollheim C.B. Hepatocyte nuclear factor 4alpha regulates the expression of pancreatic beta -cell genes implicated in glucose metabolism and nutrient-induced insulin secretion. *J Biol Chem* 2000, 275(46): 35953-35959.
Wang Q., He W., Lu C., Wang Z., Wang J., Giercksky K.E., Nesland J.M., Suo Z. Oct3/4 and Sox2 are significantly associated with an unfavorable clinical outcome in human esophageal squamous cell carcinoma. *Anticancer Res* 2009, 29(4): 1233-1241.
Wang X., Dai J. Concise review: isoforms of OCT4 contribute to the confusing diversity in stem cell biology. *Stem Cells* 2010, 28(5): 885-893.
Wang X., Zhao Y., Xiao Z., Chen B., Wei Z., Wang B., Zhang J., Han J., Gao Y., Li L., Zhao H., Zhao W., Lin H., Dai J. Alternative translation of OCT4 by an internal ribosome entry site and its novel function in stress response. *Stem Cells* 2009, 27(6): 1265-1275.
Watts C., McConkey H., Anderson L., Caldwell M. Anatomical perspectives on adult neural stem cells. *J Anat* 2005, 207(3): 197-208.
Weina K., Utikal J. SOX2 and cancer: current research and its implications in the clinic. *Clin Transl Med* 2014, 3: 19.
Wezel F., Pearson J., Kirkwood L.A., Southgate J. Differential expression of Oct4 variants and pseudogenes in normal urothelium and urothelial cancer. *Am J Pathol* 2013, 183(4): 1128-1136.
Wilson M.E., Scheel D., German M.S. Gene expression cascades in pancreatic development. *Mech Dev* 2003, 120(1): 65-80.
Wong R.S.Y. Extrinsic factors involved in the differentiation of stem cells into insulin-producing cells: an overview. *Exp Diabetes Res* 2011, 2011: 406182.
Woodbury D., Schwarz E.J., Prockop D.J., Black I.B. Adult rat and human bone marrow stromal cells differentiate into neurons. *J Neurosci Res* 2000, 61(4): 364-370.
Xu G., Stoffers D.A., Habener J.F., Bonner-Weir S. Exendin-4 stimulates both beta-cell replication and neogenesis, resulting in increased beta-cell mass and improved glucose tolerance in diabetic rats. *Diabetes* 1999, 48(12): 2270-2276.
Xu W., Zhang X., Qian H., Zhu W., Sun X., Hu J., Zhou H., Chen Y. Mesenchymal stem cells

from adult human bone marrow differentiate into a cardiomyocyte phenotype in vitro. *Exp Biol Med (Maywood)* 2004, 229(7): 623-631.

Yamanaka S. Induced pluripotent stem cells: past, present, and future. *Cell Stem Cell* 2012, 10(6): 678-684.

Yang X.F., He X., He J., Zhang L.H., Su X.J., Dong Z.Y., Xu Y.J., Li Y., Li Y.L. High efficient isolation and systematic identification of human adipose-derived mesenchymal stem cells. *J Biomed Sci* 2011, 18: 59.

Yañez R., Lamana M.L., García-Castro J., Colmenero I., Ramírez M., Bueren J.A. Adipose tissue-derived mesenchymal stem cells have in vivo immunosuppressive properties applicable for the control of the graft-versus-host disease. *Stem Cells* 2006, 24(11): 2582-2591.

Yazd E.F., Rafiee M.R., Soleimani M., Tavallaei M., Salmani M.K., Mowla S.J. OCT4B1, a novel spliced variant of OCT4, generates a stable truncated protein with a potential role in stress response. *Cancer Lett* 2011, 309(2): 170-175.

Ye F., Zhou C., Cheng Q., Shen J., Chen H. Stem-cell-abundant proteins Nanog, Nucleostemin and Musashi1 are highly expressed in malignant cervical epithelial cells. *BMC Cancer* 2008, 8: 108.

Yeung W.C., Rawlinson W.D., Craig M.E. Enterovirus infection and type 1 diabetes mellitus: systematic review and meta-analysis of observational molecular studies. *BMJ* 2011, 342: d35.

Yu J., Vodyanik M.A., Smuga-Otto K., Antosiewicz-Bourget J., Frane J.L., Tian S., Nie J., Jonsdottir G.A., Ruotti V., Stewart R., Slukvin I.I., Thomson J.A. Induced pluripotent stem cell lines derived from human somatic cells. *Science* 2007, 318(5858): 1917-1920.

Zangrossi S., Marabese M., Broggini M., Giordano R., D'Erasmo M., Montelatici E., Intini D., Neri A., Pesce M., Rebulla P., Lazzari L. Oct-4 expression in adult human differentiated cells challenges its role as a pure stem cell marker. *Stem Cells* 2007, 25(7): 1675-1680.

Zaret K.S. Hepatocyte differentiation: from the endoderm and beyond. *Curr Opin Genet Dev* 2001, 11(5): 568-574.

Zhang D., Jiang W., Liu M., Sui X., Yin X., Chen S., Shi Y., Deng H. Highly efficient differentiation of human ES cells and iPS cells into mature pancreatic insulin-producing cells. *Cell Res* 2009, 19(4): 429-438.

Zhang J., Wang X., Chen B., Xiao Z., Li W., Lu Y., Dai J. The human pluripotency gene NANOG/NANOGP8 is expressed in gastric cancer and associated with tumor development. *Oncol Lett* 2010, 1(3): 457-463.

Zhang J., Wang X., Li M., Han J., Chen B., Wang B., Dai J. NANOGP8 is a retrogene expressed in cancers. *FEBS J* 2006, 273(8): 1723-1730.

Zhong J., Rao X., Xu J.F., Yang P., Wang C.Y. The role of endoplasmic reticulum stress in autoimmune-mediated beta-cell destruction in type 1 diabetes. *Exp Diabetes Res* 2012, 2012: 238980.

Zhu Y., Liu T., Song K., Fan X., Ma X., Cui Z. Adipose-derived stem cell: a better stem cell than BMSC. *Cell Biochem Funct* 2008, 26(6): 664-675.

Zorn A.M., Butler K., Gurdon J.B. Anterior endomesoderm specification in Xenopus by Wnt/beta-catenin and TGF-beta signalling pathways. *Dev Biol* 1999, 209(2): 282-297.

Zuk P. Adipose-derived stem cells in tissue regeneration: a review. *ISRN Stem Cells* 2013, 2013: 713959.

Zuk P.A. The intracellular distribution of the ES cell totipotent markers OCT4 and Sox2 in adult stem cells differs dramatically according to commercial antibody used. *J Cell Biochem* 2009, 106(5): 867-877.

Zuk P.A., Zhu M., Ashjian P., De Ugarte D.A., Huang J.I., Mizuno H., Alfonso Z.C., Fraser J.K., Benhaim P., Hedrick M.H. Human adipose tissue is a source of multipotent stem cells. *Mol Biol Cell* 2002, 13(12): 4279-4295.

Zuk P.A., Zhu M., Mizuno H., Huang J., Futrell J.W., Katz A.J., Benhaim P., Lorenz H.P.,

Hedrick M.H. Multilineage Cells from Human Adipose Tissue: Implications for Cell-Based Therapies. *Tissue Eng* 2001, 7(2): 211-226.

Zulewski H., Abraham E.J., Gerlach M.J., Daniel P.B., Moritz W., Müller B., Vallejo M., Thomas M.K., Habener J.F. Multipotential nestin-positive stem cells isolated from adult pancreatic islets differentiate ex vivo into pancreatic endocrine, exocrine, and hepatic phenotypes. *Diabetes* 2001, 50(3): 521-533.

World Wide Web resources

https://clinicaltrials.gov/ct2/results?term=%22adipose-derived+stem+cells%22 Search results for "adipose-derived stem cells". A service of the U.S. National Institutes of Health. Accessed October 29, 2015.

https://clinicaltrials.gov/ct2/results?term=%22mesenchymal+stem+cells%22 Search results for "mesenchymal stem cells". A service of the U.S. National Institutes of Health. Accessed October 29, 2015.

http://viacyte.com/products/vc-01-diabetes-therapy/ VC-01 Diabetes Therapy. ViaCyte. Accessed May 26, 2015.

http://www.bmdw.org/index.php?id=statistics_cordblood Total number of cord blood units. Bone Marrow Donors Worldwide. Accessed April 17, 2015.

http://www.idf.org/sites/default/files/EN_6E_Atlas_Full_0.pdf IDF Diabetes Atlas, 6th Edition. International Diabetes Federation. Accessed May 19, 2015.

http://www.nobelprize.org/nobel_prizes/medicine/laureates/2012/ The Nobel Prize in Physiology or Medicine 2012. The official web site of the Nobel Prize. Accessed April 16, 2015.

http://www.spkc.gov.lv/veselibas-aprupes-statistika/ Statistikas dati par 2014. gadu. Cukura diabēts. Slimību profilakses un kontroles centrs. Accessed September 25, 2015.

Appendix

Appendix 1

Comparison of *OCT4A* gene product sequence, amplified with OCT4 primers, to *OCT4* pseudogene 3 (*OCT4P3*), pseudogene 4 (*OCT4P4*), and pseudogene 1 (*OCT4P1*) sequences of current primary reference assembly (GRCh38) (using Clustal Omega software). Sequences of primers used in the assay are underlined and written in bold. Distinct nucleotides found in the pseudogenes, but not in the original *OCT4A* gene, are marked in yellow. Unique sites of *OCT4A* gene are marked in green. The corresponding sequences of pseudogenes 2, 5, 6, 7, and 8 are not shown, since they display no similarity to the region of interest.

```
OCT4A     TGAGGTGTGGGGGATTCCCCCATGCCCCCCGCCGTATGAGTTCTGTGGGGGGATGGCGTA
OCT4P3    TGAGGAGTGGGGGATTCCCCCATGTCCCCCGCCGTATGAGTTCTGCGGGGGGATGGCGTA
OCT4P4    TGAGGTGTGGGGGATTCCCCCATGCCCCCCGCTGTATGAGTTCTGTGGGGGGATGGCGTA
OCT4P1    TGAGGTGTGGGGGATTCCCCCTTGCCCCCCGCCGTATGAGTTATGTGGGGGGATGGCGTA
          ***** *************** ** ******* ********* ** **************

OCT4A     CTGTGGGCCCCAGGTTGGAGTGGGGCTAGTGCCCCAAGGCGGCTTGGAGACCTCTCAGCC
OCT4P3    CTGTGGGCCTCAGACTGGAGTGGGGCTAGTGCCCCAAGACGGCTTGGAGACCTCTCAGCC
OCT4P4    CTGTGGGCCTCAGGTTGGAGTGCGGCTAGTGCCCCAAGGCGGCTTGGAGACCTCTCAGCC
OCT4P1    CTGTGGGCCTCAGGTTGGAGTGGGGCTAGTGCCCCAAGGCGGCTTGGAGACCTCTCAGCC
          ********* ***  ******* ************** ********************

OCT4A     TGAGGGCGAAGCAGGAGTCGGGGTGGAGAGCAACTCCGATGGGGCCTCCCCGGAGCCCTG
OCT4P3    TGAGGGCGAAGCAGGAGTCGGGGTGGAGAGCAACTCCGATGGGGCCTCCCCGGAGCCCTG
OCT4P4    TGAGGGCGAAGCAGGAGTCAGGGTGGAGAGCAACTCCGATGGCACCTCCCTGGAGCCCTG
OCT4P1    TGAGAGCGAAGCAGGAGTCGGGGTGGAGAGCAACTCCAATGGGGCCTCCCCGGAACCCTG
          **** ************** ***************** ****  ****** *** *****

OCT4A     CACCGTCACCCCTGGTGCCGTGAAGCTGGAGAAGGAGAAGCTGGAGCAAAACCCGGAGGA
OCT4P3    CACCGTCCCCTCTGGTGCCGTGAAGCTGGAGAAGGAGAAGCTGGAGCAAAACCCGGAGGA
OCT4P4    CACCGTCCCCCCTGGTGCCGTGAAACTGGAGAAGGAGAAGCTGGAGCAAAACCCGCAGGA
OCT4P1    CACCGTCCCCCCTGGTGCCGTGAAGCTGGAGAAGGAGAAGCTAGAGCAAAACCCGGAGAA
          ******* ** ************* ***************** ************ ** *

OCT4A     GTCCCAGGACATCAAAGCTCTGCAGAAAGAACTCGAGCAATTTGCCAAGCTCCTGAAGCA
OCT4P3    GTCCCAGGACATCAAAGCTCTGCAGAAAGAACTCGAGCAATTTGCCAAGCTCCTGAAGCA
OCT4P4    GTCCCAGAACATCAAAGCTCTGCAGAAAGAACTCGAACAATTTGCCAAGCTCCTGAAGCA
OCT4P1    GTCCCAGGACATCAAAGCTCTGCAGAAAGAACTCGAGCAATTTGCCAAGCTCCTGAAGCA
          ******* ************************** ***********************
```

Appendix 2-1

Comparison of *NANOG* gene product sequence, amplified with NANOG_1 primers, to *NANOGP1-NANOGP11* pseudogene sequences of current primary reference assembly (GRCh38) (using Clustal Omega software). Sequences of primers used in the assay are underlined and written in bold. Distinct nucleotides found in the pseudogenes, but not in the original *NANOG* gene, are marked in yellow. The site that distinguishes *NANOGP8* from *NANOG* is marked in green.

```
NANOG       ---------GTCTCTCCTCTTC<u>**CTTCCTCCATGGATCTGCTTATTCA**</u>GGACAGCCCTGAT
NANOGP8     ---------GTCTCTCCTCTTCCTTCCTCCATGGATCTGCTTATTCAGGACAGCCCTGAT
NANOGP1     TTTCCAACAGTCTCTCCTCTTCCTTCCTCCATGGATCTGCCTATTCAGGACAGCCATGAT
NANOGP2     ---------GTCTCTCCTCTTCCTTCCTCCATGGATCTG-------AGGATAGTCCTGAT
NANOGP4     ---------GTCTCTCCTCTTC-TTCCTCCATGGATCTGCTTATTCAGGACAGCCCTGAT
NANOGP7     ---------GTCTCTCCTCTTCCTTCCTCCGTGGATCTGCTTATTTAGGACAGCCCTGAT
NANOGP9     ---------GTCTCTCCTCTTCCTTCCTCCATGGATCTGCTTATTCAGGACAGCCCTGAT
NANOGP10    ---------GTCTCTCCTCTTCCTTCCGCCATGGATCTGCTTATCCAGGACAGCCCTGAT
NANOGP11    ------------------------------------------------------------
NANOGP6     ---------CTCTCTCATCTTCCTTCCTCCGTGGATCTATTTATTCAGGAAAGCTCTAAT
NANOGP5     ------------------------------------------------GACAGCTCTAAT
NANOGP3     ------------------------------------------------------------

NANOG       TCTTCCACCAGTCCCAAAGGCAAACAACCCACTTCTGCAGAGAAGAGTGTCGCAAAA-AA
NANOGP8     TCTTCCACCAGTCCCAAAGGCAAACAACCCACTTCTGCAGAGAATTAGTGTCGCAAAA-AA
NANOGP1     TCTTCCACCAGTCCCAAAGGCAAACAACCCACTACTGCAGAGAAGAGTGCCACAAAA-AA
NANOGP2     TCTCCTACCAGTCCCAAAGGCAAACAACCCACTGCTGCAGAGAATAGCGCCACAAAAGAA
NANOGP4     TCTTCCACCAGTCCCAAAGGCAAACAACCCATTGCTGCAGAGAATAATGCCCCAAAA-AA
NANOGP7     TCTTCCACCCCTCCCAAAGGCAAACAACCCACTTCTGCAGAGAAGAGTGCCAGAAAA-AA
NANOGP9     TCTTCCACCAGTCCCAAAGGCAAGCAACCCACTTCTGCAGAGAAGAGTGCCACAAAA-AA
NANOGP10    TCTTCTACCAGTCCTAAAGGCAAAAAACCCACTTCTGCAGAGAAGAGCACCACAAAA-AA
NANOGP11    ------------------------------------------------------------
NANOGP6     TCTTCCACTAGTCCCAGAGTAAAACTACACATTTCTGCAGAGAAGAGCACAGTG-AAGAA
NANOGP5     TCTTTCACGAGTCCCAAAGGCAGACAACTCACTTCTGCAGAGAAGAGCACCGCAAAA-AA
NANOGP3     ------------------------------------------------------------

NANOG       GGAAGACAAGGTCCCGGTCAAGAAACAGAAGACCAGAACTGTGTTCTCTTCCACCCAGCT
NANOGP8     GGAAGACAAGGTCCCGGTCAAGAAACAGAAGACCAGAACTGTGTTCTCTTCCACCCAGCT
NANOGP1     GGAAGACAAGGTCCCGGTCAAGAAACAGAAGACCAGAACTGTGTTCTCTTCCACCCAGCT
NANOGP2     GGAAGACAAGGTCCCAGTCAAGAAACAGAAGACCAGAACTGTGTTCTCTTCCACCCAGCT
NANOGP4     GGGAGACGAGGTCCCAGTCAAGAAACAGAAGACCAGAACTGTGTTTTCTTCCACCCAGCT
NANOGP7     GGAAGACAAGGTCCCATTCAAGAAACAGAAGACCAGAACTGTGTTCTCTTCCACACAGCT
NANOGP9     GGAAAACAAGGTCCCAGTCAAGAAACAGAAGACCAGAACTCTGTTCTCTTCCAACCAGCT
NANOGP10    GGAAGACAAGGTCCTGGTCAAGAAACAGAAGACCAGAACTGTGTTCCGTTCCACCCAGCT
NANOGP11    ------------------------------------------------------------
NANOGP6     TGAAGATAAGATCCAGGAGAAGAAACAGAAGACCAGAATCATGTTCTCTCCGGCCCAGCT
NANOGP5     GGAAGACAAAGTCCTGGTCAAGAAACAGATGACCAGAACTGTGTTCTCTTCCACCCAGCT
NANOGP3     ------------------------------------------------------------

NANOG       GTGTGTACTCAATGATAGATTTCAGAGACAGAAATACCTCAGCCTCCAGCAGATGCAAGA
NANOGP8     GTGTGTACTCAATGATAGATTTCAGAGACAGAAATACCTCAGCCTCCAGCAGATGCAAGA
NANOGP1     GTGTGTACTCAATGATAGATTTCAGAGACAGAAATACCTCAGCCTCCAGCAGATGCAAGA
NANOGP2     GTGTGTACTCAATGATAGATTTCAGAGACAGAAATACCTCAGCCTTCAACAGATGCAAGA
NANOGP4     GTGTGTACTCAATGATAGATTTCAGAGACAGAAATACCTTAGCCTCCAGCAGATGCAAGA
NANOGP7     GTTTGTACTCAATGATAGATTTCAGGGACAGAAATACTTCAGCCTCCAGCAGATGCAAGA
NANOGP9     GTGTGTACTCAATGATAGATTGCAGAGACAGAAATACTTCAGCCTCCAGCAGATGCAAGA
NANOGP10    GTGTGTACTCAATGATAGATTTCACGGACAGAAATACCTCAGCCTCCAGCAGATGCAAGA
NANOGP11    ------------------------------------------------------------
NANOGP6     GTGTGTAATTAATGATGGATTTCAGAGACAGAAACACCGCAGCCTCCAGCAGCTGCAAGA
NANOGP5     GTGTGTACTCAGTGATAGATTTCAGAGACAGAAATACCTCAGCCTCCAGCAGATGCAAGA
NANOGP3     ------------------------------------------------------------
```

Appendix 2-2

```
NANOG       ACTCTCCAACATCCTGAACCTCAGCTACAAACAGGTGAAGACC-----TGGTTCCA-GAA
NANOGP8     ACTCTCCAACATCCTGAACCTCAGCTACAAACAGGTGAAGACC-----TGGTTCCA-GAA
NANOGP1     ACTTTCCAACATCCTGAACCTCAGCTACAAACAGGTAGGCTTATTTTGTCGTTGCAATAA
NANOGP2     ACTTTCCAATATCCTGAACCTTAGCTACAAACAGGTGAAGACC-----TGGTTCCA-GAA
NANOGP4     ACTCTCCAATATCTGGAACCTCAGCTACAAACAGGTGAAGACC-----TGGTTCTA-GAA
NANOGP7     ACTTTCCAACATCCTGAACCTCAGCTACAAACAGGTTAAGACG-----TGGTTCCA-GAA
NANOGP9     ACTTTCCAACATCCTGAACCTCAGCTACAA--AGGTGAAGACC-----TGGTTCCA-GAA
NANOGP10    ACTTTCCAACATCCTGAACCTTAGCTACAAACAGGTTAAGACC-----TGGTTCCA-GAA
NANOGP11    ------------------------------------------------------------
NANOGP6     ACTTTCCAATACCCTGAATCTTAGCTACAAACAGCATACAAGC-----TAGTTACA----
NANOGP5     ACTTTACAGCATCCTGAATCTTAGCTACAAACAGGTTAAGACT-----TGGTTCCA-GAA
NANOGP3     ------------------------------------------------------------
```

Comparison of *NANOG* gene product sequence, amplified with NANOG_2 primers, to *NANOGP1-NANOGP11* pseudogene sequences of current primary reference assembly (GRCh38) (using MAFFT software). Sequences of primers used in the assay are underlined and written in bold. Distinct nucleotides found in the pseudogenes, but not in the original *NANOG* gene, are marked in yellow. The sites that distinguish *NANOGP8* from *NANOG* are marked in green. **!** sign means that a part of the certain pseudogene sequence, not similar to the original gene, is not shown.

```
NANOG       CCAGCTTGTCCCCAAAGCTTGCCTTGCTTTGAAGCATCCGACTGTAAAGAATCT-TCACC
NANOGP8     CCAGCTTGTCCCCAAAGCTTGCCTTGCTTTGAAGAATCCGACTGTAAAGAATCT-TCACC
NANOGP1     CCAGCTTGTCCATAAAGCCTGCCTTGCTCCAAAGCATCTGACTGTAAAGACTGG-TCACC
NANOGP2     CCAGCTTGTCCCCAA-ACCTGCCTGGCTTCAAAGCATCTGATTGTAAAGAATCT-TCACC
NANOGP4     CTGGCTTGTCTGCAAAGCTTGCCTTGCTTCGAAGCATCCGACTGTAAAGAATCT-TAACC
NANOGP7     CCAGCTTGTTCACAAAGCCTGCCTTGCTCCAACGCATCCGTCTGTAAAGACTCT-TCACT
NANOGP9     TCAGCTTGTTCACAAAGCCTGCCTTTCTCTGAAGCATCCGACTGTAAAGACTTT-TCACC
NANOGP10    CCAACCTATGCCCAAAGCCTGCCTTGTTCTGAAGCATCCAACTGTAAAGAATCT-TCACC
NANOGP11    ------------------------------------------------------------
NANOGP6     CCAGCTTGTCTCCAAAGCCTGCCTTATTCTAAAGCATCCAATTCTAGGGACTCTTTCACC
NANOGP5     CCAGCTTGTCCCCAAAACCTGCCTTGCTCTGAAGCATCCAACTGTAAAGACTCT-TTGCC
NANOGP3     ------------------------------------------------------------

NANOG       TATGCCTGTGATTTGTGGGCCTGAAGAAAACTATCCATCCTTGCAAATGTCTTCTGCTGA
NANOGP8     TATGCCTGTGATTTGTGGGCCTGAAGAAAACTATCCATCCTTGCAAATGTCTTCTGCTGA
NANOGP1     TATACCTGTGATTTGTGGGCCTGAAGAAAACCATCCATCCTTGCAAATGTCTTCTGCTGA
NANOGP2     TATGCCTGTCATTTGTGGGCCTGAAGA-AACTATCCATCCTTGCAAATGTCTCCTGCTGA
NANOGP4     TATGGCTGTGATTTGTGGGCCTGAAGAAAACTATCCATCCTTGCAAATGTCTTCTGCTGA
NANOGP7     TACACCTGTGATTTGTGGGCCTGAAGAAAACTATCCATCCTTGCAAATGTCTTCTGCTGA
NANOGP9     TACACCTGTAATTTGTGGGCCTGAAGAAAACTATCCATCCTTGCAAATGTCTTCTGCTGA
NANOGP10    TACGCCGGTGACTTGTGGGCCTGAAGAAAACTATCCATCCCTGCAAATGTCTTCTGCTGA
NANOGP11    ------------------------------------------------------------
NANOGP6     AATGCCTGTGACTCGTGGCCCTGATGAAAGTTATCCATCCTTGCAAATGACATATGAGGA
NANOGP5     AATGTCTGTGATTTGTGGGCCCAAAACAAACTATCCATCCTTGCATATATCTTCTGCTGA
NANOGP3     ------------------------------------------------------------

NANOG       GATGCCTCACACGGAGACT------------------------------------------
NANOGP8     GATGCCTCACACAGAGACT------------------------------------------
NANOGP1     GATGCCTCACACAGAGACTGGTAAGAAAGAAATTTATCCTTGAAAGAAAGGCCTTATTTG!
NANOGP2     GATGCCTCACACTGCGACT------------------------------------------
NANOGP4     GATGCCTCACACGGAGACT------------------------------------------
NANOGP7     GATGCCTCACATGGAGACT------------------------------------------
NANOGP9     GATGCCTCACACAGAGACT------------------------------------------
NANOGP10    GATGCCTCACTCAGAGACT------------------------------------------
NANOGP11    ------------------------------------------------------------
NANOGP6     GGTGTCCCACTCAGAGG-------------------------------------------
NANOGP5     GATGCCTCACACAGAGTCTG----------------------------------------
NANOGP3     ------------------------------------------------------------

NANOG       ---------GTCTCTCCTCTTCCTTCCTCCATGGATCTGCTTATTCAGGACAGCCCTGAT
NANOGP8     ---------GTCTCTCCTCTTCCTTCCTCCATGGATCTGCTTATTCAGGACAGCCCTGAT
NANOGP1     TTTCCAACAGTCTCTCCTCTTCCTTCCTCCATGGATCTGCCTATTCAGGACAGCCATGAT
NANOGP2     ---------GTCTCTCCTCTTCCTTCCTCCATGGATCTG-------AGGATAGTCCTGAT
NANOGP4     ---------GTCTCTCCTCTTC-TTCCTCCATGGATCTGCTTATTCAGGACAGCCCTGAT
NANOGP7     ---------GTCTCTCCTCTTCCTTCCTCCGTGGATCTGCTTATTTAGGACAGCCCTGAT
NANOGP9     ---------GTCTCTCCTCTTCCTTCCTCCATGGATCTGCTTATTCAGGACAGCCCTGAT
NANOGP10    ---------GTCTCTCCTCTTCCTTCCGCCATGGATCTGCTTATCCAGGACAGCCCTGAT
NANOGP11    ------------------------------------------------------------
NANOGP6     ---------CTCTCTCATCTTCCTTCCTCCGTGGATCTATTTATTCAGGAAAGCTCTAAT
NANOGP5     ------------------------------------------------GACAGCTCTAAT
NANOGP3     ------------------------------------------------------------
```

```
NANOG       TCTTCCACCAGTCCCAAAGGCAAACAACCCACTTCTGCAGAGAAGAGTGTCGCAAAA-AA
NANOGP8     TCTTCCACCAGTCCCAAAGGCAAACAACCCACTTCTGCAGAGAATAGTGTCGCAAAA-AA
NANOGP1     TCTTCCACCAGTCCCAAAGGCAAACAACCCACTACTGCAGAGAAGAGTGCCACAAAA-AA
NANOGP2     TCTCCTACCAGTCCCAAAGGCAAACAACCCACTGCTGCAGAGAATAGCGCCACAAAAGAA
NANOGP4     TCTTCCACCAGTCCCAAAGGCAAACAACCCATTGCTGCAGAGAATAATGCCCCAAAA-AA
NANOGP7     TCTTCCACCCCTCCCAAAGGCAAACAACCCACTTCTGCAGAGAAGAGTGCCAGAAAA-AA
NANOGP9     TCTTCCACCAGTCCCAAAGGCAAGCAACCCACTTCTGCAGAGAAGAGTGCCACAAAA-AA
NANOGP10    TCTTCTACCAGTCCTAAAGGCAAAAAACCCACTTCTGCAGAGAAGAGCACCACAAAA-AA
NANOGP11    ------------------------------------------------------------
NANOGP6     TCTTCCACTAGTCCCAGAGTAAAACTACACATTTCTGCAGAGAAGAGCACAGTG-AAGAA
NANOGP5     TCTTTCACGAGTCCCAAAGGCAGACAACTCACTTCTGCAGAGAAGAGCACCGCAAAA-AA
NANOGP3     ------------------------------------------------------------

NANOG       GGAAGACAAGGTCCCGGTCAAGAAACAGAAGACCAGAACTGTGTTCTCTTCCACCCAGCT
NANOGP8     GGAAGACAAGGTCCCGGTCAAGAAACAGAAGACCAGAACTGTGTTCTCTTCCACCCAGCT
NANOGP1     GGAAGACAAGGTCCCGGTCAAGAAACAGAAGACCAGAACTGTGTTCTCTTCCACCCAGCT
NANOGP2     GGAAGACAAGGTCCCAGTCAAGAAACAGAAGACCAGAACTGTGTTCTCTTCCACCCAGCT
NANOGP4     GGGAGACGAGGTCCCAGTCAAGAAACAGAAGACCAGAACTGTGTTTTCTTCCACCCAGCT
NANOGP7     GGAAGACAAGGTCCCATTCAAGAAACAGAAGACCAGAACTGTGTTCTCTTCCACACAGCT
NANOGP9     GGAAAACAAGGTCCCAGTCAAGAAACAGAAGACCAGAACTCTGTTCTCTTCCAACCAGCT
NANOGP10    GGAAGACAAGGTCCTGGTCAAGAAACAGAAGACCAGAACTGTGTTCCGTTCCACCCAGCT
NANOGP11    ------------------------------------------------------------
NANOGP6     TGAAGATAAGATCCAGGAGAAGAAACAGAAGACCAGAATCATGTTCTCTCCGGCCCAGCT
NANOGP5     GGAAGACAAAGTCCTGGTCAAGAAACAGATGACCAGAACTGTGTTCTCTTCCACCCAGCT
NANOGP3     ------------------------------------------------------------
```

Sequence alignment of current primary reference assembly (GRCh38) of the open reading frames (ORFs) of human *NANOG* and *NANOGP8* sequences (using EMBOSS Needle software). Sequences of NANOG_1 primer pair used in the study are coloured in purple and written in bold. Sequences of NANOG_2 primer pair used in the study are coloured in orange and written in bold. 14 coloured nucleotides represent variants between *NANOG* and *NANOGP8* ORF sequences. Two fixed variants detected by comparison of current primary and alternate reference assemblies are marked in red. Eight polymorphic variants detected by comparison of current primary and alternate reference assemblies are marked in green. Four polymorphic variants not present in the comparison of primary and alternate reference assemblies of *NANOGP8* or in other studies, but observed in at least two individuals by Fairbanks et al. 2012 are marked in blue. The numbers above coloured nucleotides depicts their position in the reading frame, relative to the first nucleotide in the ATG initiation codon. The letters above (for *NANOG*) or under (for *NANOGP8*) coloured nucleotides represent the polymorphic variants at this site.

```
                                                                      47
NANOG_ORF          1 ATGAGTGTGGATCCAGCTTGTCCCCAAAGCTTGCCTTGCTTTGAAGCATC      50
                     |||||||||||||||||||||||||||||||||||||||||||||||.|||
NANOGP8_ORF        1 ATGAGTGTGGATCCAGCTTGTCCCCAAAGCTTGCCTTGCTTTGAAGAATC      50
                                                                    C/A
NANOG_ORF         51 CGACTGTAAAGAATCTTCACCTATGCCTGTGATTTGTGGGCCTGAAGAAA     100
                     ||||||||||||||||||||||||||||||||||||||||||||||||||||
NANOGP8_ORF       51 CGACTGTAAAGAATCTTCACCTATGCCTGTGATTTGTGGGCCTGAAGAAA     100
                                          126                 144
NANOG_ORF        101 ACTATCCATCCTTGCAAATGTCTTCTGCTGAGATGCCTCACACGGAGACT     150
                     ||||||||||||||||||||||||||||||||||||||||||.|||||||
NANOGP8_ORF      101 ACTATCCATCCTTGCAAATGTCTTCTGCTGAGATGCCTCACACAGAGACT     150
                           T/C           T/C
                          165                       190
NANOG_ORF        151 GTCTCTCCTCTTCCTTCCTCCATGGATCTGCTTATTCAGGACAGCCCTGA     200
                     ||||||||||||||||||||||||||||||||||||||||||||||||||||
NANOGP8_ORF      151 GTCTCTCCTCTTCCTTCCTCCATGGATCTGCTTATTCAGGACAGCCCTGA     200
                                                       G/T    T/G
                                                            246
NANOG_ORF        201 TTCTTCCACCAGTCCCAAAGGCAAACAACCCACTTCTGCAGAGAAGAGTG     250
                     ||||||||||||||||||||||||||||||||||||||||||||||.||||
ENANOGP8_ORF     201 TTCTTCCACCAGTCCCAAAGGCAAACAACCCACTTCTGCAGAGAATAGTG     250
                                      G/A
                                      276
NANOG_ORF        251 TCGCAAAAAAGGAAGACAAGGTCCCGGTCAAGAAACAGAAGACCAGAACT     300
                     ||||||||||||||||||||||||||||||||||||||||||||||||||||
NANOGP8_ORF      251 TCGCAAAAAAGGAAGACAAGGTCCCGGTCAAGAAACAGAAGACCAGAACT     300

NANOG_ORF        301 GTGTTCTCTTCCACCCAGCTGTGTGTACTCAATGATAGATTTCAGAGACA     350
                     ||||||||||||||||||||||||||||||||||||||||||||||||||||
NANOGP8_ORF      301 GTGTTCTCTTCCACCCAGCTGTGTGTACTCAATGATAGATTTCAGAGACA     350
                           C/T
                          363
NANOG_ORF        351 GAAATACCTCAGCCTCCAGCAGATGCAAGAACTCTCCAACATCCTGAACC     400
                     ||||||||||||||||||||||||||||||||||||||||||||||||||||
NANOGP8_ORF      351 GAAATACCTCAGCCTCCAGCAGATGCAAGAACTCTCCAACATCCTGAACC     400

NANOG_ORF        401 TCAGCTACAAACAGGTGAAGACCTGGTTCCAGAACCAGAGAATGAAATCT     450
                     ||||||||||||||||||||||||||||||||||||||||||||||||||||
NANOGP8_ORF      401 TCAGCTACAAACAGGTGAAGACCTGGTTCCAGAACCAGAGAATGAAATCT     450

NANOG_ORF        451 AAGAGGTGGCAGAAAAACAACTGGCCGAAGAATAGCAATGGTGTGACGCA     500
                     ||||||||||||||||||||||||||||||||||||||||||||||||||||
NANOGP8_ORF      451 AAGAGGTGGCAGAAAAACAACTGGCCGAAGAATAGCAATGGTGTGACGCA     500
```

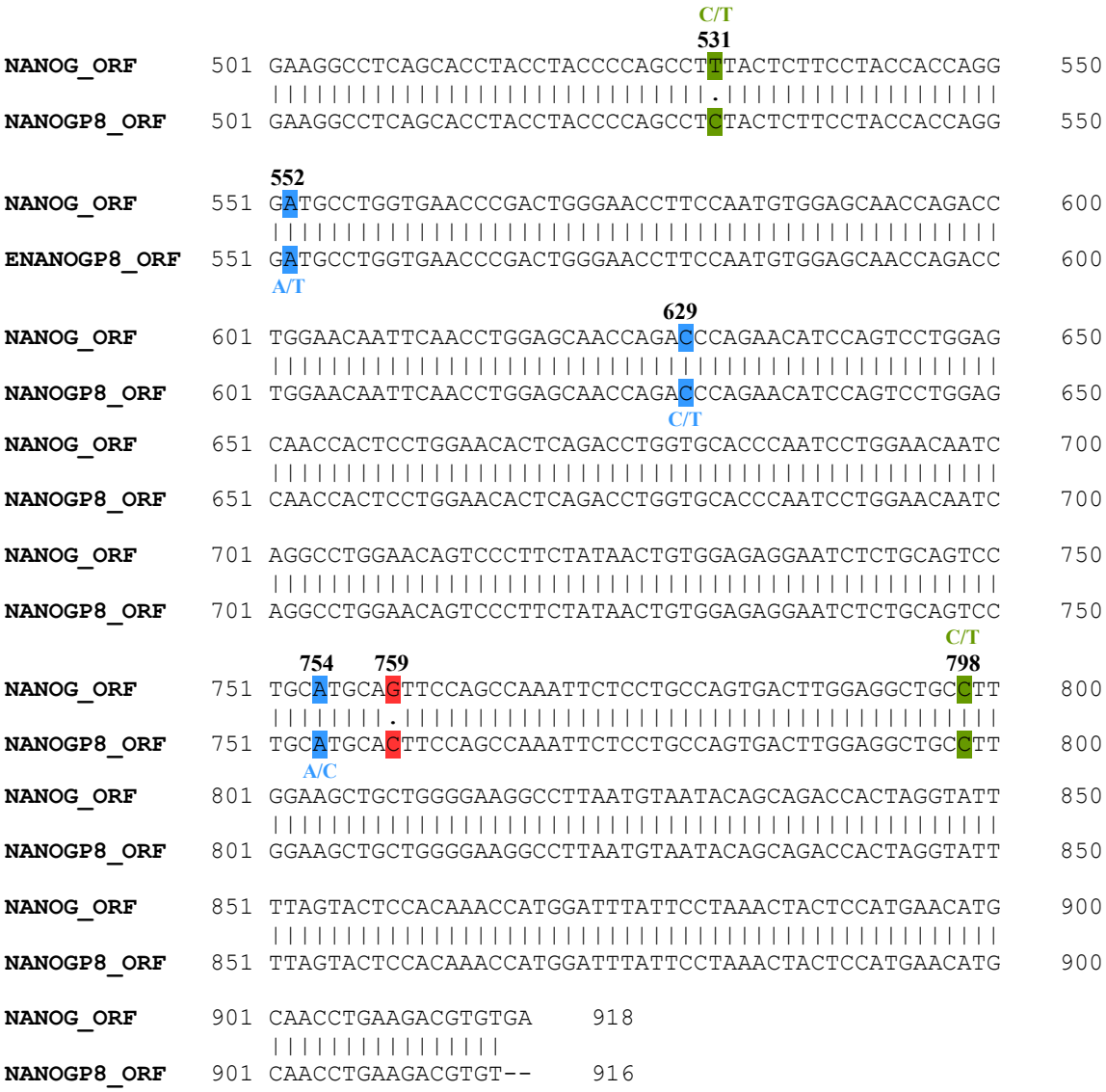
C/T
531
NANOG_ORF 501 GAAGGCCTCAGCACCTACCTACCCCAGCCTTTACTCTTCCTACCACCAGG 550
NANOGP8_ORF 501 GAAGGCCTCAGCACCTACCTACCCCAGCCTCTACTCTTCCTACCACCAGG 550
552
NANOG_ORF 551 GATGCCTGGTGAACCCGACTGGGAACCTTCCAATGTGGAGCAACCAGACC 600
ENANOGP8_ORF 551 GATGCCTGGTGAACCCGACTGGGAACCTTCCAATGTGGAGCAACCAGACC 600
A/T
629
NANOG_ORF 601 TGGAACAATTCAACCTGGAGCAACCAGACCCAGAACATCCAGTCCTGGAG 650
NANOGP8_ORF 601 TGGAACAATTCAACCTGGAGCAACCAGACCCAGAACATCCAGTCCTGGAG 650
C/T
NANOG_ORF 651 CAACCACTCCTGGAACACTCAGACCTGGTGCACCCAATCCTGGAACAATC 700
NANOGP8_ORF 651 CAACCACTCCTGGAACACTCAGACCTGGTGCACCCAATCCTGGAACAATC 700
NANOG_ORF 701 AGGCCTGGAACAGTCCCTTCTATAACTGTGGAGAGGAATCTCTGCAGTCC 750
NANOGP8_ORF 701 AGGCCTGGAACAGTCCCTTCTATAACTGTGGAGAGGAATCTCTGCAGTCC 750
C/T
754
759
798
NANOG_ORF 751 TGCATGCAGTTCCAGCCAAATTCTCCTGCCAGTGACTTGGAGGCTGCCTT 800
NANOGP8_ORF 751 TGCATGCACTTCCAGCCAAATTCTCCTGCCAGTGACTTGGAGGCTGCCTT 800
A/C
NANOG_ORF 801 GGAAGCTGCTGGGGAAGGCCTTAATGTAATACAGCAGACCACTAGGTATT 850
NANOGP8_ORF 801 GGAAGCTGCTGGGGAAGGCCTTAATGTAATACAGCAGACCACTAGGTATT 850
NANOG_ORF 851 TTAGTACTCCACAAACCATGGATTTATTCCTAAACTACTCCATGAACATG 900
NANOGP8_ORF 851 TTAGTACTCCACAAACCATGGATTTATTCCTAAACTACTCCATGAACATG 900
NANOG_ORF 901 CAACCTGAAGACGTGTGA 918
NANOGP8_ORF 901 CAACCTGAAGACGTGT-- 916

Appendix 5

Comparison between *OCT4A* gene fragment and sequencing result of RT-PCR product of ASCs from the donor No.4, amplified with OCT4 reverse (R) primer (using EMBOSS Needle software). Unique sites of *OCT4A* gene are marked in green.

```
OCT4A R              1 TGGGACTCCTCCGGGTTTTGCTCCAGCTTCTCCTTCTCCAGCTTCACGGC   50

OCT4A ASCs No.4      1 --------------------------------------------------    0

OCT4A R             51 ACCAGGGGTGACGGTGCAGGGCTCCGGGGAGGCCCCATCGGAGTTGCTCT  100
                        ....|||||.|||||||||||||||||||||.|||||||..
OCT4A ASCs No.4      1 --------NNNTGTGCANGGCTCCGGGGAGGCCCCATCGGNGTTGCTNN   41

OCT4A R            101 CCACCCCGACTCCTGCTTCGCCCTCAGGCTGAGAGGTCTCCAAGCCGCCT  150
                        ..........|||||||||||||||.||||||||||||..||......|
OCT4A ASCs No.4      42 NNNNNNNNNNTCCTGCTTCGCCCTCANGCTGAGAGGTCTNNAANNNNNNT   91

OCT4A R            151 TGGGGCACTAGCCCCACTCCAACCTGGGGCCCACAGTACGCCATC-  195
                        ||||||||||.||||||||||||||||||||||||||||||
OCT4A ASCs No.4      92 TGGGGCACTANCCCCACTCCAACCTGGGGCCCACAGTACGCCATCA  137
```

Appendix 6

Comparison between *OCT4A* gene fragment and sequencing result of RT-PCR product of ASC aggregates (aggr.) from the donor No.4, amplified with OCT4 reverse (R) primer (using EMBOSS Needle software). Unique sites of *OCT4A* gene are marked in green.

```
OCT4A R              1 TGGGACTCCTCCGGGTTTTGCTCCAGCTTCTCCTTCTCCAGCTTCACGGC   50

OCT4 ASC aggr.       0 --------------------------------------------------    0

OCT4A R             51 ACCAGGGGTGACGGTGCAGGGCTCCGGGGAGGCCCCATCGGAGTTGCTCT  100
                          ..|||||..|||||.|||||||||||||||||||....
OCT4 ASC aggr.       1 --------NN--NNGTGCNNGGCTCNGGGGAGGCCCCATCGGAGTTGNNNN   39

OCT4A R            101 CCACCCCGACTCCTGCTTCGCCCTCAGGCTGAGAGGTCTCCAAGCCGCCT  150
                        .........|||||||||||||||||||||||||||.........||||||
OCT4 ASC aggr.       40 NNNNNNNNNNCTCCTGCTTCGCCCTCAGGCTGAGAGGNNNNNNNNNCCGCCT   89

OCT4A R            151 TGGGGCACTAGCCCCACTCCAACCTGGGGCCCACAGTACGCCATC-  195
                        ||||||||||||||||||||||||||||||||||||||||||||
OCT4 ASC aggr.       90 TGGGGCACTAGCCCCACTCCAACCTGGGGCCCACAGTACGCCATCN  135
```

Appendix 7

Comparison between *OCT4A* gene fragment and sequencing result of RT-PCR product of ESCs, amplified with OCT4 forward (F) primer (using EMBOSS Needle software). Unique sites of *OCT4A* gene are marked in green.

```
OCT4A F             1 GATGGCGTACTGTGGGCCCCAGGTTGGAGTGGGGCTAGTGCCCCAAGGCG   50
                                                             ....|||
OCT4A ESCs          1 -----------------------------------------NNNNGCG    7

OCT4A F            51 GCTTGGAGACCTCTCAGCCTGAGGGCGAAGCAGGAGTCGGGGTGGAGAGC  100
                      ||||||.||||||||||||||||||||||||||||||||||||...|
OCT4A ESCs          8 GCTTGGNGACCTCTCAGCCTGAGGGCGAAGCAGGAGTCGGGGTGGANNNC   57

OCT4A F           101 AACTCCGATGGGGCCTCCCCGGAGCCCTGCACCGTCACCCCTGGTGCCGT  150
                      ||||||||||||||||||||||||||||||||||||||||||||||||||
OCT4A ESCs         58 AACTCCGATGGGGCCTCCCCGGAGCCCTGCACCGTCACCCCTGGTGCCGT  107

OCT4A F           151 GAAGCTGGAGAAGGAGAAGCTGGAGCAAAACCCGGAGGAGTCCCA  195
                      ||||||||||||||||||||||||||||||||||||||||||||
OCT4A ESCs        108 GAAGCTGGAGAAGGAGAAGCTGGAGCAAAACCCGGAGGAGTCCCA  152
```

Appendix 8

Comparison between *OCT4A* gene fragment and sequencing result of RT-PCR product of ESCs, amplified with OCT4 reverse (R) primer (using EMBOSS Needle software). Unique sites of *OCT4A* gene are marked in green.

```
OCT4A R             1 TGGGACTCCTCCGGGTTTTGCTCCAGCTTCTCCTTCTCCAGCTTCACGGC   50
                                                           ....||||
OCT4A ESCs          1 ---------------------------------------NNNNCGGC    8

OCT4A R            51 ACCAGGGGTGACGGTGCAGGGCTCCGGGGAGGCCCCATCGGAGTTGCTCT  100
                      .||||||||||||||||||||||||||||||||||||||||||||||||
OCT4A ESCs          9 NCCAGGGGTGACGGTGCAGGGCTCCGGGGAGGCCCCATCGGAGTTGCTCT   58

OCT4A R           101 CCACCCCGACTCCTGCTTCGCCCTCAGGCTGAGAGGTCTCCAAGCCGCCT  150
                      .........||||||||||||||||||||||||||||||||.........
OCT4A ESCs         59 NNNNNNNNNCTCCTGCTTCGCCCTCAGGCTGAGAGGTCTCCNNNNNNNNN  108

OCT4A R           151 TGGGGCACTAGCCCCACTCCAACCTGGGGCCCACAGTACGCCATC-  195
                      .|||||||||.|||||||||||||||||||||||||||||||||
OCT4A ESCs        109 NGGGGCACTANCCCCACTCCAACCTGGGGCCCACAGTACGCCATCA  154
```

Appendix 9

Comparison between *NANOG* gene fragment and sequencing result of RT-PCR product of ASCs from the donor No.4, amplified with NANOG_1 forward (F) primer (using EMBOSS Needle software). The nucleotides representing polymorphic variants that allow to distinguish *NANOG* gene from *NANOGP8* are marked in green.

```
NANOG_1 F            1 CTTCCTCCATGGATCTGCTTATTCAGGACAGCCCTGATTCTTCCACCAGT   50

NANOG_1 ASCs No.4    0 --------------------------------------------------    0

NANOG_1 F           51 CCCAAAGGCAAACAACCCACTTCTGCAGAGAAGAGTGTCGCAAAAAAGGA  100
                        ...|||||||||||||||||||.||||||||||||||||
NANOG_1 ASCs No.4    1 ---------NNNCAACCCACTTCTGCAGAGAATAGTGTCGCAAAAAAGGA   41

NANOG_1 F          101 AGACAAGGTCCCGGTCAAGAAACAGAAGACCAGAACTGTGTTCTCTTCCA  150
                        |.|.........|||||||||||||||||||||||||||.....||.
NANOG_1 ASCs No.4   42 ANANNNNNNNNNNGTCAAGAAACAGAAGACCAGAACTGTGTTNNNNNCCN   91

NANOG_1 F          151 CCCAGCTGTGTGTACTCAATGATAGATTTCAGAGACAGAAATACCTCAGC  200
                        |||.|||||||||.|||||||||||||||||||||||||||||||||||
NANOG_1 ASCs No.4   92 CCCNGCTGTGTGTNCTCAATGATAGATTTCAGAGACAGAAATACCTCAGC  141

NANOG_1 F          201 CTCCAGCAGATGCAAGAACTCTCCAACATCCTGAACCTCAGCTACAAACA  250
                        ||||||||||||||||||||||||||||||||||||||||||||||||||
NANOG_1 ASCs No.4  142 CTCCAGCAGATGCAAGAACTCTCCAACATCCTGAACCTCAGCTACAAACA  191

NANOG_1 F          251 GGTGAAGACCTG-  262
                        ||||||||||||
NANOG_1 ASCs No.4  192 GGTGAAGACCTGA  204
```

Appendix 10

Comparison between *NANOG* gene fragment and sequencing result of RT-PCR product of ASC aggregates (aggr.) from the donor No.4, amplified with NANOG_1 reverse (R) primer (using EMBOSS Needle software). The nucleotides representing polymorphic variants that allow to distinguish *NANOG* gene from *NANOGP8* are marked in green.

```
NANOG_1 R            1 CAGGTCTTCACCTGTTTGTAGCTGAGGTTCAGGATGTTGGAGAGTTCTTG   50

NANOG_1 ASC aggr.    0 --------------------------------------------------    0

NANOG_1 R           51 CATCTGCTGGAGGCTGAGGTATTTCTGTCTCTGAAATCTATCATTGAGTA  100
                        .||||||||..|||||||||||||||||||||||||.|||||...
NANOG_1 ASC aggr.    1 ----NGCTGGAGGNNGAGGTATTTCTGTCTCTGAAATCTATCNTTGANNN   46

NANOG_1 R          101 CACACAGCTGGGTGGAAGAGAACACAGTTCTGGTCTTCTGTTTCTTGACC  150
                        ...........|||||||||||||||||||||||||...........||
NANOG_1 ASC aggr.   47 NNNNNNNNNNNNTGGAAGAGAACACAGTTCTGGTCTTNNNNNNNNNNNC   96

NANOG_1 R          151 GGGACCTTGTCTTCCTTTTTTGCGACACTCTTCTCTGCAGAAGTGGGTTG  200
                        ||||||||||||||||||||||||||||.||||||||||||||||||||
NANOG_1 ASC aggr.   97 GGGACCTTGTCTTCCTTTTTTGCGACACTATTCTCTGCAGAAGTGGGTTG  146

NANOG_1 R          201 TTTGCCTTTGGGACTGGTGGAAGAATCAGGGCTGTCCTGAATAAGCAGAT  250
                        ||||||..............|||||||||||||.||||||||||.|||
NANOG_1 ASC aggr.  147 TTTGCCNNNNNNNNNNNNNNNGAATCAGGGCTGTACTGAATAAGCNGAT  196

NANOG_1 R          251 CCATGGAGGAAG--  262
                        ||.|||||||||
NANOG_1 ASC aggr.  197 CCNTGGAGGAAGAN  210
```

Appendix 11

Comparison between *NANOG* gene fragment and sequencing result of RT-PCR product of ESCs, amplified with NANOG_1 forward (F) primer (using EMBOSS Needle software). The nucleotides representing polymorphic variants that allow to distinguish *NANOG* gene from *NANOGP8* are marked in green.

```
NANOG_1 F            1 CTTCCTCCATGGATCTGCTTATTCAGGACAGCCCTGATTCTTCCACCAGT   50
                                                                .|||||
NANOG_1 ESCs         1 --------------------------------------------NCCAGT    6

NANOG_1 F           51 CCCAAAGGCAAACAACCCACTTCTGCAGAGAAGAGTGTCGCAAAAAAGGA  100
                       ||||||||||||||||||||||||||||||||.||||||||||||||||
NANOG_1 ESCs         7 CCCAAAGGCAAACAACCCACTTCTGCAGAGAATAGTGTCGCAAAAAAGGA   56

NANOG_1 F          101 AGACAAGGTCCCGGTCAAGAAACAGAAGACCAGAACTGTGTTCTCTTCCA  150
                       ||||||||||||.||||||||||||||||||||||||||||||||||||
NANOG_1 ESCs        57 AGACAAGGTCCCAGTCAAGAAACAGAAGACCAGAACTGTGTTCTCTTCCA  106

NANOG_1 F          151 CCCAGCTGTGTGTACTCAATGATAGATTTCAGAGACAGAAATACCTCAGC  200
                       ||||||||||||||||||||||||||||||||||||||||||||||||||.
NANOG_1 ESCs       107 CCCAGCTGTGTGTACTCAATGATAGATTTCAGAGACAGAAATACCTCAGT  156

NANOG_1 F          201 CTCCAGCAGATGCAAGAACTCTCCAACATCCTGAACCTCAGCTACAAACA  250
                       ||||||||||||||||||||||||||||||||||||||||||||||||||||
NANOG_1 ESCs       157 CTCCAGCAGATGCAAGAACTCTCCAACATCCTGAACCTCAGCTACAAACA  206

NANOG_1 F          251 GGTGAAGACCTG-  262
                       ||||||||||||
NANOG_1 ESCs       207 GGTGAAGACCTGA  219
```

Appendix 12

Comparison between *NANOG* gene fragment and sequencing result of RT-PCR product of ESCs, amplified with NANOG_1 reverse (R) primer (using EMBOSS Needle software). The nucleotides representing polymorphic variants that allow to distinguish *NANOG* gene from *NANOGP8* are marked in green.

```
NANOG_1 R            1 CAGGTCTTCACCTGTTTGTAGCTGAGGTTCAGGATGTTGGAGAGTTCTTG   50
                                                              ..|||||
NANOG_1 ESCs         1 ------------------------------------------NNTCTTG    7

NANOG_1 R           51 CATCTGCTGGAGGCTGAGGTATTTCTGTCTCTGAAATCTATCATTGAGTA  100
                       ||||||||||||.||||||||||||||||||||||||||||||||||..
NANOG_1 ESCs         8 CATCTGCTGGAGACTGAGGTATTTCTGTCTCTGAAATCTATCATTGAGNN   57

NANOG_1 R          101 CACACAGCTGGGTGGAAGAGAACACAGTTCTGGTCTTCTGTTTCTTGACC  150
                       ......||||||||||||||||||||||||||||||||||||||||||||.
NANOG_1 ESCs        58 NNNNNNGCTGGGTGGAAGAGAACACAGTTCTGGTCTTCTGTTTCTTGACT  107

NANOG_1 R          151 GGGACCTTGTCTTCCTTTTTTGCGACACTCTTCTCTGCAGAAGTGGGTTG  200
                       ||||||||||||||||||||||||||||||.||||||||||||||||||||
NANOG_1 ESCs       108 GGGACCTTGTCTTCCTTTTTTGCGACACTATTCTCTGCAGAAGTGGGTTG  157

NANOG_1 R          201 TTTGCCTTTGGGACTGGTGGAAGAATCAGGGCTGTCCTGAATAAGCAGAT  250
                       ||||||||||||||||||||||||||||||||||||||||||||||||||||
NANOG_1 ESCs       158 TTTGCCTTTGGGACTGGTGGAAGAATCAGGGCTGTCCTGAATAAGCAGAT  207

NANOG_1 R          251 CCATGGAGGAAG-  262
                       ||||||||||||
NANOG_1 ESCs       208 CCATGGAGGAAGA  220
```

Appendix 13

Comparison between *NANOG* gene fragment and sequencing result of RT-PCR product of ASCs from the donor No.4, amplified with NANOG_2 forward (F) primer (using EMBOSS Needle software). The nucleotides representing polymorphic variants that allow to distinguish *NANOG* gene from *NANOGP8* are marked in green. The letters in green under the unique site represent the nucleotides detected in a sequencing graph.

```
NANOG_2 F              1 GCTTGCCTTGCTTTGAAGCATCCGACTGTAAAGAATCTTCACCTATGCCT   50

NANOG_2 ASCs No.4      1 ------------------------------------------------     0

NANOG_2 F             51 GTGATTTGTGGGCCTGAAGAAAACTATCCATCCTTGCAAATGTCTTCTGC  100

NANOG_2 ASCs No.4      1 ---------NNNCCTGAAGAAAACTATCCATCCTTGCAAATGTCTTCTGC   41

NANOG_2 F            101 TGAGATGCCTCACACGGAGACTGTCTCTCCTCTTCCTTCCTCCATGGATC  150

NANOG_2 ASCs No.4     42 TGAGANNNNNNNNNNGAGACTGTCTCTCCTCTTCCTTCCTCCATGGATC   91
                                       A/G
NANOG_2 F            151 TGCTTATTCAGGACAGCCCTGATTCTTCCACCAGTCCCAAAGGCAAACAA  200

NANOG_2 ASCs No.4     92 TGCTTATTCAGTACAGCCCTGATTCTTCCACCAGTCCCAAAGGCNAACAA  141

NANOG_2 F            201 CCCACTTCTGCAGAGAAGAGTGTCGCAAAAAAGGAAGACAAGGTCCCGGT  250

NANOG_2 ASCs No.4    142 CCCACTTCTGCAGAGAATAGTGTCGCAAAAAAGGAAGACAAGGTCCCGGT  191

NANOG_2 F            251 CAAGAA--  256

NANOG_2 ASCs No.4    192 CAAGAAAA  199
```

Appendix 14

Comparison between *NANOG* gene fragment and sequencing result of RT-PCR product of ASCs from the donor No.4, amplified with NANOG_2 reverse (R) primer (using EMBOSS Needle software). The nucleotides representing polymorphic variants that allow to distinguish *NANOG* gene from *NANOGP8* are marked in green.

```
NANOG_2 R              1 TTCTTGACCGGGACCTTGTCTTCCTTTTTTGCGACACTCTTCTCTGCAGA   50

NANOG_2 ASCs No.4      1 --------------------------------------------------     0

NANOG_2 R             51 AGTGGGTTGTTTGCCTTTGGGACTGGTGGAAGAATCAGGGCTGTCCTGAA  100

NANOG_2 ASCs No.4      1 ---------NNNGCCTTTGGGACNGGTGGAAGAATNAGGGNTGTACTGAA   41

NANOG_2 R            101 TAAGCAGATCCATGGAGGAAGGAAGAGGAGAGACAGTCTCCGTGTGAGGC  150

NANOG_2 ASCs No.4     42 TAAGNNNNNNNNNNANGAAGGANGAGGAGAGACAGTCTCTGTGNGAGGN   91

NANOG_2 R            151 ATCTCAGCAGAAGACATTTGCAAGGATGGATAGTTTTCTTCAGGCCCACA  200

NANOG_2 ASCs No.4     92 ATCTCAGNAGAAGACATTTGCAAGGNTGGATAGTTTTCTTCAGGCCCNCN  141
NANOG_2 R            201 AATCACAGGCATAGGTGAAGATTCTTTACAGTCGGATGCTTCAAAGCAAG  250

NANOG_2 ASCs No.4    142 AATCACNGGCATAGGTGAAGATTCTTTACAGTCGGATGCTTCTAAGCNNG  191

NANOG_2 R            251 GCAAGC-  256

NANOG_2 ASCs No.4    192 GCAAGCA  198
```

Appendix 15

Comparison between *NANOG* gene fragment and sequencing result of RT-PCR product of ASC aggregates (aggr.) from the donor No.4, amplified with NANOG_2 forward (F) primer (using EMBOSS Needle software). The nucleotides representing polymorphic variants that allow to distinguish *NANOG* gene from *NANOGP8* are marked in green. The letters in green under the unique site represent the nucleotides detected in a sequencing graph.

```
NANOG_2 F              1 GCTTGCCTTGCTTTGAAGCATCCGACTGTAAAGAATCTTCACCTATGCCT   50
                                                                        ...
NANOG_2 ASC aggr.      1 ------------------N----------------------------NNN    3

NANOG_2 F             51 GTGATTTGTGGGCCTGAAGAAAACTATCCATCCTTGCAAATGTCTTCTGC  100
                          |.||||||||||||||||||||||||||||||||||.||||||||||||
NANOG_2 ASC aggr.      4 GNGATTTGTGGGCCTGAAGAAAACTATCCATCCTTGCANATGTCTTCTGC   53

NANOG_2 F            101 TGAGATGCCTCACACGGAGACTGTCTCTCCTCTTCCTTCCTCCATGGATC  150
                          |||.........|||.|||||||||||||||||||||||||.|||||
NANOG_2 ASC aggr.     54 TGANNNNNNNNNCACNGAGACTGTCTCTCCTCTTCCTTCCTCCANGGATC  103
                                      A/G
NANOG_2 F            151 TGCTTATTCAGGACAGCCCTGATTCTTCCACCAGTCCCAAAGGCAAACAA  200
                          ||||||||||.||||||||||||||||||.||||||||||||||||||
NANOG_2 ASC aggr.    104 TGCTTATTCAGTACAGCCCTGATTCTTCCANCAGTCCCAAAGGCAAACAA  153

NANOG_2 F            201 CCCACTTCTGCAGAGAAGAGTGTCGCAAAAAAGGAAGACAAGGTCCCGGT  250
                          ||||||||||||||||...||||||.|||||||||||||||||||||||
NANOG_2 ASC aggr.    154 CCCACTTCTGCAGAGAATNNTGTCGNAAAAAAGGAAGACAAGGTCCCGGT  203

NANOG_2 F            251 CAAGAA-  256
                          ||||||
NANOG_2 ASC aggr.    204 CAAGAAA  210
```

Appendix 16

Comparison between *NANOG* gene fragment and sequencing result of RT-PCR product of ASC aggregates (aggr.) from the donor No.4, amplified with NANOG_2 reverse (R) primer (using EMBOSS Needle software). The nucleotides representing polymorphic variants that allow to distinguish *NANOG* gene from *NANOGP8* are marked in green.

```
NANOG_2 R              1 TTCTTGACCGGGACCTTGTCTTCCTTTTTTGCGACACTCTTCTCTGCAGA   50

NANOG_2 ASC aggr.      1 --------N------------------------------N-----------    0

NANOG_2 R             51 AGTGGGTTGTTTGCCTTTGGGACTGGTGGAAGAATCAGGGCTGTCCTGAA  100
                             ...|||||||||||||||||||||||||||||||||.....
NANOG_2 ASC aggr.      1 ------NNNTTTGCCTTTGGGACTGGTGGAAGAATCAGGGCTGTNNNNNN   44

NANOG_2 R            101 TAAGCAGATCCATGGAGGAAGGAAGAGGAGAGACAGTCTCCGTGTGAGGC  150
                          .......||||.|||||||||||||||||||....|||||||||
NANOG_2 ASC aggr.     45 NNNNNNNATCCNTGGAGGAAGGAAGAGGAGAGACAGTNNNNGTGTGAGGC   94
NANOG_2 R            151 ATCTCAGCAGAAGACATTTGCAAGGATGGATAGTTTTCTTCAGGCCCACA  200
                          ||||||||||||||||||||||||||||||||||||||||||||||||
NANOG_2 ASC aggr.     95 ATCTCAGCAGAAGACATTTGCAAGGATGGATAGTTTTCTTCAGGCCCACA  144

NANOG_2 R            201 AATCACAGGCATAGGTGAAGATTCTTTACAGTCGGATGCTTCAAAGCAAG  250
                          ||||||||||||||||||||||||||||||||||||||||||||||||
NANOG_2 ASC aggr.    145 AATCACAGGCATAGGTGAAGATTCTTTACAGTCGGATGCTTCAAAGCAAG  194

NANOG_2 R            251 GCAAGC-  256
                          ||||||
NANOG_2 ASC aggr.    195 GCAAGCA  202
```

Appendix 17

Comparison between *NANOG* gene fragment and sequencing result of RT-PCR product of ESCs, amplified with NANOG_2 forward (F) primer (using EMBOSS Needle software). The nucleotides representing polymorphic variants that allow to distinguish *NANOG* gene from *NANOGP8* are marked in green.

```
NANOG_2 F            1 GCTTGCCTTGCTTTGAAGCATCCGACTGTAAAGAATCTTCACCTATGCCT   50
                                                                ...||
NANOG_2 ESCs         1 ------------------------------------------NNNCT    5

NANOG_2 F           51 GTGATTTGTGGGCCTGAAGAAAACTATCCATCCTTGCAAATGTCTTCTGC  100
                       ||||||||||||||||||||||||||||||||||||||||||||||||||
NANOG_2 ESCs         6 GTGATTTGTGGGCCTGAAGAAAACTATCCATCCTTGCAAATGTCTTCTGC   55

NANOG_2 F          101 TGAGATGCCTCACACGGAGACTGTCTCTCCTCTTCCTTCCTCCATGGATC  150
                       |||||......||||||||||||||||||||||.||||||||||||||
NANOG_2 ESCs        56 TGAGANNNNNNACACGGAGACTGTCTCTCCTCTTCCCTCCTCCATGGATC  105

NANOG_2 F          151 TGCTTATTCAGGACAGCCCTGATTCTTCCACCAGTCCCAAAGGCAAACAA  200
                       ||||||||||||||||||||||||||||||||||||||||||||||||||
NANOG_2 ESCs       106 TGCTTATTCAGGACAGCCCTGATTCTTCCACCAGTCCCAAAGGCAAACAA  155

NANOG_2 F          201 CCCACTTCTGCAGAGAAGAGTGTCGCAAAAAAGGAAGACAAGGTCCCGGT  250
                       ||||||||||||||||.||||||||||||||||||||||||||||||||
NANOG_2 ESCs       156 CCCACTTCTGCAGAGAATAGTGTCGCAAAAAAGGAAGACAAGGTCCCGGT  205

NANOG_2 F          251 CAAGAA-  256
                       ||||||
NANOG_2 ESCs       206 CAAGAAA  212
```

Appendix 18

Comparison between *NANOG* gene fragment and sequencing result of RT-PCR product of ESCs, amplified with NANOG_2 reverse (R) primer (using EMBOSS Needle software). The nucleotides representing polymorphic variants that allow to distinguish *NANOG* gene from *NANOGP8* are marked in green.

```
NANOG_2 R            1 TTCTTGACCGGGACCTTGTCTTCCTTTTTTGCGACACTCTTCTCTGCAGA   50
                                                                   ...|
NANOG_2 ESCs         1 --------------------------------------------NNNA    4

NANOG_2 R           51 AGTGGGTTGTTTGCCTTTGGGACTGGTGGAAGAATCAGGGCTGTCCTGAA  100
                       ||||||||||||||||||||||||||||||||||||||||||||||||||
NANOG_2 ESCs         5 AGTGGGTTGTTTGCCTTTGGGACTGGTGGAAGAATCAGGGCTGTCCTGAA   54

NANOG_2 R          101 TAAGCAGATCCATGGAGGAAGGAAGAGGAGAGACAGTCTCCGTGTGAGGC  150
                       |||......||||||||||.|||||||||||||||||||||.....|
NANOG_2 ESCs        55 TAANNNNNNCCATGGAGGAGGGAAGAGGAGAGACAGTCTCCGTGNNNNNC  104

NANOG_2 R          151 ATCTCAGCAGAAGACATTTGCAAGGATGGATAGTTTTCTTCAGGCCCACA  200
                       ||||||||||||||||||||||||||||||||||||||||||||||||||
NANOG_2 ESCs       105 ATCTCAGCAGAAGACATTTGCAAGGATGGATAGTTTTCTTCAGGCCCACA  154

NANOG_2 R          201 AATCACAGGCATAGGTGAAGATTCTTTACAGTCGGATGCTTCAAAGCAAG  250
                       ||||||||||||||||||||||||||||||||||||||..||||||
NANOG_2 ESCs       155 AATCACAGGCATAGGTGAAGATTCTTTACAGTCGGATGCTTCNNAGCAAG  204

NANOG_2 R          251 GCAAGC-  256
                       ||||||
NANOG_2 ESCs       205 GCAAGCA  211
```

Appendix 19

Expression of SOX17 in ASCs of the donors No.4 and No.9 after their differentiation into cells of endodermal lineage using the Protocol 5. Cell nuclei counterstained with DAPI. Magnification 200x.

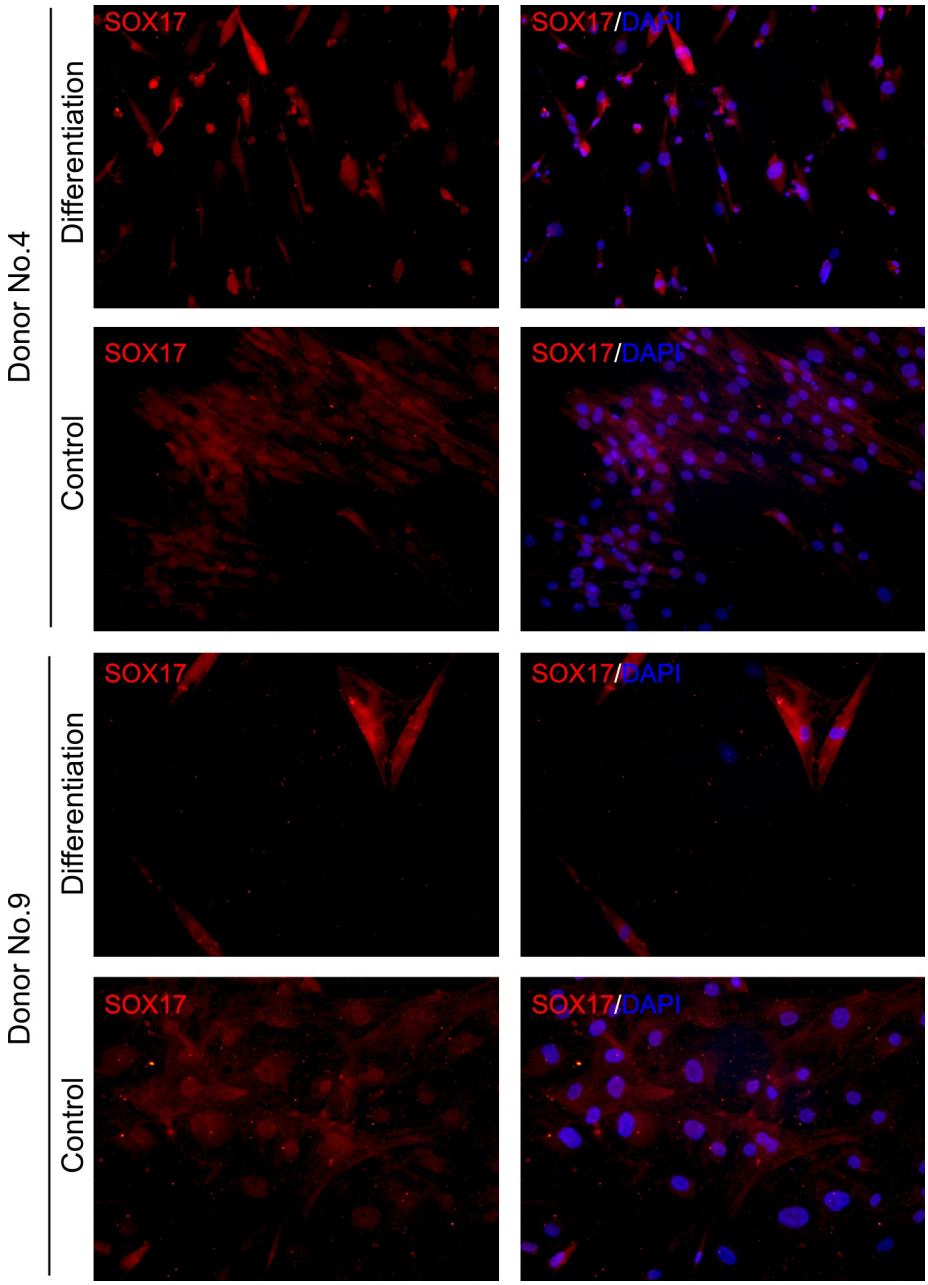

Appendix 20

Expression of SOX17 in ASCs of the donors No.4 and No.9 after their differentiation into cells of endodermal lineage using the Protocol 6. Cell nuclei counterstained with DAPI. Magnification 200x.

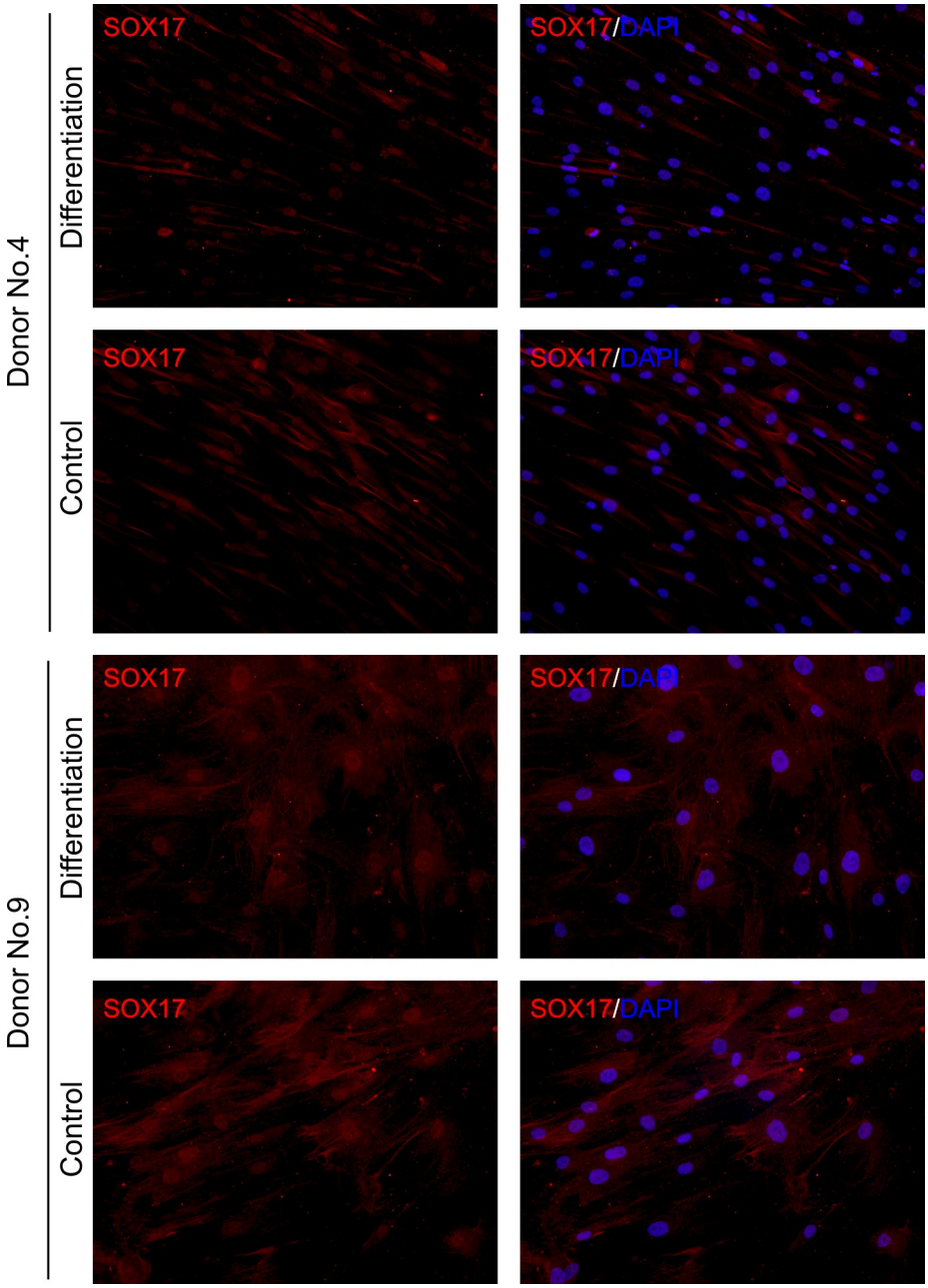

Appendix 21

Expression of SOX17 in ASCs of the donors No.4 and No.9 after their differentiation into cells of endodermal lineage using the Protocol 7. Cell nuclei counterstained with DAPI. Magnification 200x.

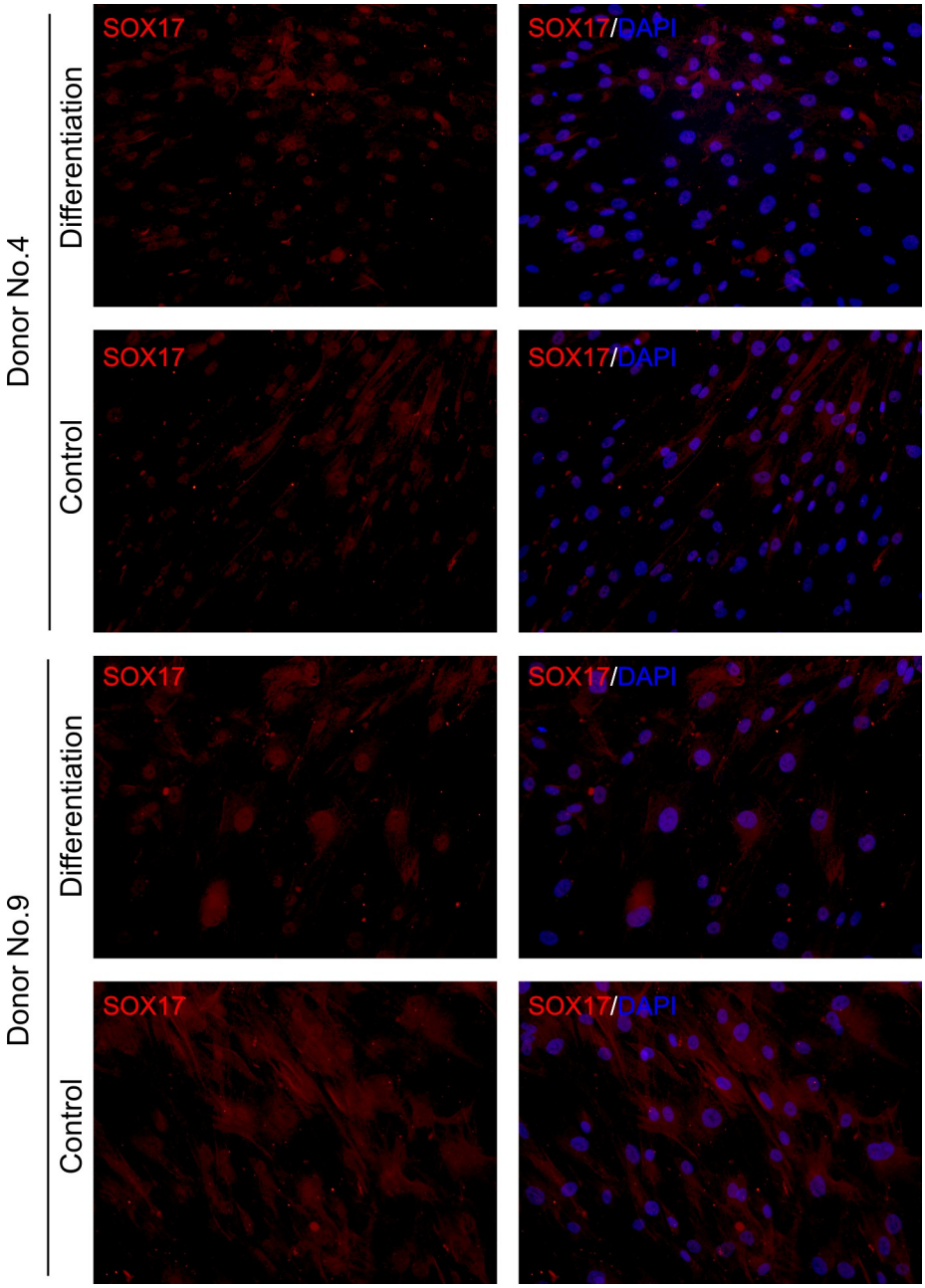

Appendix 22

Expression of SOX17 in ASCs of the donors No.4 and No.9 after their differentiation into cells of endodermal lineage using the Protocol 8. Cell nuclei counterstained with DAPI. Magnification 200x.

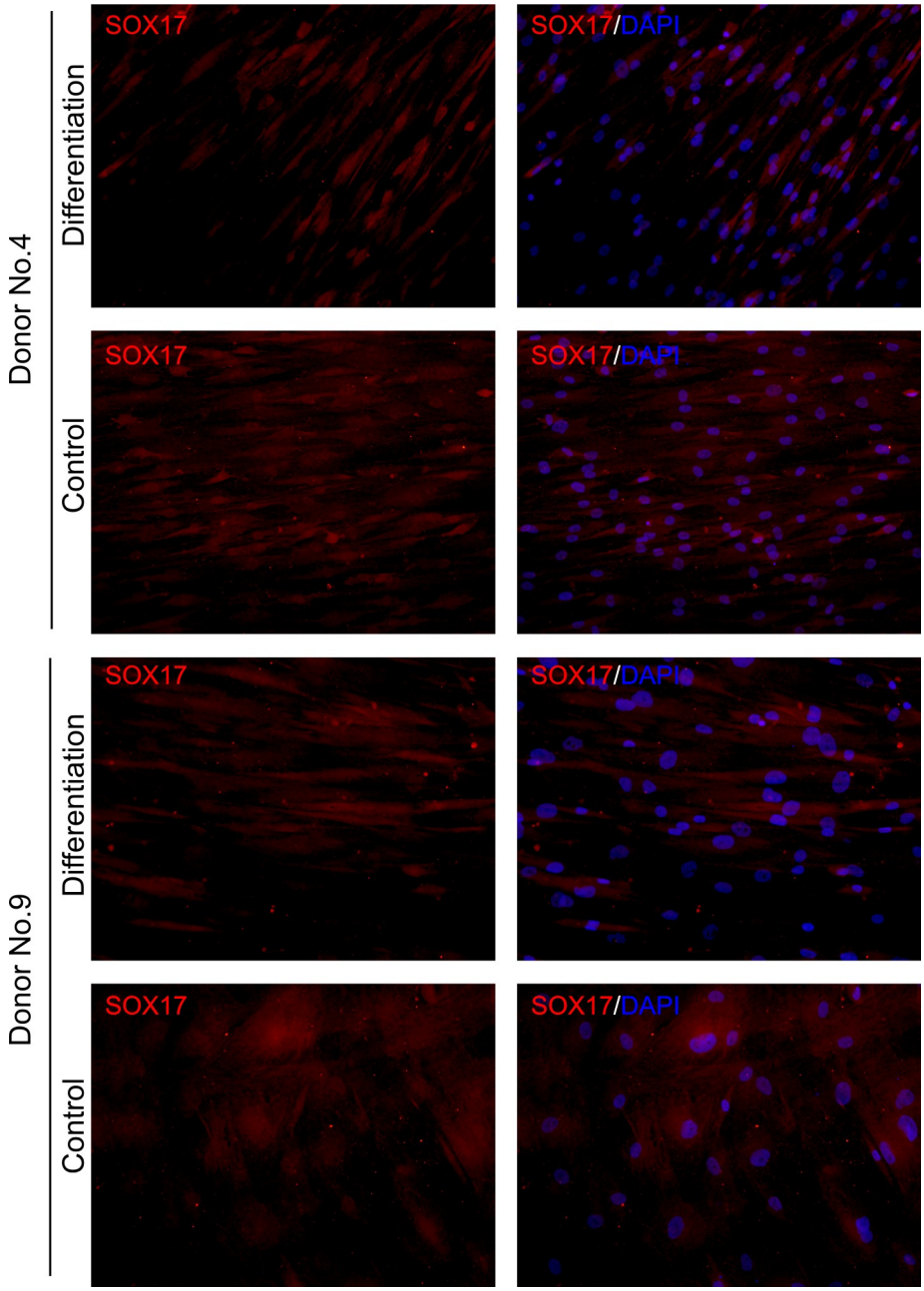

Appendix 23

Expression of PDX1 in ASCs of the donors No.4 and No.9 after their differentiation into cells of endodermal lineage using the Protocol 5. Cell nuclei counterstained with DAPI. Magnification 200x.

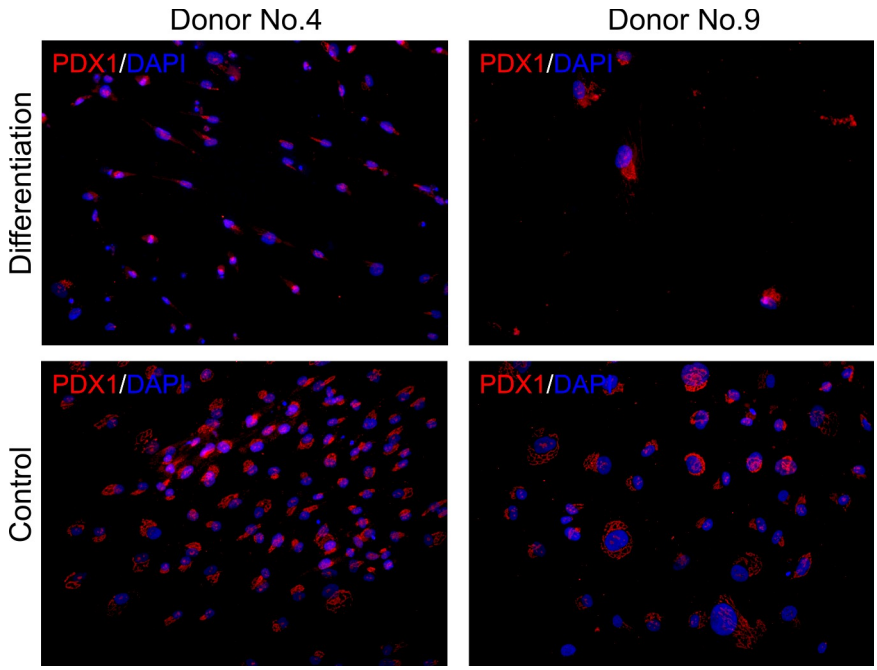

Appendix 24

Expression of PDX1 in ASCs of the donors No.4 and No.9 after their differentiation into cells of endodermal lineage using the Protocol 6. Cell nuclei counterstained with DAPI. Magnification 200x.

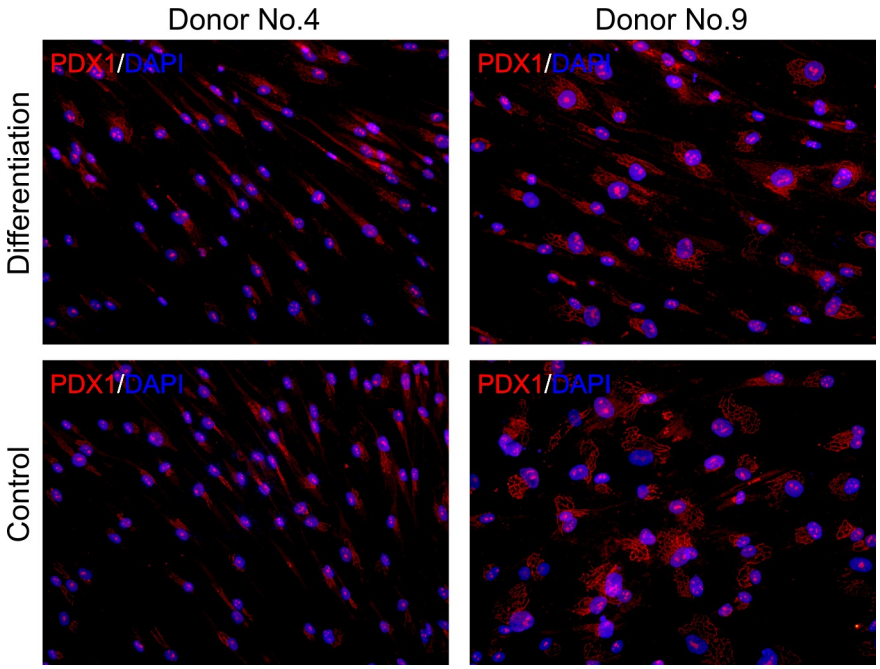

Appendix 25

Expression of PDX1 in ASCs of the donors No.4 and No.9 after their differentiation into cells of endodermal lineage using the Protocol 7. Cell nuclei counterstained with DAPI. Magnification 200x.

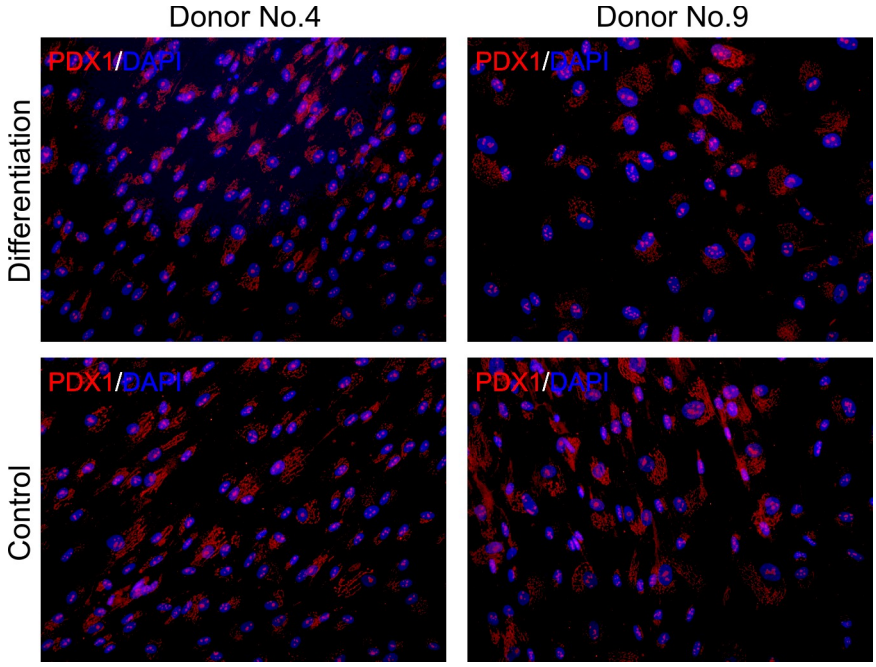

Appendix 26

Expression of PDX1 in ASCs of the donors No.4 and No.9 after their differentiation into cells of endodermal lineage using the Protocol 8. Cell nuclei counterstained with DAPI. Magnification 200x.

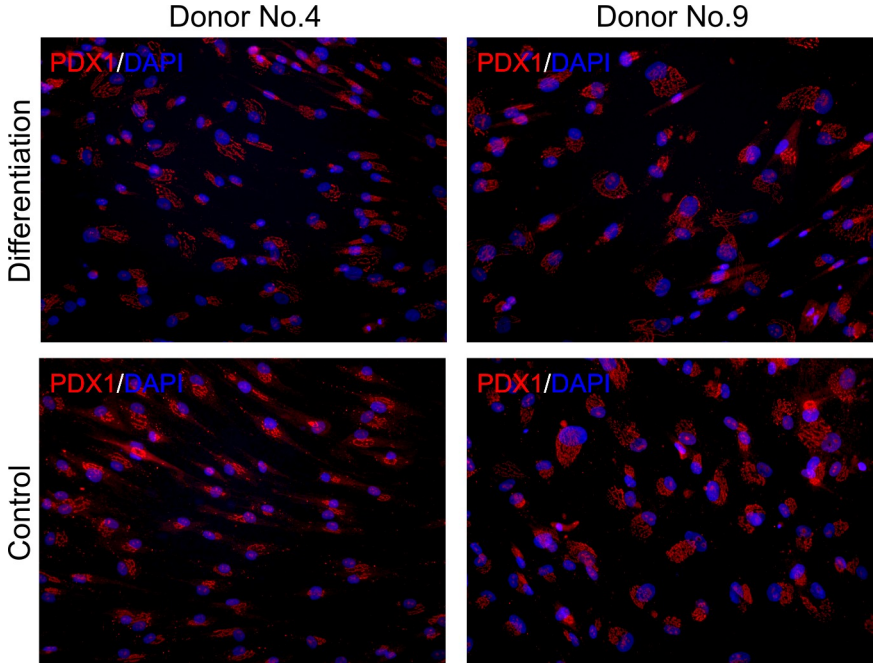

Appendix 27

Detection of INS, C-PEPT, GCG and SST in cryosections of mouse pancreas (islets of Langerhans). Cell nuclei counterstained with DAPI. Magnification 400x.